



University
of Glasgow

AL Ibrahim, Abdulqader (2019) *Studies to characterise ovarian tumours in the mare*. PhD thesis.

<https://theses.gla.ac.uk/70981/>

Copyright and moral rights for this work are retained by the author

A copy can be downloaded for personal non-commercial research or study, without prior permission or charge

This work cannot be reproduced or quoted extensively from without first obtaining permission in writing from the author

The content must not be changed in any way or sold commercially in any format or medium without the formal permission of the author

When referring to this work, full bibliographic details including the author, title, awarding institution and date of the thesis must be given

Enlighten: Theses

<https://theses.gla.ac.uk/>
research-enlighten@glasgow.ac.uk

Studies to Characterise Ovarian Tumours in the Mare

Abdulqader Awadh AL Ibrahim
BVMSc, MSc

Submitted in fulfilment of the requirements for the Degree
of

Doctor of Philosophy (PhD)



School of Veterinary Medicine
College of Medical, Veterinary and Life Sciences
University of Glasgow

14th January 2019

Abstract

Reason for performing this study: Granulosa cell tumours (GCT) are the most common type of ovarian tumours associated with mare infertility requiring highly invasive treatment, yet knowledge of GCT prevalence, pathogenesis and early diagnostic options is lacking. Text mining of UK veterinary practice data was used to enable the estimation of equine GCT (and ovarian pathology) prevalence in the UK. Gene sequencing studies were undertaken to investigate an important point mutation found in the coding region of the forkhead transcription factor gene *FOXL2* (C402G) in adult human GCT biopsies. Antral follicle wave development in mares is highly regulated and leads to differing outcomes in follicles (differentiation versus atresia) with consequences for cellular morphology and function. As rapidly growing GCT must transform from normal ovarian follicles, specifically the granulosa cell, but also the theca compartment, a detailed histological and functional comparison of normal (control) follicle walls to diseased, solid or cystic GCT tissues was also carried out. While the influence of the time of year on follicular function has previously been studied in mares, the cellular effects of other factors such as disease or age of the mare are less clear, yet important for understanding and controlling mare reproduction. In addition, the mare is also considered an excellent model for ovarian function in women, thus our understanding of both regulated and dysregulated follicle growth may benefit from our studies using mare ovaries.

Objective: The general aims were to determine the prevalence of ovarian pathology and particularly GCT in UK equine practice; determine the effects of GCT formation in mare ovaries, which may dysregulate follicular granulosa (GC) or theca cell (THC) proliferation in very healthy (VH), healthy (H), early atretic (EA) and late atretic (LA) antral follicles using morphometric and functional histological approaches; determine whether the *FOXL2* gene mutation identified in human GCT also exists in the equine GCT; and finally determine the *FOXL2* protein localization in GCT samples compared with medium and large healthy and atretic antral follicles.

Materials and Methods: Data mining of clinical records (515,832 records) from seven veterinary practices from around the UK was used in this study.

Sixty-three follicles H&E sections were dissected from the normal ovaries of 19 mares classified as healthy (n= 35), or suffering from chronic clinical disease (n= 4) or severe systemic illness (n= 24) unrelated to the reproductive system. Follicle walls were processed for histological categorisation and (granulosa and theca layer, and a subset for granulosa cell nuclear circumference) measurements using H&E sections. Forty follicle walls recovered from 16 mares were functionally examined for hormone (inhibin), enzyme (aromatase, CYP17A), receptor (AMHR2) or transcription factor (FOXL2) expression parameters (stain intensity, distribution and % area covered) using immunohistochemistry. Similarly, ten GCT tissue samples from five mares (each mare provided two tissue section samples, one from cystic and one from solid areas of the GCT) were histologically categorised using H&E sections, followed by measurement of the nuclear circumference of granulosa cells within the GCT and the same immunohistochemical evaluations. Data were analysed using non-parametric statistical analyses, including correlation analyses between protein expression (% area covered) and functional follicle parameters (diameter and follicular fluid oestradiol concentration).

In addition, the *FOXL2* gene was partially sequenced from a subset of GCT (from seven mares) and control follicle wall samples (from five mares) using in house molecular approaches followed by next generation sequencing (Illumina NextSeq 500 at Glasgow Polyomics), to analyse the region spanning the *FOXL2* C→G mutation discovered in human adult GCT.

Results: Data mining of clinical records from 26,019 mares revealed 115 potential GCT cases, but with only 11 cases being true GCT positive on further reading, resulting in a prevalence estimate of 0.04% (1: 2,365 mares); 143 potential ovarian pathology cases were found of which 65 cases were truly positive resulting in a prevalence estimate of 0.25% (1 in 400 mares).

Follicles measured on average 21 mm in diameter, which was not associated with mare disease status ($p>0.05$), and were allocated to very healthy (VH), healthy (H), early atretic (EA) and late atretic (LA) categories based on the histological appearance of the GC and THC layers. Mare disease status was not associated with the follicle health category ($p>0.05$), and was not associated with percentages of basal, intermediate or antral GC, or GC layer thickness

($p > 0.05$). However, the THC layer thickness was greater ($p = 0.01$) in follicles from mares with severe disease compared with follicles from healthy mares. More healthy than diseased mares were in seasonal transition at the time of ovary recovery ($p = 0.001$), and transitional follicles showed reduced THC layer thickness and percentages of basal GC and large THC, compared with follicles recovered from those in deep anoestrus (all p -values < 0.05). Follicle categorization into VH, H or EA was correlated with follicular fluid oestradiol concentrations, but not associated with follicle diameter or any GC layer characteristics (all p -values > 0.05); however, H follicles had a thicker THC layer than EA follicles ($p = 0.001$). In LA follicles the GC layer was not present, and the percentage of large THC was reduced, while the percentage of small THC was increased compared to VH and H follicles ($p < 0.001$), reducing the THC layer thickness in LA versus H follicles ($p = 0.001$).

Inhibin expression was detected only in GC of normal follicular walls (FW) and GCT categories, not in THC. Similarly, aromatase expression was detected only in GC of normal FW; no aromatase stain was detected in any of the GCT samples and categories. Conversely, CYP17 expression was only detected in THC of normal FW and in interstitial TH like cells in diseased GCT samples. Both compartments of GC and THC in normal FW demonstrated the expression of AMHR2, which was also highly expressed in GC of cysts and solid areas in GCT samples, where it showed only little expression in the interstitial stromal tissue.

Within normal ovaries the nuclear circumference of GC nuclei decreased from basal (62.9 ± 3.1) to intermediate (54.5 ± 1.6) and antral cells (44.7 ± 1.9) ($p = 0.001$), with follicle atresia being associated with reduced basal GC nuclear size ($p = 0.04$). In GCT1 and GCT2 cysts, basal GC nuclei (73.3 ± 3.9) were also larger than antral (53.7 ± 3.1) ($p = 0.001$) and intermediate cell nuclei (63.9 ± 4.7) ($p = 0.03$), and antral GC nuclei of GCT1 and 2 (52.8 ± 2.8) were larger than those in normal ovaries (44.7 ± 1.9) ($p = 0.03$). The nuclear circumference of solid GC nests (74.0 ± 4.1) varied more between tumours and was larger than antral GC nuclei within cysts (53.7 ± 3.1) ($p = 0.001$).

The *FOXL2* C→G (C402G) human mutation was detected very rarely, and considered to be a result of sequencing error. However, a second, proximal C→T mutation was identified in 25% of all reads (mean \pm SEM: GCT 27.2 ± 4.3 , controls

25.5± 3.0, P=0.4), even though this was not predicted to change the amino acid within the protein. Nuclear expression of FOXL2 was seen in GC and THC of all control FW, and expression declined with follicle atresia; FOXL2 was very highly expressed in GC of GCT cysts and solid areas, yet showed only a low level of expression in interstitial stromal tissue of GCT.

Conclusion: A very low prevalence of GCT in horses attending UK veterinary practices was identified. Differences in histomorphological and functional GC and THC measurements in equine large antral follicles appear more associated with season and follicle atresia than with disease. Location within normal antral follicle and tumour cyst walls, tumour transformation, and GCT compartment are associated with GC nuclear size, likely reflecting differing nuclear activity. While this study could not link the specific human *FOXL2* SNP to equine GCT in the samples that were collected, a further frequent mutation in the small region amplified was identified. Therefore, further investigation of the complete equine *FOXL2* gene may identify other mutations with functional significance in GCT formation in the horse and thus potentially also in the woman.

Table of Contents

Contents

Abstract	2
List of Tables.....	10
List of Figures.....	14
Acknowledgement	22
Author's Declaration	23
Abbreviations	24
Chapter 1 Literature Review	26
1.1 Introduction	26
1.2 Epidemiology	28
1.2.1 Background	28
1.3 Anatomical aspects in the mare.....	31
1.3.1 Gross anatomy and topography of the ovary	31
1.3.2 Histology of the ovary.....	33
1.4 Physiology	34
1.4.1 Oestrous cycle and seasonality	34
1.5 Ovarian pathology in the mare	35
1.5.1 Differential diagnosis of ovarian enlargements	35
1.6 Granulosa Cell tumour (GCT)	37
1.6.1 GCT size & weight	38
1.7 Functional and hormonal changes within the GCT and ovary.....	39
1.7.1 Oestradiol (E2)	39
1.7.2 Aromatase	40
1.7.3 Inhibin	40
1.7.4 CYP17.....	41
1.7.5 Anti-Müllerian hormone (AMH).....	41
1.8 Histopathology	42
1.9 FOXL2 gene	45
1.9.1 Definition	45
1.9.2 FOXL2 mutation	46
1.9.3 FOXL2 Immunohistochemistry	46
1.10 Hypotheses	46
Chapter 2 Materials, methods and refining techniques.....	47
2.1 Text mining methods.....	47
2.1.1 UK data.....	47
2.2 Animals from which ovarian samples were recovered	47
2.3 Ultrasonography	48

2.3.1	Measurements of follicles and corpus luteum	48
2.4	Follicular fluid (FF) samples	49
2.5	Ovaries, stroma and follicular wall samples.....	49
2.6	Blood sample	50
2.7	Hormonal assay	50
2.7.1	Oestradiol (E2) ELISA Protocol.....	51
2.8	Histopathology	53
2.8.1	Measurement of ovaries and ovarian follicles	53
2.8.2	Hemisecting of ovaries, cutting of stroma, peeling off the follicular wall (FW) and preservation	55
2.8.3	Tissue processing protocol (wax blocks).	55
2.8.4	Haematoxylin and Eosin (H&E) staining	56
2.8.5	Histological (normal follicular wall) and histopathological (GCT) slide examinations.....	56
2.8.6	Cells counting and measuring the thickness of granulosa and theca cells	61
2.8.7	Nuclear circumferences	62
2.8.8	Generic Immunohistochemistry (IHC) Protocol using Dako Autostainer	63
2.8.9	IHC analysis.....	64
2.9	FOXL2 sequence determination gene extraction	65
2.9.1	First experiment	65
Chapter 3	Text mining.....	84
3.1	Introduction	85
3.2	Materials and Methods	86
3.2.1	Data.....	86
3.2.2	Development of the categorisation dictionary in free text mining software	87
3.2.3	Inclusion dictionary	88
3.2.4	Statistical analyses	89
3.3	Results	89
3.3.1	Data details.....	89
3.3.2	Prevalence of different ovarian conditions.	91
3.3.3	Sensitivity and specificity	97
3.3.4	Risk factors for ovarian pathology and GCT	98
3.4	Discussion	100
3.5	Conclusion	103
Chapter 4	Morphometric analysis of the granulosa and theca layer of equine antral follicles	104
4.1	Introduction	104

4.1.1	Aim:.....	108
4.1.2	Objectives:	109
4.2	Materials and Methods	109
4.2.1	Animals and tissue samples	109
4.2.2	Follicle processing.....	112
4.2.3	Histology of the follicular wall	114
4.2.4	Histological assessment of follicle health status and morphometric measurements	115
4.2.5	Statistical analysis.....	119
4.3	Results	120
4.3.1	Gross findings	120
4.3.2	Histological findings.....	122
4.3.3	Analysis of the association between the different follicle health categories and other parameters	125
4.4	Discussion	138
4.5	Conclusion	141
Chapter 5 Identifying histomorphological and immunohistochemical alterations in mare granulosa cell tumours (GCT) and antral follicles		142
5.1	Introduction	142
5.1.1	Aim:.....	144
5.1.2	Objectives:	144
5.2	Materials and Methods:	144
5.2.1	Animal and tissue samples	144
5.2.2	Immunohistochemistry (IHC) technique on follicle wall and GCT sections.....	145
5.2.3	IHC and nuclear measurements.....	146
5.2.4	Statistical analysis.....	147
5.3	Results:	148
5.3.1	Immunohistological findings.....	148
5.3.2	Analysis of the association between follicle health or GCT category and FW and GCT functional parameters	175
5.3.3	Nuclear Circumference between FW and GCTs	201
5.4	Discussion	211
5.5	Conclusion	214
Chapter 6 Mutation of the forkhead box L2 (<i>FOXL2</i>) gene and <i>FOXL2</i> expression in control ovaries and GCT of mares		215
6.1	Introduction	215
6.1.1	Aim:.....	218
6.1.2	Objectives:	218
6.2	Materials and Methods	219

6.2.1	Next Generation Sequencing (NGS)	219
6.2.2	Immunohistochemistry (IHC) procedures.....	222
6.2.3	Statistical analysis.....	223
6.3	Results	224
6.3.1	Next generation sequencing of PCR products	224
6.3.2	Immunohistochemical findings	233
6.4	Discussion	247
6.5	Conclusion	250
Chapter 7	General Discussion.....	251
Appendices	261
Appendix 1	Method of using the software SimStat/WordStat	261
Appendix 2	Dictionary used in Text mining	277
2.1	Ovarian Tumour dictionary	277
2.2	Ovarian pathology dictionary	279
2.3	GCT dictionary	285
List of References	288

List of Tables

Table 2-1: An example of ovary and follicular size measurements from five mares with normal follicles	49
Table 2-2: H& E stain preparation steps	57
Table 2-3: The dilution of the primary antibodies, secondary antibodies and enzymatic antigen retrieval used	64
Table 2-4: Mares used in the study	65
Table 2-5: DNA concentration of final samples sequenced	67
Table 2-6: Primers details.....	69
Table 3-1: Number of records of female horses from each practice with veterinary reports	90
Table 3-2: Number of records for female horses per breed.....	90
Table 3-3: Cases of ovarian pathology as identified by the text mining process and confirmed (or otherwise) as such by the reading in detail of each 'case' record (represented by 'Test +ve' or 'Test-ve').....	92
Table 3-4: Ovarian tumours as identified by text mining and confirmed (or otherwise as such) following detailed examination of each 'case'.	93
Table 3-5: Positive granulosa cell tumour case	95
Table 3-6: Potential GCT cases identified by text mining that were, upon detailed examination deemed to be false positives.....	96
Table 3-7: Sensitivity and specificity of the ovarian pathology dictionary	97
Table 3-8: Contingency table of GCT text mining.	97
Table 3-9 Univariable logistic regression analysis for ovarian pathology	98
Table 3-10: Multivariable logistic regression analysis for ovarian pathology	99
Table 3-11: Univariable logistic regression analysis for GCT.....	99
Table 3-12 Multivariable logistic regression analysis for GCT.....	100
Table 4-1: Classification of atretic follicle (Follicle regression)	107
Table 4-2: Mares used in this experiment	111
Table 4-3: Association between a range of parameters and FWD. VH (very Healthy), H (Healthy). EA (Early Atretic), LA (Late Atretic), LF (Large follicles from 20mm), SF (Small Follicles < 20mm). Bold indicates a statistically significant p-value.....	126
Table 4-4: Association between the predictive follicle and mare parameters and FFE2 concentration. VH (very Healthy), H (Healthy). EA (Early Atretic), LA (Late Atretic), LF (Large follicles from 20mm), SF (Small Follicles < 20mm). Bold indicates a statistically significant p-value.....	127
Table 4-5: Association between follicle health category and mare factors and basal, intermediate and antral GC counts and thickness. VH (very Healthy), H (Healthy). EA (Early Atretic), LA (Late Atretic), LF (Large follicles from 20mm), SF (Small Follicles < 20mm). Bold indicates a statistically significant p-value..	128
Table 4-6: Association between the follicle size category and GC counts and thickness. VH (very Healthy), H (Healthy). EA (Early Atretic), LA (Late Atretic), LF (Large follicles from 20mm), SF (Small Follicles < 20mm). Bold indicates a statistically significant p-value.....	129
Table 4-7: Association between the breeding season and GC counts and thickness. VH (very Healthy), H (Healthy). EA (Early Atretic), LA (Late Atretic), LF (Large follicles from 20mm), SF (Small Follicles <20mm). Bold indicates a statistically significant p-value.....	130
Table 4-8: Association between the breed category and GC counts and thickness. VH (very Healthy), H (Healthy). EA (Early Atretic), LA (Late Atretic), LF (Large	

follicles from 20mm), SF (Small Follicles < 20mm). Bold indicates a statistically significant p-value.....	131
Table 4-9: Association between the age of the mare and GC counts and thickness. VH (very Healthy), H (Healthy). EA (Early Atretic), LA (Late Atretic), LF (Large follicles from 20mm), SF (Small Follicles < 20mm). Bold indicates a statistically significant p-value.....	132
Table 4-10: Association between mare disease status and GC counts and thickness. VH (very Healthy), H (Healthy). EA (Early Atretic), LA (Late Atretic), LF (Large follicles from 20mm), SF (Small Follicles < 20mm). Bold indicates a statistically significant p-value.....	133
Table 4-11: Association between follicle health status and THC counts and thickness. VH (very Healthy), H (Healthy). EA (Early Atretic), LA (Late Atretic), LF (Large follicles from 20mm), SF (Small Follicles < 20mm). Bold indicates a statistically significant p-value.....	134
Table 4-12: Association between follicle size category and THC counts and thickness. VH (very Healthy), H (Healthy). EA (Early Atretic), LA (Late Atretic), LF (Large follicles from 20mm), SF (Small Follicles < 20mm). Bold indicates a statistically significant p-value.....	135
Table 4-13: Association between breeding season and THC counts and thickness. VH (very Healthy), H (Healthy). EA (Early Atretic), LA (Late Atretic), LF (Large follicles from 20mm), SF (Small Follicles < 20mm). Bold indicates a statistically significant p-value.....	136
Table 4-14: Association between breed category and THC counts and thickness. VH (very Healthy), H (Healthy). EA (Early Atretic), LA (Late Atretic), LF (Large follicles from 20mm), SF (Small Follicles < 20mm). Bold indicates a statistically significant p-value.....	136
Table 4-15: Association between mare age and THC counts and thickness. VH (very Healthy), H (Healthy). EA (Early Atretic), LA (Late Atretic), LF (Large follicles from 20mm), SF (Small Follicles < 20mm). Bold indicates a statistically significant p-value.....	137
Table 4-16: Association between mare disease status and THC counts and thickness. VH (very Healthy), H (Healthy). EA (Early Atretic), LA (Late Atretic), LF (Large follicles from 20mm), SF (Small Follicles < 20mm). Bold indicates a statistically significant p-value.....	138
Table 5-1: IHC antibodies	146
Table 5-2: Association between FW health status and FWD and FFE2 concentration	176
Table 5-3: Association between FW and GCT categories and inhibin GC stain intensity, distribution and percentage area covered.	178
Table 5-4: Association between FW categories and aromatase GC stain intensity, distribution and percentage area covered.....	180
Table 5-5: Association between FW and GCT categories and CYP17 THC stain intensity, distribution and percentage area covered.	182
Table 5-6: Association between FW and GCT categories and AMHR2 GC and THC stain intensity, distribution and %area	184
Table 5-7: the combined FW (VH, H and EA) with the combined GCT categories in the hormone (inhibin) , enzyme (CYP17) and receptor (AMHR2) expression measurements in GC.	186
Table 5-8: Comparing the combined FW (VH, H and EA) with the combined GCT categories in the hormone (inhibin) , enzyme (CYP17) and receptor (AMHR2) expression measurements in THC/interstitial cells.	187

Table 5-9: Association between inhibin GC stain intensity and distribution and FWD.....	188
Table 5-10: Association between aromatase GC stain intensity and distribution and FWD.	189
Table 5-11: Association between CYP17 THC stain intensity and distribution and control FWD.	190
Table 5-12: Association between AMHR2 GC and THC stain intensity and distribution and FWD.....	191
Table 5-13: Association between inhibin GC stain intensity and distribution and FFE2 concentration.....	192
Table 5-14: Association between aromatase stain GC intensity and distribution and control FFE2 concentration	193
Table 5-15: Association between CYP17 THC stain intensity and distribution and FFE2 concentration.....	194
Table 5-16: Association between AMHR2 GC and THC stain intensity and distribution and FFE2 concentration.....	195
Table 5-17: Correlation of the percentage area covered in GC or THC with FWD and FFE2 concentration in control follicles. FWD (NO. =30 follicles), FFE2 concentration (NO. =25 follicles).	196
Table 5-18: Comparison of FW GC nuclear circumferences by health status. No represent 5 different follicles	207
Table 5-19: Comparison of follicle size categories in their FW GC nuclear circumferences.	207
Table 5-20: Effect of categories on GCT GC nuclear circumferences. No. represent 5 different GCT tumours which were used for each GCT category. ...	209
Table 5-21: Comparison of health status and combined nuclear GC layers within GCT categories.....	209
Table 5-22: Comparison of all categories of FW and GCT in their GC nuclear circumferences. Note that GCT4 did not have different GC layers, but top, middle and bottom nuclei were measured within one view.	210
Table 5-23: Comparison of the GC nuclear circumference between all VH, H and EA FW combined and all GCT1, GCT2 and GCT4 combined.	211
Table 6-1: PCR products for GCTs and for controls	222
Table 6-2: GCT samples: GT is Genotype, DP is Depth, RO is Reference allele count, QR is Reference allele quality, AO is Alternate count, QA is Alternate quality and GL is Genotype likelihood (0/0 is Ref and 1/1 is Alt and both are Homozygous, 0/1 is Heterozygous). * Please note that Freebayes identified 'no mutation' in samples 3 and 4 because %Alt is less than 10%, thus we consider the genotype of the sample as 0/0.	229
Table 6-3: Control samples. * Please note that Freebayes identified the mutation in sample 10 but as %Alt is less than 10% we consider the genotype of the sample as 0/0.	230
Table 6-4: Association between FW and GCT categories and FOXL2 GC and THC stain intensity, distribution and percentage area covered.....	241
Table 6-5: Comparing the difference in combined health status of GC and THC in FW and GCT categories on FOXL2 stain measurements.....	242
Table 6-6: Effect of FOXL2 GC and THC stain intensity and distribution on FWD	243
Table 6-7: Effect of FOXL2 GC and THC stain intensity and distribution on FFE2 concentration	244

Table 6-8: Correlation of GC and THC percentage area covered and FWD and FFE2 concentration. FWD (NO.=30 follicles) and FFE2 concentration (NO.=25 follicles)245

List of Figures

Figure 1-1: Mare reproductive tract. (Ab. AL Ibrahim, Thesis Image)	32
Figure 1-2: Demonstration of mare rectal palpation on a dummy mare illustrating the topography of the mare's tract. The images were acquired by Ab. AL Ibrahim.	32
Figure 1-3: Mare oestrous cycle. DF (dominant follicle), CL (corpus luteum)	35
Figure 1-4: Follicular cavity filled with blood: Anovulatory haemorrhagic follicle, 49.1x38.2 mm. (Ab. AL Ibrahim, Thesis Image).	36
Figure 1-5: Gross appearance of the complete and hemisected GCT tumour. (Ab. AL Ibrahim, Thesis image).	38
Figure 1-6: Classified GCT1; cystic structure looks like a healthy follicular wall. GCT1 has all antral (Yellow arrow), intermediate (Red arrow) and basal (Black arrow) granulosa cells (GCs). 400x magnification. (Ab. AL Ibrahim, Thesis image)	43
Figure 1-7: Classified GCT2: cystic like structure but appear as a closed circle cyst. It has all antral (Yellow arrow), intermediate (Red arrow) and basal (Black arrow) GCs. 400x magnification (Ab. AL Ibrahim, Thesis image).	44
Figure 1-8: Classified GCT3: cystic like structure but appear as a closed circle cyst. It has only few antral (Yellow arrow) GCs. 400x magnification (Ab. AL Ibrahim, Thesis image).	44
Figure 1-9: Classified GCT4: solid nests of granulosa cells. 400x magnification (Ab. AL Ibrahim, Thesis image).	45
Figure 2-1: Standard curve and calibrator diluent	52
Figure 2-2: Examining the uterine tract immediately after euthanasia	53
Figure 2-3: Ovary diameter measurement	54
Figure 2-4: Follicle diameter measurement using ultrasonography	55
Figure 2-5: Illustration of how views are taken from a selected follicular wall sample. This sample is taken as 200X magnification; the boxes are representative of the five successive views taken for further assessment at 400x magnification.	58
Figure 2-6: Rectangle view of follicular wall image 200x magnification	59
Figure 2-7: Counting granulosa and theca cells at 400x magnification, No.1: Basal GCs, No.2: Antral GCs, No.3: Intermediate GCs, No. 4: Large THC's, No. 5: Small THC's	60
Figure 2-8: Measuring (White lines) the thickness of granulosa and theca cell at 200x magnification	61
Figure 2-9: Setting a scale (pixel: μm) ratio using ImageJ at 40 magnifications. 100 μm equal to 398.0201 pixels, thereby producing a scale of 3.9802 pixels/ μm	62
Figure 2-10: Gel of extracted DNA from tissues of varying ages using 150ng/ μl DNA per well. Fixed tissues: (GCT1, GCT2A, GCT6, GCT5), Frozen tissue (GCT2B), Frozen blood (Non GCT4), Fresh blood (Non GCT 7A), Fresh tissue (Non GCT 7B)	68
Figure 2-11: An Extracted DNA result generated by the NanoDrop1000.....	69
Figure 2-12: The nucleotide sequence of Equine <i>FOXL2</i> , with the position of the forward and reverse primers shown and the expected site of the mutation highlighted in yellow.....	70
Figure 2-13: Gel of primary PCR using P2 of fixed GCT & Non GCT tissues (with exception of fresh Non GCT 7B (FW) tissue).....	74
Figure 2-14: Nested PCR of one fixed GCT and two fixed Non GCT samples using P1.	75

Figure 2-15: Gel of nested PCR of the frozen samples: GCT 2C (Solid), GCT 2B (Cystic) and NON-GCT 4 blood (a DNA from WBC); using P2 followed by P1.	75
Figure 2-16: Gel of nested PCR using P3 (after P2) of fixed tissues, alongside primary PCR using P3 of frozen samples (bottom 3 wells, Blood= NON GCT4 is a DNA from WBC), GCT2B&C solid and cystic frozen). Primer dimer bands of <100bp can be seen from fixed tissues, and a product of around 100-150bp can be seen from frozen tissue.....	76
Figure 2-17: Gel of primary PCR using P2 of fresh tissue (LO = Non GCT 7D, LFW = Non GCT 7B, RO = Non GCT 7E and RFW = Non GCT 7C), and blood (Non GCT 7A is a DNA from WBC). LO is left ovary, RO is right ovary, LFW is left follicle wall and RFW is right follicle wall	77
Figure 2-18: Gel of nested PCR using P1 after P2. Blood (Non GCT 7A is a DNA from WBC) and FW tissue (LFW = Non GCT 7B, RFW = Non GCT 7C) underwent purification between PCRs, while ovarian tissue (LO = Non GCT 7D and RO = Non GCT 7E) did not.....	77
Figure 2-19: Gradient PCR on Non GCT 7 (FW) DNA at 4ng/ μ l using both P1 and P2.	79
Figure 2-20: The sequence of forward Non GCT 7 (LFW) spanning mutation site, highlighted in black. A single read can be seen, with defined peaks and no overlapping sequences occurring.....	80
Figure 2-21: The extracted forward nucleotide sequences from the fresh tissue (Non GCT) compared to the Equine <i>FOXL2</i> P1 sequence. The mutation site possible is highlighted in yellow and as expected no mutation was seen in the four different samples. LFW: Left follicle wall, RFW: Right follicle wall, LO: Left ovary, RO: Right ovary.....	80
Figure 2-22: A section of the generated forward sequence from Non GCT 7A (Blood) with at least 3 overlapping sequences observed. One of the potential sequencing matches for the mutation site is highlighted.	81
Figure 2-23: Sequencing results of the P3 blank compared to the <i>FOXL2</i> sequences generated by the use of P3 with area of the mutation highlighted in yellow.	81
Figure 2-24: DNA (DNA and ID number) and PCR products (ID number) bioanalyzer. The x-axis is the size of the fragments and the Y-axis is the amount of sample at any point.	82
Figure 2-25: The first two graphs are the repeated DNA samples and the other 7 are control PCR products.	83
Figure 2-26: The first 6 graphs are the GCT PCR products and the other 5 are the control PCR product.....	83
Figure 3-1: The number of records for female horses by age.....	91
Figure 4-1: Measuring the diameter of the ovary.....	113
Figure 4-2: Blunt dissection of the follicle showing the follicular cavity after fluid aspiration	113
Figure 4-3: Cube section of the stroma close to ovulation fossa.	114
Figure 4-4: Illustration of how views are taken from a selected FW sample. This sample is taken at 200x magnification, and the boxes are representative of the 5 successive views taken for further assessment at 400x magnification	116
Figure 4-5: Rectangle view of a FW image at 200x magnification	117
Figure 4-6: Counting GC and THC at x400 magnification, A: shows Basal GC (no.1 purple colours), B: shows Intermediate GC (no.3 green colours), C: shows Antral GC (no.2 blue colours), D: shows small THC (no.5 yellow colours), E: shows large THC (no.4 pink colours)	118

Figure 4-7: Measuring the thickness of GC (Blue arrows) and THC (Black arrows) at x200 magnification.....	119
Figure 4-8: The peeled FW containing GC and THC layers from an healthy or EA follicle which has a reddish appearance because of its high vascularisation and blood vessels being visible.	121
Figure 4-9: Fatty brownish appearance between the follicular wall following its dissection and the theca externa/stroma.	121
Figure 4-10: Very healthy follicular wall category. A (FWD 10.3x11.8 mm measured in two dimensions), B (FWD 25x18.8 mm), C (FWD 13.8x13.3 mm), D (FWD 19x17 mm): Examples from different follicles.....	122
Figure 4-11: Healthy follicular wall category. A (FWD 29.6x34.9 mm measured in two dimensions), B (FWD 17.7x17.3 mm), C (FWD 25.5x16.6 mm) D (FWD 38.2x31.2 mm): Examples from different follicles	123
Figure 4-12: Early Atretic FW category. A (FWD 18.2 mm) B (FWD 22.1x20.4 mm measured in two dimensions), C (FWD 29.6x29.2 mm) D (FWD 17x18 mm): Examples from different follicles	124
Figure 4-13: Late atretic FW category. A (FWD 6.15 mm), B (FWD 13.6 mm) C (FWD 16.35 mm), D (FWD 40.9 mm): Examples from different follicles	125
Figure 5-1: Inhibin expression exclusively in GC in VH (A1 and A2) and H (B1 and B2) follicles. A1 and B1 are at 200x magnification, and A2 and B2 are at 400x magnification.	149
Figure 5-2: Inhibin expression exclusively in GC of EA follicles (A1 and A2). As the GC layer has disappeared in LA follicles, no positive immunoreactivity is seen (B1 and B2). A1 and B1 are at 200x magnification, and A2 and B2 are at 400x magnification.	150
Figure 5-3: Inhibin expression exclusively in GC of GCT categorised as GCT1 (A1 and A2) and GCT2 (B1 and B2). A1 and B1 are at 200x magnification, and A2 and B2 are at 400x magnification.	151
Figure 5-4: Inhibin expression exclusively in GC of GCT categorised as GCT3 (A1 and A2) and GCT4 (B1 and B2). A1 and B1 are at 200x magnification, and A2 and B2 are at 400x magnification.	152
Figure 5-5: Inhibin expression exclusively in GC showing different stain intensity at 200x magnification (ABCD1) and 400x magnification (ABCD2); A1 & A2 show H follicle walls with high expression and B1 & B2 H follicle walls with medium expression, C1 & C2 show GCT2 with low expression and D1 & D2 show GCT2 with relatively high expression.	153
Figure 5-6: Inhibin expression exclusively in GC showing examples of different stain distribution and %area at 200x magnification (ABC1) and 400x magnification (ABC2); A1&A2 show FW with continuous distribution and almost 100% GC area covered from a H follicle, B1&B2 show FW with individual distribution and almost 70% area covered from a H follicle; C1&C2 show a GCT4 with continuous distribution and almost 90% area covered. There are no images for clustered distribution as inhibin always stained continuously or on occasion individually. No THC or stromal stain was seen.	154
Figure 5-7: Aromatase expression exclusively in GC in VH (A1 and A2) and some cells of H (B1 and B2) FW categories. A1 and B1 are at 200x magnification, and A2 and B2 are at 400x magnification.	155
Figure 5-8: Aromatase expression exclusively in GC in cells of the EA FW category (A1 and A2) but not in LA follicles where the GC compartment is lacking (B1 and B2) . A1 and B1 are at 200x magnification, and A2 and B2 are at 400x magnification.	156

Figure 5-9: No positive aromatase immunoreactivity was seen in GCT categorised as GCT1 (A1 and A2) and GCT2 (B1 and B2). A1 and B1 are at 200x magnification, and A2 and B2 are at 400x magnification.	157
Figure 5-10: No positive aromatase immunoreactivity was seen in GCT categorised as GCT3 (A1 and A2) and GCT4 (B1 and B2). A1 and B1 are at 200x magnification, and A2 and B2 are at 400x magnification.	158
Figure 5-11: Aromatase expression exclusively in GC of FW showing different stain intensities at 200x (ABC1) magnification and 400x (ABC2) magnification; A1 & A2 show VH FW with high expression, B1 & B2 H FW with medium expression and C1 & C2 H FW with low expression.	159
Figure 5-12: Aromatase exclusively in GC of FW showing different stain distribution and %area at 200x (ABC1) magnification and 400x (ABC2) magnification; A1&A2 show FW with continuous distribution and almost 85% GC area covered from a H follicle, B1&B2 show FW with individual distribution and almost 40% area covered from a EA follicle.	160
Figure 5-13: CYP17 expression in THC of VH (A1 and A2) and H (B1 and B2) FW categories. A1 and B1 are at 200x magnification, and A2 and B2 are at 400x magnification.	161
Figure 5-14: CYP17 expression expression in THC of EA (A1 and A2) and LA (B1 and B2) FW categories. A1 and B1 are at 200x magnification, and A2 and B2 are at 400x magnification.....	162
Figure 5-15: CYP17 expression in interstitial stromal tissue of GCT1 (A1 and A2) and GCT2 (B1 and B2) categories. A1 and B1 are at 200x magnification, and A2 and B2 are at 400x magnification.	163
Figure 5-16: CYP17 expression in interstitial stromal stromal tissue of GCT3 (A1 and A2) and GCT4 (B1 and B2) categories. A1 and B1 are at 200x magnification, and A2 and B2 are at 400x magnification.	164
Figure 5-17: CYP17 expression in THC showing different stain intensity at 200x magnification (ABC1) and 400x magnification (ABC2); A1 & A2 show a VH follicle with high expression, B1 & B2 a H follicle with medium expression and C1 & C2 a LA follicle with low expression.	165
Figure 5-18: CYP17 expression in THC and interstitial stromal tissue showing different stain distribution and %area examples with 200x magnification (ABC1) and 400x magnification (ABC2); A1&A2 show frequent clustering and almost 70% GC area covered from a VH FW, B1&B2 show less frequent clustering and almost 25% area covered from GCT1, and C1&C2 shows individual cells and very small clusters and only 10% area covered from a GCT3.....	166
Figure 5-19: CYP17 expression in THC and interstitial stromal tissue showing a severe reduction in staining of LA FW and GCT categories with 200x magnification (ABCD1) and 400x magnification (ABCD2); A1&A2 show a low stain from a LA FW, B1&B2 shows even less staining from another LA FW, C1&C2 shows only two localised small clusters or individual cells from a LA FW, and D1&D2 shows a low number of flat interstitial cells stained from GCT1 (Black arrows).	167
Figure 5-20: CYP17 expression in interstitial stromal tissue cells in GCT some of which appear like individual or clustered Large THC (Black arrows) at 200x magnification (ABCD1) and 400x magnification (ABCD2); A1&A2 show GCT1, B1&B2 GCT2, C1&C2 GCT3 and D1&D2 an example of GCT4.....	168
Figure 5-21: AMHR2 protein expression in GC and THC of VH (A1 and A2) and H FW (B1 and B2). A1 and B1 are at 200x magnification, and A2 and B2 are at 400x magnification.	169

Figure 5-22: AMHR2 protein expression in GC and THC of an EA follicle (A1 and A2), and AMRH2 expression in individual THC of LA FW (B1 and B2). A1 and B1 are at 200x magnification, and A2 and B2 are at 400x magnification.	170
Figure 5-23: AMHR2 protein expression in GC and interstitial/stromal theca like cells in GCT1 (A1 and A2) and GCT2 categories (B1 and B2). A1 and B1 are at 200x magnification, and A2 and B2 are at 400x magnification.	171
Figure 5-24: AMHR2 protein expression in GC and interstitial/stromal theca like cells in GCT3 (A1 and A2) and GCT4 categories (B1 and B2). A1 and B1 are at 200x magnification, and A2 and B2 are at 400x magnification.	172
Figure 5-25: AMHR2 expression in GC and THC of FW showing different stain intensity at 200x magnification (ABC1) and 400x magnification (ABC2); A1 & A2 show H FW with high expression, B1 & B2 VH FW with medium expression and C1 & C2 VH FW with low expression.	173
Figure 5-26: AMHR2 expression in GC and THC layer or interstitial stromal tissue of GCT showing different stain distribution and %area at 200x magnification (ABC1) and 400x magnification (ABC2); A1&A2 show continuous distribution and 100% GC area covered from GCT1, B1&B2 show individual distribution and approximately 25% area covered from a LA FW, and C1&C2 show clusters and approximately 30% of the interstitial area covered from a GCT3.	174
Figure 5-27: Inhibin GC percentage area covered among GCT categories	179
Figure 5-28: Aromatase GC percentage area covered among FW categories. 1 (VH), 2 (H), and 3 (EA).	181
Figure 5-29: Scatter plots for inhibin GC percentage area covered versus FWD and FFE2 concentration in control FW. Health status: VH = very healthy), H = healthy, EA = early atretic. Follicle sizes are represented as LF (Large follicles from 20mm) SF (Small follicles < 20mm). FWD (No.= 30 follicles), FF E2 concentration (No.=25).	197
Figure 5-30: Scatter plots for aromatase GC percentage area covered versus FWD and FFE2 concentration in control FW. Health status: VH = very healthy), H = healthy, EA = early atretic. Follicle sizes are represented as LF (Large follicles from 20mm) SF (Small follicles < 20mm). FWD (No.= 30 follicles), FF E2 concentration (No.=25).	198
Figure 5-31: Scatter plots for CYP17 THC percentage area covered versus FWD and FFE2 concentration in control FW. Health status: VH = very healthy), H = healthy, EA = early atretic. Follicle sizes are represented as LF (Large follicles from 20mm) SF (Small follicles < 20mm). FWD (NO.=40 follicles), and FFE2 concentration (No.=30 follicles).	199
Figure 5-32: Scatter plots for AMHR2 GC percentage area covered versus FWD and FFE2 concentration in control FW. Health status: VH = very healthy), H = healthy, EA = early atretic. Follicle sizes are represented as LF (Large follicles from 20mm) SF (Small follicles < 20mm). FWD (No.= 30 follicles), FF E2 concentration (No.=25).	200
Figure 5-33: Scatter plots for AMHR2 THC percentage area covered versus FWD and FFE2 concentration in control FW. Health status: VH = very healthy), H = healthy, EA = early atretic. Follicle sizes are represented as LF (Large follicles from 20mm) SF (Small follicles < 20mm). FWD (NO.=40 follicles), and FFE2 concentration (No.=30 follicles).	201
Figure 5-34: Nuclear circumferences of GC in VH (A) and H (B) FW health categories at 1000x magnification. Black arrows indicate antral GC, Blue arrows intermediate GC and White arrows basal GC.	202

Figure 5-35: Nuclear circumferences of GC in the EA FW health category at 1000x magnification. Black arrows indicate antral GC, Blue arrows intermediate GC and White arrows basal GC.	203
Figure 5-36: Nuclear circumferences of GC in the GCT1 category showing basal and intermediate GC (A), and antral GC (B) at 1000x magnification. Black arrows indicate antral GC, Blue arrows intermediate GC and White arrows basal GC..	204
Figure 5-37: Nuclear circumference of GC in GCT categories GCT2 (A) and GCT4 (B) at 1000x magnification. In GCT2 Black arrows indicate antral (to the cyst antrum) GC, Blue arrows intermediate GC and White arrows basal GC. In the solid GC nests of GCT4 15 nuclear circumferences were measured across the view with colour of arrows only indicating the top, middle or bottom of the view.	205
Figure 5-38: Antral (lining the cyst antrum) GC in the GCT3 category at 200x magnification (A) and 1000x magnification (B), Black arrows indicate antral GC.	206
Figure 6-1: Equine and Human <i>FOXL2</i> gene sequences	218
Figure 6-2: The nucleotide sequence of Equine <i>FOXL2</i> (EF202823.1), with the position of forward and reverse primers shown and the expected site of the mutation highlighted in yellow and primer in blue.....	221
Figure 6-3: This screenshot shows multiple reads sequenced from one control sample with the mutation from C → T shown in position 117 bp of the reference sequence EF202823.1. Please note that the alternate base is in red when it differs from the reference base.....	225
Figure 6-4: The number and percentages of mutation localisation	226
Figure 6-5: Mutated sequences aligned with original <i>FOXL2</i> gene sequence. The yellow highlighted is the new identified SNP and the green highlighted would be the original human SNP	227
Figure 6-6: Original <i>FOXL2</i> gene sequences and mutated sequences aligned with amino acids code showing no alternative changes within protein.	232
Figure 6-7: Human vs. Equine <i>FOXL2</i> gene with known sites of mutation highlighted.	233
Figure 6-8: <i>FOXL2</i> expression in GC and THC in VH and H FW categories; A1 shows VH with 200x and A2 with 400x magnification; B1 shows H with 200x and B2 with 400x magnification. Black arrow shows positive nuclear stain, Blue arrow shows negative nuclear stain.	234
Figure 6-9: <i>FOXL2</i> expression in GC and THC in EA and LA FW; A1 shows EA with 200X and A2 with 400x magnification. B1 shows LA with 200x and B2 with 400x magnification. Black arrow shows positive nuclear stain, Blue arrow shows negative nuclear stain.	235
Figure 6-10: <i>FOXL2</i> expression in GC and few interstitial cells (Stromal cells) of GCT1 and GCT2 categories; A1 shows GCT1 with 200x and A2 with 400x magnification, B1 shows GCT2 with 200x and B2 with 400x magnification. Black arrow shows positive mesenchymal nuclear stain, Blue arrow shows negative mesenchymal irregular nuclear stain.	236
Figure 6-11: <i>FOXL2</i> expression in GC and few interstitial cells (Stromal cells) of GCT3 and GCT4 categories; A1 shows GCT3 with 200x and A2 with 400x magnification, B1 shows GCT4 with 200x and B2 with 400x magnification. Black arrow shows positive mesenchymal nuclear stain, Blue arrow shows negative mesenchymal irregular nuclear stain.	237
Figure 6-12: <i>FOXL2</i> expression in GC and THC showing different stain intensity with 200x (ABCD1) and 400x magnification (ABCD2); A1 & A2 from VH FW with high expression, B1&B2 with medium expression from EA FW, C1 & C2 with Low	

expression from LA FW, D1&D2 from GCT1 with high expression. Black arrow shows positive mesenchymal irregular nuclear stain, Blue arrow shows negative mesenchymal irregular nuclear stain.	238
Figure 6-13: FOXL2 expression in GC and THC showing different stain distribution and %area with 200x (ABC1) and 400x magnification (ABC2); A1&A2 show continuous distribution and almost 90% GC and THC area covered from VH FW, B1&B2 show individual distribution and almost 50% area covered from LA FW; C1&C2 show continuous distribution and almost 100% area covered from a GCT2. There are no images for clustered distribution as FOXL2 always stained continuously or in a few occasions individually. Black arrow shows positive mesenchymal irregular nuclear stain, Blue arrow shows negative mesenchymal irregular nuclear stain.	239
Figure 6-14: Correlation of FOXL2 GC percentage area covered with FWD (A&B) and FFE2 (C&D) concentration. A & C follicles are characterised by health status categories (VH blue, H red and EA green), B & D follicles are characterised by follicle size categories (Large follicle (LF) blue, small follicle (sF) red).	246
Figure 6-15: Correlation of FOXL2 THC percentage area covered in FWD (A&B) and FFE2 concentration (C&D). A & C follicle are characterised by health status categories (VH blue, H red and EA green, LA purple), B & D follicle are characterised by follicle size categories (Large follicle (LF) blue, small follicle (sF) red).	247
Figure 7-1: Choosing X_Y	261
Figure 7-2: Adding ID to independent column and Text to dependent column .	262
Figure 7-3: Shiffting from Simstat to Wordstat by clicking on content analysis	262
Figure 7-4: Choosing dictionary	263
Figure 7-5: Put tick in the box near categories	263
Figure 7-6: Clicking on Keyword-In-Content.....	264
Figure 7-7: Choosing a category or subcategory from the box near keyword ...	264
Figure 7-8: Case no., Keyword and Text appeared on the screen with highlighted keyword	265
Figure 7-9: Clicking on Frequency showed the frequency and percentages of cases on categories	266
Figure 7-10: Clicking on Leftover words showed words with no alphabetical order	266
Figure 7-11: Tabbing on top of the first word from the list of leftover words arranged them alphabetically	267
Figure 7-12: Choosing the required or useful word and drag it to the dictionary	267
Figure 7-13: Clicking the Red arrow to export data matrix	268
Figure 7-14: A box for exporting data to file appeared.....	268
Figure 7-15: Saving the word frequency list.....	269
Figure 7-16: Choosing the comma separated files (CSV) type to save	269
Figure 7-17: Tabbing filter	270
Figure 7-18: Filtering numbers for particular column.....	270
Figure 7-19: Sorting from largest to smallest or vice versa	271
Figure 7-20: creating pivot table by selecting table/range and choose new wroksheet.....	272
Figure 7-21: Dragging ID number to raw labels	272
Figure 7-22: Choosing the gender for example by clicking all to delete the ticks from all boxes.....	273
Figure 7-23: Choose the required gender e.g female then tab select multiple items then ok	273

Figure 7-24: Filtering ID number from smallest to largest or vice versa by clicking the Row labels274

Figure 7-25: Clicking on find and select to search for particular D number274

Figure 7-26: clicking on Find.....275

Figure 7-27: The box of Find and replace appeared275

Figure 7-28: Write the ID number required on the box of find what then tick the box close to Match entire cell contents.....276

Acknowledgement

There are many people to whom I owe thanks. Firstly, I would like to express my thanks to Professor Tim Parkin for providing invaluable knowledge in epidemiological investigation. Tim helped me in my statistical analysis and writing skills as well as he was always available when needed.

I would also like to thank Dr. Monika Mihm Carmichael for the motivation, and immense reproductive knowledge she provided to me throughout my 4 years. Monika's door was always open to allow a chat about PhD Lab work and answering endless questions about experiments.

The effort for both supervisors by helping me to shape my thesis and kept me going - particularly during this last hard year - something I will not forget. I feel extremely lucky to have been able to work with you both, supportive, knowledgeable supervisors and friends.

Thanks must also go to all staff in old cell sciences lab and veterinary diagnostic lab for their guidance and help in lab and for the staff in Weipers Centre Equine Hospital for their cooperation and facilitation of my work with collection of samples particularly Professor Sandy Love. Also I would like to thank all the veterinary practices in UK, which have agreed to provide data for the project and the others who provided samples.

I would like to thank Omani government (Royal Court Affairs and Ministry of higher Education) that provided me a PhD scholarship via the embassy of the Sultanate of Oman in London.

Finally, I must thank my loving wife Fatima who always supporting and cheering me up to relieve my stress and tension particularly during late nights work and while writing as well as my sons Mohammed, Abdullah, Ahmed and Omar for being quiet and nice during working at home. Thanks must go to my great Mum for all her support and encouragement and pushing me up to reach my goals since I was child until now.

Author's Declaration

I declare that, except where explicit reference is made to the contribution of others, that this thesis is the result of my own work and has not been submitted for any other degree at the University of Glasgow or any other institution.

Abdulqader AL Ibrahim

Signature

Abbreviations

KDD = Knowledge discovery in databases

NLP = Natural language processing

GPASS = General practice administration system for Scotland

EMR = Electronic Medical Record

GCT = Granulosa cell tumour

GTCT = Granulosa theca cell tumour

E2 = Oestradiol

AMH = Anti Müllerian hormone

AMHR2 = Anti Müllerian hormone Receptor 2

H&E = Haematoxylin and eosin

FSH = Follicle stimulating hormone

LH = luteinizing hormone

IGF = Insulin-like growth factor

CL = Corpus luteum

GnRH = Gonadotropin releasing hormone

hCG = Human chorionic gonadotropin

F1 = Largest follicle

F2 = Second largest follicle

FF = Follicular fluid

PBS = Phosphate buffer saline

NSB = Non specific binding

FW = Follicular wall

GC = Granulosa cells

THC = Theca cells

IHC = Immunohistochemistry

PCR = Polymerase chain reaction

P1 = Primer 1

P2 = Primer 2

P3 = Primer 3

LFW = Large follicle wall

VH = Very healthy

H = Healthy

EA = Early atretic

LA = Late atretic

FF = Follicular fluid

CVs = Coefficient of variations

FFE2= Follicular fluid oestradiol

FWD = Follicular wall diameter

LF = Large follicle

SF = Small follicle

GCT1 = Granulosa cell tumour 1

GCT2 = Granulosa cell tumour 2

GCT3 = Granulosa cell tumour 3

GCT4 = Granulosa cell tumour 4

QCs = Quality controls

BPES = Blepharophimosis, ptosis, and epicanthus inversus syndrome

Chapter 1 Literature Review

1.1 Introduction

Most horse breeders are rightly concerned about their mare's fertility in terms of producing foals every season. Some producers therefore categorise infertility in a mare by whether or not she cycles normally and by whether or not the mare conceives and holds a pregnancy. The mare reproductive function is seasonally polyestrous which implies that the reproductive season (oestrus) and non-reproductive season (anoestrus), followed by transitional period during the breeding season are controlled by daylight (Morel et al., 2010). In other words the mare does not show heat during winter but starts to cycle just before spring and reaches a peak in the spring and early summer (March, April and May). The mare's ovarian cyclicity is seasonal and during the short days of winter they come into a period of anoestrus where very small follicles exist in the ovaries (Watson and Ai-zi'abi, 2002). During the transitional period, which occurs between normal ovarian cyclicity and deep winter anoestrus, in many mares large follicles develop and then regress. The granulosa cells from preovulatory follicles produce more oestrogen than those originating from anovulatory transitional follicles because the latter are thought to be steroidogenically inadequate (Watson and Ai-zi'abi, 2002).

In all characterised species (Young and McNeilly, 2010) follicles have been classified into different types as follows:

Primordial follicles - prior to follicular activation and development and when only one flattened granulosa cell layer incubates the oocyte;

Primary follicles - when the granulosa cells have only one cuboidal layer;

Secondary follicles - when the number of granulosa cell layers has increased to two or four;

Large pre-antral follicles - when the follicle contains four to six granulosa cell layers;

Antral follicles - if the number of granulosa cell layers has reached more than five. So antrum develops in six granulosa cell layers.

Theca cells start to form after formation of the secondary follicle, creating a layer all over the granulosa cell structure.

Equine follicles have been categorised according to developmental stage and to normality and abnormality (Haag et al., 2013). Normal if the oocyte is intact and it is covered by one or more organised layers of granulosa cells whereas, it is 'abnormal' if the latter descriptive features are deteriorated and cells are detached from the basement membrane. According to the stage of development classification, the oocyte that is surrounded by one layer of cuboidal granulosa cells is defined as a primary follicle, while the primordial follicle is characterised by an oocyte surrounded by one layer of flattened granulosa cells.

Atretic follicles have been classified into three stages according to (Driancourt et al., 1982, Kenney et al., 1979) depending on the appearance of pyknotic nuclei and granulosa cells: Stage I - more than five pyknotic areas detected; stage II - wide distribution of pyknosis and floating of granulosa cells to the antrum; and stage III - a lack of granulosa cells apart from in the oocyte area. Moreover, healthy follicles were identified by counting the number of granulosa cells per follicle or by measuring the density of the cells in the large follicles using a circular reticule.

Common abnormal ovarian functional problems that impact a mares' fertility are haemorrhagic follicles, ovulation failure (anovulatory follicles or cystic follicles), persistent corpus luteum, premature luteolysis (endometritis), failure of follicular development and ovarian tumours (Troedsson et al., 2003). A granulosa cell tumour (GCT) is considered as one of the major causes of horse infertility, representing 85% of ovarian tumours (McCue et al., 2006). GCT are most frequently successfully treated by way of surgical removal or ovariectomy. Frequently, following ovariectomy (Crabtree et al., 2013), mares have a good chance of returning to a healthy and normal life with no complications due to the fact that the majority of GCT are benign (van der Kolk et al., 1998).

Many types of ovarian tumours (granulosa-theca cell tumour, teratoma, cystadenoma and dysgerminoma) detrimentally affect a mares' fertility, the impact varying from mild to severe. Tumour is defined as an uncontrollable growth of tissue cells and can either be malignant or benign (McCue et al., 2006, Crabtree, 2013). GCT, although most frequently benign, might reduce pregnancy rates and can cause severe behavioural changes in the mare (Crabtree et al., 2013). They can also inhibit a mare's reproductive career to some extent by damaging the internal organs (McCue et al., 2006)). This thesis will focus on various aspects of GCT, describing the prevalence of GCT (and ovarian pathology); histological classification of the normal follicular wall using haematoxylin and Eosin (H&E) based on health status by measuring the thickness of the granulosa and theca cells and their counts; comparing the control follicle wall and GCT immunohistochemically and nuclear circumferences of their granulosa cells; and finally detecting the occurrence of *FOXL2* gene mutation in equine GCT.

1.2 Epidemiology

1.2.1 Background

1.2.1.1 Text mining in knowledge discovery in databases

Text mining is defined as “deriving structured information from text, usually to fill some specific information need” (Garten et al., 2010). Text mining enables the use of data from the whole body of written records, and permits data from multiple sources to be joined and presented to clients. Some authors characterize content mining as the detection, by computer, of new obscure information, by automatically removing data from diverse written text (Garten et al., 2010). Others assert that it is characterized as mining or extracting required data from the content, as a way of providing valuable information about that text-based content (Garten et al., 2010). Moreover, the authors separate text mining into two principle steps: Identification of archives that may contain the required data followed by the extraction of the data itself. The identification process or computerized reading can be divided into four general subtasks: text arrangement, named substance labelling, reality extraction, and accumulation wide analysis (de Bruijn and Martin, 2002).

1.2.1.2 Electronic patient records in medical practice, companion animal and equine veterinary practice

There has been a dramatic increase in the use of computer databases in general practice for public health auditing and commissioning (Pringle et al., 1995). Although applying computer databases in general practice has been widely noticeable, some problems still exist such as patient data transmission and the use of or agreement regarding the common coding structure(s) for diseases.

Although the majority of veterinary practices in UK use modern electronic practice management systems (PMS), its utilisation remains a challenge for epidemiologists. This is largely because there is no central hub in veterinary practices as in the NHS, from which validated data can be collected.

In the veterinary field, the VetCompass™ project delivers significant management assistance to particular practices such as facilitating clinical audit and accelerated reviews of patient history (O'Neill, 2012). Currently VetCompass™ includes nearly 10 million animals from 1,100 UK participating veterinary practices (over 20% of all UK practices) and now contains 55 million clinical notes and 181 million treatment records. Mattin et al. (2014) noted that there were a few limitations to their present studies, for example the information analysed were not recorded for research purposes, and therefore it will contain irregularities and mistakes. Nevertheless, the authors contend that continued data gathering within the VetCompass™ project will enable larger analyses of affected animals in the future to produce more useful epidemiological analyses which, in time, will include temporal and spatial disease pattern recognition.

1.2.1.3 Free text mining in the veterinary literature

The number of projects that have been performed in recent years to gather information from veterinary clinical records or large Electronic Medical Record (EMR) datasets, both retrospectively and also prospectively, has grown (Jones-Diette et al., 2014, Lam et al., 2007, Mattin et al., 2014, O'Neill, 2012, O'Neill et al., 2012, O'Neill et al., 2013, Oswald et al., 2010, Radford et al., 2011). In addition to some regulated databases, various bespoke and specially designed recording systems have been produced in therapeutic and veterinary practice in

the previous 20 years (Lam et al., 2007). Moreover, they conducted an analysis of a large electronic database in use at the Hong Kong Jockey Club since 1970. These data included health records of more than 6000 Thoroughbred racehorses and their racing performance. The authors condensed a large number of text words that were extracted from the data based on reasons for retirement from racing for the racing seasons 1992/93 to 2003/04 using Wordstat and Simstat content analysis software. They found that more than 95% of 3,727 horse records were extracted from the database and 21 defined dictionaries of retirement categories were established in Wordstat. All these categories were filtered using Simstat and this complete process was done in approximately 2-weeks (Lam et al., 2007).

This widespread use of EMR enables epidemiological research by facilitating access to large quantities of clinical records without the preparatory work required to translate conventional paper records into electronic formats. Content mining is a part of Natural Language Processing (NLP) and aims to discover or create a structure of free text to make it useful for further automated analytic procedures (Anholt et al., 2014a). These authors reported that text mining works by two fundamental systems: The first, untrained or linguistic approach, distinguishes client-characterized terms included within the free text and gives an account of their position within dataset. The second, trained or rule based approach, applies statistical algorithms to separate predetermined sorts of data. Both these systems aim to provide structure to an essentially unstructured group of sentences. This is accomplished by the classification of sentences by the words or phrases that comprise those sentences, as indicated by pre-defined categories. The classification of these free content EMR also permits the assessments of the existence and importance of connections between those pre-defined classes. The conduct of content mining in clinical studies are different and have different aims and objectives including, retrospective investigation of data to illustrate disease prevalence (Chapman et al., 2005, Chapman et al., 2004), identification of symptoms and side effects (Chapman et al., 2004), treatment outcomes (Penz et al., 2007) and prognostication and survival examination (Penz et al., 2007, Bradley et al., 2005).

1.3 Anatomical aspects in the mare

1.3.1 Gross anatomy and topography of the ovary

The anatomy of the mare's ovary is inverted which is different than in other species. The outer layer of the ovary is what would otherwise be the medulla, which contains blood vessels and nerves, and the inner layer, which would normally be the cortex that contains the follicles. The ovulation fossa is on the concave surface where the oocyte is expelled (Carnevale et al., 1988). The cranial aspect of this kidney bean shaped ovary is smooth and attached to the mesovarium of the broad ligament that suspends the ovary and supplies the blood through the ovarian branch of the ovarian artery (Davis Morel, 2015). As the cortex consists of follicles and oocytes, the follicle needs to migrate through ovarian stroma to the ovulation fossa in order to ovulate. The thick protective layer (tunica albuginea) that covers the whole ovary, is absent at this fossa (Davis Morel, 2015).

The ovulation fossa is attached to the funnel shaped infundibulum of the oviduct. This fossa is coated with germinal epithelium whereas the bulk of the ovary is coated with visceral peritoneum or serosa (McCue, 1998, Watson, 1994, Gastal et al., 2007). The size and weight of the mare's ovary generally ranges from 35-120 cm³ in volume and 40-80 g, respectively (Aurich, 2011). The size of the ovaries depends on the season, varying from 2-4cm during anoestrus to 6-8cm during sexual activity (Davis Morel, 2015). Mare reproductive organs are similar to other mammals' organs in term of their position in the pelvis, their anatomy and physiology. The anatomical location, as presented in Figure 1-1, facilitates rectal palpation of the mare as presented in Figure 1-2 and enables the examination of the mare's reproductive stages ultrasonographically.

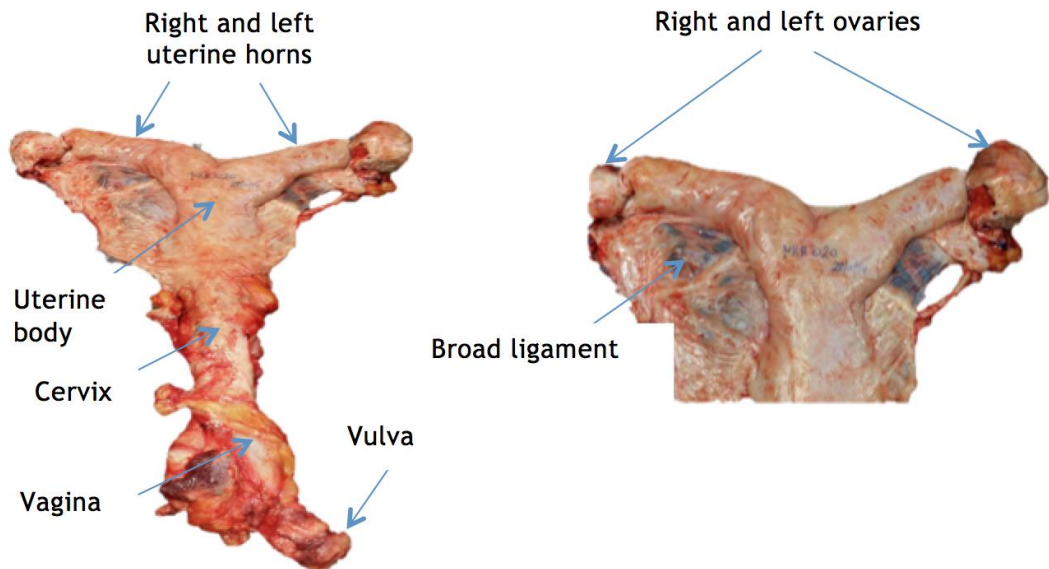


Figure 1-1: Mare reproductive tract. (Ab. AL Ibrahim, Thesis Image)

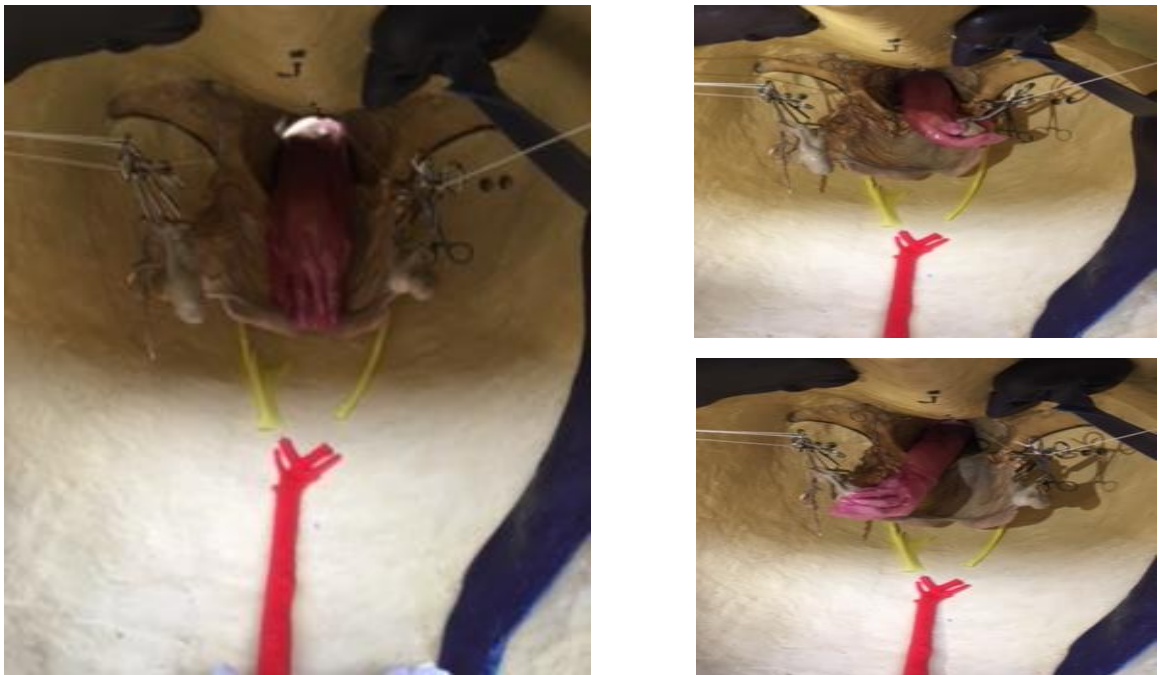


Figure 1-2: Demonstration of mare rectal palpation on a dummy mare illustrating the topography of the mare's tract. The images were acquired by Ab. AL Ibrahim.

The follicle develops a double ring of blood vessels. The outer ring is composed of venules and arterioles in the theca externa and the inner ring is composed of a prominent capillary plexus in the theca interna (Ginther et al., 2006). In the histological study conducted by (Ginther et al., 2006), it was identified that both vascular capillaries and terminal lymphatics contain the fluid between cells in the follicle wall and appear as a partially anechoic band. A rich capillary plexus

develops in the theca cells encapsulating the avascular granulosa cells during follicle growth (Watson and Ai-zi'abi, 2002).

1.3.2 Histology of the ovary

Stroma constitutes the body of the ovary, and is composed of spindle shaped cells and fine collagen fibres. Stromal cells simulate fibroblasts, however, some contain lipid droplets. The cortex is composed of follicles, which contain oocytes, in various stages of development, atretic follicles and corpora lutea. The tunica albuginea is the superficial surface of the cortex and is more fibrotic than the deep surface. The germinal epithelium covers the surface of the ovary but only where the cortex is. The medulla is highly vascular and contains hilus cells that are analogous to Leydig cells of the testes (Watson and Ai-zi'abi, 2002).

In the antral follicle the vascular theca interna and the avascular granulosa are divided by a basement membrane (Ginther et al., 2006). The granulosa cells, which attach to the basement membrane, constitute the upper layers of anovulatory and preovulatory follicles. Both transitional and preovulatory follicles can have mitotic nuclei (Watson and Ai-zi'abi, 2002). The theca interna in preovulatory follicles consists of a thick layer of plump polyhedral cells with large cytoplasm and a pale nucleus.

Developmental stages of the follicle are: germ cell, primordial, primary, secondary, antral, preovulatory, ovulation and corpus luteum (CL). It has been noted that the approximate numbers of primordial follicles and growing follicles in adult mares' ovaries is 40,000 and 100, respectively (Raz and Aharonson-Raz, 2012, Donadeu and Pedersen, 2008, Haag et al., 2013, Pedersen et al., 2003). Antral follicle formation in horses and ponies starts when the follicular diameter reaches 0.2 to 0.4 mm. Follicle regression or atresia is uncommon until their diameter reaches 1mm. There are three classified stages of the atresia based on the counting of granulosa cells pyknosis on the section: Stage I (early atresia), when five pyknotic nuclei were counted, Stage II (advanced atresia), when pyknosis is noticed to be significantly distributed and huge numbers of granulosa cell are detected in the antrum, and Stage III (late atresia), when the

appearance of the granulosa cell layer is significantly reduced except around the oocyte (Driancourt et al., 1982).

1.4 Physiology

1.4.1 Oestrous cycle and seasonality

The oestrous cycle of the mare during the normal breeding season in the Northern Hemisphere begins in late April or early May and continues through to August and September (Satué and Gardón, 2013). The duration of the oestrous cycle is 21 days \pm 3 days and it consists of two periods, oestrous (heat) and dioestrous (between heat) as presented in Figure 1-3. Oestrus usually lasts six days but it can be from 4-10 days especially in ponies (Aurich, 2011). Dioestrus lasts 15 days but it might be from 12-18 days. During oestrus ovulation could occur at any time but normally 24-48 hours before the end of the period. First oestrous cycle of the mare is usually prolonged and irregular, and might last from 20-30 days or more. The mare cycles normally under the effect of increasing daylight in spring. According to (Heidler et al., 2004), the length of oestrous cycle is influenced by reproductive stage, for instance in a lactating mare the length is 21.2 \pm 1.8 days but is 22.8 \pm 1.4 days in non-lactating mares. In young and middle aged mares the interovulatory interval is shorter than in old mares due to the delay of the growth rate of the dominant follicle in the old mares (Ginther et al., 2008). Transitional stages from winter anoestrus to the ovulatory season and once again into the anovulatory season are characterised by irregular oestrous behaviour that may last from a few days to weeks (Aurich, 2011).

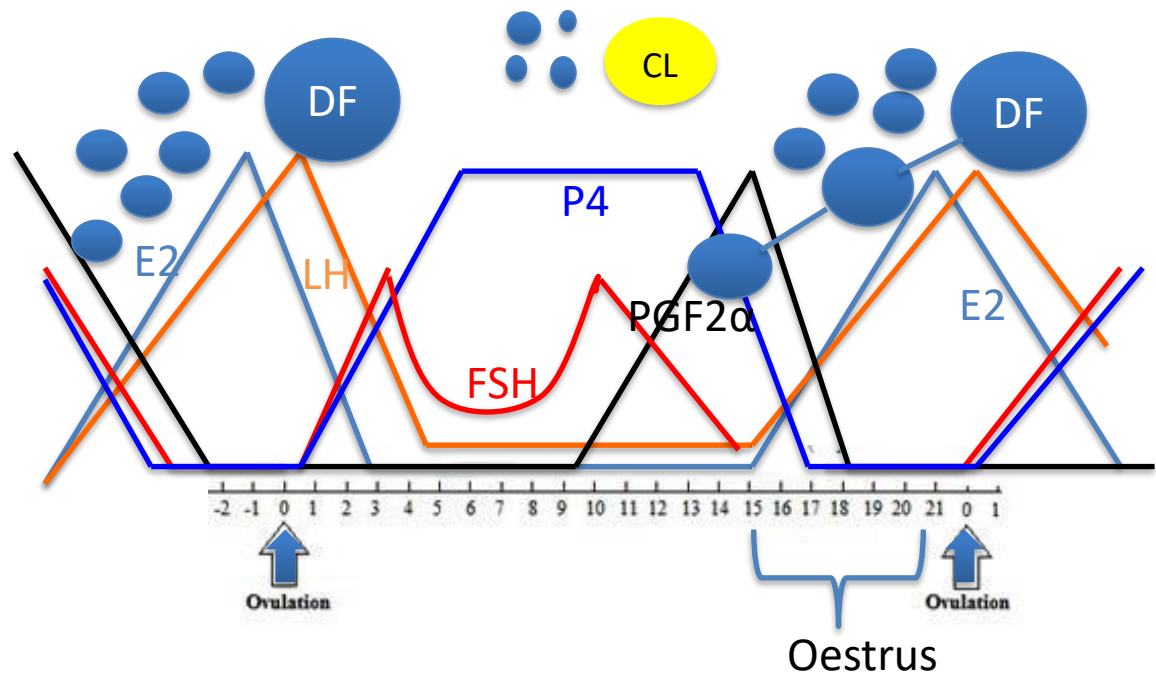


Figure 1-3: Mare oestrous cycle. DF (dominant follicle), CL (corpus luteum)

1.5 Ovarian pathology in the mare

1.5.1 Differential diagnosis of ovarian enlargements

1.5.1.1 Anovulatory follicle (follicular cyst)

The anovulatory follicle is also often referred to as a haemorrhagic anovulatory follicle or follicular cyst as presented in Figure 1-4 and it occurs due to ovulation failure from a non-ruptured dominant follicle (Cuervo-Arango and Newcombe, 2010). In a study conducted by McCue and Squires (2002), the diameter of an anovulatory follicle was approximately 50.9 ± 11.2 mm and the occurrence of persistent anovulatory follicles increased with age of the mare. The main cause of this condition is unclear, however it might be due to low follicular oestrogen (Pierson, 1993), low FSH and LH levels (Mckinnon, 1997), or follicular internal haemorrhage inside the lumen of the follicle (McCue and Squires, 2002). In addition, the majority of mares that had developed an anovulatory follicle have elevated progesterone concentrations due to luteinisation. Anovulatory follicles might persist for many months and their lumen is filled with echogenic particles on ultrasound investigation.



Figure 1-4: Follicular cavity filled with blood: Anovulatory haemorrhagic follicle, 49.1x38.2 mm. (Ab. AL Ibrahim, Thesis Image).

1.5.1.2 Haematomas

Haematomas are always non pathological, not affecting the mare breeding capability and do not have external clinical signs (Beachler et al., 2016). They occur after ovulation due to an accumulation of blood in the follicular cavity and can be palpated or examined by ultrasound. The size of haematomas can become a quite large and might reach 10 cm in diameter. This enlargement might result in confusion with the diagnosis of a tumour (Curtin, 2003). After the absorption of the blood from this mass, a firm and calcified area remains on ovary. Haematomas can be differentiated from other neoplastic masses such as granulosa cell tumour (GCT) by monitoring inhibin secretion (Curtin, 2003). Moreover, the low testosterone level is also an indication that the mass is not a GCT. Ultrasound is considered to be a useful tool for differentiation from GTC in that haematomas often also have a honeycomb structure due to clustered cysts, but they may reduce in size when rechecked a few months later, due to regression and reabsorption of fluid (Curtin, 2003).

1.5.1.3 Teratoma

Teratoma is a type of ovarian tumour in mares, which arises from germ cells and is also named “dermoid cyst” if they arise from ectoderm, skin and hair (Vanhaesebrouck et al., 2010). They are also benign and unilateral as GCT,

however, the unaffected ovary remains active and the mare cycle normally and can carry an embryo despite the presence of a tumour (Catone et al., 2004, McCue and McKinnon, 2011, da Encarnacao Fiala et al., 2011). The occurrence of this tumour is extremely rare (Lefebvre et al., 2005). The problem of this tumour is that it causes pain and discomfort to the mare and can result in colic-like symptoms, which can mislead the diagnosis. The discomfort and pain is most likely due to the bigger size of teratoma tumour which includes many different tissue types such as hair, teeth, bone, cartilage, nerve and adipose (fat) tissue (Catone et al., 2004). Although teratomas are benign in nature, Vancamp et al. (1989) stated that teratomas might lead to adenocarcinoma.

1.5.1.4 Dysgerminoma

This tumour also comes from germ cells as with teratomas. However, it originates from only one germ cell layer and is very rare and malignant (Gehlen et al., 2006, McLennan and Kelly, 1977, Chandra et al., 1998) as it can spread quickly from the ovary to the rest of the abdominal cavity and even to the chest cavity (Harland et al., 2009). Fortunately, dysgerminoma tumour are infrequently found in horses (Harland et al., 2009).

1.5.1.5 Cystadenoma

Cystadenomas originate from the ovarian capsule or surface epithelium that covers the ovary and produce multiple cyst-like structures inside the ovary (McCue and McKinnon, 2011). Most of the normal ovarian tissue and thus the ovary itself can be destroyed by a cystadenoma because it is considered locally invasive (Hinrichs et al., 1989). However, this kind of tumour is benign and will not spread to the horse's body. Affected mares usually have normal oestrous cycles due to the functioning of the unaffected ovary (McCue et al., 2006, Son et al., 2005). Although many cases of mares' cystadenoma tumour are expected to have high levels of testosterone, they generally do not result in any behavioural changes (Hinrichs et al., 1989).

1.6 Granulosa Cell tumour (GCT)

The most common equine ovarian tumour is GCT (Watson, 1999) and its occurrence affects the mares' behaviour, disrupts hormone levels and causes

illness. According to Watson (1994) metastasis of this tumour is rare, although it has been reported (van der Kolk et al., 1998).

1.6.1 GCT size & weight

The diameter of a GCT ovary can range from 10 to 20 cm with yellowish cystic stroma (Watson, 1994, McCue et al., 2006). The weight of a GCT reported by vanderZaag et al. (1996) was 31.5 kg and the largest reported weight was 59.1 kg (McCue et al., 2006). Its gross appearance is firm, oval with a smooth surface and subcapsular cystic processes. The size of one of the GCT cases used as part of this study was 30 cm in diameter with a weight of 15 kg, as presented in Figure 1-5.

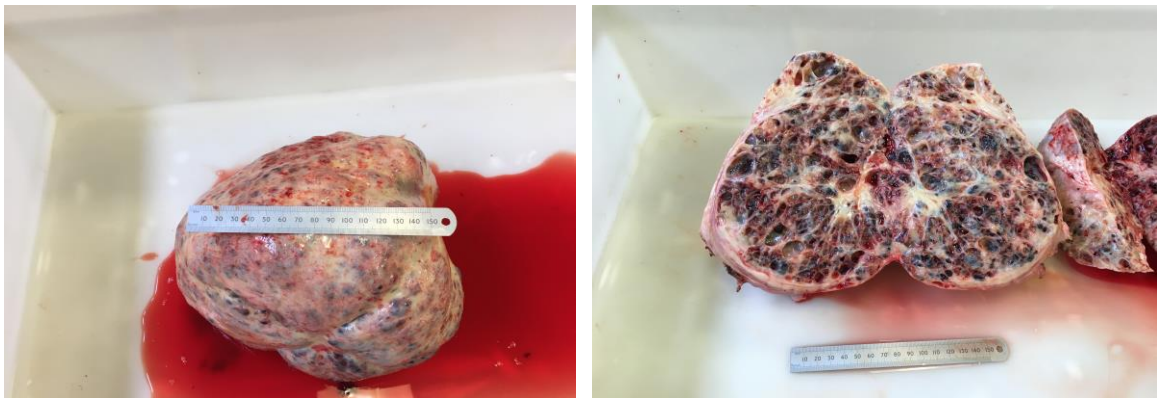


Figure 1-5: Gross appearance of the complete and hemisected GCT tumour. (Ab. AL Ibrahim, Thesis image).

1.6.1.1 Clinical signs

As a consequence of the tumour growth, it can have a negative impact on a mare's gait resulting in vague lameness. The reason for this is that the weight of the ovary pulls on the ovarian broad ligament suspending the ovary within the abdominal cavity (Crabtree, 2013). In addition, the hormonal levels of an affected mare might change to cause behaviour changes, in particular aggressiveness. Abnormal behaviours include stallion-like aggressiveness, mounting other horses and lunging at other mares. There may be an absence of normal oestrous cycles, with intermittent or continuous (Assis Neto et al., 2010).

1.7 Functional and hormonal changes within the GCT and ovary

A GCT secretes steroid hormones impeding the normal reproductive cycle. This tumour enhances several different hormones in the mare such as oestrogens, progesterone, and testosterone, which lead to many different behavioural abnormalities. Recently inhibin and anti Müllerian hormones (AMH) have been reported (Ball et al., 2013) and approximately 90% of mares with GCT have high levels of inhibin (Bailey et al., 2002). Previously (Bailey et al., 2000) an inhibin test was considered the gold standard in confirming a diagnosis of a GCT but nowadays high AMH concentrations are considered the better test. Testosterone produced by theca cells of the tumour also used to diagnosis granulosa theca cell tumour (GTCT), but it should be noted that testosterone can be elevated for other reasons such as during the development of fetal gonads which can cross the placenta into the mare's blood stream.

1.7.1 Oestradiol (E2)

Oestradiol is believed to regulate oestrous behaviour (Pycock et al., 1995). During the oestrous cycle, the luteal phase length is approximately 16 days and the follicular phase length is seven days. A few days before the end of the luteal phase, there is a wave of follicle growth. The largest follicle (22-24 mm) is selected near the end of the luteal phase, with deviation occurring when one follicle continues to grow with regression of the remaining follicles at the end of a common growth phase (Ginther et al, 2007). One to two days before this deviation the concentration of E2 and LH starts to increase.

Goudet et al. (1999) identified that the E2 concentration increases with follicular diameter expansion. The level of E2 was measured by Knudsen and Velle (1961) at anoestrus, oestrus and dioestrus and it was recorded as (7.5 µg, 37.5 µg and 6.0 µg/100ml, respectively). The normal E2 concentration in serum of a non-pregnant mare was from 20-45 pg/ml (Ball et al., 2014). Yoshida et al. (2000) reported that the E2 of normal follicular fluid was 200-7000 pg/ml. During follicular development at early and late dioestrus or in the late oestrus but before ovulation the E2 concentration of follicular fluid gradually increases. Furthermore, the follicular wall, which consists of granulosa cells and theca

interna, produces more E2 in early and late oestrus compared to late dioestrus (Sirois et al., 1990). Almadhidi et al. (1995) noted that the level of E2 concentration is low in small follicles and that it gradually increases in large follicles.

1.7.2 Aromatase

Oestrogen is derived from androgen under the impact of aromatase (Almadhidi et al., 1995, Belin et al., 2000, Almeida et al., 2011b). During development of the dominant follicle the level of E2 is elevated and this is under the influence of a steroidogenic enzyme such as aromatase (Belin et al., 2000). Its expression is reduced in subordinate follicles with reduced concentration of E2 level. This reduction of steroidogenic enzymes might explain the onset of atresia.

The expression of aromatase has been detected in the mare granulosa cells as well as in granulosa cells of many mammalian species (Goudet et al., 1999, Nagamine et al., 1998). However, the expression of aromatase using immunohistochemistry was not detected in a healthy small follicle investigated by (Nagamine et al., 1998). It has been confirmed that aromatase activity in mare granulosa cells is elevated, whereas it was also suggested that aromatase activity in the theca interna was low (Almadhidi et al., 1995).

1.7.3 Inhibin

Inhibin is a disulphide-linked heterodimeric glycoprotein produced by granulosa cells (Piquette et al., 1990). It has a negative effect on FSH which leads to a decrease in its secretion, and thus inactivity of the contralateral ovary (Ellenberger et al., 2007). Inhibin was recorded as a GCT tumour marker in human medicine in 1989 (Koebel et al., 2009) whereas, in mares it was reported in 1993 and 2002 by (McCue, 1993, Watson et al., 2002a). The inhibin dimer consists of an alpha subunit (α) and 2-beta subunits (BA and BB), which create, equally active dimers: inhibin A (α BA) and inhibin B (α BB) (Bailey et al., 2002, Piquette et al., 1990). According to the experiment conducted by Ellenberger et al. (2007) inhibin is situated intra-cytoplasmically and demonstrated in granulosa cells. Davis et al. (2005) stated that a positive immunoreactivity for inhibin α -subunit was expressed in the cytoplasm of neoplastic GC in GCT tumour.

Using radioimmunoassay (RIA) for the determination of α -inhibin was considered to be a more accurate indicator of GCT occurrence than a specific measurement of α BA-inhibin using immunoradiometric assay (IRMA) (Bailey et al., 2002). According to a study conducted by Ellenberger et al. (2007) the concentration of inhibin B was higher in mares before ovariectomy than in ovariectomised mares (1817 pg/ml and 15 pg/ml, respectively) and was more or less similar to the concentration of mares in oestrus. Furthermore, it has been stated that approximately 90% using RIA of mares diagnosed with GCT have high inhibin level.

1.7.4 CYP17

CYP17 is detected in ovaries, testis and the adrenal cortex of some mammals (Almeida et al., 2011b). In addition, it has been stated that CYP17 acts as an enzyme for oestrogen synthesis. Furthermore, CYP17 expression was localized in Leydig like cells of newborn pigs and male wild mature pigs. The immunolabelling of CYP17 in the preovulatory follicle is localised in the theca interna layer (Albrecht and Daels, 1997).

1.7.5 Anti-Müllerian hormone (AMH)

Anti- Müllerian hormone (AMH) is a 140 KD dimeric glycoprotein and a member of the transforming growth factor superfamily of growth and differentiation factors (Almeida et al., 2011a). It is secreted by the Sertoli cells of the testis from fetal sexual differentiation to puberty, and is responsible for regression of the Müllerian ducts during male sexual differentiation (Ball et al., 2008b). According to immunohistochemistry the granulosa cells of the small growing and antral follicles produce AMH normally and it can be shown in normal mare ovaries as well as in GCTs (Ball et al., 2013). However, its expression is reduced in large antral follicles based on the experiment done by Ball et al., (2008).

AMH has been considered a useful biomarker for GCT in mares. AMH concentration is increased (≥ 4.0 ng/ml) in mares with GCT and reduced to normal level post-ovariectomy. For example, the AMH concentration in a 13 year old Arabian mare suffering from GCT was recorded as 21.6 ng/ml compared with normal cyclic mares of 0.36 ± 0.02 ng/ml (Gharagozlou et al., 2013). Following

ovariectomy the AMH concentration in this mare reduced to 0.1 ng/ml (Gharagozlou et al., 2014).

1.8 Histopathology

Hultgren et al. (1987) classified histologically the juvenile GCT into two types with either a macrofollicular or diffuse pattern. The macrofollicular type has smaller granulosa cell lined follicles compared to the adult GCT, whereas the diffuse type has a distribution of granulosa and theca cells with a possibility of lipid accumulation. In addition, this follicular tumour pattern is classified by multiple large and small follicles as well as cysts separated by thick fibromyxomatous septa. Those structures contain amorphous, basophilic material, which is lined by follicular epithelium, appeared as a single layer of cuboidal cells. Some of these structures have solid nests and trabeculae, and others have cells with round or oval hyperchromatic nuclei covered by different shaped and sized eosinophilic cytoplasm (Hultgren et al., 1987). On the other hand, the diffuse type includes large cells with prominent plasma membranes and large amount of small or rough vacuolated cytoplasm. The stroma that supports the neoplastic granulosa cells also comprises large, oval or elongated theca cells which have hyperchromatic nuclei and a large amount of clear cytoplasm (Hultgren et al., 1987, Davis et al., 2005). Large Leydig like cell and polyhedral cells have also been detected between theca cells and beneath granulosa cells (Crabtree, 2011, Crabtree, 2013, Bailey et al., 2002, Bustamante, 1998). These cells had a finely granular eosinophilic cytoplasm. Clusters of cells were observed in tubular form, and cells had round nuclei and finely dotted dense chromatin and mild anisokaryosis (Crabtree, 2011, Chopin et al., 2002). Ball et al. (2008a) pointed out that the GCT have different shapes: tubular, trabecular and cystic. The tubular granulosa cells had a sertoli cell like structure and there were polyhedral Leydig like cells in the stroma and no antral follicle were detected. Connective tissue cells surrounded cystic structures, which were localized all over the fibrous tissue (Charman and McKinnon, 2007). Other stated that the GCT consists of cords and trabeculae of neoplastic GC supported by a moderate fibrovascular stroma ((Davis et al., 2005).

Histologically, and based on our findings, the cysts are surrounded by one or more layers of cubic or cylindrical cells, arranged in a palisade manner with

small round nuclei as presented in Figure 1-6, Figure 1-7 and Figure 1-8. Some cells are found as solid clusters as presented in Figure 1-9.

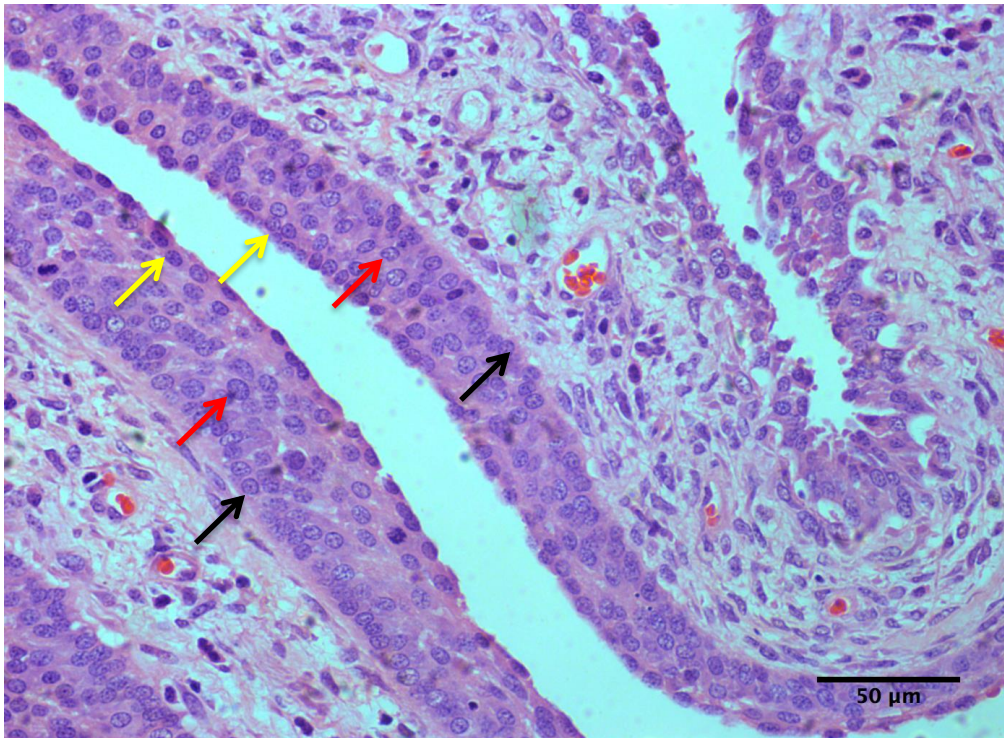


Figure 1-6: Classified GCT1; cystic structure looks like a healthy follicular wall. GCT1 has all antral (Yellow arrow), intermediate (Red arrow) and basal (Black arrow) granulosa cells (GCs). 400x magnification. (Ab. AL Ibrahim, Thesis image)

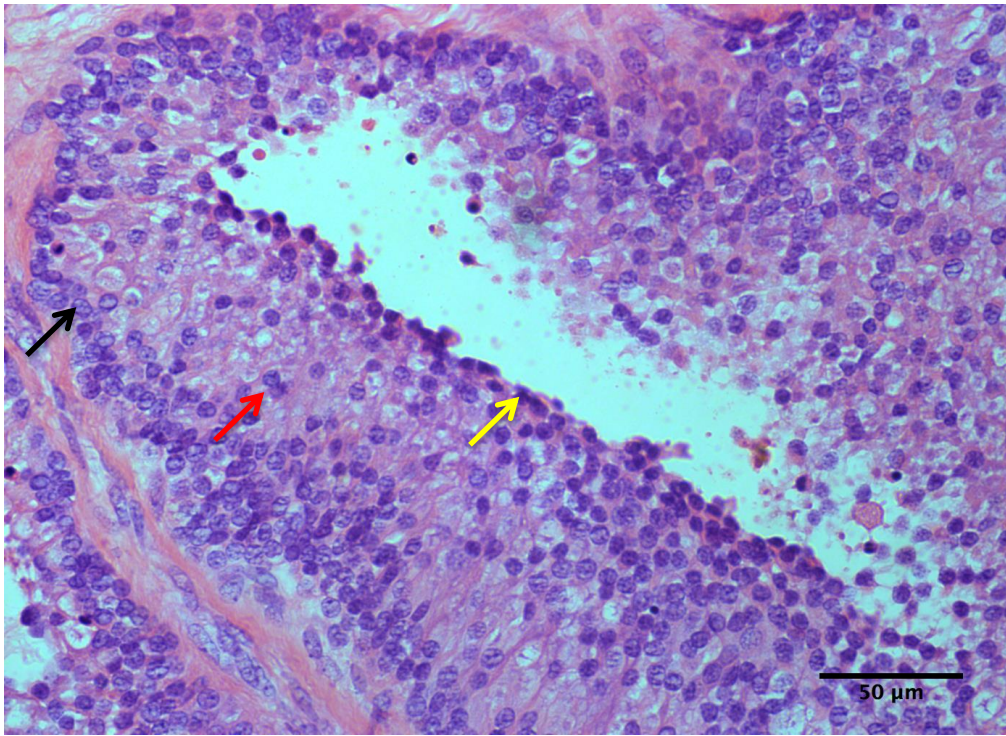


Figure 1-7: Classified GCT2: cystic like structure but appear as a closed circle cyst. It has all antral (Yellow arrow), intermediate (Red arrow) and basal (Black arrow) GCs. 400x magnification (Ab. AL Ibrahim, Thesis image).

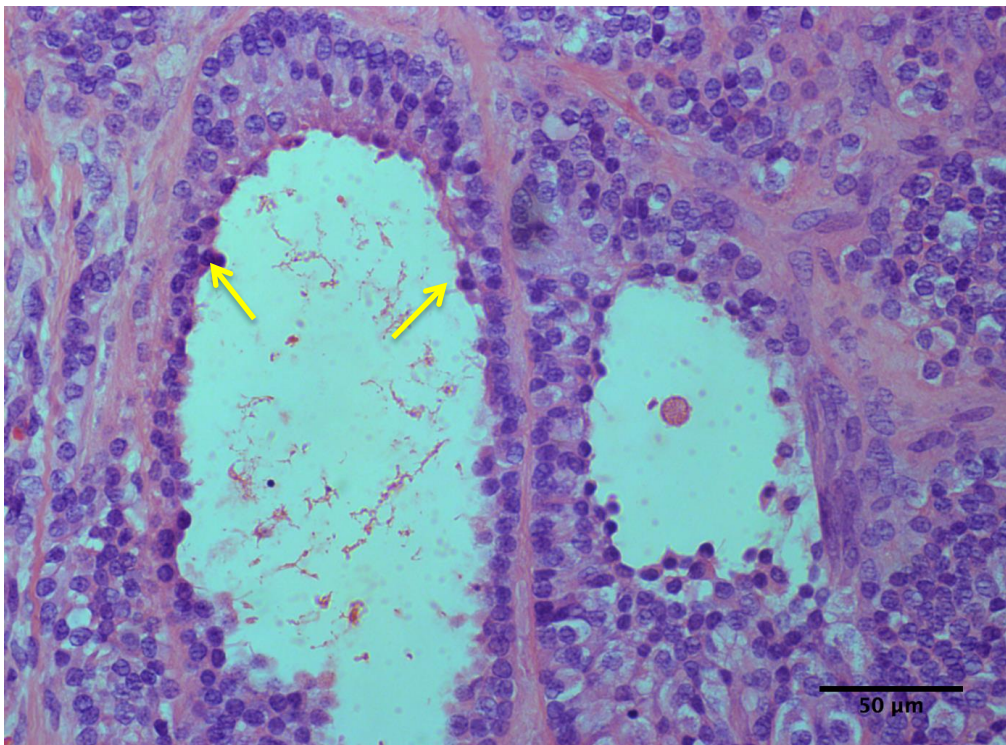


Figure 1-8: Classified GCT3: cystic like structure but appear as a closed circle cyst. It has only few antral (Yellow arrow) GCs. 400x magnification (Ab. AL Ibrahim, Thesis image).

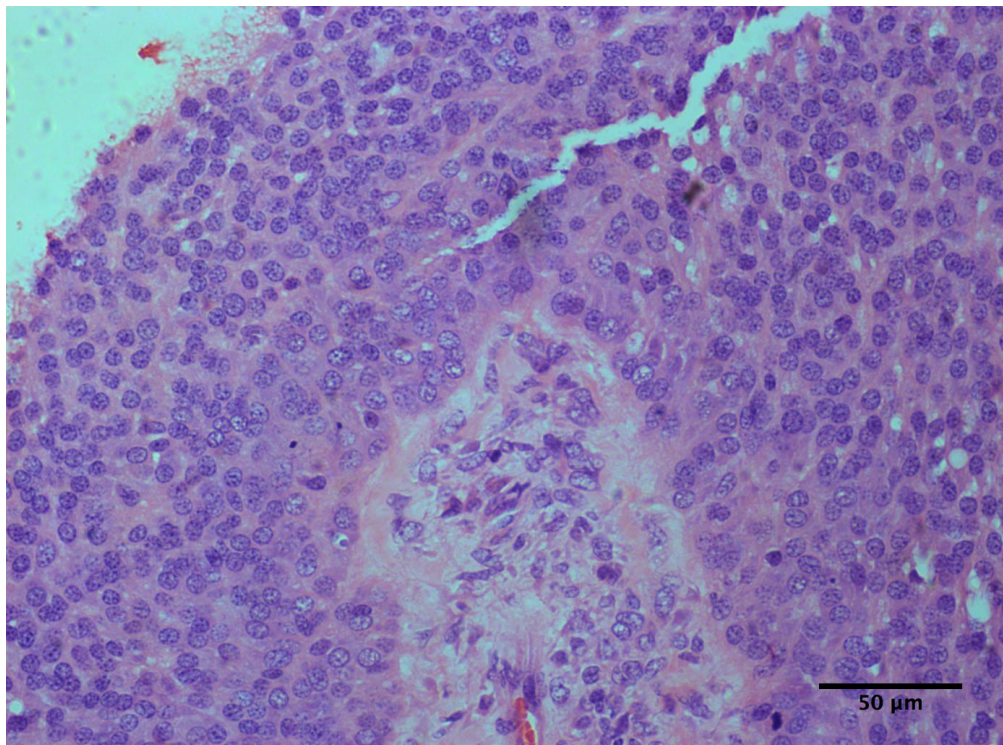


Figure 1-9: Classified GCT4: solid nests of granulosa cells. 400x magnification (Ab. AL Ibrahim, Thesis image).

1.9 FOXL2 gene

1.9.1 Definition

The term FOXL2 is derived from a large family of forkhead/winged-helix transcription factors. The name forkhead is obtained from the *Drosophila* gene, whereas the term winged-helix came about because of the butterfly shape. FOXL2 is a single-exon gene of 2.7 kb encoding a highly conserved protein of 376 amino acids containing a 110-amino-acid DNA-binding forkhead domain. This classifies FOXL2 to the family of forkhead transcription factors involved in a wide variety of biological processes during development and postnatal life. FOXL2 has been recognised as an ovarian differentiation marker in mammals and plays a significant role in follicular development and the maintenance of adult female fertility (Cocquet et al., 2002). FOXL2 gene is known to be involved in Blepharophimosis, ptosis, and epicanthus inversus syndrome (BPES), eyelid abnormalities occur during development and leading to vision limitation due to an inability to fully opening the eyelid, as well as the development of ovarian GCT (Caburet et al., 2012).

1.9.2 FOXL2 mutation

A range of disease conditions has been associated with a mutation in the isolated FOXL2 gene. This is due to the major role it plays in sex regulation, ovarian development and GC differentiation. FOXL2 can be considered as an ovarian follicle proliferation inhibitor in small and medium follicle whose purpose is to prevent premature depletion of ovarian follicles resulting in ovarian failure and malignancy (Pisarska et al., 2011). Some findings proposed that FOXL2 might act as a cancer suppressor. For instance, follistatin has been seen to be up-regulated by overexpression of wild-type FOXL2, compared with the FOXL2 mutation C134W. It has been found that activin A-stimulated cell proliferation is constrained by follistatin (Cheng et al., 2014).

1.9.3 FOXL2 Immunohistochemistry

Most follicular developmental stages; primordial, primary and larger secondary follicles express *FOXL2* protein as detected immunohistochemically (Pisarska et al., 2011). The nuclear expression of the *FOXL2* gene was identified in almost 100% of adult GCT patients (Kommos et al., 2013, Al-Agha et al., 2011) and in juvenile GCT patients (Al-Agha et al., 2011). Moreover, one study found that all examined cases of GCT patients positively expressed nuclear *FOXL2* protein (Hes et al., 2011, Yanagida et al., 2017, Takahashi et al., 2013). In a separate study, most GCT patient samples were immunostained with *FOXL2* (Jamieson et al., 2010). This has not been shown in any domestic animal species.

1.10 Hypotheses

This PhD project will have three main broad aims:

1. To study epidemiological aspects of ovarian pathology and tumours in the mare using text mining.
2. To study morphometric features of the granulosa and theca cell layers of equine antral follicles and granulosa cell tumours using H and E stain.
3. To find new immunohistochemical or genetic marker(s) for GCT of mares.

Chapter 2 Materials, methods and refining techniques

2.1 Text mining methods

2.1.1 UK data

Text mining techniques were used to identify individual records of horses with and without ovarian pathology, ovarian tumours and more specifically granulosa cell tumours (GCT). Proprietary software (Provalis Research) was used for this purpose and full detailed instructions on the process involved are provided in Appendix 1. In brief, data were uploaded to the software, dictionaries created which included a list of as many words as possible that could relate to the outcome of interest (ovarian pathology, ovarian tumour or GCT). These dictionaries are also provided at Appendix 2. An automated search of the text was initiated which identified any record in which any of the words contained in each dictionary were present. These records were downloaded in spreadsheet format for further investigation that ultimately results in a count of the number of individual animals with each condition such that prevalence estimates can be calculated.

2.2 Animals from which ovarian samples were recovered

The mares used in this study were primarily sourced from University of Glasgow, Weipers Centre Equine Hospital cases (n=31 mares), but some (n=5 mares) came from practices around the UK. Ovaries recovered from 18 mares were examined following euthanasia in a variety of reproductive states: oestrus, dioestrus and anoestrus because they arrived in different seasons such as late spring, summer, early autumn and winter. Other ovaries recovered from 15 mares were ovariectomised and also from three mares with unknown reason of collection.

All procedures were carried out in accordance with ethical research (Ref 41a/16), and were approved by the local Research Ethics Committee, School of Veterinary Medicine, University of Glasgow.

2.3 Ultrasonography

Ultrasonography on specimens in saline was used to determine the number and size of the follicles and occurrence of luteal structures on ovaries. A real time digital ultrasonic imaging scanner (Shenzhen Mindray Bio- Medical Electronics CO. LTD, Model DP-30 Vet) with to a 7.5 MHZ linear array transducer was used. The ovaries were collected, placed in a bag filled with phosphate buffered saline (PBS) and placed in an icebox. The linear probe was applied on each ovary scanning from lateral to medial or vice versa to detect all follicles or any corpus luteum present on each ovary.

2.3.1 Measurements of follicles and corpus luteum

The ovaries were scanned approximately one hour after each mare had been euthanized or between 1- and 2-hours after ovariectomy. The images of the follicles were frozen on the screen of the ultrasound scanner and individually measured. All findings of location and follicular size of individual follicle and corpus luteum were recorded on ovarian sheet, which then assisted fluid aspiration with individual follicle. This also ensured work commenced with the largest follicle first. A vertical and horizontal 'diameter' (mm) of each follicle was written on the ovarian diagram. The largest follicle from both ovaries was given number F1 and the second largest given F2 and so on as presented in Table 2-1. The diameter of any corpus luteum present was also drawn and measured as described above.

Table 2-1: An example of ovary and follicular size measurements from five mares with normal follicles

Mare	Date	Ovary size	ex vivo Scan	Structure	Left or right ovary	Size	FF
1	06.08.14	L 9.3x6.5cm	Yes	Follicle 1	Left	29.6 x34.9	Yes
			Yes	Follicle	Left	23.6 x 36.8	No
		R 11.5x8.5cm	Yes	Follicle	Right	22.4x21.4	No
			Yes	Follicle 2	Right	28.4x27.2	Yes
				Follicle	Right	62.7x60.3	No
2	14.08.14	L 4.8x3.5cm	Yes	Follicle	Left	12.5x8.9	No
				Follicle	Left	12.7x13.1	No
				Follicle LF F2	Left	27.2x28.1	Yes
		R 8.5x6.5cm	Yes	Follicle	Right	18x13.7	No
				Follicle MF	Right	20.7x19.2	Yes
				Follicle RF F1	Right	37.3x32.7	Yes
3	21.08.14	L 3.5x2.5cm	Yes	Follicle MF3	Left	10.3x11.8	Yes
		R 5.3x4cm	Yes	Follicle MF1	Right	15.4x13.2	Yes
				Follicle MF2	Right	11.5	Yes
4	11.11.14	L 6.7x5.5 cm	Yes	Follicle F1	Left	30.4x24	Yes
				Follicle F2	Left	17.7x15	Yes
		R 6.2x6 cm	Yes	Follicle F3	Right	17.3x14.4	Yes
				Follicle F4	Right	15.4x12.5	No
5	28.11.14	L 4.5x4 cm	Yes	Follicle F2	Left	18.3x17.9	Yes
		R 7.5 x 5.4 cm	Yes	Follicle F1	Right	36.3x31.3	Yes
				Follicle F3	Right	20.6x13.8	Yes

2.4 Follicular fluid (FF) samples

Follicular fluid samples were collected in the laboratory from individual follicle for analysis of Oestradiol (E2) concentration using a five or 10ml syringe with 20 G 1.5" needle after ultrasound procedures were complete. Follicular fluid was collected in 15ml tubes and placed in the icebox while aspiration of other follicles was taking place. All tubes were stored in a freezer at -20 °C until the E2 hormonal assay was performed.

2.5 Ovaries, stroma and follicular wall samples

One ovary at a time was taken from the Phosphate buffer saline (PBS) plastic bag that was in the icebox and placed on a sterile petri dish with fresh PBS. The follicle was penetrated with an incision by Westcott curved blunt tenotomy scissors to visualize the follicular cavity. The follicular wall of each follicle was peeled off by blunt dissection and put in a sterile petri dish filled with PBS. This

follicular wall was cut into three rectangular shaped pieces. A cube of stroma was then cut from the ovary and the ovary hemisected from lateral to medial splitting the ovulation fossa into two pieces. Each follicular wall of one follicle as well as stroma from each ovary that collected earlier was fixed in an individual 50 ml tube of Bouins solution fixative (VWR Chemicals, VWR International, 7000.1000). The two pieces of left and right ovaries were put in two different jars filled with Bouins solution fixative (VWR Chemicals, VWR International, 7000.1000). All tubes were kept at room temperature for 48 hours and then changed to 70% ethanol for the first time and after another 48 hours for the second time until ready for histopathology. The more recently collected ovaries with their follicular wall (n=7) and GCTs (n=5) were fixed in 10% neutral buffer formaldehyde for DNA extraction and PCR procedures and some were stored in -80 °C freezer as fresh samples either from a normal ovaries (n=2) or GCT (n=1) ovaries. In addition, two GCT and three normal ovaries from three mares had been preserved in 10% neutral buffer formaldehyde at the beginning of the study, and were also used for DNA extraction and PCR procedures.

2.6 Blood sample

A blood sample was collected from one euthanized mare under a different licence, which allowed the use of leftover blood for research via indwelling jugular vein catheters inserted prior to euthanasia. The blood sample was withdrawn and transferred to 10 ml EDTA tubes. The tube was centrifuged for 20 minutes at a temperature of 3 °C, speed 3800 rpm and low brake. The buffy coat from the EDTA tube was transferred in a 15 ml tube and filled with distilled water, centrifuged to wash and then removed red blood cells, poured off, and this process was repeated twice to recover a white blood cell pellet. The white cell sediment was stored in the freezer at - 80 °C until DNA extraction.

2.7 Hormonal assay

Follicular fluid (FF) oestradiol-17 β concentration collected during Chapter 4 was measured by an ELISA using the Parameter™ Estradiol kit from catalogue number (KGE014), R&D System a biotechne® brand, USA (Dou et al., 2017) and a LabTech LT-4500 microplate reader. All laboratory analyses were carried out in accordance with Control of Substances Hazardous to Health (COSHH) guidelines.

2.7.1 Oestradiol (E2) ELISA Protocol

Plates for ELISA were prepared as follows: Two wells for non-specific binding (NSB) that contained buffer (Calibrator diluent RD5-62) and Tracer (Oestradiol conjugate); two wells for maximum binding or total binding or zero binding (TB) that contained buffer (Calibrator diluent RD5-62), E2 primary antibody and Tracer (Oestradiol conjugate); twelve duplicated wells of six standards were prepared; and four wells of Quality Controls (two wells QCs low + two wells QCs High) at the beginning and end of the plates. Follicular fluid samples were added to all remaining wells in duplicate.

2.7.1.1 Quality controls (QCs) preparation

The following steps made the QCs 'low' and QCs 'high': 10 µl of each individual FF sample were collected in one tube to make a pooled sample. 10 µl of pooled sample was added to 990µl of distilled water to make 1000µl (1ml) of 1:100 dilution. 20 µl of the 1:100 dilutions was added to 80µl of calibrator diluent to make 100µl (0.1ml) of 1:500 dilution (QC High). 10 µl of the 1:100 dilution was added to 90 µl of calibrator diluent to make 100µl (0.1ml) of 1: 1000 dilution and finally 25 µl of the 1:1000 dilutions was added to 25 µl of calibrator diluent (double dilution) to make a 1: 2000 dilution (QC Low).

2.7.1.2 Follicular fluid dilution

The individual frozen FF sample was thawed and diluted four times, 1:100 in distilled water and (1:500, 1:1000 & 1:2000) in calibrator diluent buffer as follows: 10 µl of FF was added to 990µl of distilled water to make 1000µl (1ml) 1:100, 20 µl of 1:100 was added to 80 µl of calibrator diluent to make 100 µl (0.1ml) 1:500, 10 µl of 1:100 was added to 90 µl of calibrator diluent to make 100µl (0.1ml) 1:1000 and finally double the dilution of 1:1000 to make 1:2000, 25µl of 1:1000 in 25 µl of calibrator diluent to make 50 µl (0.05ml) 1:2000.

2.7.1.3 Preparation of the standard curve

The standard curve was prepared by adding 1ml of deionized or distilled water to Estradiol standard solution of 30,000 pg/ml. This was left for a minimum of 15 minutes with gentle mixing prior to making dilutions. 900 µl of Calibrator Diluent

RD5-62 was pipetted into the first tube (3000 pg/ml) tube and 400 μ l of Calibrator Diluent RD5-62 into the remaining tubes. Each tube was mixed gently but thoroughly before the next transfer, then 100 μ l of stock solution (Estradiol Standard 30,000pg/ml) was transferred into 3000pg/ml tube to make 1000 μ l. 200 μ l was transferred from 1st tube to another starting from the top standard or (high standard) 3000pg/ml tube until the low standard 12.3pg/ml tube. The top (high) standard starts from 3000pg/ml then 1000pg/ml, 333pg/ml, 111pg/ml, 37pg/ml, and 12.3pg/ml as presented in Figure 2-1 Calibrator diluent RD5-62 serves as the zero standard (0pg/ml)

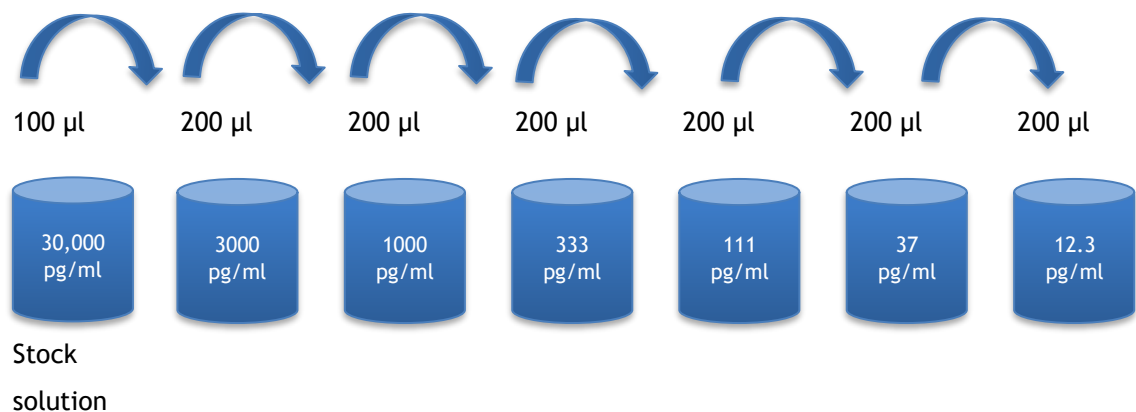


Figure 2-1: Standard curve and calibrator diluent

2.7.1.4 Assay procedures

100 μ l of Oestradiol primary antibody solution was added to each well, excluding the Non specific binding (NSB) wells, then covered with the adhesive strip provided and followed by one hour incubation at room temperature on a horizontal orbital micro plate shaker (0.12" orbit) set at 500 \pm 50 rpm. Each well was aspirated and washed with Wash Buffer (400 μ l) using a squirt bottle and this step was repeated three times for a total of four washes. After the fourth wash the plate was inverted and blotted against clean paper towels. 100 μ l of standard, control, or samples was added to the appropriate wells. 100 μ l of Calibrator Diluent RD5-62 was added to the zero standard (Bo) wells and NSB wells. 50 μ l of the E2 conjugate was added to all wells then covered with the adhesive strip provided and followed by two hours incubation at room temperature on the shaker. Aspiration and washing was repeated four times then a 200 μ l of substrate solution was added to each well followed by 30 minutes

incubation at room temperature on the bench top, protected from light. 100 μ l of stop solution was added to each well. At this point, if the colour in the wells did not change from blue to yellow or remained green, the plates were gently tapped to ensure thorough mixing. The optical density of each well was determined within 30 minutes, using a LabTech LT-4500 microplate reader set to 450 nm.

2.8 Histopathology

All ovaries and uteri were examined, inspected for any abnormalities and images were taken as shown on Figure 2-2. Those that were collected and scanned after euthanasia were transferred to the laboratory for histopathological procedures, apart from one ovary that was received from a different practice, which was already stored in 10% neutral buffer formaldehyde. Ovarian maps were used to identify the position of the follicle on the ovary. The ovary was placed on a petri dish filled with PBS and the follicular wall removed after aspiration of FF completed.



Figure 2-2: Examining the uterine tract immediately after euthanasia

2.8.1 Measurement of ovaries and ovarian follicles

Horizontal and vertical diameters of each ovary were measured using a ruler as shown on the Figure 2-3, whereas the horizontal and vertical diameter of each

follicle on the monitor screen of the ultrasound scanner was measured as on the Figure 2-4.



Figure 2-3: Ovary diameter measurement



Figure 2-4: Follicle diameter measurement using ultrasonography

2.8.2 Hemisecting of ovaries, cutting of stroma, peeling off the follicular wall (FW) and preservation

Following all procedures related to follicular fluid aspiration, peeling off the FW, cutting stroma, hemisecting the ovaries and preserving as described earlier, samples were sent for histopathology embedding and H&E staining (Kiernan, 2008). Many ways were investigated to identify the optimal alignment of follicular wall in order to view the layers of granulosa cell, theca cell and stroma. The FW was cut as a small rectangular piece of tissue. Individual samples were placed in a small container filled with Bouins solution fixative (VWR Chemicals, VWR International, 7000.1000) or 10% neutral buffer formaldehyde, labelled with a specific code number and maintained at room temperature for both histology and immunohistochemistry. The GCT ovaries were also dissected into small (approximately 10mm) pieces for the same examination.

2.8.3 Tissue processing protocol (wax blocks).

Histology and immunohistochemistry staining was carried out by Veterinary Diagnostic Services at the University of Glasgow, School of Veterinary Medicine

which is recommended by (Oliver and Jamur, 2010) . Preparation of H&E staining wax has many steps for small tissue samples as presented in the Table 2-2.

2.8.4 Haematoxylin and Eosin (H&E) staining

Follicular walls were embedded in wax using Thermo Scientific, Histostar machine sections. The block was cut using a Thermo Scientific, FINESSE ME+ microtome machine by placing the block in a position where the machine could trim the first 10µm in order to get a full face of the block before then setting the machine to 2.5µm slice thickness. The section was stretched and placed on the warm water bath. The best section was chosen and mounted onto a slide and left on hotplate for at least 5-10 minutes, then placed in the 60° c oven for at least one hour to ensure it was fixed properly to the slide and that the wax had melted. The 2.5µm-backed section was deparaffinised by immersion in xylene substrate called a Histo-clear (National Diagnostics, New Jersey, USA), for three minutes. The slides were rehydrated for three minutes by passing through (100%, 90%, 70%) alcohol baths and rinsing in water. Slides were placed in Haematoxylin for five minutes, washed with water, then placed in mixed of acid and alcohol (70%) and rinsed in Scott's tap water substitute for three minutes. The slides placed in Eosin for five minutes, then washed with water. Sections were dehydrated with (70%, 90%, 100%). Finally the section cleared with Histo-clear and mounted in mounting media using Histomount (National Diagnostics, New Jersey, USA).

2.8.5 Histological (normal follicular wall) and histopathological (GCT) slide examinations

The granulosa and theca cell layers in each FW section, were quantitatively assessed using a Leica DM4000B microscope (Leica Microsystem, Switzerland) connected to Leica Application Suite software (version 4.3.0; Leica Microsystems, Switzerland) to acquire images. ImageJ (1.49v, Wayne Rasband, National Institute of Health, USA) software was used for cell count and thickness measurements. Five consecutive rectangular views were spaced over the whole length of the follicle wall capturing both the granulosa cell and theca cell layers (all at 40 x magnifications) as shown in Figure 2-5. Each rectangle measured

140.70x255.27 μm^2 as shown in Figure 2-6. All magnifications were viewed by multiplying with 10X microscope binocular.

Table 2-2: H& E stain preparation steps

Station	Content	Time
1	70% ALCOHOL	30MINS
2	95% ALCOHOL	30MINS
3	ABS ALCOHOL	30MINS
4	ABS ALCOHOL	30MINS
5	ABS ALCOHOL	45MINS
6	ABS ALCOHOL	45MINS
7	ABS ALCOHOL	1 HR
8	ABS ALC/XYLENE	30MINS
9	XYLENE	30MINS
10	XYLENE	30MINS
11	WAX	30MINS
12	WAX	30MINS
13	WAX	45MINS
14	WAX	45MINS

In each of the five views granulosa (GC) and theca cells (THC) were counted at x40 magnification as shown in Figure 2-7. These cell types were differentiated from each other on the basis of cellular morphology. Basal GC were classified as cells that were situated at the base of the GC layer. Antral GC were classified as cells that were situated closest to the antral surface of the follicle. Intermediate GC were classified as the cells that were laid in between the basal and antral GC. The thicknesses of the granulosa and theca cells were measured on five views under 20x magnification images in order to examine the whole stretch of the tissue as shown in Figure 2-8. The thickness of GC layers started from the antral GC to the basal GC and thickness of THCs layers started from the top of the theca interna cell directly beneath the basal GCs to the end of theca interna. The large THC and small THC cells make up the composition of the theca layer. The large THC cells exhibit a well-defined cell membrane with large cytoplasm, whereas the small THC cells tend to be smaller in size with less

cytoplasm. The cells that were included in the assessment had distinct nuclei. The entire cell had to be visible for it to be counted.

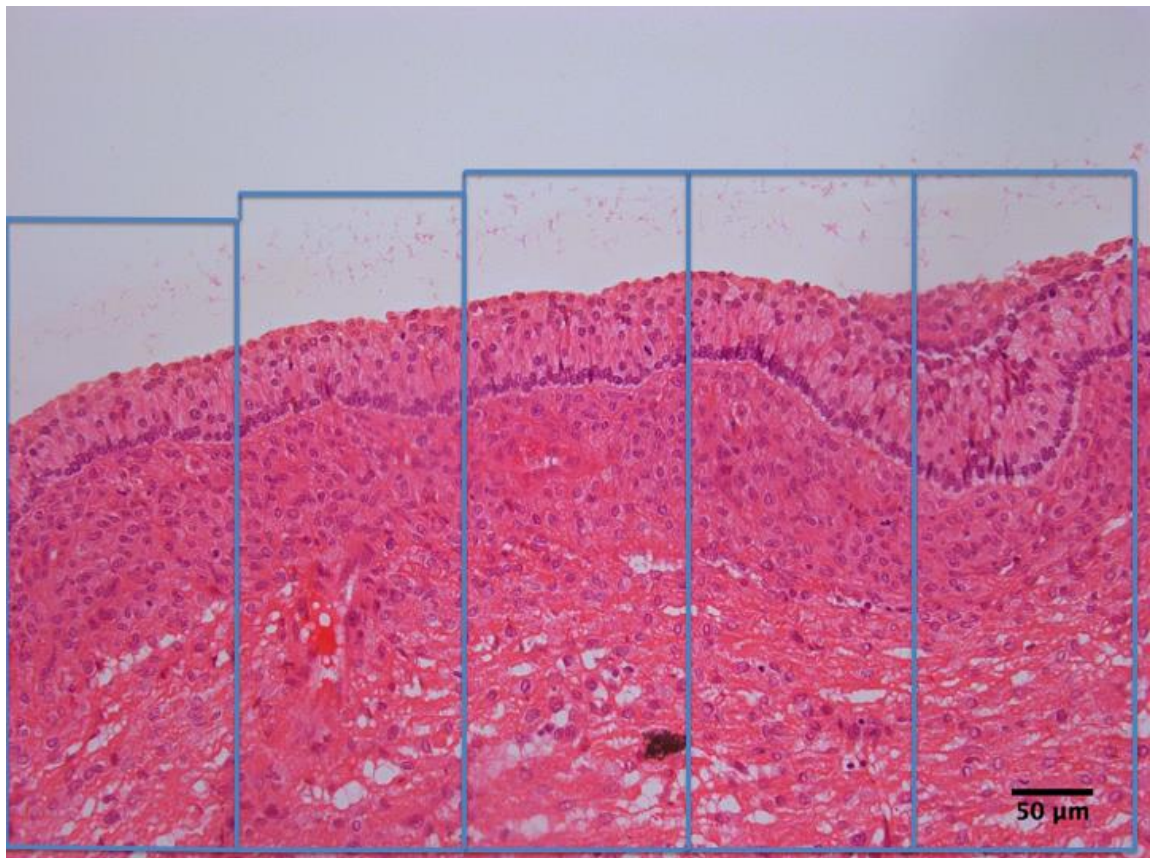


Figure 2-5: Illustration of how views are taken from a selected follicular wall sample. This sample is taken as 200X magnification; the boxes are representative of the five successive views taken for further assessment at 400x magnification.

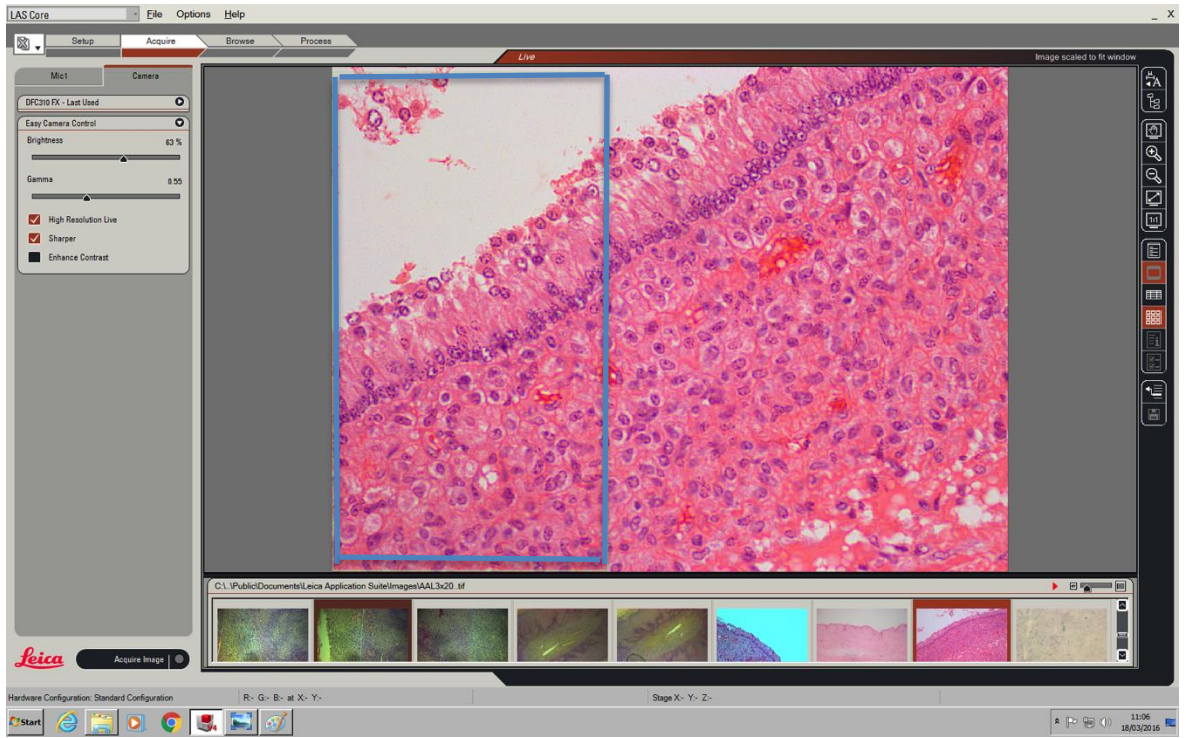


Figure 2-6: Rectangle view of follicular wall image 200x magnification

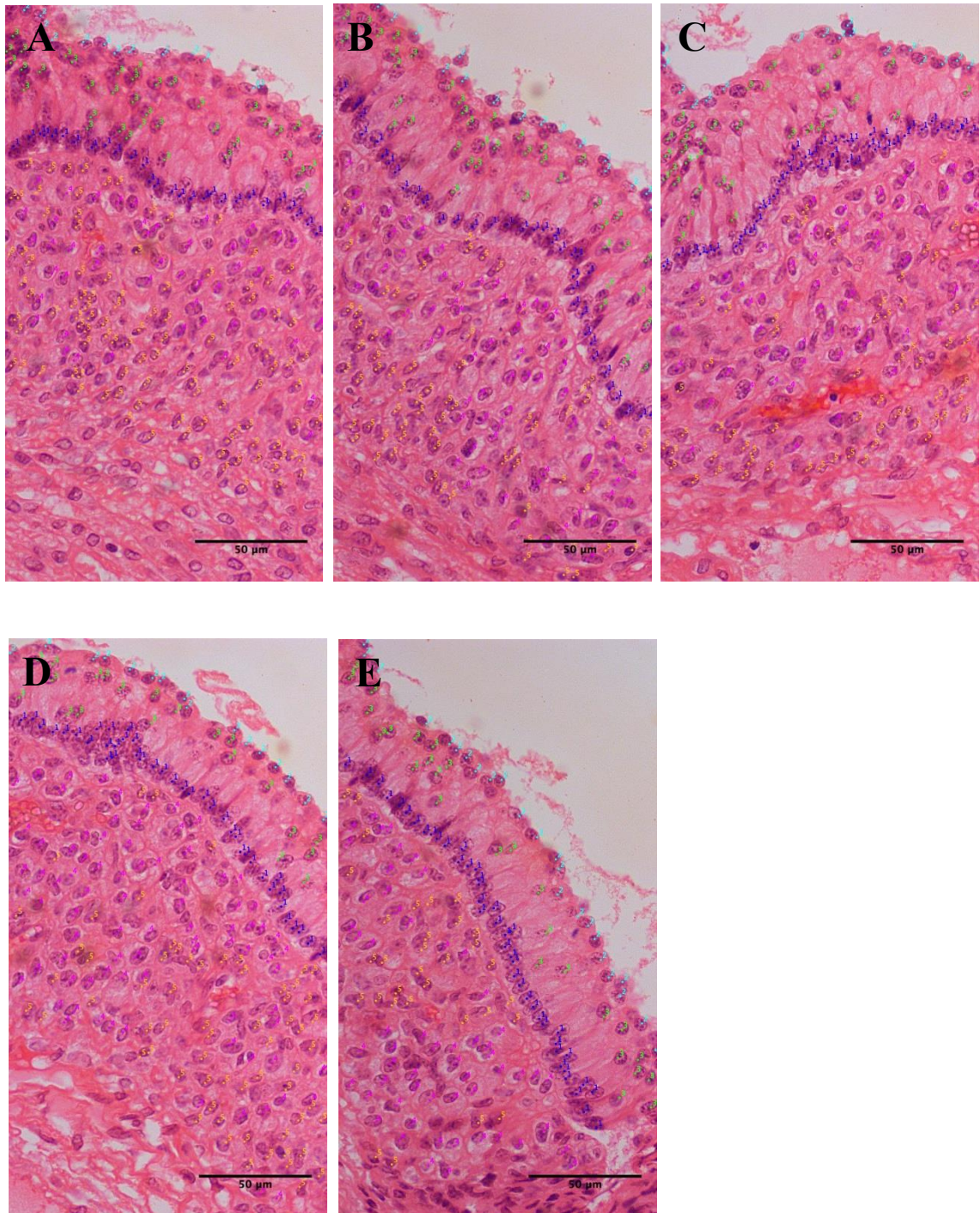


Figure 2-7: Counting granulosa and theca cells at 400x magnification, No.1: Basal GCs, No.2: Antral GCs, No.3: Intermediate GCs, No 4: Large THCs, No. 5: Small THCs



Figure 2-8: Measuring (White lines) the thickness of granulosa and theca cell at 200x magnification

2.8.6 Cells counting and measuring the thickness of granulosa and theca cells

Granulosa cells and small and large theca cells were counted by using Image J (1.49v, Wayne Rasband, National Institute of Health, USA) software. Only those cells with distinct nuclei were included. Granulosa and theca layers thicknesses were acquired under 200x magnification using a Leica DM4000B microscope (Leica Microsystem, Switzerland) connected to a Leica Application Suite software (version 4.3.0; Leica Microsystems, Switzerland) followed by analysis using ImageJ software. The scale was first calibrated with the use of a graticule taken with the same magnification to enable measurement of the cell layers in μm based on the number of pixels as shown on Figure 2-9. This distance was then converted to a measured length on the basis of a standardized scale.

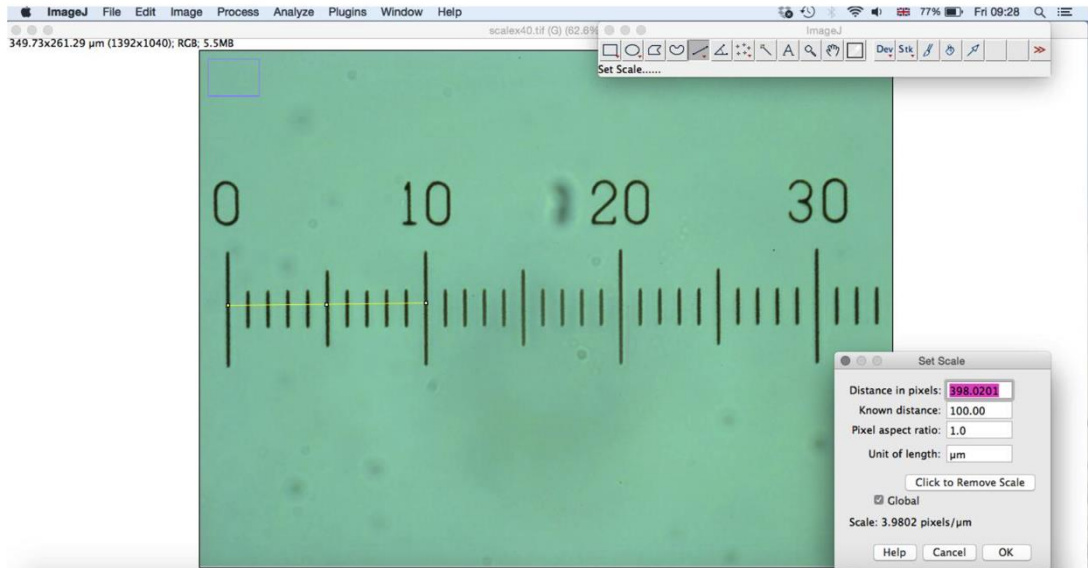


Figure 2-9: Setting a scale (pixel: μm) ratio using ImageJ at 40 magnifications. $100\mu\text{m}$ equal to 398.0201 pixels, thereby producing a scale of 3.9802 pixels/ μm .

2.8.7 Nuclear circumferences

Image J software was also used on nuclear circumferences for basal, intermediate and antral nuclear cells for both follicular wall of antral follicle and for GCT. The scale was set using 50 graticule scale image taken under 100 magnifications to calibrate the software that enable conversion of pixels to a known length unit on μm so the scale ratio will be pixels/ μm , then measurements of the nucleus were taken. All various views at 100x (under oil immersion) magnification (multiplied with 10X microscope binocular) were taken of a characteristically healthy follicular wall samples (VH, H, EA) and granulosa cell tumour samples (GCT1, GCT2, GCT4) in interest of comparison of cellular morphology using an Olympus BX51 microscope and Stream Basic (version 1.9.2; Olympus soft Imaging Solutions GmbH). In normal follicular wall samples, five basal GC, five intermediate GC and five antral GC were randomly selected in each view (three views measurement). In other words, 15 basal, 15 intermediate and 15 antral GC in three views per section were measured. In GCT samples, five cells in three views were randomly selected on the same requirements. In total 15 basal, 15 intermediate and 15 antral GC in 3 views per sections in GCT1 (large, follicle-like) and GCT2 cysts (small, thick wall), and in GCT3 cysts (single cell layer surrounding fluid antrum, only antral GC), and in GCT4 45 GC within solid nests because there is no distinct basal or intermediate or antral GC.

2.8.8 Generic Immunohistochemistry (IHC) Protocol using Dako Autostainer

All procedures were done at room temp and slides were placed for five minutes in buffer to rinse all Tris buffer pH7.5 + Tween. HIER (Heating-Induced Epitope Retrieval) was done using Access Retrieval Unit (Menarini, UK), Buffer Sodium Citrate pH6 1 min 40 sec at 125°C full pressure and Enzymatic antigen retrieval using Proteinase K RTU (Agilent, Dako, USA) was used for antigen retrieval. Slides were loaded on to a Dako Autostainer (Agilent, Dako, USA) then rinsed in a buffer and placed in Dako Real TM Peroxidase blocking solution (3% hydrogen peroxide in PBS made in house) for five minutes followed by a five minutes buffer rinse. The first antibody dilution was performed using (universal diluent, Dako) for 30 minutes then followed by two buffer rinses for five minutes. The appropriate second reagent was applied for 30 minutes depending on which species has been raised on first antibody then followed by two buffer rinses for five minutes. Slides were loaded on Dako K5007 DAB (Dako, UK) twice for five minutes followed by three water rinses and counterstaining with Gills Haematoxylin (made in house) for 27 seconds. The slides were then washed in water (Scotts Tap Water Substitute) dehydrated, cleared and mounted in synthetic resin (DPX, Sigma), which ready for analysis. The details of the primary antibodies, enzymatic antigen retrieval agent and secondary antibodies are presented in Table 2-3.

Table 2-3: The dilution of the primary antibodies, secondary antibodies and enzymatic antigen retrieval used

No.	Antibodies	Antigen Retrieval	Antibodies dilution	Secondary Antibodies
1	INHIBIN clone R1 Dako Cat. NO. M3609	HIER Sod Citrate pH6	1:20	Dako Envision+System HRP Labelled polymer Ant- mouse Cat. No. K4001 ready to use
2	AROMATASE ABBIOTEC Cat. No. 250549	Proteinase K 15 minutes	1:100	Dako Envision+System HRP Labelled polymer Ant- Rabbit Cat. No. K4003 ready to use
3	CYP17A1 Santa Cruz Cat. No. se- 374244	HIER Sod Citrate pH6	1:1500	Dako Envision+System HRP Labelled polymer Ant- mouse Cat. No. K4001 ready to use
4	AMHR2 N- Term Antibodies- online Cat. No. ABIN2616027	HIER sodium citrate pH6	1:200	Dako Envision+System HRP Labelled polymer Ant- Rabbit Cat. No. K4003 ready to use
5	FOXL2 Abcam Cat. No. ab5096	HIER Sod Citrate pH6	1:600	ImmPRESS HRP reagent kit anti-Goat IgG Cat. No. MP- 7405 made up as per suppliers instruction

2.8.9 IHC analysis

All images were examined under 200x magnification plus 10X objective binocular using a Leica DM4000B microscope (Leica Microsystem, Switzerland) connected to a Leica Application Suite software (version 4.3.0; Leica Microsystems, Switzerland) followed by analysis using ImageJ software (1.49v, Wayne Rasband, National Institute of Health, USA). Each image was given a category or a percentage of coverage depending on a judgment of the stain intensity, distribution at the section and %area covered. For the stain intensity; '0' implies no stain, '1' was low stain, '2' was medium stain and '3' was high stain and for the spread or distribution '1' was continuous, '2' was individual and '3' implied clusters of cells. The area covered was given according to the number of granulosa cells, and percentage of cells covered because, for example in those classified as GCT3, the total number of GCS is reduced.

2.9 FOXL2 sequence determination gene extraction

2.9.1 First experiment

2.9.1.1 Samples

Eight GCT samples from six mares and eleven control samples from seven mares were used in this study. All had been fixed in 10% neutral buffered formalin. One of the GCT samples (No.2) stored fresh in -80 °C and one mare (No.1) was presented in both groups because both ovaries were removed during ovariectomy. Fresh tissue and blood from the mare (No.7) that is a non-GCT tissue sample alongside frozen washed buffy coat from another non-GCT mare (No.4) were analysed. The University of Glasgow School of Veterinary Medicine Research Ethics Committee - Reference number 41a/16, approved the use of tissue and blood for this study. Details of the origin of samples used in the study are shown in Table 2-4.

Table 2-4: Mares used in the study

Samples	Mares No.	Collecting Date	Comment
GCT	1 Left Ovary	16.10.13	13yo Welsh Pony
	2	17.06.14	Unknown mare - 20cm GCT on RHS
	3	07.03.16	Chestnut Thoroughbred - foaled 12d before admission
	4	31.05.16	GCT of 8.5cm diameter with large cystic cavity of 6x4x3cm
	5	10.06.16	8yo Cob
	6	14.09.16	8yo L. ovary weighed 5 kg
Non GCT	1 Right Ovary	16.10.13	13yo Welsh Pony
	2	03.04.13	9yo Irish Sport Horse with persistent oestrus and difficult behaviour
	3	22.05.13	4yo Piebald Draft horse
	4	09.02.15	1.5yo Welsh Mountain Pony
	5	02.04.16	10yo Thoroughbred Cross with masculine behaviour
	6	01.04.16	10yo Connemara Cross
	7	03.02.17	Recently Foaled. Had sarcoid and difficult behaviour

2.9.1.2 Purification of total DNA from animal tissues (spin-column protocol)

A few important steps were performed before starting the procedures. All centrifugation steps were carried out at room temperature (15-25 °C) in a microcentrifuge and vortexing was performed by pulse-vortexing for 5-10s. The buffer ATL and buffer AL were warmed to 56 °C until the precipitates had fully dissolved to prevent the formation of precipitates upon storage. The appropriate amount of ethanol (96-100%) was added to Buffer AW1 and Buffer AW2 as indicated on the bottle to obtain a working solution before using for the first time. To prevent reducing DNA size, the frozen tissue samples were equilibrated to room temperature and repeated thawing and freezing was avoided.

QIAGEN DNeasy® Blood and Tissue Kit and its protocol (Qiagen. DNeasy® Blood & Tissue Handbook. Qiagen; 2006) was used to extract the DNA from samples. Tissue samples between 15-20 mg were cut and washed twice in PBS to remove any formalin. Tissue was put into 1.5ml DAN/RNA-free Eppendorf tubes and 180µl of Buffer ATL was added. Then 20µl proteinase K was added, mixed thoroughly by vortexing, and incubated in a water bath at 56 °C until the tissue was completely lysed. It is worth noticing that some tissue required many hours of water bath incubation. 200 µl of Buffer AL was added to the sample, and mixed thoroughly by vortexing. This was followed by the addition of 200µl ethanol (96-100%), and mixing again thoroughly by vortexing. The mixture including any precipitate was added to the DNeasy Mini spin column placed in a 2-ml collection tube then centrifuged at $\geq 6000 \times g$ (8000 rpm) for one minute. The collection tube was discarded and placed the DNeasy Mini spin column in a new 2-ml collection tube, then 500 µl Buffer AW1 was added, and centrifuged for one minute at $\geq 6000 \times g$ (8000 rpm). The collection tube was discarded and placed the DNeasy Mini spin column in a new provided 2-ml collection tube, then 500 µl Buffer AW2 was added, and centrifuged for three minutes at 20,000 $\times g$ (14,000 rpm) to dry the DNeasy membrane. The collection tube was discarded and placed the DNeasy Mini spin column in a clean 1.5 ml or 2 ml microcentrifuge tube, and pipetted 30µl Buffer AE directly onto the DNeasy membrane. This was then incubated at room temperature for one minute, and then centrifuged for one minute at $\geq 6000 \times g$ (8000 rpm). Elution with 30µl

(instead of 200 µl) increased the final DNA concentration in the eluate, but also decreased the overall DNA yield. 50µl Buffer AE was used for blood. DNA yield and quality (260/280 ratio) were measured using the NanoDrop 1000 Spectrophotometer, after which the DNA was stored at -20°c until required.

Extracted DNA yield from tissues that eventually went on to sequencing are presented in Table 2-5. Although for most DNA extraction overall positive results were achieved, *FOXL2* amplification from fixed and frozen tissues was unsuccessful, indicating DNA degradation. A gel was run of the DNA extracted from tissues of various ages presented in Figure 2-10. It can be observed that DNA is highly degraded in fixed tissue, with fewer longer reads remaining compared to frozen and fresh tissue. Although for reasons unknown, Non-GCT 7B DNA appeared very faint in this gel, all downstream reactions and sequencing were successful.

Table 2-5: DNA concentration of final samples sequenced

Mare Samples	Collecting Date	Tissue origin	Tissue state	Weight (mg)	DNA conc. (ng/ml)	260/280 Ratio
GCT 1	16.10.13	L. Ovary	Fixed	19.2	87.56	1.75
GCT 2A	17.06.14	R. Ovary	Fixed	18.8	181.94	1.76
GCT 2B	17.06.14	R. Cyst wall	Frozen	15.9	141.39	2.03
GCT 2C	17.06.14	R. Stroma	Frozen	19.5	368.79	2.05
GCT 3	07.03.16		Fixed	18.5	135.03	1.86
GCT 4	31.05.16		Fixed	19.9	446.05	1.76
GCT 5	10.06.16		Fixed	17.8	132.09	1.77
GCT 6	14.09.16		Fixed	18.1	197.25	1.9
Non- GCT 1	16.10.13		Fixed	17.5	43.41	1.67
Non- GCT 2	03.04.13		Fixed	19	95.67	1.69
Non- GCT 3	22.05.13	L. Ovary	Fixed	19.1	101.85	1.78
Non- GCT 4	09.02.15	Blood	Frozen		37.18	1.92
Non- GCT 5	02.04.16	R. Ovary	Fixed	18.9	157.99	1.78
Non- GCT 6	01.04.16		Fixed	18.3	114.22	1.7
Non- GCT 7A	03.02.17	Blood	Fresh		666.54	1.88
Non- GCT 7B	03.02.17	L. Follicle wall	Fresh	17.6	145.4	2.02
Non- GCT 7C	03.02.17	R. Follicle wall	Fresh	16.8	141.02	2.13
Non- GCT 7D	03.02.17	L. Ovary	Fresh	19.2	101.91	2.04
Non- GCT 7E	03.02.17	R. Ovary	Fresh	18.9	83.77	2.04

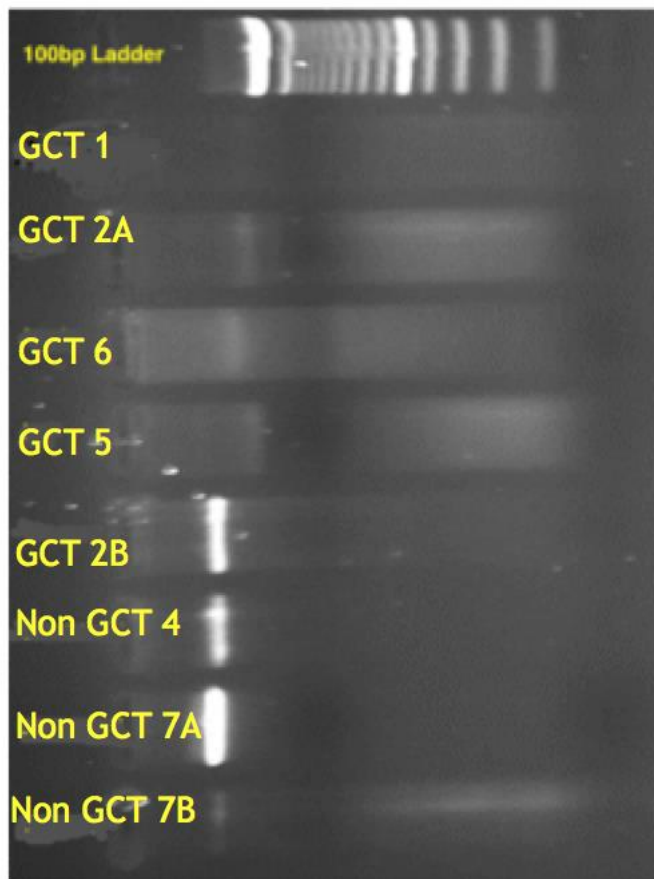


Figure 2-10: Gel of extracted DNA from tissues of varying ages using 150ng/ μ l DNA per well. Fixed tissues: (GCT1, GCT2A, GCT6, GCT5), Frozen tissue (GCT2B), Frozen blood (Non GCT4), Fresh blood (Non GCT 7A), Fresh tissue (Non GCT 7B)

2.9.1.3 DNA extraction from blood

The collected blood in EDTA tubes was spun at 2500 rpm, 4°C for 15 minutes. The buffy coat layer was extracted and placed in a 1.5 ml eppendorf tube and the DNA extracted from the buffy coat on the same day using DNeasy® Blood and Tissue kit or the buffy coat was frozen at -80°C until ready for use. The DNA yield was measured using NanoDrop 1000 spectrophotometer. The AE buffer provided in the DNA extraction kit was used (to set a blank) then stored at -80°C.

2.9.1.4 Nanodrop protocol

Initially 1.5 μ l of water was loaded on the lower measurement pedestal then the sampling arm was closed to initiate. Loading 1.5 μ l of AE buffer onto the lower measurement pedestal set the blank. The pedestal was wiped with a clean laboratory wipe and 1.5 μ l of the DNA sample was loaded and read. An example of a good quality DNA curve created by DNA samples is as presented in Figure 2-11. The pedestals were wiped after each sample. The last run was performed with AE buffer to check for contamination.

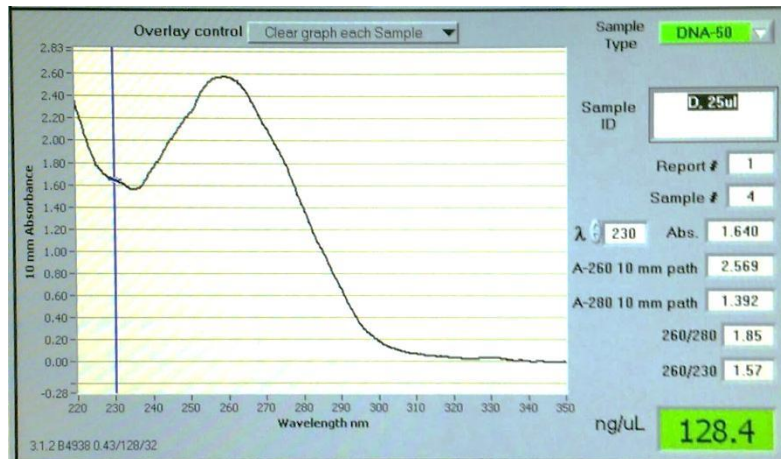


Figure 2-11: An Extracted DNA result generated by the NanoDrop1000

2.9.1.5 Primer Design

The primer design software Primer-BLAST, available on NCBI were used to design three sets of primers for Equine *FOXL2* as shown in Table 2-6 based on the sequence available on NCBI. Primers were prepared to 100pmol/ μ l with (molecular grade) water. For the Polymerase chain reaction (PCR) a Primer Mix of both Forward (F) and Reverse (R) primers were prepared to 20pmol/ μ l of each primer. For the Sequencing PCR, the primers were individually prepared to 3.2pmol/ μ l, as instructed in the BigDye[®] Kit Protocol. The binding positions of the primers in relation to the equine *FOXL2* sequence are presented in Figure 2-12.

Table 2-6: Primers details

Primer		Sequences (5'-3')	Melting Temp.	Product size
P1	F	CAACCTCAGCCTCAACGAGT	59.4 °C	294bp
	R	TTGTTGAGGAAGCCCGACTG	59.4 °C	
P2	F	GCCAAGTTCCCGTTCTACGA	59.4 °C	355bp
	R	ACGAGTTGTTGAGGAAGCCC	59.4 °C	
P3	F	CAACCTCAGCCTCAACGAGT	59.4 °C	119bp
	R	GGTAGTTGCCCTTCTCGAACA	59.8 °C	

```

1  aggctcagc  tgtccggcat  ctaccagtac  atcatcgcca agttcccgtt ctaccgagaag
61  aacaagaagg  gctggcagaa  tagcatccgc  caaacctca gcctcaacga gtgcttcac
121 aagggtgccg  gggagggcgg  cggcgagcgc  aagggcaact actggacgct ggaccggcc
181 tgcgaggaca  tggtcgagaa gggcaactac cggcgccgcc gccgcatgaa gggcccttc
241 cggccgccgc  cagcgcactt  ccagcccggc  aaggggctct tcggggcggg aggcgccgcg
301 gggggctgcg  gtgtggcggg  cgggggggcc  gacggctacg gctacctggc gcccccaag
361 tacctgcagt cgggcttct caacaactcg t

```

Primer 1
Primer 2
Primer 3

Figure 2-12: The nucleotide sequence of Equine *FOXL2*, with the position of the forward and reverse primers shown and the expected site of the mutation highlighted in yellow

2.9.1.6 PCR PROTOCOL

Decontamination of the PCR working area with 70% ethanol was performed followed by PCR preparation with Applied Biosystems AmpliTaq Gold® reagent. PCR procedures were applied according to the method of (Walsh et al., 2012, Mihm et al., 2006). The PCR products for the three sets of primers ranged from 118-355 bp were designed. A nested PCR was performed by using the primer pair (P2) for the initial PCR, followed by a nested primer pair (P1 or P3) for the secondary reaction. The bench top of the flow hood was treated with UV for five minutes prior to setting up the PCR reactions. Each of the reagents was thawed and gently mixed, and the enzyme solution was gently spun down in a micro centrifuge before pipetting. All pipetting steps were carried out in the flow hood. PCR was in 30 µl reactions. Along with the reactions required for the total number of samples, additional reactions to serve as blank (one for each primer pair) were included. In case of one primer pair, the master mix was prepared by first adding 3µl of 10X PCR buffer II and 2.4µl of 25mM MgCl₂ per reaction and water was added to this mixture. The volume of water will vary according to the volume of template DNA. The total volume of master mix, primers and template was equal to 30 µl. The mixture was gently vortexed followed by a pulse spun in the micro centrifuge then UV treated. The master mix was completed by adding 0.6µl of dNTP mix and 0.3µl of AmpliTaq® Gold DNA polymerase per reaction. Each of the primers was prepared to a concentration of 20 pmol/µl. 0.6 µl of forward as well as 0.6 µl of reverse primer per reaction was added to the master mix then gently vortexed by a short pulse spin. The final concentration of each primer in the reaction was 0.4 pmol/µl (400 nmol/l). The mixture was divided into each of the PCR tubes. The different DNA templates were added in different tubes leaving one tube blank per primer pair. DNA template was added to a final

concentration of 4 ng/ μ l. The final volume was made up to 30 μ l and followed by a brief vortex and a short pulse spin to each of the PCR tubes. Thermo Hybaid Px2 thermal cycler was used to run PCR. For different primers with varying annealing temperatures, the temperature of the gradient block was set accordingly. The following 35 PCR cycling conditions were used:

- Stage 1: 95°C, three minutes.
- Stage 2: Step 1) 95°C, 30 seconds. Step 2) Annealing temperature (57°C), 30 seconds. Step 3) 72°C, one minute.
- Stage 3: 72°C, five minutes and hold at 4°C.

2.9.1.7 Agarose Gel electrophoresis

Agarose Gel electrophoresis was performed to identify the presence of any amplified DNA and the size of PCR products. 2.5 L of 5X TBE was prepared by adding 135g of Tris base and 68.75g of boric acid and 50ml of 0.5 M EDTA (pH 8.0). 5X solution of TBE was diluted by 10 times to prepare a working solution of 0.5X TBE. 2% agarose gel was prepared by adding 3g of agarose to 150 ml of 0.5 X TBE. The agarose was melted in a microwave until the solution became clear then was cooled down to about 50-55°C while swirling the flask occasionally to cool evenly. 0.5 μ l of Ethidium bromide was added to the gel with a gentle mix. The ends of the casting tray were sealed with two layers of tape. The combs were placed in the gel-casting tray. The melted agarose solution was poured into the casting tray and left to cool until solid. The combs were pulled out carefully and the tape was removed. The gel was placed in the electrophoresis chamber to which was added enough 0.5 X TBE Buffer so that there is about 2-3 mm of buffer over the gel. For loading the gel, 5 μ l of the PCR products in separate eppendorf tubes were added to 3 μ l of loading buffer and 10 μ l of water. For the ladder, 1 μ l of Invitrogen 100bp DNA ladder (Invitrogen 15628019) and 3 μ l of loading buffer were added to 14 μ l of water. Each of these tubes was spun down in a micro centrifuge. 18 μ l of sample/sample loading buffer mixture were carefully pipetted into separate wells in the gel. 18 μ l of the ladder/loading buffer mixture were pipetted into at least one well of each row of the gel. The lid on the gel tank was closed and connected the electrodes then the gel was run at 110-125V for approximately one hour. Finally the gel image was viewed and recorded under UV trans-illumination.

2.9.1.8 Purification of PCR product

The PCR product was purified to eliminate any unincorporated PCR reagents or products <100bp in length that could interfere in subsequent sequencing reactions. Purification was performed on the remaining 25µl of PCR product using the Qiagen QIAquick[®] PCR Purification Kit, according to kit protocol with 20µl of Elution Buffer PE used to elute the samples. The column was incubated at room temperature for one minute followed by centrifugation at 17,000g for one minute.

2.9.1.9 Sequencing PCR

Sequencing reactions (10µl) were performed on a 96-well plate using the BigDye[®] Terminator v3.1 Cycle Sequencing Kit (Applied Biosystems, 4337456). All the reagents were thawed and gently mixed. 10µl reactions for the sequencing PCR was set up and all primers were prepared to a concentration of 3.2 pmol/µl. The master mix was prepared by adding 3µl of BigDye sequencing buffer and 1µl BigDye terminator ready reaction premix per reaction. 1µl of forward primer per reaction was added. The master tube was gently vortexed followed by a short pulse spin in a micro centrifuge. The mix was pipetted out into separate wells of the 96- well plate. 1µl of the purified PCR product and 4µl of water were added to each of the wells. The plate was sealed with caps and followed by a short spin. The plate for the sequencing PCR was loaded on Hybaid PCR express thermal cycler then run the sequencing PCR with the following (25 cycles) thermal cycling conditions:

- Stage 1: 96°C, one minute
- Stage 2: Step 1- 96°C, 10 seconds. Step 2- 50°C, five seconds. Step 3- 60°C, four minutes
- Hold at 4°C

2.9.1.10 Precipitation

PCR products precipitation was performed to eradicate any proteins, nucleotides and salts from the solution that might interfere with the sequencing machine. After the completion of sequencing PCR, the plate was removed and given a

short spin before carefully removing the caps. 8µl of deionized water and 32µl of molecular grade 100% ethanol were added to each of the wells. The wells were resealed, the tray was inverted a few times, and the plate was pulse-spun. The plate was incubated at room temperature for 20-30 minutes and was centrifuged at 4,000 rpm at 4 °C for 30 minutes. The supernatant was removed by tapping onto a paper towel then 150µl of 70% ethanol was added and the plate was sealed followed by inverting it once or twice and centrifugation at 4,000 rpm for 10 minutes. The supernatant was removed by tapping and inverting the tray on a tissue. The inverted tray along with the tissue was placed in a centrifuge and spun at 800 rpm for one minute. The plate was placed in an open PCR block at 90 °C for three minutes to ensure it was dry. Then the plate was ready to be sequenced using the Genetic Analyzer as described under 2.9.1.12

2.9.1.11 PCR and Gel Electrophoresis

A visualised single thin product band on the gel is required in order to immediately progress to sequencing. The majority of samples, however, were of insufficient quality to successfully sequence despite successful DNA extraction.

1. Fixed Tissue

Primary PCR of fixed tissue using P2 produced faint smears instead of the thin, clean bands needed, as presented in Figure 2-13. Primer dimer of <100bp can be clearly identified in all wells, while a band can only be detected with the fresh Non GCT 7B (FW) samples. Smears above or higher to the expected product size of 350bp, are visible for the fixed tissue, indicating DNA degradation.

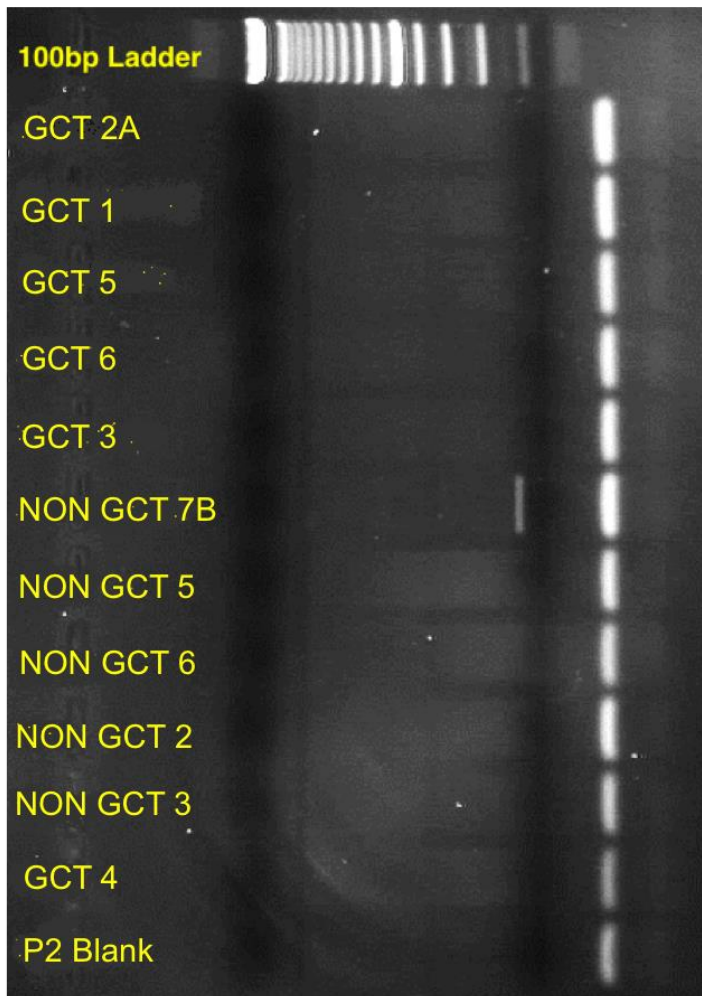


Figure 2-13: Gel of primary PCR using P2 of fixed GCT & Non GCT tissues (with exception of fresh Non GCT 7B (FW) tissue).

A nested PCR was then performed on the fixed tissues using P1 (shorter primer pair read length) to see if it would provide better bands. Similar results were identified from all fixed tissues, which did not detect any clean bands as presented in Figure 2-14.

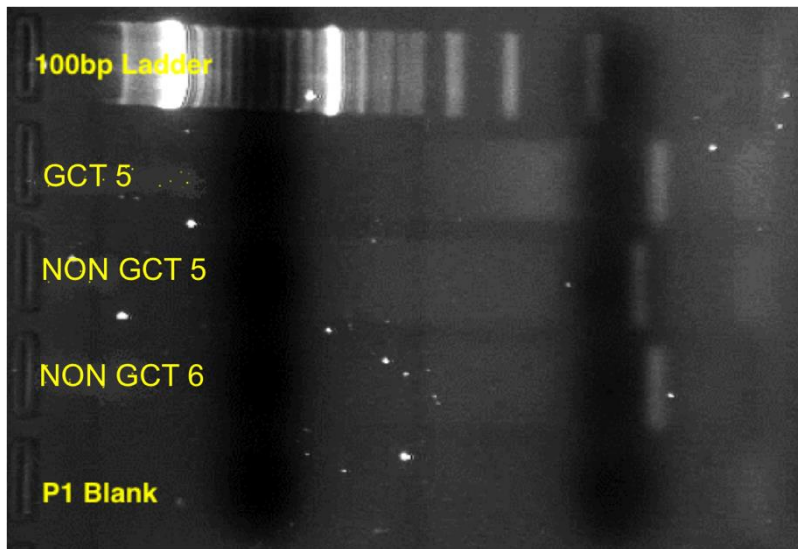


Figure 2-14: Nested PCR of one fixed GCT and two fixed Non GCT samples using P1.

2. Frozen Samples

A nested approach using primer 2 (P2) followed by primer 1 (P1) was also examined on the frozen samples as presented in Figure 2-15 and that produced smeared bands identical to fixed tissues. The shorter primer 3 (P3) was applied to perform both a primary PCR on frozen tissue and nested PCR of fixed tissues as presented in Figure 2-16. The result revealed no clear bands in the fixed tissue despite the shorter product length. Bands of the correct length were observed in the primary PCR of the frozen tissue. However, a band was also found in the P3 Blank, indicating contamination.

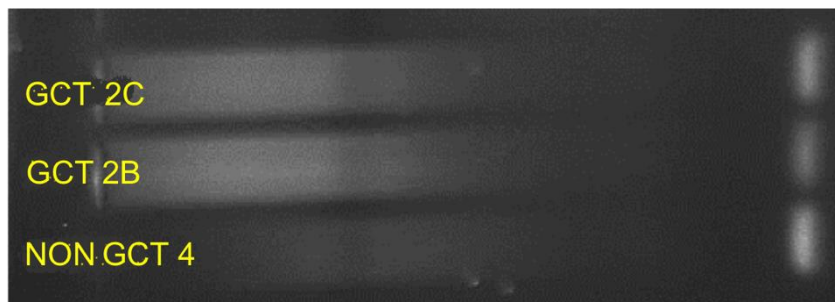


Figure 2-15: Gel of nested PCR of the frozen samples: GCT 2C (Solid), GCT 2B (Cystic) and NON-GCT 4 blood (a DNA from WBC); using P2 followed by P1.

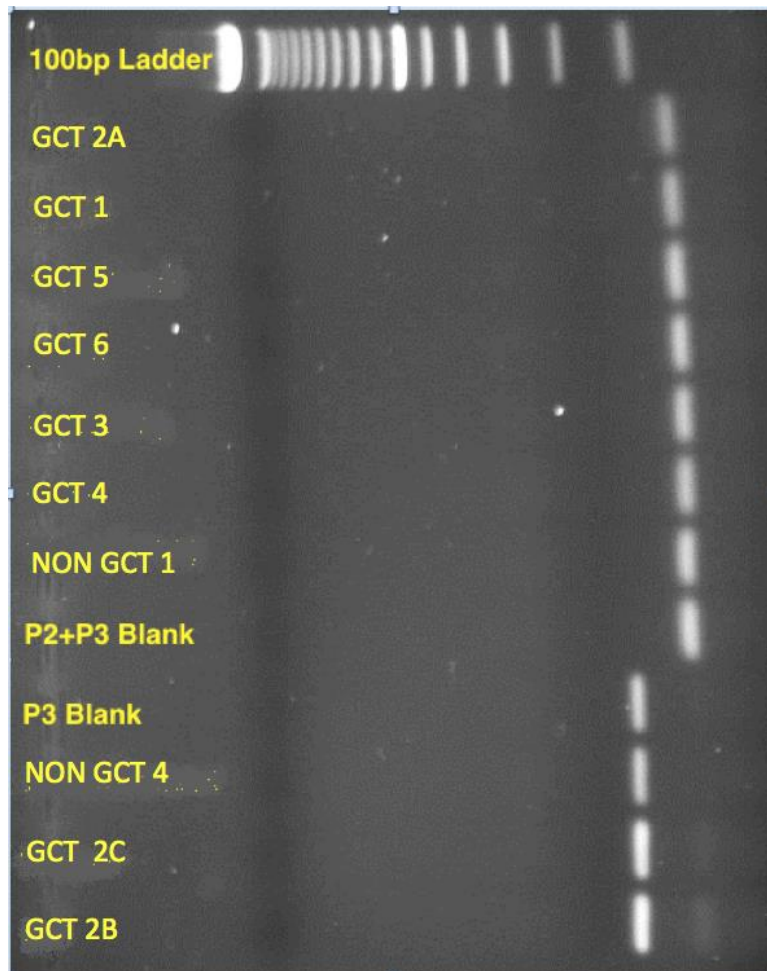


Figure 2-16: Gel of nested PCR using P3 (after P2) of fixed tissues, alongside primary PCR using P3 of frozen samples (bottom 3 wells, Blood= NON GCT4 is a DNA from WBC), GCT2B&C solid and cystic frozen). Primer dimer bands of <100bp can be seen from fixed tissues, and a product of around 100-150bp can be seen from frozen tissue.

3. Fresh Samples

Primary PCR of fresh Non GCT 7 DNA tissue using P2, showed several clean bands for all samples, with the exception of blood (NON GCT 7A), as presented below in Figure 2-17. The required result from a nested PCR became apparent, as there were multiple bands using only P2, something that could not be observed with PCRs of the fixed tissues. A nested PCR using P1 was performed to resolve any non-specific binding; the gel of these PCR products is presented in Figure 2-18, which represented clean, single bands in the expected position for the product size of 294bp, which were suitable for sequencing.

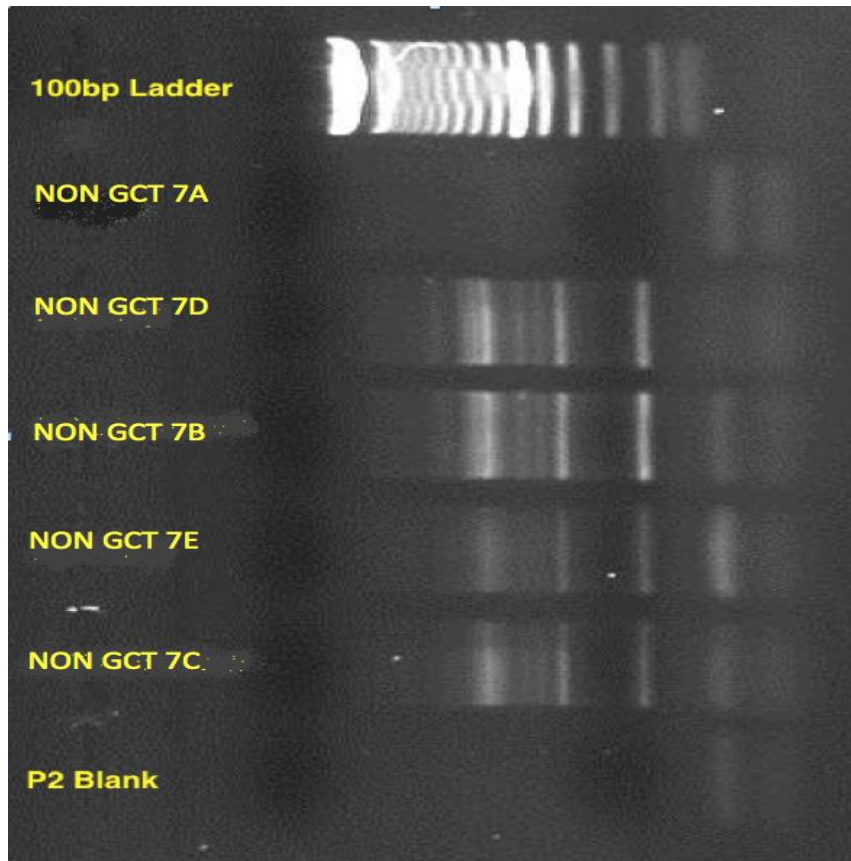


Figure 2-17: Gel of primary PCR using P2 of fresh tissue (LO = Non GCT 7D, LFW = Non GCT 7B, RO = Non GCT 7E and RFW = Non GCT 7C), and blood (Non GCT 7A is a DNA from WBC). LO is left ovary, RO is right ovary, LFW is left follicle wall and RFW is right follicle wall

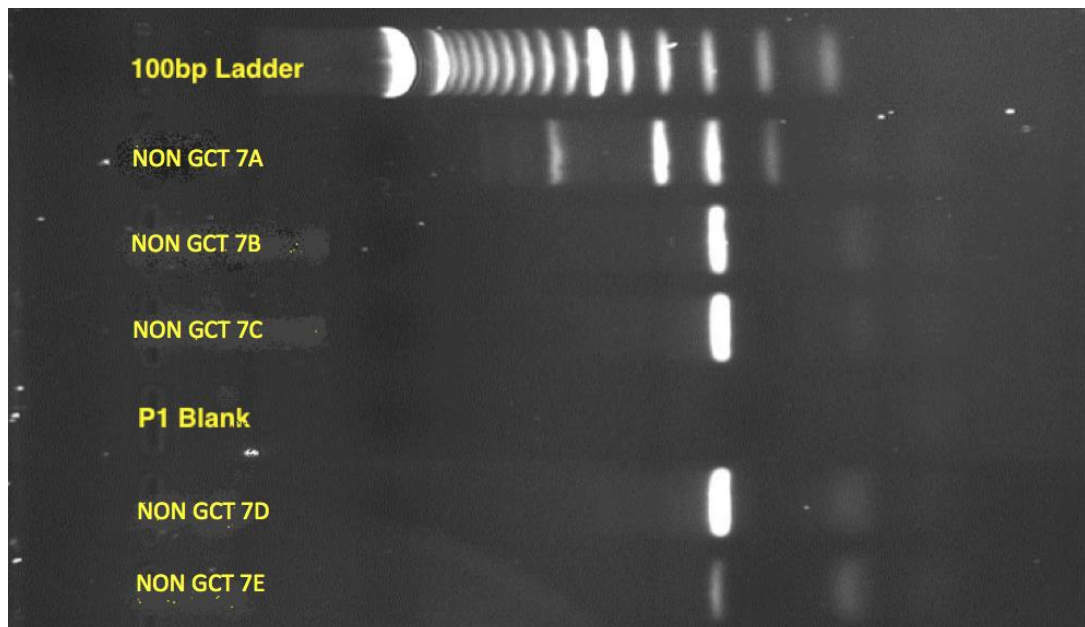


Figure 2-18: Gel of nested PCR using P1 after P2. Blood (Non GCT 7A is a DNA from WBC) and FW tissue (LFW = Non GCT 7B, RFW = Non GCT 7C) underwent purification between PCRs, while ovarian tissue (LO = Non GCT 7D and RO = Non GCT 7E) did not

A fundamental difference between gene amplification in blood and tissue can be observed from both primary and nested PCR of the fresh samples. In addition, it was unclear whether purification between PCR products was required.

Therefore, in the nested PCR of fresh tissue both 50ng/reaction of purified PCR product (Blood and Follicle wall tissue) and 3µl of unpurified PCR product were used (Ovarian tissue). This revealed that purification between the PCRs was not necessary.

4. Gradient PCR

Following the identification of smeared PCR bands obtained from frozen tissue and the multiple bands observed in fresh tissue, it was thought that primer-annealing temperature might be the cause and needed to be adjusted. To do this, gradient PCRs were performed using the Thermo Hybaid Px2 PCR machine. However, it was not until fresh tissue became available that it was confirmed that the optimum annealing temperature for P2 was 57°C. The results of a gradient PCR using fresh tissue is presented in Figure 2-19 showing that the number of bands does not decrease between 57.0°C and 57.8°C, and that bands drop off after 57.8°C. As there was no clear amplification using P1 in the gradient primary PCR, and as a nested approach resolved the appearance of multiple bands at 57°C, an annealing temperature of 57°C was also continued for P1. Despite contamination observed in P3 and the appearance of multiple bands in P2, it can be confirmed that all the primers designed worked to amplify *FOXL2*.

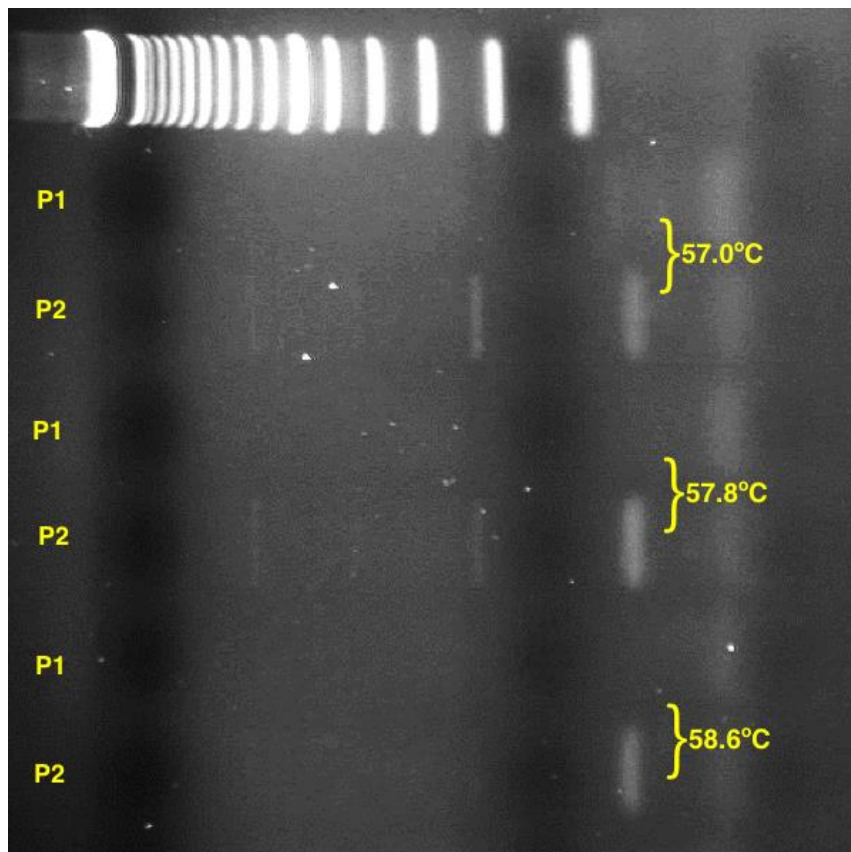


Figure 2-19: Gradient PCR on Non GCT 7 (FW) DNA at 4ng/ μ l using both P1 and P2.

2.9.1.12 Sequencing

The plate was sequenced using an Applied Biosystems Genetic Analyzer 3130xl. Before the sequencing a few steps were performed: 20 μ l Hi-Di™ formamide (Applied Biosystems, part number 4311320) was added to each well and left in the plate for two minutes followed by a brief vortex. The plate was placed into a PCR block at 95°C for two minutes then immediately removed directly onto ice. The plate was spun at 100g for one minute to remove any bubbles if necessary. Finally the plate was sequenced or stored at 4°C until ready to run.

The fresh Forward Non GCT tissue large follicle wall (LFW) was sequenced after a nested PCR with P2 followed by P1 presented in Figure 2-20.

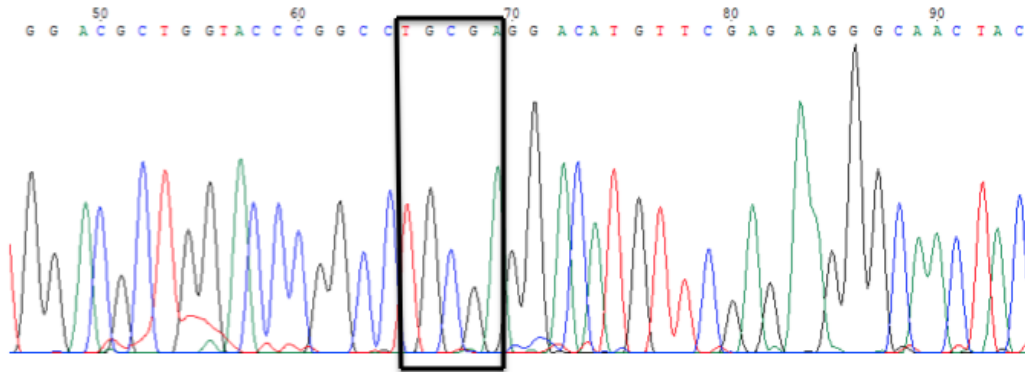


Figure 2-20: The sequence of forward Non GCT 7 (LFW) spanning mutation site, highlighted in black. A single read can be seen, with defined peaks and no overlapping sequences occurring.

The generated sequences from the fresh tissue (Non GCT) compared to the Equine *FOXL2* sequence created by P1 are presented in Figure 2-21.

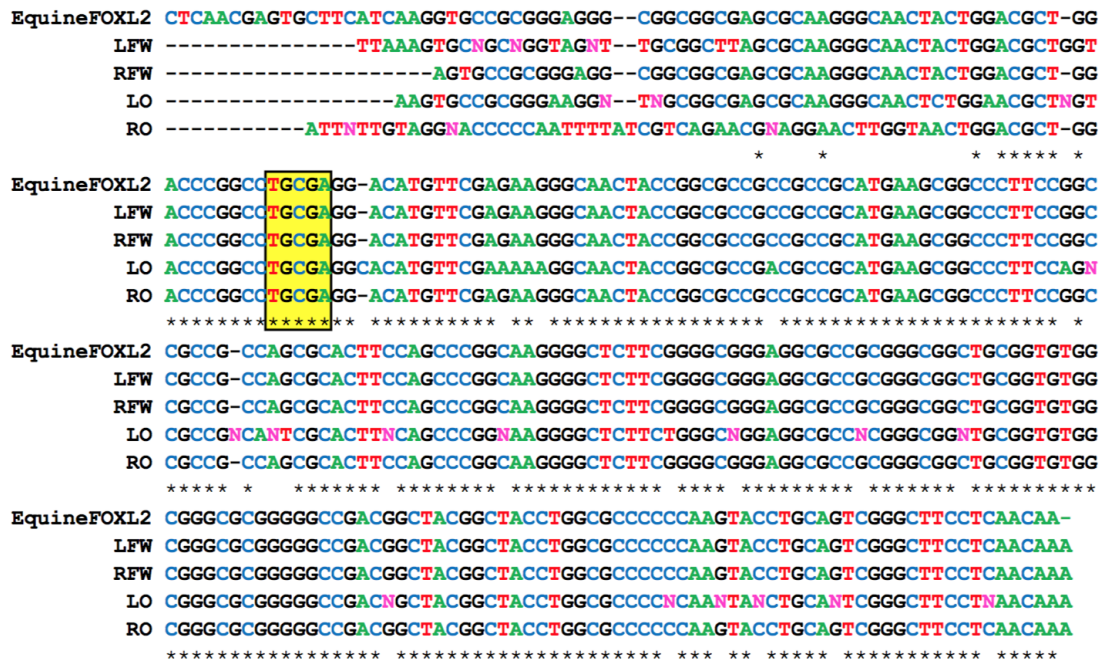


Figure 2-21: The extracted forward nucleotide sequences from the fresh tissue (Non GCT) compared to the Equine *FOXL2* P1 sequence. The mutation site possible is highlighted in yellow and as expected no mutation was seen in the four different samples. LFW: Left follicle wall, RFW: Right follicle wall, LO: Left ovary, RO: Right ovary.

As expected none of the successfully sequenced equine control tissue contained the 402C-G nucleotide mutation found in human GCTs. As no other samples (fixed, frozen or blood) produced single, clean bands, all sequences generated from these PCR products presented long, overlapping reads. This made generating an accurate sequence impossible. The data generated from the Non GCT 7A blood, processed at the same time as the fresh tissue, is presented in

Figure 2-22 showing similar results that were obtained from all fixed and frozen samples.

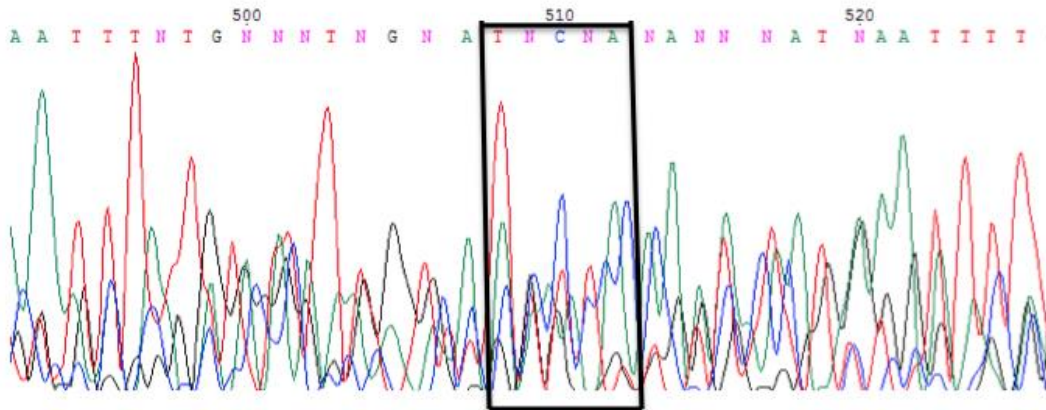


Figure 2-22: A section of the generated forward sequence from Non GCT 7A (Blood) with at least 3 overlapping sequences observed. One of the potential sequencing matches for the mutation site is highlighted.

Due to the contamination of P3 blank that appeared on the gel in Figure 2-16 a P3 PCR sequencing was performed to identify the source as presented in Figure 2-23. The contamination was suspected to be from the primer stock solution but it can be identified as the FOXL2 gene and it was probably from one of the frozen GCT sample, although the main source is unknown.

Blank	1	-----TTNGTTCTAAAAGGTNGCCTTTTNT-----	26
		
P3_seq	1	CAACCTCAGCCTCAACGAGTGCCTTCATCAAGGT-GCC-----GCGGG	41
Blank	27	AGGGCGGACCGNGAGCGCAAGGGCAACTATCTNCGACGCTGGACCCGGC	75
		.	
P3_seq	42	AGGGCGG-CGGCGAGCGCAAGGGCAACTA-CT-GGACGCTGGACCCGGC	87
Blank	76	CTGCCAGGACATGTTTCGAGAGGGCAACTACC	107
P3_seq	88	CTGCCAGGACATGTTTCGAGAGGGCAACTACC	119

Figure 2-23: Sequencing results of the P3 blank compared to the FOXL2 sequences generated by the use of P3 with area of the mutation highlighted in yellow.

2.9.1.13 Bioanalyzer findings

Some of the extracted DNA samples described above and some new nested PCR products extracted samples were analysed for quality using the Bioanalyzer of the Polyomics Glasgow facility. This is because we suspected primer dimer contamination or low quality DNA to interfere with PCR and BigDye sequencing results. The DNA samples are the first seven peak graphs and the other four are

GCT PCR products as seen in Figure 2-24. The peak at 35nt (nucleotides) is a marker peak, which is part of the kit. PCR product is the peak at about 127nt. The other peaks (about 35nt) are the primers or primer dimers. The first three plots show much more degradation than the other four. The mares called DNA NON GCT 3 and DNA NON GCT 6 were rerun on the Figure 2-25 since they were slightly over diluted on the first chip. The bioanalyzer traces for the PCR products have also been included Figure 2-26. When the chip runs it has a marker peak at 35nt (nucleotides) to align all the traces but some of samples have additional peaks next to the marker, which are probably PCR primers. These may have interfered with the sequencing that was done during the first experiment giving a double sequence. In some samples the primer peaks are much larger than PCR product such as NON GCT 1 on Figure 2-25.

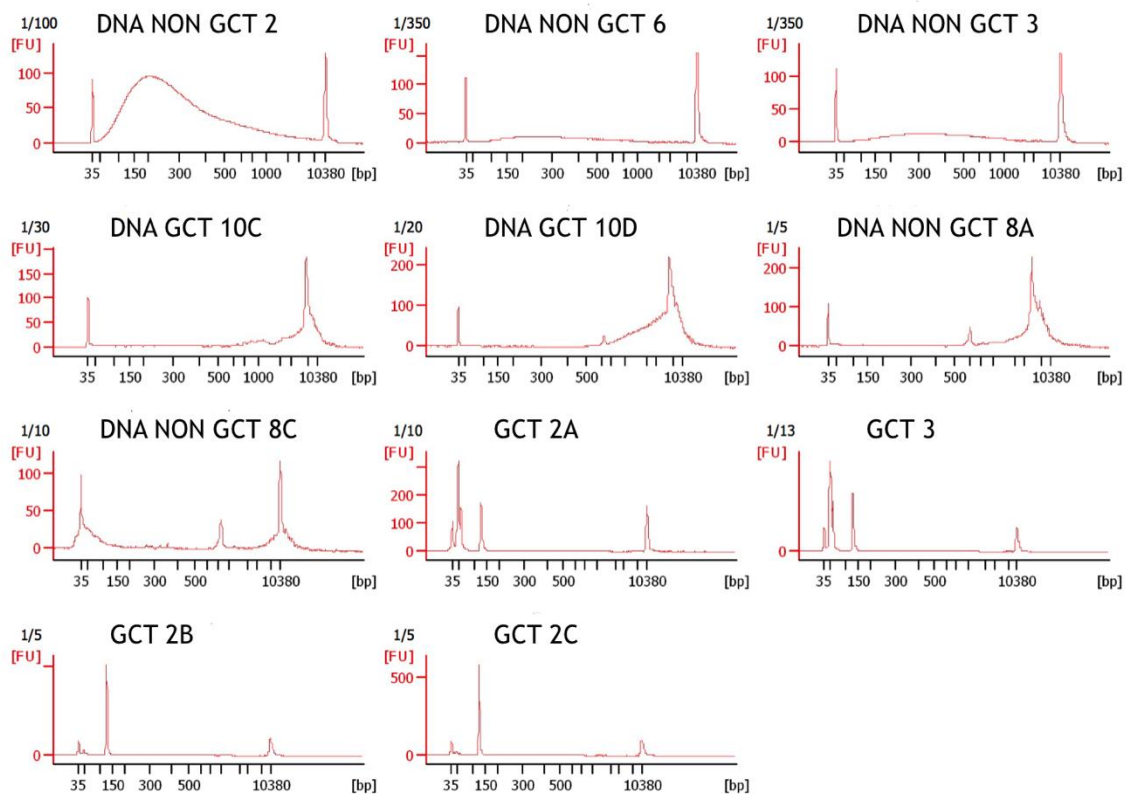


Figure 2-24: DNA (DNA and ID number) and PCR products (ID number) bioanalyzer. The x-axis is the size of the fragments and the Y-axis is the amount of sample at any point.

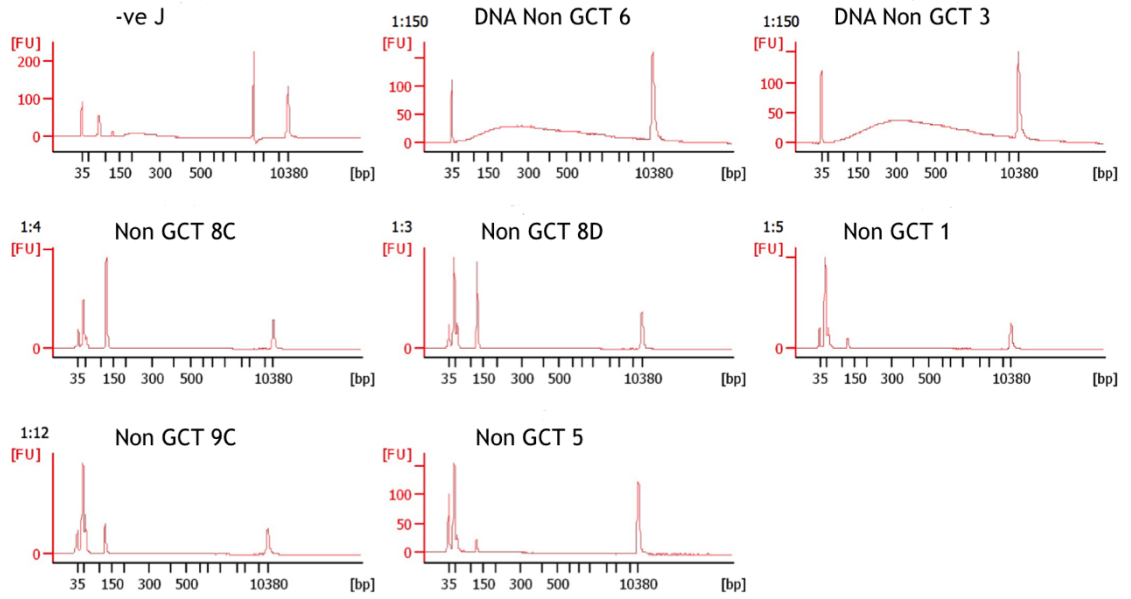


Figure 2-25: The first two graphs are the repeated DNA samples and the other 7 are control PCR products.

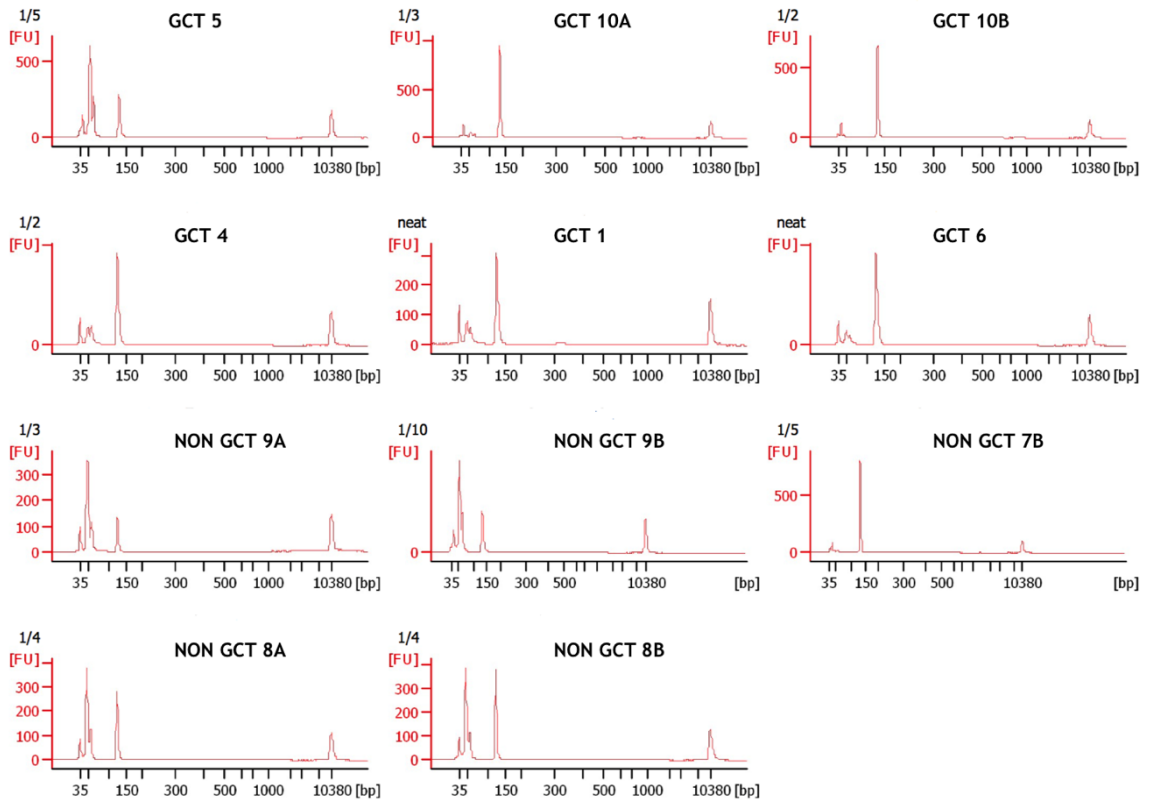


Figure 2-26: The first 6 graphs are the GCT PCR products and the other 5 are the control PCR product

Chapter 3 Text mining

Aims:

1. Investigate epidemiological aspects of mare ovarian pathology and granulosa cell tumours.
2. Text-mine a UK veterinary practice clinical database to facilitate the epidemiological investigation of ovarian pathology and ovarian tumours, in particular granulosa cell tumours (GCT).

Objectives:

1. Use Simstat and WordStat¹ software to apply text mining to a large UK veterinary clinical database.
2. Estimate the prevalence of ovarian pathology, ovarian tumours and GCT in seven first opinion veterinary practices in the UK.
3. Identify risk factors for the development of ovarian pathology, ovarian tumour and GCT to determine clinical features that may aid early diagnosis or indicate future risk.

¹ Provalis Research

3.1 Introduction

The equine breeding industry perceives abnormalities of the ovary(s) to be the most significant concern reflecting negatively on breeding productivity (McCue and McKinnon, 2011). According to (McCue et al., 2006), the susceptibility of horses to ovarian tumours is greater than other domestic species accounting for approximately 2.5 % of all equine cancers. There does not appear to be any breed (McCue et al., 2006, Crabtree, 2013) or age predisposition with ovarian tumours having been identified in newborn, 3-month old and 2-20 years olds (Gunduz et al., 2010, Crabtree, 2013) as well as in a 15 month old pre-pubertal filly (Charman and McKinnon, 2007).

Mares ovaries are known to be affected by many other pathological diseases apart from ovarian tumours such as anovulatory follicle (McCue and Squires, 2002), ovarian haematoma and luteal dysfunction (Troedsson et al., 2003). Examples of ovarian tumours are GCT, teratoma, cystadenoma and dysgerminoma, the most common of these being GCT (Watson, 1999). A retrospective study of laparoscopic ovariectomy on 157 mares with various clinical problems such as infertility, abnormal behaviour due to hormonal disturbance, ovarian tumours and neutering was conducted by (Roecken et al., 2011). The authors used a medical database that had been gathered between 1996 and 2009 by the Justus-Liebig University, Germany and Utrecht University, The Netherlands. The aim of that study was to evaluate the most appropriate ovarian treatment and surgical approach amongst the range performed by various surgeons during 206 surgeries. They concluded that the best treatment for ovarian tumour was indeed surgical removal (ovariectomy), particularly if it is unilateral, allowing the contralateral ovary to carry on functioning 6-months post operation (De Bont et al., 2010) and that a unilateral laparoscopic approach was optimal.

Significant changes have occurred over the last five decades in the modern computing system for medical records (Salton and Lesk, 1968, de Bruijn and Martin, 2002). Moreover, the use of computer databases in general practice for public health auditing and commissioning has increased significantly ((Pringle et al., 1995). The collection of data retrospectively and prospectively from either veterinary practice records or electronic medical records for research purposes

has gradually expanded (Jones-Diette et al., 2014, Lam et al., 2007, Mattin et al., 2014, O'Neill, 2012, O'Neill et al., 2012, O'Neill et al., 2013, Oswald et al., 2010, Radford et al., 2011). Structured and unstructured knowledge types are the two main kinds of system used for information storage, data usage and investigation. Both are used to extract and analyse stored data (de Bruijn and Martin, 2002, Garten et al., 2010).

A previous analysis using Wordstat and Simstat content analysis software was conducted by Lam et al. (2007) to identify reasons for racehorse retirement from racing at the Hong Kong Jockey Club over a period of 10 years. Analysis of a total of 3,727 retirement records revealed 95% of the text records could be successively extracted in approximately 2-weeks of work. In addition, Anholt et al. (2014) has used the same software for disease surveillance in small animal veterinary practice in Canada collected from 12 practices over a period of three years (2007 to 2009, inclusive). Text-mining allowed the authors to recover cases of enteric disease, with high sensitivity and specificity, which they were then able to investigate further.

Natural language processing (NLP) considers text mining as an important element to contribute positively in automated analytic procedures (Anholt et al., 2014a). Text mining in scientific research has been used to achieve specific objectives such as retrospective work to clarify disease prevalence (Chapman et al., 2005, Chapman et al., 2004), investigating clinical symptoms and unwanted secondary effects (Chapman et al., 2004), medical care outcomes (Penz et al., 2007) and prognostication and survival examination (Penz et al., 2007, Bradley et al., 2005). In this chapter text-mining is used to first estimate the prevalence of ovarian pathology, ovarian tumours and more specifically GCT and then to aid in the identification of risk factors or prodromal clinical signs for ovarian pathology or GCT.

3.2 Materials and Methods

3.2.1 Data

The dataset used in this investigation was collated in 2013 and includes clinical data from 1987 to 2012, from seven veterinary practices in the UK (Duz et al.,

2016). These data included a total of 515,832 records of which 194,466 referred to female horses and contain details of identification, date of veterinary record, gender, practice, breed and date of birth, which ranged from January 1952 to November 2012.

3.2.2 Development of the categorisation dictionary in free text mining software

WordStat v 7.0¹ a modular constituent of statistical software Simstat v 2.6² is a linguistic based product that enables distinguishing of pre-defined words or compound expressions incorporated into a self-characterized categorisation dictionary within any given free-text. The output is all rows of information ("cases") that match any word or words contained within the categorisation dictionary. The program includes a feature to ignore terms of minimal semantic use (terms between pronouns, conjunctions and verb modifiers) unless these are incorporated into the categorisation word dictionary. This element accelerates the procedure by removing many repeated words throughout the text that have little bearing on the translation of the content.

The "Frequency tab" in WordStat produces a table of every remaining word inside of the dataset and this list can be utilized to facilitate further characterisation of the categorisation "inclusion dictionary". This feature makes it significantly easier to identify and then include (unpredictable) spelling errors and abbreviations that would otherwise not be included as 'case' records. This list of words and phrases can be exported as a spreadsheet and assessed utilizing other software, such as ³MS Excel.

The software also offers the ability to include words with the same root by including the character "*" at the end of the regular root. For instance, "ovar*" would identify all cases including a word starting as "ovar", such as "ovary", "ovarian", "ovaries", and so on. The 'word list' is an extremely valuable tools as it provides the user the means to describe a lexicon that includes every applicable term and their varieties that are actually present in the dataset. It is

³ MS Excel

essential to note that this element makes the dictionary exceptionally 'dataset-specific' and if significant quantities of new data are added the lexicon should be updated to incorporate new terms that may be present in the new data that were not part of the original database.

As the identification of a particular single word may not always indicate a 'case', negations must be considered. For example, if the characterisation dictionary includes the word "oestrus", a sentence, such as "the mare is not in oestrus" would be classified as positive, which is clearly incorrect. Recognisable proof of such false positives is a critical procedure as it characterizes the specificity of the analysis (Anholt et al., 2014b). WordStat also supports the utilization of boolean functions ("AND", "OR", "NOT") or different modifiers ("NO", "IF", "WHICH") and proximity operators ("NEAR", "BEFORE", "AFTER"). For instance, an investigator may determine that any sentence for which "not" is present within three words of "oestrus" be categorised in the "not oestrus" group rather than "oestrus" group. A list of rules to eliminate false positive cases can be incorporated into an "exclusion dictionary" that could then give a list of those cases that ought to be removed from the "inclusion dictionary".

Together these features of the software help to maximise the sensitivity and specificity of the process such that 'cases' and 'unaffected' animals are correctly identified. Nevertheless, the degree of variability in expression in free-text records is wide and finding rules that fit perfectly is frequently impractical and a level of error is always likely to be present. Consequently it is important to report sensitivity and specificity of the inclusions dictionaries utilised for the specific dataset being mined as has been done as part of this work.

3.2.3 Inclusion dictionary

The clinical records dataset was imported into SimStat and by identifying the 'horse' column as the independent variable and the clinical 'note' column as the dependent variable WordStat was initiated.

Three separate dictionaries were created in order to identify cases of: ovarian pathology; ovarian tumours; and more specifically GCT. The complete lists of words and phrases for each of these dictionaries are included in Appendix 2.

3.2.4 Statistical analyses

The prevalence and 95% confidence intervals for each outcome were calculated using the methods proposed by Wilson (1927) and recommended by (Agresti and Coull, 2000, Brown et al., 2001), which is appropriate for rare outcomes.

The records of all cases were checked and read in detail. The dates of each outcome were confirmed as well as the age at which they occurred. Potential risk factors such as vaccination, worming, respiratory disease, digestive or orthopaedic diseases etc. were recorded from the preceding clinical records for each case horse. The presence or absence of those risk factors was coded numerically. For each of the positive cases of each outcome three unaffected horses, from the same practice as the case horse and that were represented in the dataset at the same time as the case horse, were randomly selected from the main database. The same risk factors were evaluated for each of those horses from the first entry record to the last entry prior to the date of the relevant case.

Univariable (factors with $p < 0.2$ were available for inclusion in the next stage), followed by multivariable logistic regression analysis was used to identify any clinically recorded indicators associated with an increase or decrease in the likelihood of a horse ultimately being diagnosed with ovarian pathology or more specifically GCT.

3.3 Results

3.3.1 Data details

The 515,832 records included 194,466 records for female horses, 91,724 records for male horses, 176,966 records for geldings and 52,676 records with unspecified gender. These data included details of variable numbers of female horses from each practice with an absolute number of veterinary reports for each as presented in Table 3-1. Of the seven practices six of them had similar numbers of records per horse (range 5.1 to 8.8). However practice number '7' had significantly more records per horse (13.6) compared with the average of the other practices (T-test p -value < 0.001). The female horses included in future analyses were of different breeds as presented in Table 3-2. However, the

greatest proportion of the records (57%) was of unknown breed. The age of those females are presented in Figure 3-1. For 23,163 females age was not recorded. The mean horse age of records representing female horses was 11.31 years (median; 9.95 years).

Table 3-1: Number of records of female horses from each practice with veterinary reports

Practice number	Number of records for female horses	Number of horses	Average number of records per horse
1	10,933	1245	8.8
2	107,622	14601	7.4
3	3,001	589	5.1
4	31,720	4996	6.3
5	16,585	1953	8.5
6	16,879	2066	8.2
7	7,726	569	13.6
Total	194466	26019	7.5

Table 3-2: Number of records for female horses per breed

Breeds	Number of female records
Arab	3,315
Cob	5,100
Draught	3,606
Native	5,387
Other	19,374
Pony	3,921
Thoroughbred	27,455
Unknown	111,067
Warm Blood (WB)	6,759
Welsh	8,482
Total	194,466

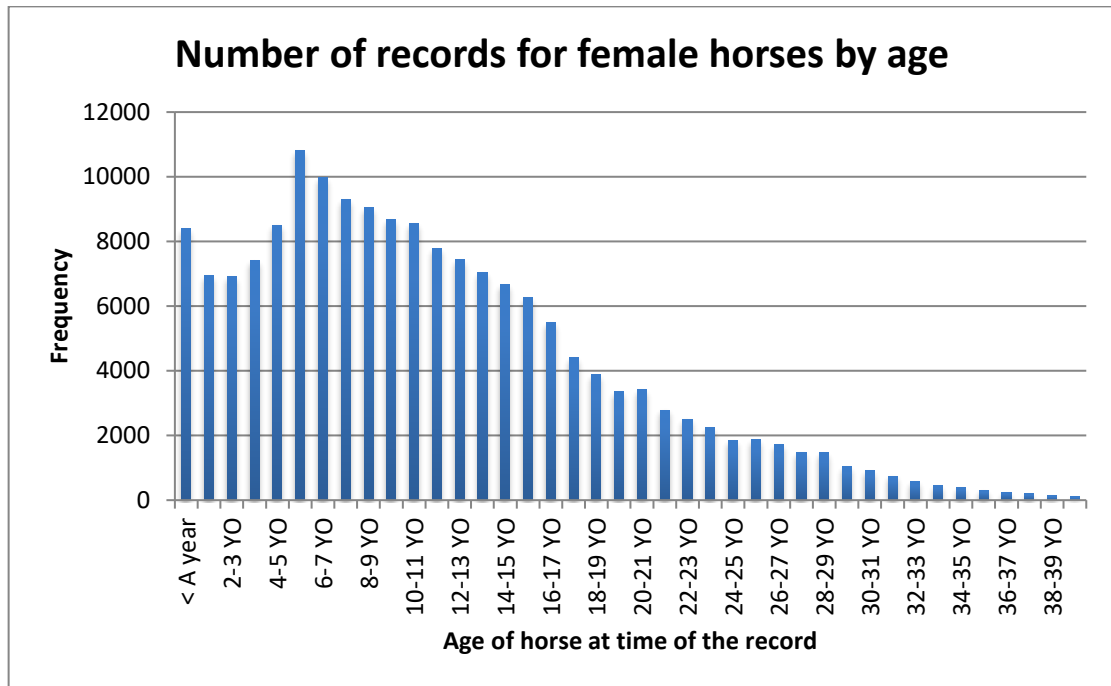


Figure 3-1: The number of records for female horses by age.

3.3.2 Prevalence of different ovarian conditions.

3.3.2.1 Ovarian Pathology

In the ovarian pathology dictionary, 143 cases were initially identified from 194,466 records representing 26,019 female horses. All entries of those cases were checked in the main database and 65 cases from all categories were truly positive representing cases of anovulatory follicles, cyst-like structure, inactive ovaries, irregular oestrus, infertility and so on as shown on Table 3-3. Therefore, this gives an ovarian pathology prevalence of 0.25 percent.

Table 3-3: Cases of ovarian pathology as identified by the text mining process and confirmed (or otherwise) as such by the reading in detail of each 'case' record (represented by 'Test +ve' or 'Test-ve').

No.	Categories	Wordstat +ve	Test -ve	Why test -ve	Test +ve	Why test +ve
1	Follicular development abnormalities/ Hormonal exogenous	64	58	Gynecology exam/ P4 lab test/ scan mare	6	Irregular ovary/inactive ovary/ behavioural and painful ovary/no cycling
2	Follicular development abnormalities/ovarian dysfunction	4	1	Uterine biopsy infertility	3	Long time infertility
3	Miscellaneous abnormalities	2	1	Same ID no extracted on GCT Cat.	1	Ref for GCT removal
4	Ovarian tumor/Cystadenoma	5	4	Cystic like structure on uterine horn	1	Enlarged ovary cystic like structure
5	Ovarian tumor/GCT	59	11	Suspect GCT	48	GCT/ ovariectomy/irregular oestrus/ Inactive ovary
6	Ovarian tumor/Teratoma	2	0		2	Teratoma
7	Ovulation abnormalities/anovulatory follicles	7	3	Possible haemorrhagic follicle/no sign of cystic	4	Haemorrhagic follicle/treat cystic ovary
Total		143	78		65	

3.3.2.2 Ovarian Tumours

The dictionary of ovarian tumours had four categories as described in Table 3-4. One of them was dysgerminoma that had no record in the database, while teratoma had two potential false positives because it was mentioned as likely teratoma or a question mark had been written after the word teratoma. Cystadenoma had also five false positive cases due to the sentence that was extracted as “cystic like structure”. Overall the category of ovarian tumours identified 85 cases from 26,019 female horses, two were GCT positive but as expected these two were also extracted as part of the GCT dictionary and 83 were false positive simply stating ‘large ovary’ or ‘small inactive ovary’ without further information relating specifically to tumours. Ultimately the tumour dictionary was discarded from the statistical analysis because it added nothing more than the GCT dictionary, due to almost complete overlap in case identification.

Table 3-4: Ovarian tumours as identified by text mining and confirmed (or otherwise as such) following detailed examination of each ‘case’.

No of cases	Reason for identification	Positive cases	Not true positive	Why not confirmed?	
1	Teratoma	0	1	Teratoma?	
1	Teratoma	0	1	Likely teratoma	
1	Cystadenoma	0	1	-ve x ray dense bone visible at the site of cystadv	
5	Cystadenoma	0	5	Cystic like structure	
1	Dysgerminoma	0	1	-	
1	GCT	0	1	Multilocular ovaries symmetry in sizes. Both ovaries enlarged	
17		0	17	Enlarged ovaries	
8		0	8	Ovarian cysts	
2		0	2	Ovarian adhesion	
3		0	3	Ovarian haematoma	
24		0	24	Painful ovary	
1		0	1	Anoestrus ovaries	
17		0	17	Small inactive ovaries	
1		0	1	Persistent oestrus	
1		1	0	LO Large mass (grapefruit), multilobulated lesion	
1		1	0	Ovarian tumour	
Total			2	83	

3.3.2.3 GCT

In the dictionary of GCT, 115 potential cases were exported in five categories from the dataset and out of these only 11 cases were truly positive for GCT (Table 3-5). The software extracted those negative cases because the GCT was written in the text such as 'possible GCT', 'suspect GCT', 'likely GCT' and so on (Table 3-6). Five cases from the false positive table were discarded because the software extracted them as tumours on penis and sheath. This occurred due to some practices used the same ID number of the dam to their offspring even if they were males.

Table 3-5: Positive granulosa cell tumour case

No.	Positive cases text	Ovary site
1	GCT of the LO reported to [REDACTED] started June 2009	Left
2	LO GCT, RO very small	Left
3	Referred to [REDACTED] for GCT removal	Right
4	Clinical Hx and ovarian appearance consistent with GCT	Right
5	RO small 3-3.5 cm, LO 7cm firm. This finding combined with recent behavioural changes, which are consistent with early GTCT. Discussing with [REDACTED] for L ovariectomy laparoscopically.	Left
6	Visit Hx of behavioural problems > ovariectomy > rectal exam, RO palpably normal 6cmx3cm GCT	Left
7	LO 15 cm Diam GCT	Left
8	Large mass consistent with GCT, ovary size of grapefruit, RO CL and 45mm follicles	Left
9	Multilobulated (Multiloculated) Granulosa, mounting other mares in field 3 weeks LO very large	Left
10	Stallion like behaviour last 4 mo large granulosa cell tumour LO	Left
11	R O granulosa cell T Multi loculated ovary orange size 11ml regulate SID 10 D then re assess behaviour	Right

Table 3-6: Potential GCT cases identified by text mining that were, upon detailed examination deemed to be false positives.

No. of not true cases	Why not true?
3	Possible GCT
5	Suspect GCT
2	Likely GCT
1	To rule out GCT
3	Blood taken for inhibin Test for GCT
5	Question mark (?) for GCT
7	No evidence of GCT
2	No sign of GCT
2	No GCT seen on scan
2	Haemorrhagic follicle or GCT
1	Appearance GCT
1	Owner concern about GCT
1	Results do not support GCT
1	If GCT owner will not go for surgery
1	Discussed GCT
1	Highly suggestive of GCT
25	Eosinophilic Granulomas
17	Granulomatous
1	GCT232
1	Connective tissue tumors
1	Sarcoid tumours
2	Multiple tumours prop. Melanomas
1	No clear tumors
1	Round tumours
2	Eye tumours
1	Tumours under jaw
1	Tumors increase in size
1	No sign of tumours
1	Gluteal tumours
1	Detect tumours
1	Anal tumours
1	Nostril tumours
1	Spindle cell tumors, fibrosarcoma
2	Equine mast cell tumors on horse neck
Total = 99	

3.3.3 Sensitivity and specificity

The sensitivity of the text mining process to identify cases of ovarian pathology was 100% (65/65) and the specificity to correctly identify truly negative cases of ovarian pathology (i.e. unaffected horses) was 99.7% (25,876/25,954) - see Table 3-7.

Table 3-7: Sensitivity and specificity of the ovarian pathology dictionary

Word stat/Test	True status		Total cases no.
	+ ve ovarian pathology	- ve ovarian pathology	
Word stat as +ve	65	78	143
A Test - ve	0	25876	25876
	65	25954	26019

With 65 confirmed cases of ovarian pathology amongst 26,019 female horses, the prevalence estimate for definite cases of ovarian pathology was 0.25% (95% confidence interval = 0.20% - 0.32%).

The sensitivity of the text mining process to identify cases of GCT was 100% (11/11) and the specificity to correctly identify truly negative cases of GCT (i.e. unaffected horses) was 99.6% (25,904/26,008) - see Table 3-8.

Table 3-8: Contingency table of GCT text mining.

Word stat	True status upon detailed examination		Total
	+ ve GCT	- ve GCT	
+ve	11	104	115
- ve	0	25,904	25,904
	11	26,008	26,019

With 11 confirmed cases of GCT (Table 3-5) amongst 26,019 female horses, the prevalence estimate for definite cases of GCT was 0.04% (95% confidence interval = 0.02% - 0.08%). If the 15 'possible and suspect' cases of GCT (highlighted in bold in Table 3-6) were also included the prevalence estimate would have increased to 0.1% (95% confidence interval = 0.07% to 0.15%).

3.3.4 Risk factors for ovarian pathology and GCT

Table 3-9 Univariable logistic regression analysis for ovarian pathology

Variables - type of clinical examination	P- Value	Cases (n= 65)	Control (n = 195)	Odds Ratio	95% CI
Orthopaedics	< 0.001	29 (44.62%)	150 (76.92%)	0.24	(0.13, 0.44)
Anti-inflammatory	< 0.001	25 (38.46%)	120 (61.54%)	0.39	(0.22, 0.69)
Antibiotics	0.003	14 (21.54%)	81 (41.54%)	0.39	(0.20, 0.74)
Sedation	0.003	15 (23.08%)	84 (43.08%)	0.40	(0.21, 0.75)
Respiration	0.006	6 (9.23%)	47 (24.10%)	0.32	(0.13, 0.79)
Dressing	0.010	4 (6.15%)	36 (18.46%)	0.29	(0.10, 0.85)
Digestive disease	0.093	17 (26.15%)	73 (37.44%)	0.59	(0.32, 1.10)
Vaccination	0.14	20 (30.77%)	80 (41.03%)	0.64	(0.35, 1.16)
Internal/Ext parasite, Deworming, Fungicides	0.175	4 (6.15%)	23 (11.79%)	0.49	(0.16, 1.47)
Behaviour	0.183	3 (4.62%)	3 (1.54%)	3.10	(0.61, 15.74)
Eye Treatment	0.188	6 (9.23%)	9 (4.62%)	2.10	(0.72, 6.15)
Antiviral	0.279	2 (3.08%)	2 (1.03%)	3.06	(0.42, 22.20)
Reproductive clinical record	0.339	12 (18.46%)	47 (24.10%)	0.71	(0.35, 1.45)
Physiotherapy	0.457	2 (3.08%)	3 (1.54%)	2.03	(0.33, 12.43)
Dietary supplement	0.539	3 (4.62%)	13 (6.67%)	0.68	(0.19, 2.45)
Hormonal	0.560	5 (7.69%)	11 (5.64%)	1.39	(0.46, 4.17)
Age	0.59	Mean=14.47 Median=14.80	Mean=13.73 Median=12.20	1.01	(0.97, 1.05)

In the univariable analysis for ovarian pathology, six separate categories of clinical record (as indicated by a **bold p-value**) prior to the case date were associated with a reduced likelihood of the horse being ultimately diagnosed with ovarian pathology Table 3-9.

Table 3-10: Multivariable logistic regression analysis for ovarian pathology

Variables	P- Value	Cases (n= 65)	Control (n = 195)	Odds Ratio	95% CI
Orthopedics	< 0.001	29 (44.62%)	150 (76.92%)	0.22	(0.12, 0.41)
Respiration	0.005	6 (9.23%)	47 (24.10%)	0.29	(0.11, 0.75)
Eye Treatment	0.030	6 (9.23%)	9 (4.62%)	3.83	(1.19, 12.28)

In the final multivariable analysis for ovarian pathology two types of prior clinical record were associated with a reduced likelihood of ovarian pathology (previous orthopaedic or respiratory examination) and one type of record (previous record of eye treatment) was associated with an increased likelihood of ovarian pathology Table 3-10.

Table 3-11: Univariable logistic regression analysis for GCT

Variables	P- Value	Cases (n= 11)	Control (n = 33)	Odds Ratio	95% CI
Reproduction	< 0.001	9 (81.82%)	7 (21.21%)	16.71	(2.92, 95.68)
Sedation	0.004	3 (27.27%)	25 (75.76%)	0.12	(0.02, 0.56)
Physiotherapy	0.026	3 (27.27%)	1 (3.03%)	12.00	(1.097, 131.24)
Digestive disease	0.045	4 (36.36%)	3 (9.09%)	5.71	(1.03, 31.53)
Age	0.064	Mean=8.16 Median=8.05	Mean=13.15 Median=11.60	0.88	(0.75, 1.03)
Antibiotics	0.153	5 (45.45%)	23 (69.70%)	0.36	(0.09, 1.47)
Orthopedics	0.256	8 (72.73%)	29 (87.88%)	0.37	(0.07, 1.99)
Antiviral	0.436	1 (9.09%)	1 (3.03%)	3.20	(0.18, 55.95)
Anti-inflammatory	0.443	7 (63.64%)	25 (75.76%)	0.56	(0.13, 2.42)
Dressing	0.577	3 (27.27%)	12 (36.36%)	0.66	(0.14, 2.95)
Vaccination	0.596	4 (36.36%)	15 (45.45%)	0.68	(0.17, 2.80)
Internal/Ext parasite, Deworming, Fungicides	0.672	2 (18.18%)	8 (24.24%)	0.694	(0.12, 3.90)
Dietary supplement	0.737	1 (9.09%)	2 (6.06%)	1.55	(0.13, 18.95)
Respiration	0.828	2 (18.18%)	7 (21.21%)	0.82	(0.14, 4.72)

In the univariable analysis for GCT, four separate categories of clinical record (as indicated by a **bold p-value**) prior to the case date were associated with the likelihood of the horse being ultimately diagnosed with GCT Table 3-11.

Table 3-12 Multivariable logistic regression analysis for GCT

Variables	P- Value	Cases (n= 11)	Control (n = 33)	Odds Ratio	95% CI
Reproduction	< 0.001	9 (81.82%)	7 (21.21%)	18.37	(2.55, 132.26)
Sedation	0.012	3 (27.27%)	25 (75.76%)	0.11	(0.01, 0.72)

In the final multivariable analysis for GCT two types of prior clinical records were associated with the likelihood of GCT. Having had a previous reproductive examination was associated with an 18-fold increase in the likelihood of subsequently being diagnosed with GCT. In contrast horses that had a previous record of sedation were associated with a reduced likelihood of subsequent GCT Table 3-12.

3.4 Discussion

A retrospective analysis of equine ovarian pathology in particular ovarian GCT and health records of horses collected from seven equine practices distributed all over United Kingdom was executed. An analysis of the content of the free text records was conducted to ascertain the prevalence of equine ovarian pathology and GCT. Most practices had similar numbers of records per horse apart from practice number '7' which had significantly more records per horse, despite of low number horses compared, with the average of the other practices. This practice is located in a remote, rural part of the UK, where the density of horses is likely to be low, as is the number of equine veterinary practices. It may be that this practice genuinely serves the majority of horses in the area and that, due to the relative lack of competition from other equine practices, has a more 'loyal' client base, demonstrated as significantly more visits per horse than the other practices. It is also possible that the type of horse and/or horse owner in this area is different. A greater number of visits per horse would result if horse owners in the area keep their horses for longer (maybe due to the lack of opportunity, market or need to sell).

This study determined that content mining recovered ovarian pathology and ovarian GCT cases from electronic veterinary medical records with high

sensitivity and specificity (100%, 99.7% & 100%, 99.6%, respectively). From these analyses it is clear that, in the population of female horses represented by these records, both ovarian pathology and GCT are rare. No previous estimates of the prevalence of either ovarian pathology or GCT have been identified in the literature. Anecdotal reports, and clinical experience, would suggest that these conditions are indeed rare, but it is possible that due to the nature of the data recorded these estimates are underestimates of the true population prevalence. Teratoma and dysgerminoma were not encountered in this study and the wider literature also indicates that their occurrences are very rare compared to other domestic animals (Catone et al., 2004, da Encarnacao Fiala et al., 2011, Lefebvre et al., 2005, Gehlen et al., 2006, Chandra et al., 1998, McLennan and Kelly, 1977, Vanhaesebrouck et al., 2010).

Logistic regression analysis was performed to attempt to identify routinely recorded clinical features of horses that may be used to predict likely future development of ovarian pathology or GCT. For the analysis of ovarian pathology the clear finding is that previous orthopaedic or respiratory examinations were associated with a reduced likelihood of subsequent ovarian pathology. It is highly unlikely that these findings represent any true protective effect of these two types of clinical examination. The reason for these findings most likely lies with the way the control population were selected at random and the fact that these two particular types of examination are very common. So it would appear that this analysis simply identified, in the control population, two common types of veterinary examination that may be less common in horses that are susceptible to ovarian pathology. The reasons for the positive association between previous eye treatment and subsequent ovarian pathology are equally difficult to understand. The final multivariable model of ovarian pathology suggested that previous eye treatment was associated with a 3.8 fold greater risk of ovarian pathology. Without any clear aetiological reason or pathway for this association this is most likely to be a chance finding. Indeed with only six cases and nine controls having had a previous eye treatment this is the most likely explanation of this finding.

With respect to the logistic regression analysis for GCT a similar finding was identified (as with respiratory and orthopaedic examination for ovarian

pathology) for sedation. However, in this analysis it was clear that previous reproductive examination, as one might expect, was very strongly associated with subsequent GCT. Four of the cases of GCT that had previous reproductive examinations had those examinations on the day that GCT was confirmed, clearly indicating a suspicion of GCT on that day. The other five cases had initial reproductive examinations between 12 and 108 days before the diagnosis of GCT was confirmed. Six out of nine GCT cases that also had a previous reproductive examination showed behavioural changes such as mounting other mares, stallion like behaviour and most developed these behaviours between three and four weeks prior detecting GCT. In all six cases regumate treatment did not alleviate their behaviour problems. In addition, two cases had GCT diagnosed around foaling or while in-foal: One mare was diagnosed with a GCT post foaling and one had a twin on day 40 then aborted on day 90 the same day that GCT was confirmed. It is likely that for some of these the prior reproductive examinations may have been totally unrelated to any suspicion or clinical signs of GCT. However, without greater detail included within the clinical records it is not possible to confirm this.

The mares' age when the GCT was confirmed in all eleven positive cases ranged from 2.4 to 14.9 years. This findings concurred with previous literature which reported a variation in age of GCT occurrence that ranged from 2-20 years (Watson, 1994).

Content mining software, that utilizes a phonetic methodology, requires the researcher to have a background understanding of the area of investigation, text meaning and importance of the words and phrases contained within the data (Raja et al., 2008). One of the considerable obstacles as identified by Lam et al. (2007) was preparing terminology that can be recognized and common to all technicians and users. The recorded veterinary electronic information used in these analyses was not initially collected for research purposes, but rather for clinical and charging reasons, as with other similar studies (Mattin et al., 2015). An unknown number of cases will have been misclassified because of the phonetic divergence among veterinary practice data entries as well as missing information. In the particular case of CGT, some cases may have irregular oestrus cycles and stallion like behaviour but may have no GCT appearance or

any follicular activity on ultrasound examination. Additionally, on occasion, clinical notes indicated the suspicion of GCT and that a 'hormonal test for GCT confirmation was taken' but there were no further clinical details, at a later date confirming or not a GCT. In cases such as this it is impossible to state if the horse ended up with a GCT or not.

3.5 Conclusion

Even with the clear limitations, outlined above, related to the use of clinical data for research purposes, it is possible to estimate the prevalence (with confidence intervals) of different conditions and also identify clinical factors that may be used to predict future more serious veterinary problems. However, in this particular case the retrieved data did not provide any clear predictive factors that could reliably be related to future GCT occurrence.

Chapter 4 **Morphometric analysis of the granulosa and theca layer of equine antral follicles**

4.1 Introduction

Months of the year with shorter day length have an impact on the number and diameter of the follicles by suppressing the follicular activity in mares (anovulatory season). For the months in which day light is increasing (during the transitional period) the number and diameter of follicles increases until the ovulation occurs (ovulatory season)(Ginther, 1990). During this transition period there are consecutively growing and regressing follicles. During the mid-anovulatory period the maximum diameter of the largest follicle is from 17.8 - 20.8 mm while the largest follicle in transitional period ranges from 22.4 to 30 mm (Donadeu and Ginther, 2002). The initiation of follicular development is an indication of beginning of the spring transitional period that might last from 30 to 90 days with the size of dominant follicle ranging from 20 mm to 30mm (Aurich, 2011).

The length of the mare's oestrous cycle in the breeding season is 21 days although it can range from 18-24 days and the length of dioestrus is from 14-15 days (Raz and Aharonson-Raz, 2012). The actual length of oestrus consists of 4-7 days of the cycle although this is affected by season, sometimes ranging from 7-12 days at the beginning and at the end of the reproductive season while in summer it may last just from 3-4 days (Raz and Aharonson-Raz, 2012). However, in ponies it has been reported that this period might be extended by two days (Aurich, 2011). The mean (SD) ovarian diameter during early oestrus and late oestrus has been reported as 51.2mm (± 8 mm) and 65.0mm (± 10 mm), respectively and the mean (SD) number of antral follicles during early oestrus and late oestrus reported as 12 (± 2) and 2 (± 1), respectively. The mean (SD) diameter of the largest follicle during early oestrus and late oestrus has been reported as 20.0mm (± 2 mm) and 46.0mm (± 4 mm), respectively, and the mean (SD) ovarian diameter during early dioestrus and late dioestrus has been reported as 45.0mm (± 25 mm) and 40.0mm (± 10 mm), respectively). The mean (SD) number of antral follicles during early dioestrus and late dioestrus is 6 (± 1)

and 11 (± 4), respectively and mean (SD) diameter of the largest follicle during early dioestrus and late dioestrus has been reported as 12.5mm (± 2 mm) and 23.7mm (± 3.7 mm), respectively (Smok S and Rojas R, 2010).

During the 24 day oestrous cycle of pony mares, there is normally one major follicular wave (Gastal et al., 1999a). The largest follicles during this wave reach approximately 23 mm in diameter after growing from an emergent 6mm follicle. The largest follicle will continue growing to become a preovulatory follicle with a diameter of about 30 mm while the remainder (subordinate follicles) will follow an atretic pathway. Detection of largest follicles (> 20 mm in diameter) in the pony are generally not recorded until the middle of March (in the Northern Hemisphere) or approximately 60 days prior to the ovulatory season (Donadeu and Ginther, 2002).

Mares have two waves of follicular activity waves during an oestrous cycle (anovulatory wave and ovulatory wave). The first follicular development wave takes place during diestrus and several follicles become atretic. The second wave occurs after luteolysis and is associated with oestrus in which the dominant follicle becomes the ovulatory follicle (Ginther, 1990). The majority of mares ovulate when the size of the follicle reaches 40- 45 mm in diameter (Ginther et al., 2007). During each cycle mares exhibit one or two follicular waves. Major waves produce dominant and subordinate follicles and minor waves have a large follicle, which does not reach the same diameter as a dominant follicle (Raz and Aharonson-Raz, 2012). The second wave is the origin of the ovulatory follicle and the growing follicles (15 mm in diameter) continue to grow until one ovulates and the others undergo atresia (Sirois et al., 1989). According to Ginther et al. (2003) the emergence of the largest follicle occurs when it reaches 6-13 mm in diameter.

Developing follicles are surrounded by the ovarian stroma (fibroblast like cell tissue) and these particular cells become theca interna cells either in developing follicles or in interstitial cells. During any phase of follicular development most follicles become either atretic or undergo an involution. The large extension of the granulosa cell layer has an impact on the development of preovulatory follicle (Aurich, 2011). Luteal cells in mares originate from the granulosa cells of the preovulatory follicle, which is different from other species where luteal cells

are formed from thecal cells (Aurich, 2011). In the mare a single follicle is selected from the cohort of follicles to be a dominant follicle (Gerard et al., 1998). This largest follicle suppresses FSH which is a requirement of small follicles, resulting in their regression (Danica Marković¹, 2003). Thus, the majority of follicles will become atretic after one follicle has been 'selected' to be dominant (Sessions et al., 2009). In addition, subcategories of follicles that are unable to ovulate or become atretic become persistent anovulatory follicles.

Preovulatory and transitional follicles differ in their wall colour (Watson and Aizi'abi, 2002). For instance, the preovulatory follicles have an orange to red colour whereas the transitional follicles have a yellowish to pale pink colour. However, histologically there were no differences between transitional anovulatory and preovulatory follicles in terms of granulosa cell arrangement above the basement membrane or granulosa cell thickness. These granulosa cells were distributed randomly in the upper layers of both follicles with an infrequent appearance of mitotic nuclei and pyknotic nuclei. Preovulatory follicles contain a thick layer of pulp polyhedral cells with a pale cytoplasm and nucleus, whereas the anovulatory follicles have a thin and poorly developed theca. In addition, the majority of theca cells maintain a fibroblast type morphology with a spindle-shaped darkly staining nucleus. The follicular fluid content and the external granulosa layer thickness varied between small antral follicles (up to 25 mm) and large antral follicles (> 30 mm). The external layer of the larger antral follicles is thin (24 ± 2 mm) and has an aqueous follicular fluid, whereas the smaller antral follicles have a jelly like fluid and a thick external layer (40 ± 7 mm) that consists of six or seven follicular cell layers (Smok S and Rojas R, 2010).

The granulosa cells in follicles and the follicle wall are similar to those of the theca interna in terms of having a huge amount of eosinophilic cytoplasm, being luteinised, rarely apoptosed and with multiple mitosis. However, there are differences in vacuolation, shape and location (Mueller et al., 2009). For example, the granulosa cells are partially vacuolated, the cell borders are distinctive and have a columnar palisade arrangement, whereas the theca interna cells are highly vacuolated and have large round bulbous hyperchromatic nuclei that include one or two nucleoli. The theca externa cells are arranged

partially in a circle, slightly irregular and are plump in shape. The antral follicles have no haemorrhage or blood component. The vascular structures are fully developed especially the theca interna, which is dilated distinctively and hyperaemic. The basement membrane in a preovulatory follicle separates the avascular granulosa and theca interna layers. This theca interna consists of glandular cell layers that contain a rich capillary plexus. Moreover, the theca externa is composed of a fibrous layer including arterioles and venules (Gastal et al., 2006). Kenney et al. (1979), Driancourt et al. (1982) categorised theca interna layers into three types: smooth theca, mixed theca (composed of smooth layers with islands of large luteal like cells), and hypertrophied theca (which contains a thick layer of luteal like cells).

(Rodgers et al., 2001), reported that the membrane of granulosa cells in the bovine is not stable but starts with a single layer that then proliferates into several layers as it matures laterally during follicle development. This maturation ends during follicular atresia. In addition, this membrane of granulosa cells differs from one area to another and is situated on a basal lamina. This differentiation of cells is based on their shape, age and biochemical properties as well as the manner of death in atresia. The follicular epithelium during degeneration at the atretic phase sloughs toward the antrum and appears as a cuboidal layer or flattened lining cells (Oshea, 1968). Apoptosis of the ovarian granulosa cells play an essential part in follicular atresia (Peter and Dhanasekaran, 2003, Ginther et al., 2007). The regression follicles were classified into four groups (Atresia- 0, 1, 2, & 3) based on apoptosis (fragmented nuclei) in a study conducted by Pederson et al (2003) as presented on Table 4-1.

Table 4-1: Classification of atretic follicle (Follicle regression)

Atresia groups	Classification based on apoptosis
Atresia 0	Follicle had no sign of Atresia
Atresia 1	Follicle had apoptotic granulosa cells (GC) and pyknosis with an intact remaining thickness of GC and theca cell (THC) layers
Atresia 2	Follicle classified with hyaline membrane appearance between GC and THC layer with pyknosis and apoptosis
Atresia 3	Follicle had GC layer with few pyknosis and apoptosis as well as a thick hyaline membrane

Occurrence of pyknotic foci and karyorrhexis in the nuclei of granulosa cells is an indication of an atretic subordinate follicle (Stage I) and they are classified as advanced atretic (Stage II) when pyknosis and karyorrhexis are widely distributed (Watson et al., 2002b). In addition, two layers of flattened granulosa cells with a thick basement membrane in these follicles can be detected. Kenney et al. (1979) also mentioned that the Stage III occurs when the granulosa and theca cells separate with only a small amount of connective tissue remaining with the thick basal membrane. Furthermore, in Stage II and Stage III the detection of capillaries within the theca interna layer is difficult. Kenney and co-authors reported that in atretic follicles the oestradiol concentration is very low compared to viable follicles (between 600-900 ng/ml) as follows: (stage I - 1150 ng/ml, stage II - 302 ng/ml, stage III - 15 ng/ml).

Oestradiol FF concentrations have already been described (Watson and Ai-zi'abi, 2002). The concentration in preovulatory follicles was higher than the concentration in transitional follicle (1063 ± 169.2 ng/ml and 345 ± 112.3 ng/ml, respectively). During the breeding season the concentration of E2 was higher in dominant follicles than in those aspirated during transition (Watson et al., 2002b). One day prior to deviation or selection the amount of E2 gradually increases and remains raised for one or two days prior to ovulation. The E2 concentration in the follicular fluid of the healthy mare has been found to be high, in the region of 300 to more than 5000 ng/ml (Forst et al., 2003, Bailey et al., 2002, Meinecke and Gips, 1987, Peter and Dhanasekaran, 2003, Gastal et al., 1999b).

4.1.1 Aim:

To categorise the ovarian follicular wall specifically the GC and THC compartments by measuring their thickness and describing their cellular pattern using histology and to examine relationships with follicle health markers (intrafollicular steroid hormone concentration and follicle size) and mare characteristics (age, reproductive state and disease status).

4.1.2 Objectives:

1. To categorise the follicle walls (FW) into four groups based on histological criteria: Very healthy (VH), Healthy (H), Early atretic (EA) and Late atretic (LA).
2. To count and compare between the four groups the three layers of GC: basal, intermediate and antral, and the two types of THC: large THC and small THC
3. To measure the thickness of the GC and THC layers
4. To determine the E2 hormone concentration in the follicular fluid of the four histologically classified categories.
5. To determine any associations between follicular factors (such as the follicle health categories or intrafollicular estradiol) and mare factors (such as season of ovary collection, breed type, age or disease status) with GC and THC measurements.

4.2 Materials and Methods

4.2.1 Animals and tissue samples

Follicle wall samples were recovered from a total of 63 follicles collected from 19 mares between August 2014 and May 2016. Mares differed in breed, health status, age, season of the year (therefore breeding season), and stages of the oestrous cycle when the ovaries were collected. All experimental procedures were approved by the University of Glasgow, School of Veterinary Medicine Research Ethics Committee (Ref 41a/16). Where required client consent was sought. The ovaries were collected from 14 mares after euthanasia, and from five mares after surgical ovariectomy carried out at the School of Veterinary Medicine, University of Glasgow. A summary of the mare details is presented below in Table 4-2.

The ovaries were each placed in a plastic laboratory bag filled with chilled 0.05M Phosphate buffered saline (PBS), and briefly transported on ice or within an icebox to the laboratories for measuring and processing.

Measurements and ovarian maps: ruler and ultrasound procedures. Ovaries were ultrasound scanned using a linear 7.5MHz transducer, applied to each ovary

scanning from lateral to medial or vice versa to detect all follicles and corpora lutea on each ovary. Using the ovulation fossa in the middle of the ovary as a landmark the ovary was placed in a petri dish and measured as shown in Figure 4-1. The diameter of each palpated follicle was measured from the external surface using a metal ruler by taking an average width and height in mm.

Table 4-2: Mares used in this experiment

Mares ID	Date of ovary collection	Horse/pony	Age	Disease
Unknown	14.08.14	Unknown	Unknown	Behavioural problem during oestrus, On regumate
NKR 008	06.08.14	Belgian Warm blood	18 years old	Chronic lameness in left forelimb
NKR 010	21.08.14	Appaloosa pony "Dotty"	7-9 years old	Increasing lameness in front (reason for PTS)
NKR016	10.10.14	Very small pony	5 years old	Secondary parathyroidism nutritional
NKR18	11.11.14	Sport horse = TB	5 years old	PTS because of multiple limb lameness
NKR 020	28.11.14	TB X	9 years old	Deteriorating multi-limb lameness
NKR021	01.12.14	Chestnut, Welsh A mare	12 years old	PPID, Laminitis, COPD (PTS)
NKR 023	22.12.14	Highland pony	12 years old	Chronic lameness =PTS, Had focal ulcers along GIT (PM finding)
NKR 025	09.02.15	Welsh mountain	1.5 years old	Unknown
NKR 027	11.02.15	Welsh mountain	1.5 years old	Unknown
NKR 029	13.02.15	Welsh mountain	1.5 years old	Unknown
NKR 034	18.02.15	Welsh mountain	1.5 years old	Unknown
NKR 036	06.03.15	TB X	20 years old	LH lame, Laminitis, Mammary gland mass
NKR 046	05.06.15	TB	7 years old	RDA horse with a chronic forelimb lameness
Violet	29.10.15	WB	7 year old	Abnormal behaviour. Stallion like behaviour. Regumate treatment. Ovariectomy
Squiggy	27.04.16	Sport horse	9 years old	Behavioural issues. Squamous and glandular gastric ulceration. Ovariectomy
Maggie	01.04.16	Connemara X pony	10 year old	Behavioural problem. Not responded to regumate. Ovariectomy
Molly	02.04.16	Connemara x pony	10 years old	Masculine behaviour, ovariectomy due to Owner request
Nia	19.05.16	Mare	11 years old	Behavioural issue. Responded well to regumate but not cycling well. Ovariectomy

4.2.2 Follicle processing

Based on the ovarian map and also manual palpation of the ovaries to locate and distinguish large follicles, the largest follicle(s) (ranging from one to two per mare) present were aspirated and their follicle walls dissected for histological processing. Follicular fluid (FF) was collected slowly without causing turbulence using 5- and 10- ml syringes and 20 G 1.5" needles, by puncturing the follicle wall through the stroma at the laboratory bench. Fluid from each follicle was stored in 15ml tubes and maintained at -20 °C until hormone (oestradiol) assay. The follicle was penetrated with an incision by Westcott curved blunt tenotomy scissors to visualize the follicular cavity. A blunt dissection of the follicle wall followed whereby the wall was peeled off carefully and then placed in a sterile petri dish filled with PBS for further processing as shown in Figure 4-2.

The oestradiol (E2) hormone assay was carried out using an ELISA kit (R&D system® a biotechne® brand, Catalogue number KGE014) per manufacturer's instructions, which have also been described in detail in chapter 2. The intra assay coefficient of variation (CV) for a Low QC (65/ml), Medium QC (436 ng/ml) and High QC (1089 ng/ml) were 7%, 6% and 11% respectively. The inter-assay CV for the three QCs were 25%, 14% and 16%, respectively.

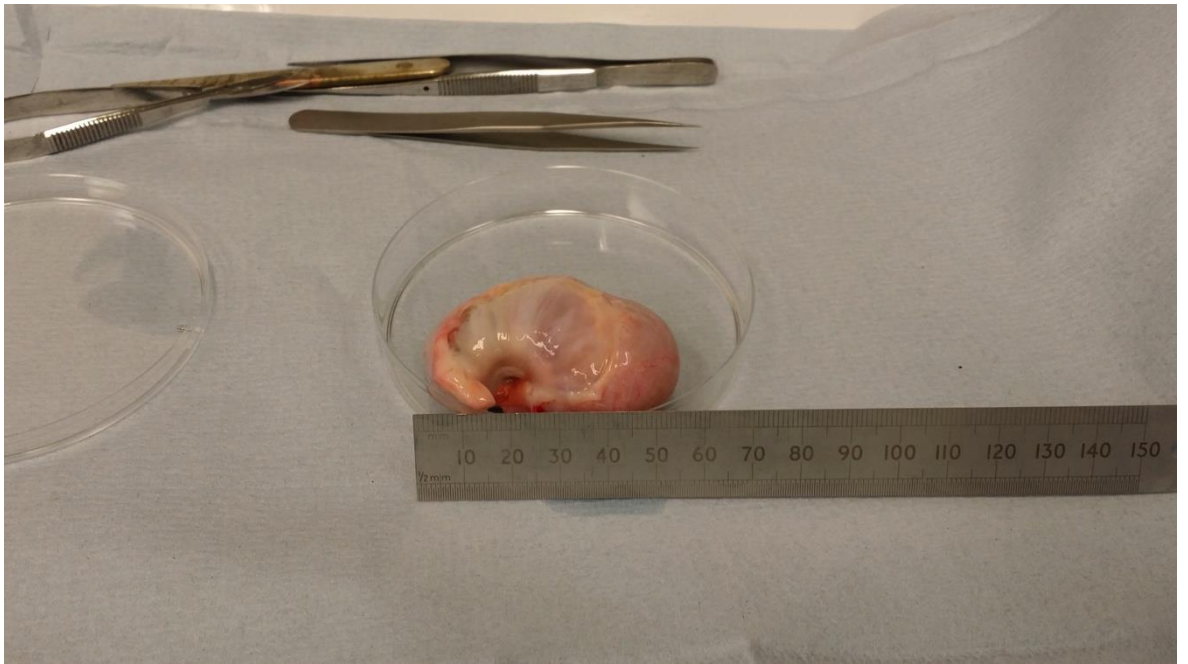


Figure 4-1: Measuring the diameter of the ovary



Figure 4-2: Blunt dissection of the follicle showing the follicular cavity after fluid aspiration

Three rectangular pieces of each dissected follicular wall were prepared. After all follicles were sampled, the ovary was hemisected sagittally through the ovulation fossa, and a cube of ovarian stroma was dissected from the two inside surfaces bordering the ovulation fossa as shown in Figure 4-3. The first collected samples were fixed in Bouins solution Fixative (VWR Chemicals, VWR International, 7000.1000) for 24-72 hours, washed twice in 70% ethanol at 48h intervals, and stored in 70% until histological processing, and some later collected samples were fixed in 10% neutral buffer formaldehyde as this was recommended by the histopathologists.

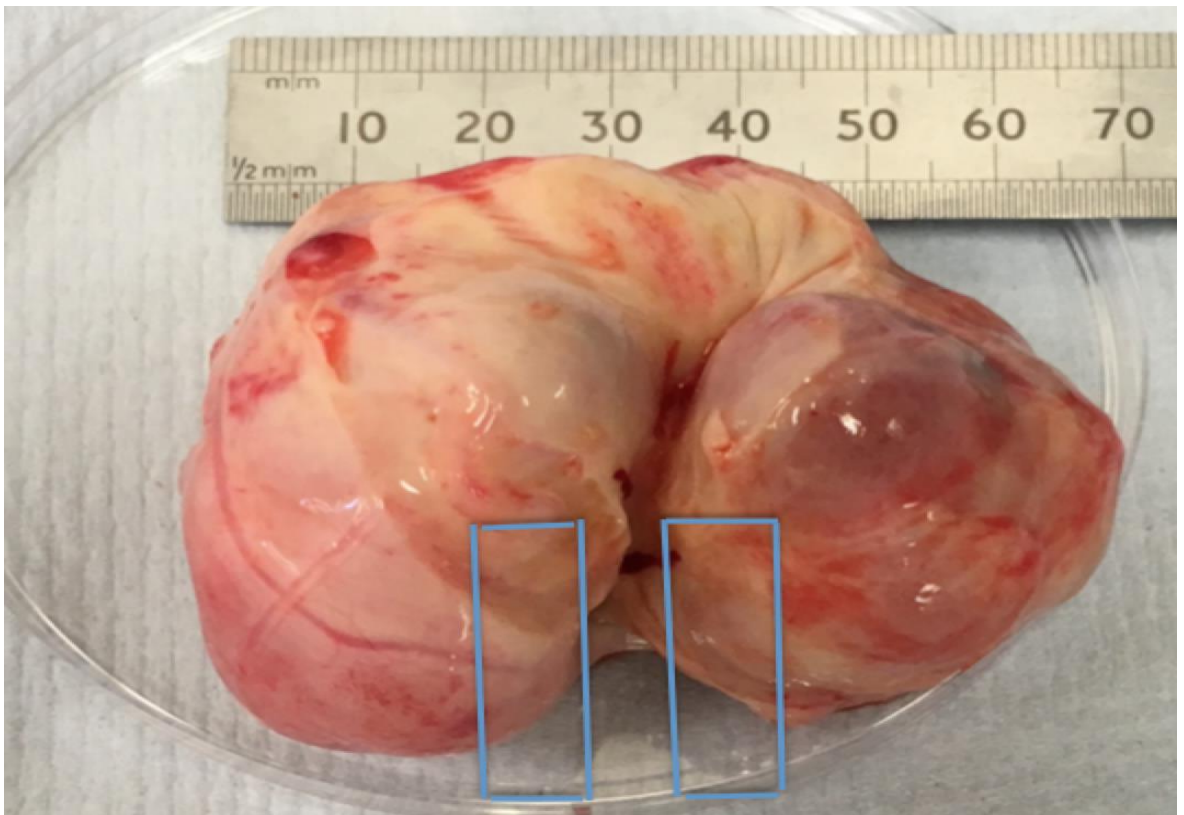


Figure 4-3: Cube section of the stroma close to ovulation fossa.

4.2.3 Histology of the follicular wall

The follicular walls (FW) were cut in small rectangular pieces of tissue and carefully placed onto the embedding cassettes in order to obtain a cross-section view of the layers of granulosa cell (GC), theca cell (THC) and the underlying stroma without any of the layers sloughing during histological processing. Follicle walls were embedded in wax in the Diagnostic Laboratories of the School of Veterinary Medicine, using their Thermo Scientific, Histostar machine, then

sectioned at 2µm thickness using a Thermo Scientific, FINESSE ME+ microtome machine, and stained with haematoxylin and eosin prepared by the Veterinary Diagnostic Services laboratory, University of Glasgow, as per standard protocol (described in Chapter 2).

4.2.4 Histological assessment of follicle health status and morphometric measurements

In this study we aimed to categorise the follicle walls into Very Healthy growing (VH), Healthy and highly differentiated (H), Early Atretic with beginning disruption of the GC and THC compartments (EA), and Late Atretic with no functional GC layer (LA) based on published histological criteria particularly relating to dominant follicles and follicle apoptosis. The morphometric measurements were then taken to a) establish a database for GC and THC compartments in developing antral follicles, and b) to see whether our subjective evaluation was supported by differences in objective measurements taken.

The granulosa and theca cell layers in each follicle wall section, were quantitatively assessed using a Leica DM4000B microscope (Leica Microsystem, Switzerland) connected to a Leica Application Suite software (version 4.3.0; Leica Microsystems, Switzerland) to acquire images, followed by measurements using the ImageJ (1.49v, Wayne Rasband, National Institute of Health, USA) software. Five consecutive rectangle views were spaced over the whole length of the follicle wall capturing both the GC and THC layers (all at 40 x magnifications) as shown in Figure 4-4. Each rectangle measured 140.70x255.27 µm² as shown in Figure 4-5. The aim was that the follicular tissue was not collapsed and laid out level on the histological slide, with no or negligible folds in the granulosa layer.

In each of the five views all GC and THC were counted at x40 magnification as shown in Figure 4-6. These cell types were differentiated from each other on the basis of cellular morphology. Basal GC were classified as GC that were located at the base of the GC layer bordering the basal lamina with nuclei mostly in laminar position. Antral GC were classified as GC that were located at the antral surface, closest to the fluid-filled antrum of the follicle. Intermediate GC were

classified as the GC that were located in between the basal and antral GC. The thicknesses of the GC and THC were measured on those five views under 20x magnification as shown in Figure 4-7 using a graticule scale measurement as described in details in Chapter 2. The thickness of GC layer was measured from the antral GC to the basal GC, and the thickness of THC layers was measured from the granulosa side of theca interna cells directly beneath the basal GC to the discernible border of the theca interna with stroma cells = theca externa. The large THC and small THC cells make up the composition of the theca layer. The large THC cells exhibit a well-defined cell membrane with large cytoplasm similar to large luteal cells, whereas the small THC cells are clearly smaller in size with a much reduced cytoplasm: nucleus ratio. The cells that were included in the assessment all had distinct nuclei. The entire cell has to be visible for it to be counted. Other cells that can be viewed partially on that particular view would not be taken into consideration.

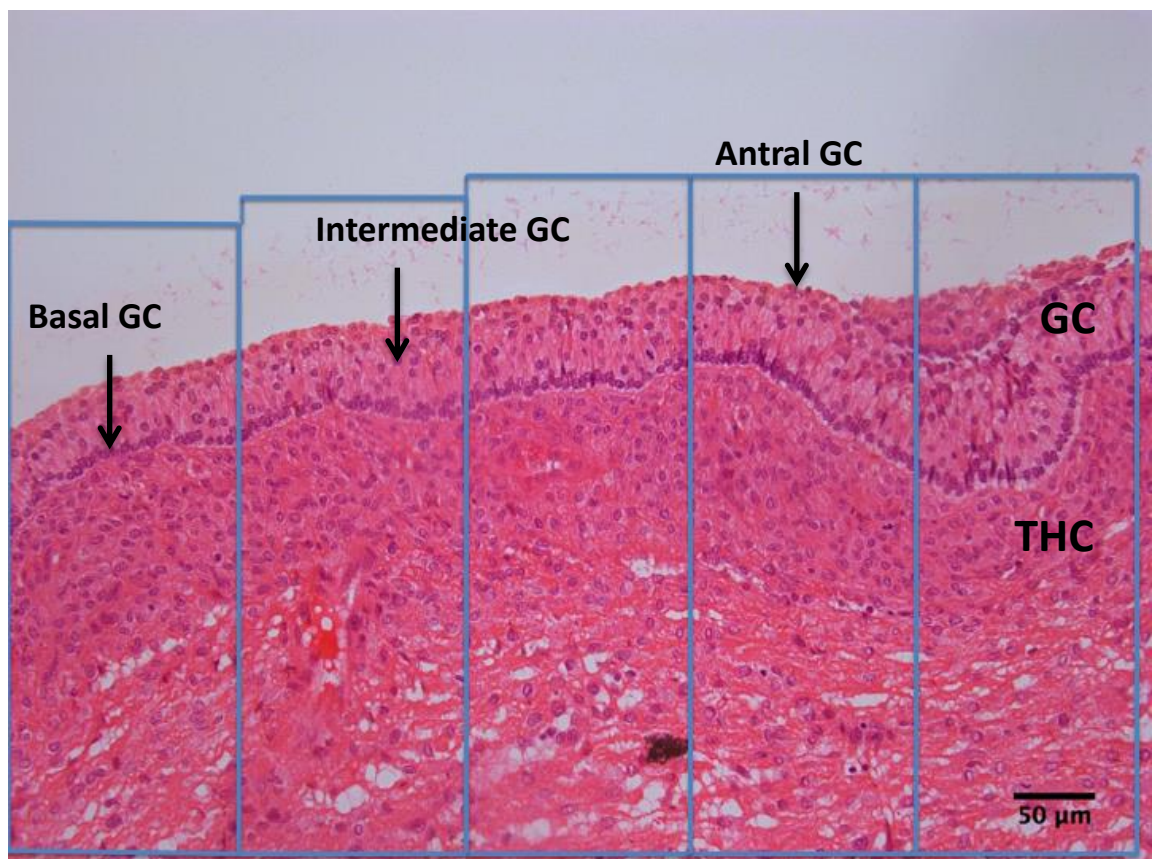


Figure 4-4: Illustration of how views are taken from a selected FW sample. This sample is taken at 200x magnification, and the boxes are representative of the 5 successive views taken for further assessment at 400x magnification

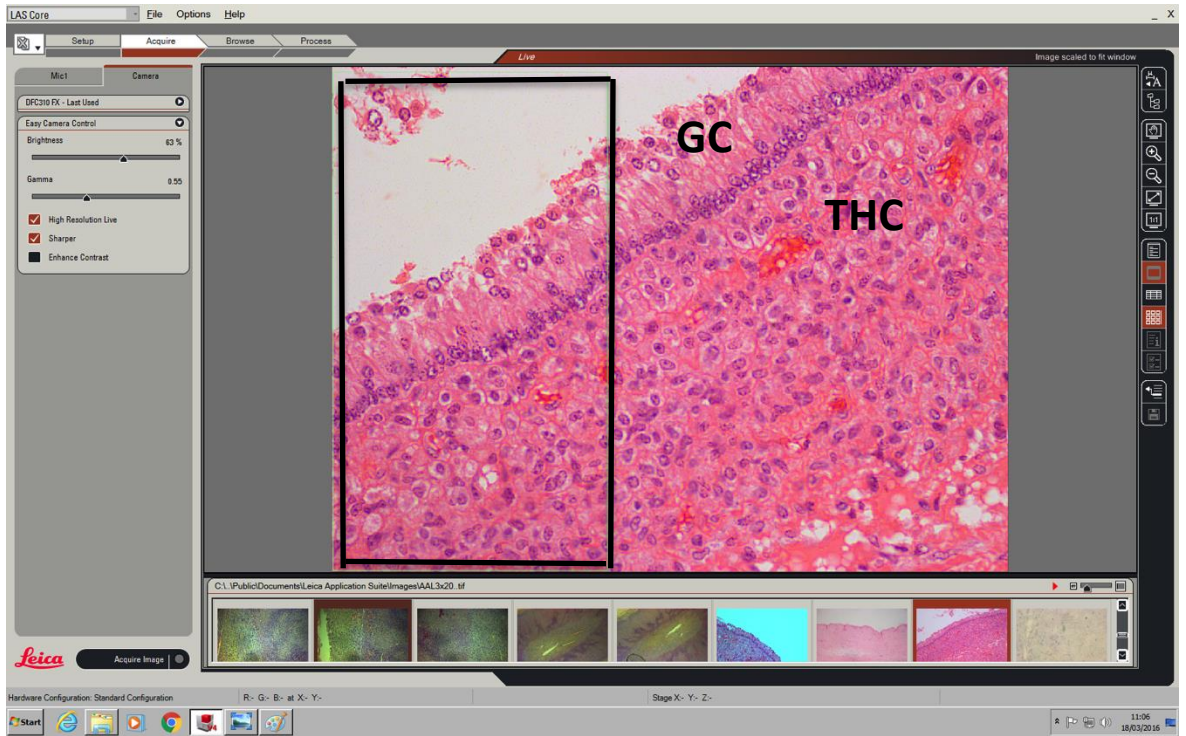


Figure 4-5: Rectangle view of a FW image at 200x magnification

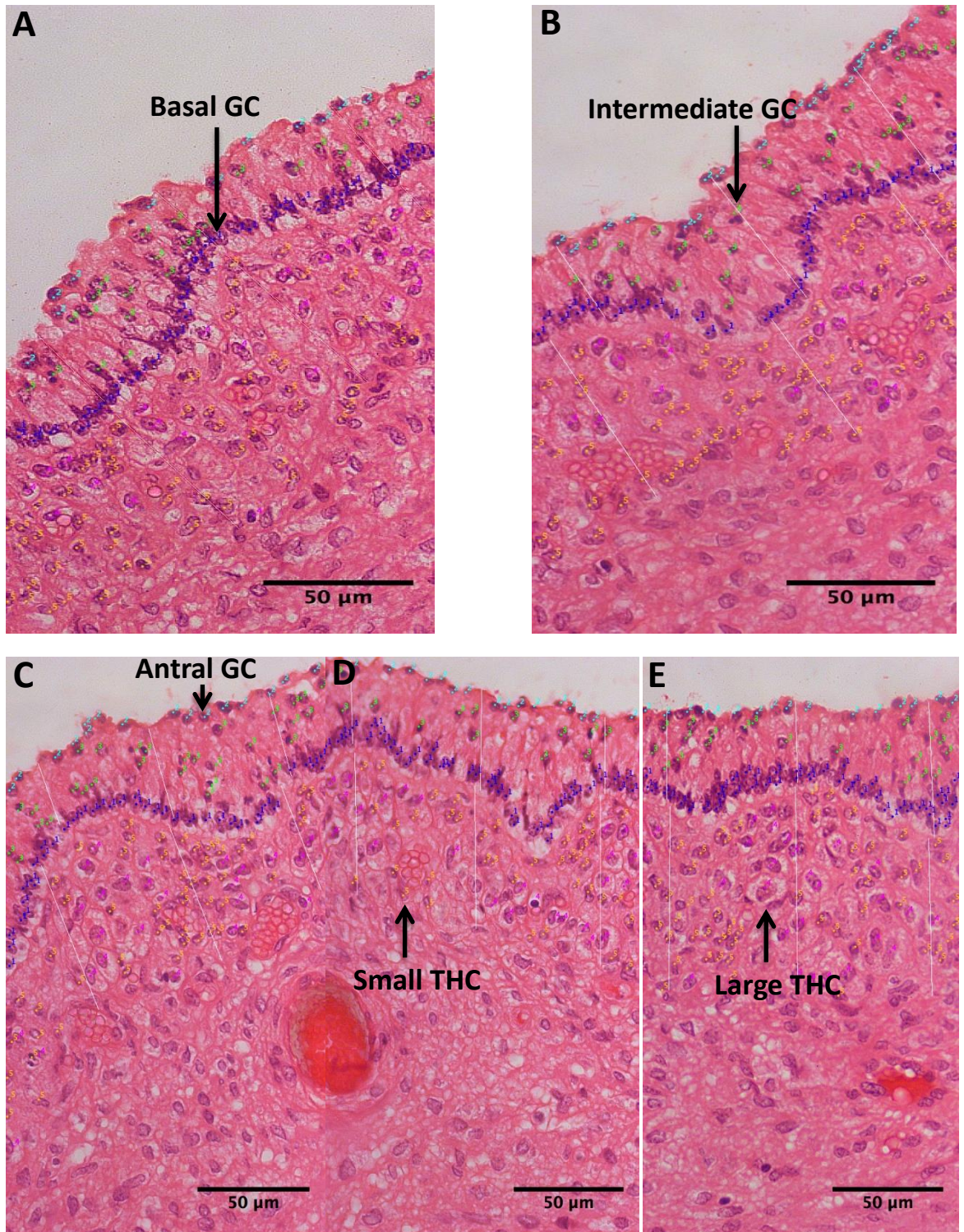


Figure 4-6: Counting GC and THC at x400 magnification, A: shows Basal GC (no.1 purple colours), B: shows Intermediate GC (no.3 green colours), C: shows Antral GC (no.2 blue colours), D: shows small THC (no.5 yellow colours), E: shows large THC (no.4 pink colours)

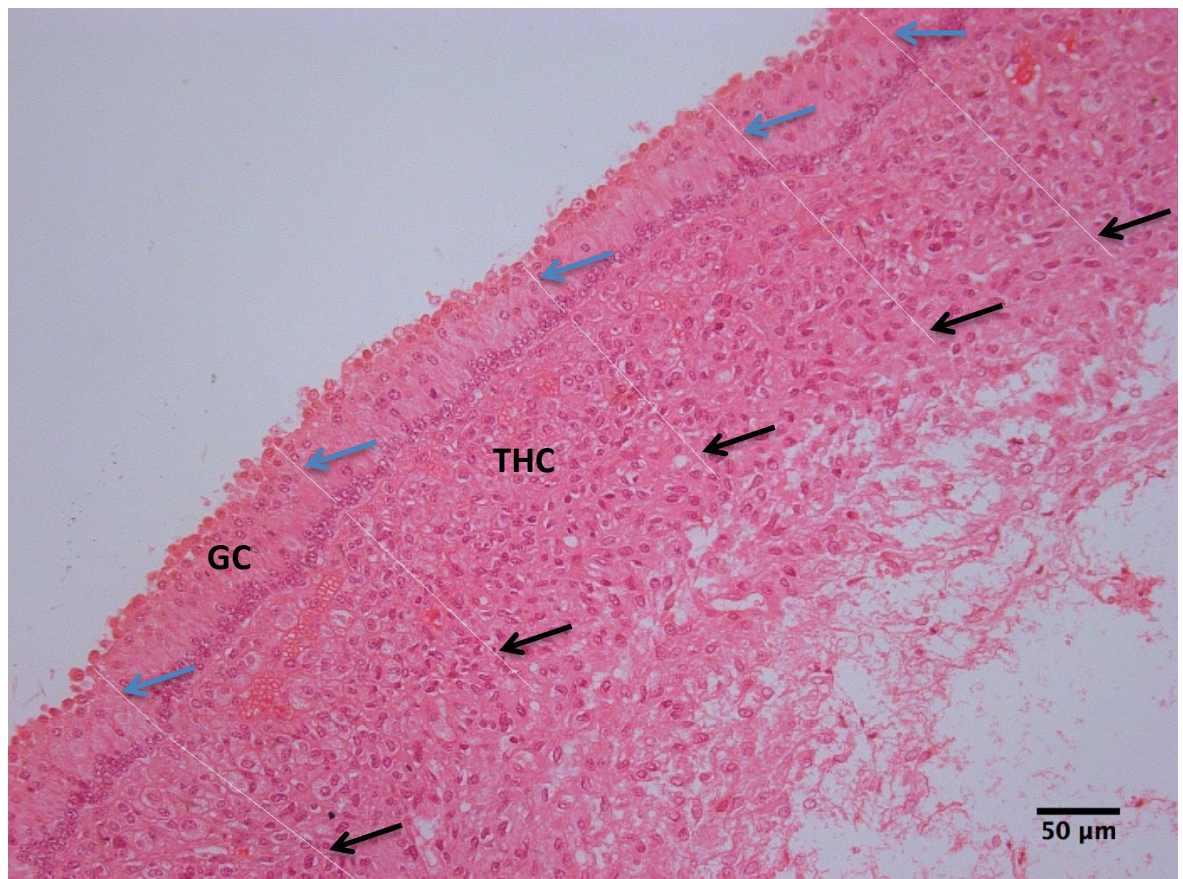


Figure 4-7: Measuring the thickness of GC (Blue arrows) and THC (Black arrows) at x200 magnification

4.2.5 Statistical analysis

The Null Hypotheses tested using statistical analyses were:

- a) There would be no difference in the thickness of GC and THC layers between follicle health categories of (control mare) follicle walls (FW)
- b) There would be no difference in cells counts between follicle health categories of FW
 - i. between the three layers of GCs: basal, intermediate and antral and
 - ii. between the two types of THCs: large THC and small THC cells
- c) There would be no difference in the FF E2 concentration of follicles belonging to the four histologically classified categories.

An initial descriptive statistical analysis of the cell numbers in the GC and THC layers (basal, intermediate and antral, large THC and small THC), follicle diameter and follicular fluid oestradiol (FFE2) concentration in follicles of different histological health categories was performed. Non-parametric Mann-Whitney or Kruskal Wallis tests were then performed after a lack of normality was detected (i.e. the distribution of the data demonstrated evidence of a lack of normality using the Shapiro-Wilks normality test) and box plots were created to identify potential differences in each of the histological measurements between each of the four follicle health categories VH, H, EA and LA. The same tests were also used to determine any associations with other potential factors, such as follicle size (large or small), breeding season (winter, summer, transition), breed category (pony or horse), age and disease status of mares (none, mild-chronic, severe) which were coded numerically. Follicular diameter and FFE2 concentration were treated as continuous variables.

4.3 Results

4.3.1 Gross findings

The wall of large fresh follicles appeared relatively smooth and it was possible to peel it off easily. In healthy or EA follicles the FW had a reddish appearance due to visible blood vessels over its surface, Figure 4-8, whereas this was not present in LA follicles. It was also noticed that in some follicles brown fat appeared between the theca externa and follicle wall, as shown in Figure 4-9.



Figure 4-8: The peeled FW containing GC and THC layers from an healthy or EA follicle which has a reddish appearance because of its high vascularisation and blood vessels being visible.



Figure 4-9: Fatty brownish appearance between the follicular wall following its dissection and the theca externa/stroma.

4.3.2 Histological findings

The follicular walls from 63 follicles were classified into four health categories VH (10 follicles), H (11 follicles), EA (10 follicles) and LA (32 follicles) as detailed below: A follicle was considered to be very healthy (VH) when the GC layer appeared to be of uniform thickness, basal GC were arranged in a palisade with a high proportion to the total of GC, slight appearance of or few intermediate GC, and the antral GC were lined up in an interrupted palisade arrangement as shown in Figure 4-10.

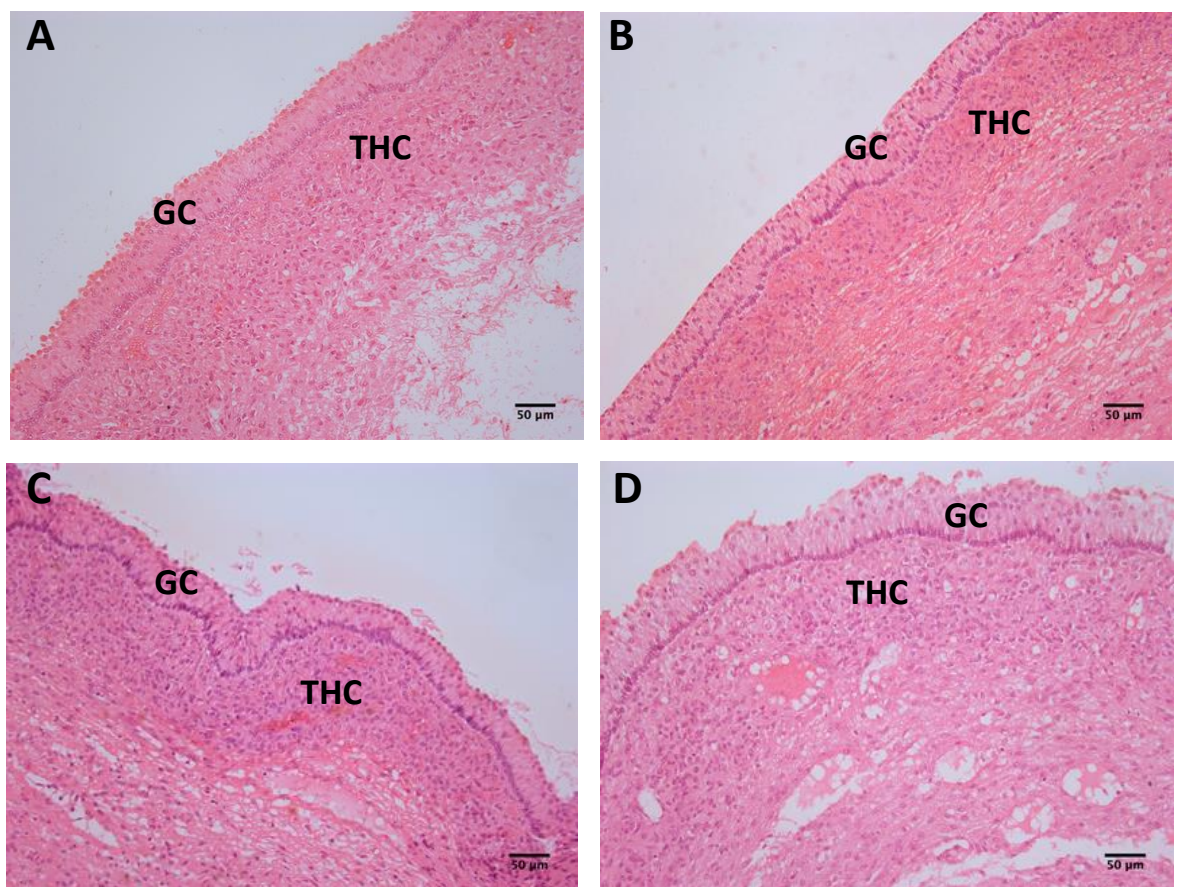


Figure 4-10: Very healthy follicular wall category. A (FWD 10.3x11.8 mm measured in two dimensions), B (FWD 25x18.8 mm), C (FWD 13.8x13.3 mm), D (FWD 19x17 mm): Examples from different follicles

Furthermore, large THC and small THC appeared within the heterogeneous population of theca cells, with approximately 1/3 of THC population being large THC. The second category included follicles classified as healthy H based on the presence of a slight disarray of basal GC, although the following may also have been present: A degree of palisade arrangement was still present, but in some

areas it was somewhat difficult to differentiate between basal, intermediate and antral GC; a few gaps or vacuolation was visible between the basal GC; and a small degree of pyknosis (<5 per view) was present, often seen in intermediate and antral GC populations. In addition, the small and large THC cells were still part of the heterogeneous THC layer; however, the large THC proportion was increased in population as shown in Figure 4-11.

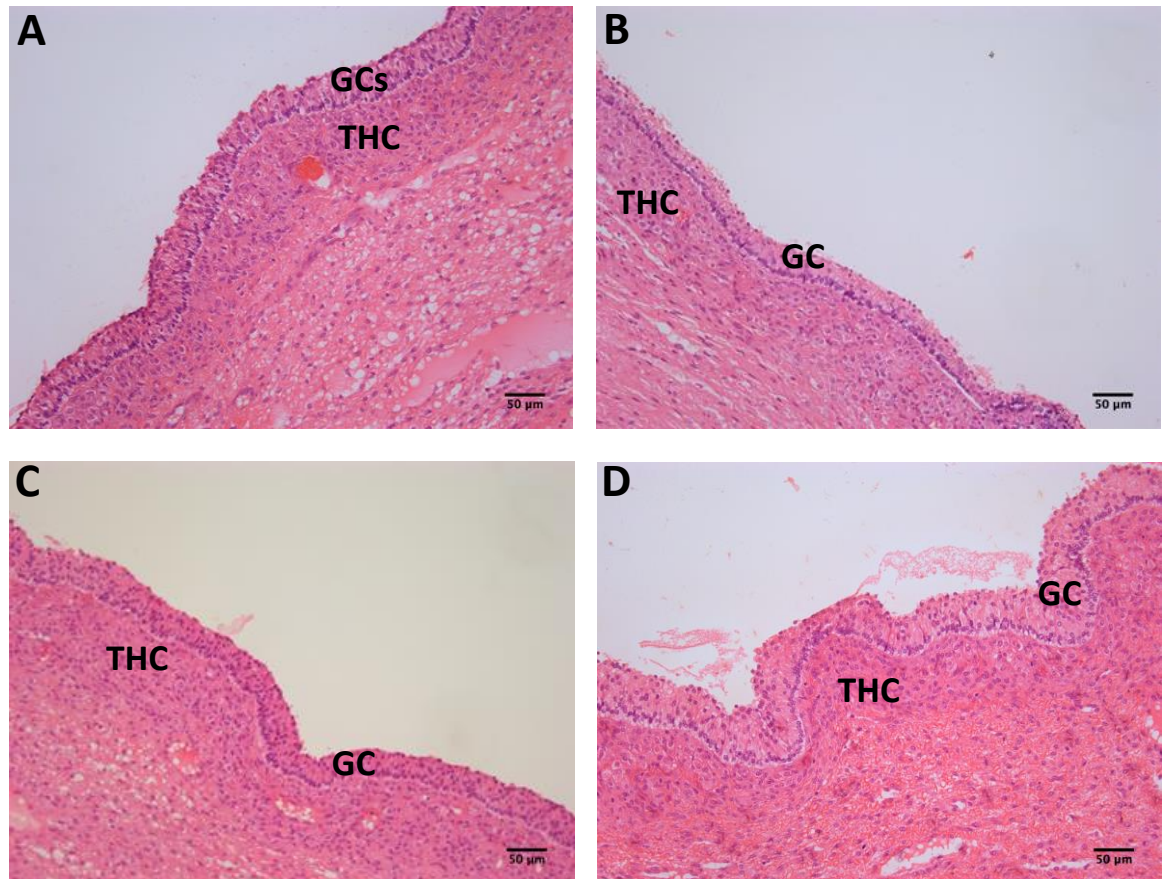


Figure 4-11: Healthy follicular wall category. A (FWD 29.6x34.9 mm measured in two dimensions), B (FWD 17.7x17.3 mm), C (FWD 25.5x16.6 mm) D (FWD 38.2x31.2 mm): Examples from different follicles

The third category is the early atresia EA follicle category. In this group the GC layer was decreased in thickness; mild sloughing of the antral granulosa cells might be present; there seem to be more intermediate GC which together with the basal GC appear more disorganised, and cells are overlapping, which led to a decrease in the adherence to the THC layer; and the degree of pyknosis was increased (> 5 per view) in the GC layer. Moreover, most of the THC were small THC, the presence of a vascular supply was evident in the theca interna; and the accumulation of an eosinophilic connective tissue substance (a thin amorphous membrane) was becoming apparent within the THC layer underlying the granulosa, as shown in Figure 4-12.

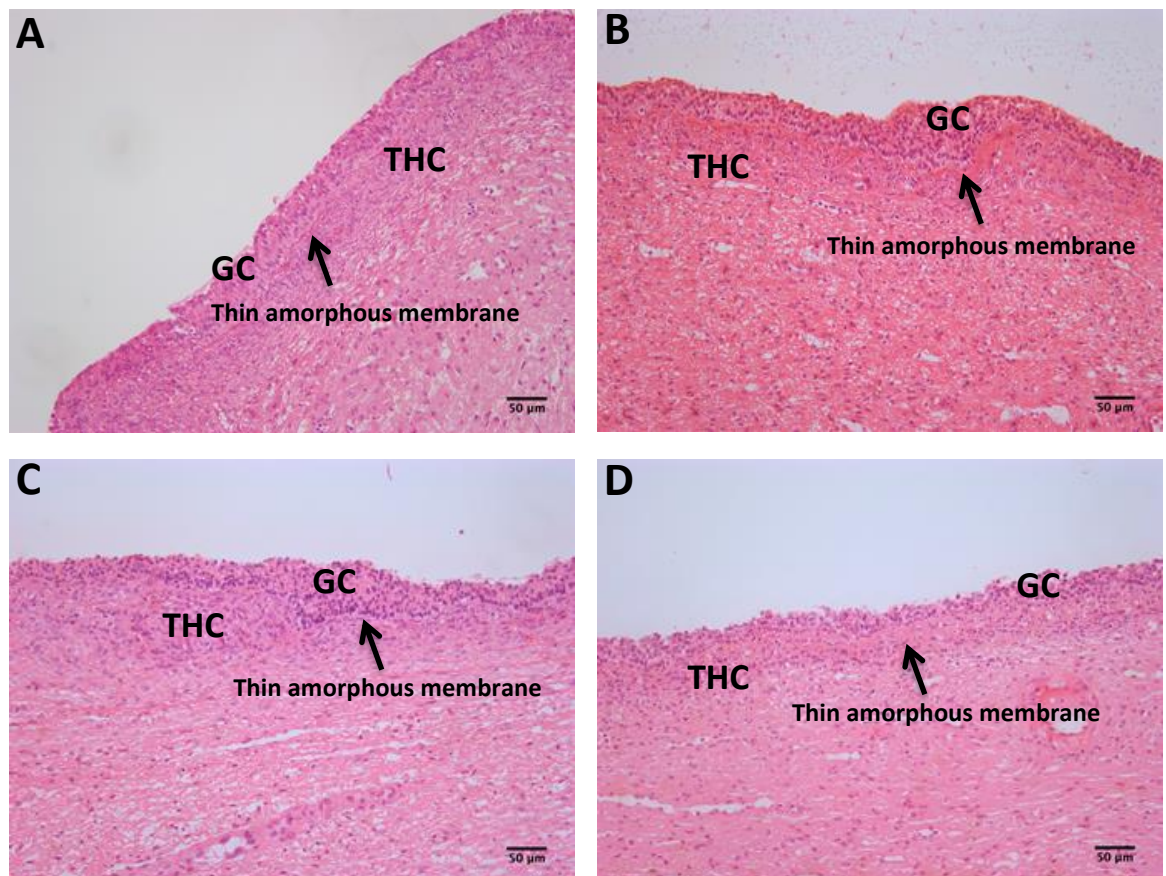


Figure 4-12: Early Atretic FW category. A (FWD 18.2 mm) B (FWD 22.1x20.4 mm measured in two dimensions), C (FWD 29.6x29.2 mm) D (FWD 17x18 mm): Examples from different follicles

Late atresia is the fourth category of histologically classified follicles: In this group there is a complete absence of GC, so the GC layer has sloughed off, (and the THC layer now contained mainly small smooth spindle like cells considered

to be small THC with an elongated darkly stained nucleus. Moreover, a distinct, thick sub-basal amorphous eosinophilic band is present. In some views sloughing of the THC layer below or above this band was seen, and the remaining THC layer now shows vasculature loss as seen in Figure 4-13.

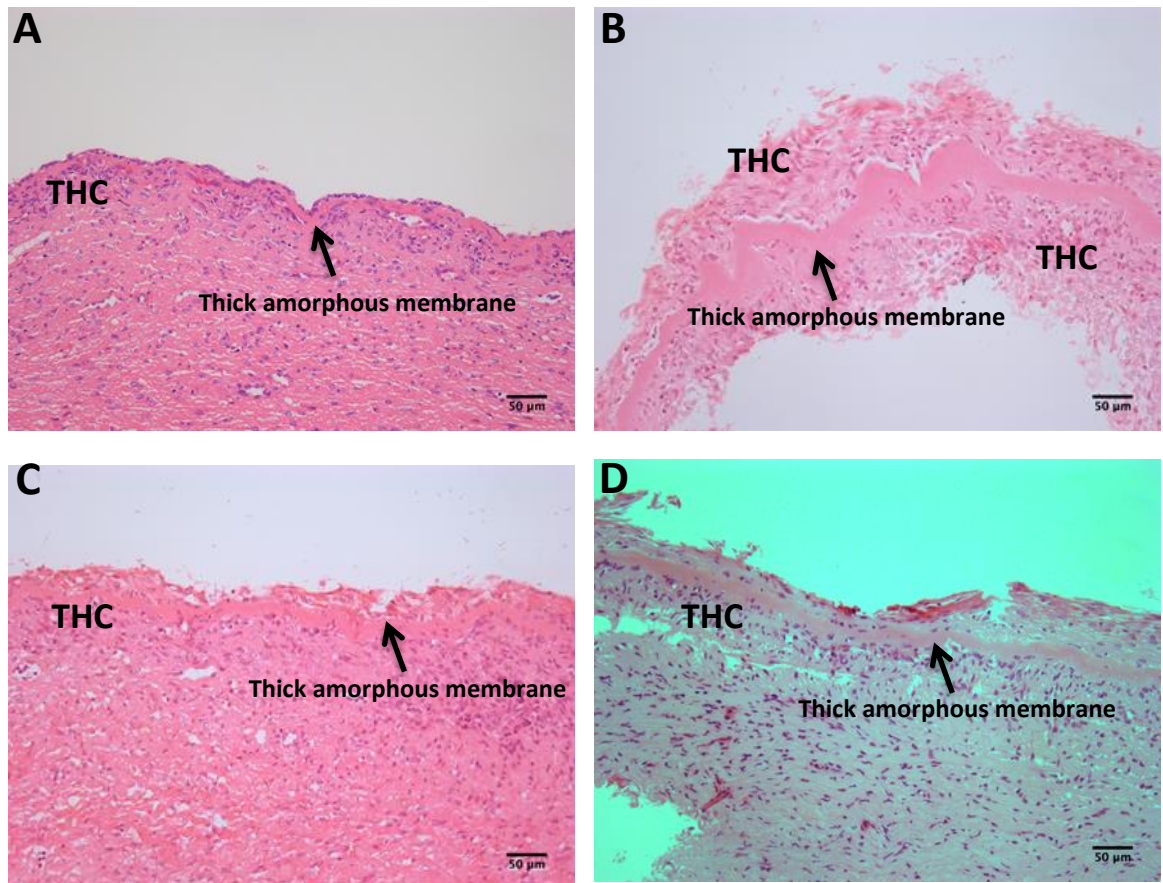


Figure 4-13: Late atretic FW category. A (FWD 6.15 mm), B (FWD 13.6 mm) C (FWD 16.35 mm), D (FWD 40.9 mm): Examples from different follicles

4.3.3 Analysis of the association between the different follicle health categories and other parameters

4.3.3.1 Follicle wall diameter (FWD)

The analysis of associations of follicle health category or time of year of follicle collection (breeding season), age and disease status of mare with follicular size is shown in Table 4-3. A tendency towards significance was observed for follicle health status ($P < 0.06$), with healthy and early atretic follicles tending to have greater diameters than very healthy or late atretic follicles. There was a significant association between FWD and disease category ($P < 0.05$), with

follicles from mares without disease having greater diameters than if collected from mares with disease. As one would expect follicle diameter was also very strongly associated with our distinction of follicle size ($p < 0.001$).

Table 4-3: Association between a range of parameters and FWD. VH (very Healthy), H (Healthy). EA (Early Atretic), LA (Late Atretic), LF (Large follicles from 20mm), SF (Small Follicles < 20mm). Bold indicates a statistically significant p-value.

Factors	P-value	No. of follicle	Follicular wall diameter (mm)	
			Mean \pm SE Mean	Median
VH	0.059	10	18.9 \pm 1.8	20.1
H		11	23.2 \pm 1.9	22.3
EA		10	23.7 \pm 1.9	21.1
LA		32	18.8 \pm 1.1	17.6
F. Size Cat				
LF	<0.001	32	22.2\pm0.8	23.1
SF		31	15.4\pm0.6	16.0
Breeding season				
Winter	0.893	11	20.1 \pm 1.9	18.1
Summer		32	20.8 \pm 1.2	20.8
Transition		20	19.9 \pm 1.4	19.2
Breed				
Horse	0.424	40	19.8 \pm 1.0	18.1
Pony		20	20.4 \pm 1.4	20.8
Age				
0-2 YO	0.506	13	20.8 \pm 0.9	20.8
2-10 YO		31	20.2 \pm 1.3	19.9
> 10 YO		17	19.1 \pm 1.3	17.5
Disease				
No disease	0.028	35	21.6\pm0.9	21.0
Chronic mild		4	12.9 \pm 2.9	12.7
Severe		24	19.8 \pm 1.5	17.8

4.3.3.2 Follicular fluid oestradiol (FFE2) concentrations

There was a significant association between follicle size class and health status and FF E2 concentration ($P = 0.014$, < 0.001 , respectively) as presented in Table 4-4. A Mann Whitney test was used to compare combined the VH and H groups versus EA and LA groups ($P < 0.001$). Large and very healthy or healthy follicles had significantly greater E2 concentrations than atretic or small follicles, respectively. It is noticeable that fluid from LA follicles still contains some E2 despite loss of the GC layer (8.7 \pm 4.9 ng/ml). Although not statistically significant at $P < 0.05$, follicular fluid from ponies tended to have greater oestradiol concentration than horses despite similar FWD. There was no association

between breeding season and follicular fluid oestradiol concentration indicating that the range of follicles recovered particularly in summer or winter contained follicles with very different health and functional status.

Table 4-4: Association between the predictive follicle and mare parameters and FFE2 concentration. VH (very Healthy), H (Healthy). EA (Early Atretic), LA (Late Atretic), LF (Large follicles from 20mm), SF (Small Follicles < 20mm). Bold indicates a statistically significant p-value.

Factor	P-value	No. of follicle	Follicular fluid E2 Concentration (ng/ml)	
			Mean \pm SE Mean	Median
VH	<0.001	10	210.5\pm87.8	103.5
H		11	167.4 \pm 41.8	107.8
EA		5	28.5 \pm 14.2	16.0
LA		20	8.7 \pm 4.9	1.2
F. Size Cat				
LF	0.014	23	151.8\pm45.5	66.9
SF		23	33.5 \pm 10.4	2.9
Breeding season				
Winter	0.730	10	128.7 \pm 76.2	48.3
Summer		16	113.1 \pm 46.5	42.1
Transition		20	58.2 \pm 21.5	9.5
Breed				
Horse	0.112	26	55.6 \pm 19.6	8.4
Pony		17	126.8 \pm 48.3	66.9
Age				
0-2 YO	0.962	13	68.4 \pm 26.2	49.0
2-10 YO		16	57.3 \pm 20.0	9.5
> 10 YO		15	120.0 \pm 57.9	37.0
Disease				
No disease	0.172	22	66.5 \pm 32.2	5.6
Chronic mild		4	44.8 \pm 21.2	43.0
Severe		20	131.0 \pm 43.7	63.6

4.3.3.3 Granulosa cell layer

The late atretic category was eliminated from the comparison because it had no GC at all. The differences in granulosa cells counts (Basal, Intermediate and Antral GC) and thickness, between VH, H and EA follicles are shown in Table 4-5. There was a reduction in the absolute number of basal GC in EA follicles (27.2 \pm 3.3) compared to VH and H follicles (39.2 \pm 1.9, 36.5 \pm 1.3, respectively, P=0.004). This led to a tendency for a higher % of basal GC in VH compared with H and EA follicles, and a concomitant tendency for lower % antral GC between VH and EA follicles. The reduction in GC thickness on which the EA classification

was partly based did not reach significance (EA follicles show a non-significant > 10 μ m reduction in thickness when compared to VH follicles).

Table 4-5: Association between follicle health category and mare factors and basal, intermediate and antral GC counts and thickness. VH (very Healthy), H (Healthy), EA (Early Atretic), LA (Late Atretic), LF (Large follicles from 20mm), SF (Small Follicles < 20mm). Bold indicates a statistically significant p-value.

Outcomes	Factor	P-value	No. of follicle	GC counts and thickness	
				Mean \pm SE	Median
Response	Health status			Mean	
Basal GC	VH	0.004	10	39.2\pm1.9	37.3
	H		11	36.5 \pm 1.3	37.6
	EA		10	27.2 \pm 3.3	24.4
% Basal GC	VH	0.142	10	51.6 \pm 2.7	51.9
	H		11	46.2 \pm 2.2	44.1
	EA		10	46.0 \pm 5.4	37.0
Antral GC	VH	0.711	10	12.9 \pm 1.0	11.6
	H		11	13.7 \pm 0.6	13.8
	EA		10	18.1 \pm 6.6	11.4
% Antral GC	VH	0.122	10	16.4 \pm 0.6	16.3
	H		11	17.1 \pm 0.9	16.8
	EA		10	21.5 \pm 2.9	19.8
Intermediate GC	VH	0.730	10	26.0 \pm 3.3	24.6
	H		11	30.4 \pm 3.2	29.0
	EA		10	26.7 \pm 5.9	28.8
% Intermediate GC	VH	0.756	10	31.9 \pm 2.8	30.9
	H		11	36.7 \pm 2.6	39.5
	EA		10	32.5 \pm 5.3	35.0
Total GC	VH	0.772	10	78.1 \pm 4.7	76.6
	H		11	80.6 \pm 3.9	81.0
	EA		10	72.0 \pm 13.1	65.5
GC Thickness	VH	0.160	10	43.4 \pm 3.8	44.1
	H		11	39.4 \pm 2.9	39.5
	EA		10	32.8 \pm 6.7	31.5

There is no effect ($P > 0.05$) of follicle size category on all GC measurements as presented in Table 4-6.

Table 4-6: Association between the follicle size category and GC counts and thickness. VH (very Healthy), H (Healthy). EA (Early Atretic), LA (Late Atretic), LF (Large follicles from 20mm), SF (Small Follicles < 20mm). Bold indicates a statistically significant p-value.

Outcomes	Factor	P-value	No. of follicle	GC counts and thickness	
				Mean \pm SE Mean	Median
Basal GC	LF (1)	0.180	20	32.3 \pm 1.9	34.6
	SF (2)		11	38.2 \pm 2.6	36.8
% Basal GC	LF (1)	0.483	20	47.3 \pm 2.7	44.0
	SF (2)		11	48.9 \pm 3.4	50.8
Antral GC	LF (1)	0.292	20	12.3 \pm 0.9	12.8
	SF (2)		11	19.5 \pm 5.7	13.8
% Antral GC	LF (1)	0.099	20	17.0 \pm 0.7	16.3
	SF (2)		11	20.7 \pm 2.6	18.9
Intermediate GC	LF (1)	0.409	20	28.9 \pm 3.3	30.9
	SF (2)		11	25.7 \pm 3.4	26.6
% Intermediate GC	LF (1)	0.148	20	35.7 \pm 2.8	40.1
	SF (2)		11	30.4 \pm 2.9	29.4
Total GCs	LF (1)	0.804	20	73.5 \pm 5.4	79.7
	SF (2)		11	83.5 \pm 8.5	69.6
GC Thickness	LF (1)	0.680	20	36.4 \pm 3.1	39.2
	SF (2)		11	42.4 \pm 5.3	36.5

The breeding season or time of year of follicle collection showed a significant association with the percentage of basal and intermediate GC: transitional follicles had less %basal GC but more intermediate and % intermediate GC and more total GC when compared to winter but particularly summer follicles, which led to a non-significant increase in GC thickness. This is illustrated in Table 4-7.

Table 4-7: Association between the breeding season and GC counts and thickness. VH (very Healthy), H (Healthy). EA (Early Atretic), LA (Late Atretic), LF (Large follicles from 20mm), SF (Small Follicles <20mm). Bold indicates a statistically significant p-value.

Outcomes	Factor	P-value	No. of follicle	GC counts and thickness	
				Mean \pm SE	Median
Response	Breeding season				
Basal GC	Winter	0.670	7	35.3 \pm 2.1	35.0
	Summer		12	32.0 \pm 3.4	34.0
	Transition		12	36.2 \pm 2.0	35.4
% Basal GC	Winter	0.025	7	50.3\pm4.3	51.6
	Summer		12	53.4 \pm 3.6	52.6
	Transition		12	40.9 \pm 2.0	38.9
Antral GC	Winter	0.224	7	12.0 \pm 0.7	12.0
	Summer		12	11.8 \pm 1.3	11.7
	Transition		12	19.6 \pm 5.2	15.0
% Antral GC	Winter	0.264	7	16.8 \pm 0.7	16.5
	Summer		12	18.4 \pm 0.8	18.8
	Transition		12	19.2 \pm 2.6	16.1
Intermediate GC	Winter	0.006	7	24.7\pm4.6	20.8
	Summer		12	20.0 \pm 3.3	20.7
	Transition		12	37.4 \pm 3.1	39.8
% Intermediate GC	Winter	0.034	7	32.9\pm4.5	32.4
	Summer		12	28.2 \pm 3.4	28.9
	Transition		12	39.9 \pm 2.6	42.9
Total GC	Winter	0.012	7	72.0\pm4.8	66.8
	Summer		12	63.8 \pm 7.3	67.9
	Transition		12	93.2 \pm 6.8	96.0
GC Thickness	Winter	0.160	7	34.5 \pm 2.4	34.6
	Summer		12	31.5 \pm 4.0	35.6
	Transition		12	47.9 \pm 4.6	47.2

Ponies tended to have a lower % antral GC with a higher %intermediate GC, which was confirmed using a Mann Whitney test, and is presented in Table 4-8.

Table 4-8: Association between the breed category and GC counts and thickness. VH (very Healthy), H (Healthy). EA (Early Atretic), LA (Late Atretic), LF (Large follicles from 20mm), SF (Small Follicles < 20mm). Bold indicates a statistically significant p-value.

Outcomes	Factor			GC counts and thickness	
Response	Breed	P-value	No	Mean \pm SE Mean	Median
Basal GC	Horse	0.443	15	35.3 \pm 1.9	35.0
	Pony		15	32.8 \pm 2.6	34.4
% Basal GC	Horse	0.494	15	48.5 \pm 2.6	50.5
	Pony		15	46.9 \pm 3.5	44.0
Antral GC	Horse	0.901	15	16.9 \pm 4.3	12.2
	Pony		15	12.8 \pm 1.2	13.0
% Antral GC	Horse	0.120	15	19.8 \pm 1.9	18.4
	Pony		15	16.8 \pm 0.9	16.0
Intermediate GC	Horse	0.078	15	24.2 \pm 2.4	25.0
	Pony		15	31.6 \pm 4.3	37.4
% Intermediate GC	Horse	0.120	15	31.7 \pm 2.5	29.6
	Pony		15	36.3\pm3.5	41.9
Total GC	Horse	0.254	15	76.5 \pm 6.4	69.0
	Pony		15	77.2 \pm 7.2	89.6
GC Thickness	Horse	0.885	15	40.2 \pm 4.1	38.1
	Pony		15	36.7 \pm 3.9	38.9

Prepubertal mares had a lower % basal GC, tended to have more antral GC, and had more intermediate GC numbers and percentage, as well as more total GC, when compared to the 2 to 10 year and older categories in Table 4-9.

Specifically, Mann Whitney analysis showed significantly higher intermediate GC numbers ($P < 0.005$) between prepubertal aged mares (0-2 years old) and adult (>2-10 year old) mares ($P < 0.005$, CI 95.57%), with a tendency between prepubertal (0-2 years old) and adult mares >10 years old ($P = 0.07$, CI 95.44%), but no difference between >2-10 and >10 year old mares.

Table 4-9: Association between the age of the mare and GC counts and thickness. VH (very Healthy), H (Healthy). EA (Early Atretic), LA (Late Atretic), LF (Large follicles from 20mm), SF (Small Follicles < 20mm). Bold indicates a statistically significant p-value

Outcomes	Factor	P-value	No	GC counts and thickness	
				Mean \pm SE Mean	Median
Response	Age				
Basal GC	0-2 YO	0.559	10	34.6 \pm 2.6	34.1
	>2-10 YO		12	31.7 \pm 3.3	34.9
	>10 YO		8	36.9 \pm 1.2	35.9
% Basal GC	0-2 YO	0.003	10	38.4\pm1.5	38.3
	>2-10 YO		12	53.3\pm3.7	53.3
	>10 YO		8	51.0\pm3.5	51.2
Antral GC	0-2 YO	0.093	10	20.9 \pm 6.1	14.9
	>2-10 YO		12	11.5 \pm 1.4	10.5
	>10 YO		8	12.2 \pm 0.8	11.6
% Antral GC	0-2 YO	0.316	10	20.3 \pm 3.0	18.5
	>2-10 YO		12	18.0 \pm 0.8	17.6
	>10 YO		8	16.3 \pm 0.6	16.3
Intermediate GC	0-2 YO	0.010	10	38.6\pm3.1	39.8
	>2-10 YO		12	20.5\pm3.6	18.2
	>10 YO		8	25.7\pm4.2	22.9
% Intermediate GC	0-2 YO	0.033	10	41.3\pm2.8	43.9
	>2-10 YO		12	28.7\pm3.5	29.3
	>10 YO		8	32.7\pm3.7	33.6
Total GC	0-2 YO	0.021	10	94.2\pm8.0	96.0
	>2-10 YO		12	63.7\pm7.5	65.4
	>10 YO		8	74.8\pm4.8	69.3
GC Thickness	0-2 YO	0.300	10	44.5 \pm 5.0	40.3
	>2-10 YO		12	32.3 \pm 4.6	30.3
	>10 YO		8	40.0 \pm 4.2	39.5

There was no association between disease status and GC counts and thickness as shown in Table 4-10.

Table 4-10: Association between mare disease status and GC counts and thickness. VH (very Healthy), H (Healthy). EA (Early Atretic), LA (Late Atretic), LF (Large follicles from 20mm), SF (Small Follicles < 20mm). Bold indicates a statistically significant p-value.

Outcomes	Factor			GC counts and thickness		
Response	Disease	P-value	No	Mean \pm SE	Mean	Median
Basal GC	No disease	0.148	17	31.8 \pm 2.4		33.4
	Chronic mild		2	45.3 \pm 7.7		45.3
	Severe		12	36.2 \pm 1.3		35.9
% Basal GC	No disease	0.324	17	46.0 \pm 3.2		44.1
	Chronic mild		2	50.7 \pm 3.0		50.7
	Severe		12	50.0 \pm 2.8		51.2
Antral GC	No disease	0.174	17	16.4 \pm 3.9		12.8
	Chronic mild		2	16.8 \pm 0.0		16.8
	Severe		12	12.4 \pm 0.6		12.4
% Antral GC	No disease	0.319	17	19.4 \pm 1.8		19.2
	Chronic mild		2	18.7 \pm 1.8		18.7
	Severe		12	16.7 \pm 0.5		16.6
Intermediate GC	No disease	0.741	17	29.1 \pm 3.8		29.6
	Chronic mild		2	28.3 \pm 1.7		28.3
	Severe		12	25.8 \pm 3.3		22.9
% Intermediate GC	No disease	0.684	17	34.5 \pm 3.3		36.2
	Chronic mild		2	30.6 \pm 1.2		30.6
	Severe		12	33.3 \pm 2.9		33.6
Total GCs	No disease	0.435	17	77.3 \pm 7.9		83.6
	Chronic mild		2	90.4 \pm 9.4		90.4
	Severe		12	74.4 \pm 3.9		69.2
GC Thickness	No disease	0.962	17	37.6 \pm 4.3		39.9
	Chronic mild		2	38.5 \pm 11.2		38.5
	Severe		12	39.8 \pm 3.3		38.5

4.3.3.4 Theca cell layer

Follicle health category affected all thecal measurements with greatest THC thickness measured in healthy follicles as shown in Table 4-11. Individual comparisons using Mann Whitney also confirmed that numbers of large THC in LA was reduced (5.1 \pm 0.9) compared to VH, H and EA (45.5 \pm 6.4, 53.2 \pm 3.8, 16.9 \pm 7.7; respectively), whereas, it is the opposite with small theca cells (80.7 \pm 5.1) compared to VH, H and EA (47.2 \pm 5.3, 49.9 \pm 6.6, 40.1 \pm 4.1; respectively). The % large and small THC was equally altered between VH and H versus LA follicles (P < 0.005, CI 95.04%). When large THC percentage was combined for VH and H follicles versus EA and LA follicles Mann-Whitney showed also a significant reduction in atretic follicles (P < 0.001, CI 95.01%). There was no difference in

absolute numbers of small THC between VH, H and EA categories, but there was a significant increase in % small THC in EA compared to VH and H follicles.

Table 4-11: Association between follicle health status and THC counts and thickness. VH (very Healthy), H (Healthy). EA (Early Atretic), LA (Late Atretic), LF (Large follicles from 20mm), SF (Small Follicles < 20mm). Bold indicates a statistically significant p-value.

Outcomes	Factor			THC counts and thickness	
Response	Health status	P-value	No	Mean \pm SE Mean	Median
Large THC	VH	<0.001	10	45.5\pm6.4	42.0
	H		11	53.2 \pm 3.8	51.0
	EA		10	16.9 \pm 7.7	7.2
	LA		32	5.1 \pm 0.9	3.3
% Large THC	VH	<0.001	10	48.9\pm5.5	47.1
	H		11	53.4 \pm 4.0	49.8
	EA		10	20.9 \pm 8.1	11.0
	LA		32	6.8 \pm 1.5	3.5
Small THC	VH	<0.001	10	47.2\pm5.3	53.6
	H		11	49.9 \pm 6.6	50.0
	EA		10	40.1 \pm 4.1	37.3
	LA		32	80.7 \pm 5.1	79.0
% Small THC	VH	<0.001	10	51.1\pm5.5	52.9
	H		11	46.6 \pm 4.0	50.2
	EA		10	79.1 \pm 8.1	89.0
	LA		32	93.2 \pm 1.5	96.5
Total THC	VH	0.001	10	92.7\pm6.4	86.5
	H		11	103.0 \pm 6.5	97.0
	EA		10	57.1 \pm 7.9	64.0
	LA		32	85.8 \pm 5.2	81.6
THC Thickness	VH	<0.001	10	99.8\pm10.5	90.4
	H		11	101.7 \pm 8.3	91.2
	EA		10	47.9 \pm 5.9	46.7
	LA		32	71.0 \pm 4.7	64.6

Examining the effect of follicle size category on the large and small THC compartment showed that large THC seemed to be one quarter and small THC three quarters of the total THC in both categories as presented in Table 4-12. This table shows a significant increase in small THC and all THC numbers in small follicles < 20mm (P= 0.04 and P= 0.03) whereas the thickness was not significantly affected.

Table 4-12: Association between follicle size category and THC counts and thickness. VH (very Healthy), H (Healthy). EA (Early Atretic), LA (Late Atretic), LF (Large follicles from 20mm), SF (Small Follicles < 20mm). Bold indicates a statistically significant p-value.

Outcomes	Factor			THC counts and thickness	
Response	F. Size Cat.	P-value	No	Mean \pm SE Mean	Median
Large THC	LF (1)	0.874	32	21.0 \pm 3.7	12.5
	SF (2)		31	22.5 \pm 5.0	8.0
% Large THC	LF (1)	0.967	32	24.7 \pm 4.2	21.7
	SF (2)		31	22.9 \pm 4.7	7.2
Small THC	LF (1)	0.041	32	55.6\pm4.4	56.2
	SF (2)		31	71.9\pm5.8	73.2
% Small THC	LF (1)	0.967	32	75.3 \pm 4.2	78.3
	SF (2)		31	77.0 \pm 4.7	92.8
Total THC	LF (1)	0.031	32	76.6\pm4.9	80.3
	SF (2)		31	94.4\pm5.1	92.6
THC Thickness	LF (1)	0.221	32	70.2 \pm 4.6	67.8
	SF (2)		31	84.7 \pm 6.6	73.1

When comparing the effect of breeding season on the large and small THC and theca thickness presented in Table 4-13 an increase in large THC numbers and percentage was seen in winter compared to summer and transition follicles (% large THC 41.0 \pm 8.3, 14.9 \pm 3.8, 28.8 \pm 5.0; respectively). In contrast, the small theca cell percentage decreased in winter compared with summer and transition follicles (58.9 \pm 8.3, 85.1 \pm 3.8, 71.2 \pm 5.0; respectively). Furthermore, a significant difference in THC thickness (P= 0.004) was detected between winter and summer follicles (100.1 \pm 10.7, 64.8 \pm 4.6; respectively; P <0.005) using a Mann Whitney test.

Table 4-13: Association between breeding season and THC counts and thickness. VH (very Healthy), H (Healthy). EA (Early Atretic), LA (Late Atretic), LF (Large follicles from 20mm), SF (Small Follicles < 20mm). Bold indicates a statistically significant p-value.

Outcomes	Factor			THC counts and thickness	
Response	Breeding season	P-value	No	Mean \pm SE Mean	Median
Large THC	Winter	0.001	11	39.6\pm9.6	45.4
	Summer		32	13.1 \pm 3.5	2.4
	Transition		20	25.8 \pm 4.8	23.9
% Large THC	Winter	0.001	11	41.0\pm8.3	43.9
	Summer		32	14.9 \pm 3.8	2.9
	Transition		20	28.8 \pm 5.0	30.9
Small THC	Winter	0.275	11	50.0 \pm 7.3	38.8
	Summer		32	63.6 \pm 4.9	60.5
	Transition		20	71.0 \pm 7.6	63.5
% Small THC	Winter	0.001	11	58.9\pm8.3	56.1
	Summer		32	85.1 \pm 3.8	97.1
	Transition		20	71.2 \pm 5.0	69.1
Total THC	Winter	0.073	11	89.6 \pm 9.6	83.4
	Summer		32	76.7 \pm 5.1	79.9
	Transition		20	96.8 \pm 5.3	87.2
THC Thickness	Winter	0.004	11	100.1 \pm10.7	94.9
	Summer		32	64.8 \pm 4.6	61.6
	Transition		20	84.7 \pm 7.1	78.4

There was no effect of breed category on large and small THC count and thickness as presented in Table 4-14.

Table 4-14: Association between breed category and THC counts and thickness. VH (very Healthy), H (Healthy). EA (Early Atretic), LA (Late Atretic), LF (Large follicles from 20mm), SF (Small Follicles < 20mm). Bold indicates a statistically significant p-value.

Outcomes	Factor			THC counts and thickness	
Response	Breed	P-value	No	Mean \pm SE Mean	Median
Large THC	1 Horse	0.188	40	20.6 \pm 4.2	7.3
	2 Pony		20	25.9 \pm 4.7	27.9
% Large THC	1 Horse	0.136	40	21.6 \pm 4.1	5.6
	2 Pony		20	29.6 \pm 5.3	35.2
Small THC	1 Horse	0.180	40	67.3 \pm 4.8	68.5
	2 Pony		20	58.0 \pm 6.6	53.6
% Small THC	1 Horse	0.136	40	78.5 \pm 4.1	94.4
	2 Pony		20	70.4 \pm 5.3	64.8
Total THC	1 Horse	0.938	40	87.8 \pm 4.6	82.9
	2 Pony		20	83.9 \pm 6.4	85.1
THC Thickness	1 Horse	0.158	40	75.0 \pm 4.5	66.6
	2 Pony		20	85.7 \pm 8.6	85.6

There was an association of large and small THC counts and thickness with mare age as presented in Table 4-15, specifically prepubertal fillies had a higher number and percentage of large THC, and a lower % small THC. Surprisingly, theca cell thickness was greatest in the older mares > 10 years of age, and they tended to have 10 and 20 more THC per view than prepubertal and 2-10 year old mares.

Table 4-15: Association between mare age and THC counts and thickness. VH (very Healthy), H (Healthy). EA (Early Atretic), LA (Late Atretic), LF (Large follicles from 20mm), SF (Small Follicles < 20mm). Bold indicates a statistically significant p-value.

Outcomes	Factor			THC counts and thickness	
Response	Age	P-value	No. of follicle	Mean \pm SE Mean	Median
Large THC	0-2 YO	0.005	13	31.2\pm5.7	27.2
	>2-10 YO		31	14.6 \pm 3.8	3.0
	>10 YO		17	28.6 \pm 7.3	12.2
% Large THC	0-2 YO	0.009	13	35.5\pm5.9	36.6
	>2-10 YO		31	17.1 \pm 4.2	2.7
	>10 YO		17	27.9 \pm 6.7	13.3
Small THC	0-2 YO	0.404	13	57.7 \pm 7.0	56.0
	>2-10 YO		31	63.1 \pm 5.9	57.6
	>10 YO		17	69.0 \pm 7.0	73.8
% Small THC	0-2 YO	0.009	13	64.5\pm5.9	63.4
	>2-10 YO		31	82.9 \pm 4.2	97.3
	>10 YO		17	72.1 \pm 6.7	86.7
Total THC	0-2 YO	0.091	13	88.9 \pm 5.6	83.4
	>2-10 YO		31	77.7 \pm 6.0	77.4
	>10 YO		17	97.7 \pm 5.8	87.8
THC Thickness	0-2 YO	0.009	13	76.7\pm5.9	80.2
	>2-10 YO		31	68.9 \pm 5.9	63.9
	>10 YO		17	95.7 \pm 8.1	91.2

Follicles from mares with severe disease tended to have more large THC, and a higher % large THC, with a lower % small THC and most total THC as shown in Table 4-16. Interestingly, it was the follicles from mares with mild disease that had greatest THC thickness (P= 0.01), although the numbers were very low. Therefore, a Mann Whitney test was applied combining follicles from mares with chronic mild and severe disease compared with follicles recovered from mares with no disease, and it confirmed that follicles from mares with disease had a thicker THC compartment (P< 0.005, CI 95.13 %).

Table 4-16: Association between mare disease status and THC counts and thickness. VH (very Healthy), H (Healthy). EA (Early Atretic), LA (Late Atretic), LF (Large follicles from 20mm), SF (Small Follicles < 20mm). Bold indicates a statistically significant p-value.

Outcomes	Factor			THC counts and thickness	
Response	Disease	P-value	No	Mean \pm SE	Median
Large THC	No disease	0.068	35	16.1 \pm 3.5	7.4
	Chronic mild		4	26.5 \pm 13.6	23.6
	Severe		24	29.3 \pm 5.7	21.0
% Large THC	No disease	0.059	35	18.0 \pm 3.7	6.7
	Chronic mild		4	29.1 \pm 12.7	31.0
	Severe		24	31.6 \pm 5.6	32.9
Small THC	No disease	0.960	35	62.4 \pm 4.4	63.4
	Chronic mild		4	62.2 \pm 19.1	50.1
	Severe		24	65.5 \pm 7.0	59.9
% Small THC	No disease	0.059	35	82.0 \pm 3.7	93.3
	Chronic mild		4	70.9 \pm 12.7	69.0
	Severe		24	68.4 \pm 5.6	67.1
Total THC	No disease	0.088	35	78.5 \pm 4.8	80.2
	Chronic mild		4	88.7 \pm 19.3	100.5
	Severe		24	94.8 \pm 5.5	89.0
THC Thickness	No disease	0.013	35	65.3\pm3.8	63.9
	Chronic mild		4	107.5 \pm 26.2	112.4
	Severe		24	89.7 \pm 6.9	79.8

4.4 Discussion

Oestrous cycles in ponies are longer compared to the mare (Aurich, 2011), with follicles emerging at 6mm and then reaching a maximum size of about 30 mm. The largest follicle > 20 mm in ponies cannot be recognized until mid-March or 60 days before ovulatory season (Donadeu and Ginther, 2002). This explains why all our collected follicles prior to mid-March had not reached the maximum size of the largest follicle. Draincourt et al. (1982) have stated that the pony mares begin their ovulatory oestrous cycles in May, which is later than large mares (in March) and stop earlier on September compared to large mares (at the end of October). Therefore, the average length of the oestrous cycles for pony mare and large mares are 25 days and 22.7 days, respectively. Small antral follicles activity in pony mares increased dramatically at the beginning of the ovulatory season compared to the end of it and in anoestrus (Donadeu and Pedersen, 2008). Our findings support this as we found many follicles in the pony mares during the beginning of the transition period. The length of the transition phase

might vary due to an intermittent period of oestrous behaviour, which could continue for several days and weeks.

The counts of growing follicles and primordial follicles were not affected by breed (Kenney et al., 1979, Driancourt et al., 1982). Our histological study showed that the counts of GC and THC were also not significantly affected by breed categories.

According to Watson and Ai-zi'abi (2002) the transitional follicles had a yellowish to pale pink colour and the preovulatory follicles had orange to red colour. In the current study the finding was exactly the same for the transitional follicles collected but we did not specifically characterise preovulatory follicles. Kenney et al. (1979) classified grossly the yellowish colour of the follicular cavity with remarkable blood vessels on the surface as representing the early atretic phase. This yellowish-coloured surface with blood vessels was noticed in some follicles in our examination, but did not contribute to our classification based on histological findings. Pedersen et al. (2003) classified atretic follicles based on apoptosis and pyknotic appearance on GC and THC, as well as the appearance of a thick membrane between both cell types. In our study, the atretic follicles were classified into early atretic, when the palisade arrangement of basal GC became irregular and mixed with intermediate and antral GC and the amorphous membrane started to appear, or as late atretic when there was no GC layer as well as the hyaline or amorphous membrane becoming very noticeable and separating the theca layers into two parts. Pyknosis and apoptosis were distinguished in atretic follicles, but could to a small extent also be seen in the healthy category. Cells undergoing apoptosis have disarray in their connections with the neighboring cells (Duvall and Wyllie, 1986), therefore, follicles with a granulosa layer showing detachment between cells and the theca would be considered to be atretic. This supports our classification into the EA category and LA category separate from that of H category. The degree of separation of cells seen in EA category and LA category are far more extensive than what was seen in H category follicles.

The thickness and the arrangement of GC above the basement membrane in transitional anovulatory and preovulatory follicles are histologically the same, but there are differences in theca interna (Watson and Al-zi'abi, 2002). The

preovulatory follicle consists of a thick layer of polyhedral cells with a nucleus and a pale cytoplasm, whereas the anovulatory follicle contains a thin and undeveloped theca.

The observed difference associated with disease conditions might be due to the fact that the majority of follicle walls were collected from mares with no diseases while only 4 follicles were collected from mares with chronic mild diseases, and follicles from mares with severe diseases actually had absolute highest intrafollicular oestradiol, thus belonged to the healthy follicle categories.

The unusual Mean and Median of follicles collected in the non-breeding season is due to the presence of one large follicle produced high levels of oestradiol (798 ng/ml) compared to those in the transitional period. We also saw an unusual tendency for a breed association (with intrafollicular oestradiol concentrations, because follicles from ponies produced more oestradiol.

Although a degeneration of follicles occurred in the LA category, those types of follicles still show some intrafollicular oestradiol. This outcome agrees with other studies (Kenney et al., 1979). Similar to our study and follicle health categorisation, Sessions et al. (2009) classified the follicles as healthy based on high concentrations of oestradiol, whereas the ones with low concentrations were categorised as atretic. These authors also detected that there were no significant changes in mean diameter between healthy and atretic follicles, which is again supported by our findings.

The variation that occurred in the intermediate GC number and percentage in the two follicle size categories might be due to the large follicle group having almost double the number of follicles than small follicles.

The thickness of the cellular layers amongst relatively healthy population does not vary that much, however, it should be noted that the granulosa cell layer in healthy samples would be relatively uniform in thickness (absence of sloughing and hyperplasia). The significant variation in the large and small theca cell numbers and percentage, and the THC thickness associated with follicle health category may be influenced by the large number of LA follicles compared to VH,

H and EA follicles in our study. However, as histomorphological alterations agree with previous reports of equine follicle atresia, we attribute the changes seen more to the health status than follicle numbers analysed.

Although mitosis was not considered in our analysis and histological categorisation, mitotic figures were found in theca cells mostly in the VH, H and EA categories. This agrees with previous descriptions (Kenney et al., 1979) where mitotic figures were observed in both granulosa and theca cells.

4.5 Conclusion

Overall histomorphological measurements of antral follicle walls in mares appeared to mostly be affected by health status rather than mare factors. However, differences were seen in follicles from prepubertal mares, ponies, diseased mares and follicles collected in transition or winter, and subsequent statistical analyses which need to include several predictive factors in one model will determine whether associations remain with season, age, disease or breed category.

Comparison of various parameters between different follicle health groups categorised visually based on histological criteria demonstrates that the GC and THC compartment thickness and the cell counts of the cell layers were similar between VH and H categories which also had similarly high intrafollicular oestradiol concentrations. However, H follicles were 4 mm larger in diameter and thus larger than the size of dominant follicles at the time of selection, while VH follicles appear to be pre-selection cohort follicles. Overall, the granulosa cell layer in healthy specimens is uniform in thickness due to an absence of sloughing or hyperplasia. The effects of follicle atresia were clearly seen in both cell compartments and in intrafollicular oestradiol, but not in diameter. Follicles categorised as LA lost their GC layer, but also showed a much reduced THC compartment even when compared with EA follicles. In fact, onset of atresia, while still maintaining a full GC layer, began to affect the THC compartment with reduced theca thickness seen during early atresia.

Chapter 5 Identifying histomorphological and immunohistochemical alterations in mare granulosa cell tumours (GCT) and antral follicles

5.1 Introduction

Granulosa cell tumours (GCT) developing within ovaries are the overarching neoplasm in mares (Watson, 1994), they develop gradually, are consistently benign and occur unilaterally (Troedsson et al., 2003). In GCT most of the ovarian tissue contains multiple macrofollicular cysts, with cysts being composed of granulosa cells surrounded by theca or luteal like cells within a fibrovascular stroma (McCue et al., 1991, vanderZaag et al., 1996). Histological examination of GCT also revealed clusters of granulosa cells isolated by stroma that contained spindle-shaped cells corresponding to thecal tissue (Fernandes et al., 2011). In addition, GCT are characterised by microfollicular Exner bodies, trabecular cords of granulosa cells, and large Leydig like polyhedral cells in the surrounding theca.

Such histological GCT analyses show that tumour transformation occurs mainly in granulosa cells (GC), leading to a dysregulation in GC proliferation. Yet we know that some functions of differentiated GC and theca cells (THC) are maintained, such as GC inhibin and THC androgen synthesis, providing systemic diagnostic markers for a large proportion of GCT in mares. This is very much in contrast to antral follicle wave and dominant follicle development where differentiation, ultimately leading to enhance oestradiol synthesis, slows proliferation of follicular cells. A comparative approach investigating the synthesis of follicular differentiation markers may, therefore, aid our understanding of GCT pathogenesis in mares.

The main functions of inhibin are in GC development and proliferation, steroid hormone secretion and oocyte growth. The production of inhibin by granulosa cells has been recognised to contribute to a reduction of the ovulatory quota (the selection mechanism) in mares by downregulation of FSH. In healthy large follicles the expression of inhibin α and β A subunits was detected in granulosa

cells (Nagamine et al., 1998). In contrast, they found that the expression of inhibin α subunit was identified in small healthy follicles but inhibin BA subunits were not found, possibly indicating that the inhibin A dimer was not synthesised.

The concentration of inhibin increases gradually and reaches a peak at preovulation ensuring low FSH and dominant follicle selection; inhibin is also elevated when GCT is present (Crabtree, 2013). Approximately 87% of GCT in mares have high inhibin concentrations. The cytoplasm of granulosa cells in GCT have been immunostained with inhibin α and also Anti-Muellerian Hormone (AMH) by (Evkuran Dal et al., 2013). While inhibin IHC has been done by many researchers, few reports exist of enzymes involved in androgen production by theca cells, such as 17 α hydroxylase and those involved in oestradiol production in GC such as the cytochrome P450 aromatase (Watson, 1999). The cytochrome P450 aromatase converts androgen to oestrogen, but its expression in the granulosa cells detected using IHC appears very low but adequate even in transitional follicles (Watson, 1999, Watson and Ai-zi'abi, 2002). Immunostaining for aromatase in granulosa cells was seen in follicles from 5mm in diameter until the preovulatory stage (Belin et al., 2000).

In contrast to inhibin and aromatase expression in GC, CYP17 only immunostains theca cells. The P450 cytochrome 17 enzyme is present in ovary, testis and adrenal cortex samples (Almeida et al., 2011b). Immunolabelling of CYP17 in the preovulatory follicle is seen in the theca interna layer (Albrecht and Daels, 1997, Watson et al., 2004).

In ovaries from healthy mares and in GCT the expression of AMH is high but is reduced in large antral follicles (Almeida et al., 2011a). Immunostaining of AMH in GCT has previously been observed in all parts containing GC, such as tubular or trabecular GC nests or cysts, as well as being found in polyhedral Leydig like cells in the interstitial tissue or the stroma (Ball et al., 2008b). It is, however, unclear whether AMH type 2 receptor (AMHR2) presence, essential for intracellular AMH actions, is regulated in antral follicles and whether its expression regulates AMH actions in GCT tumour cells.

5.1.1 Aim:

By using histological (H&E and IHC) approaches determine follicular and mare factors that are associated with granulosa and theca cell expression of proteins related to antral follicle differentiation, and investigate how such expression may be dysregulated in GCT and whether characteristic alterations in GC nucleus size occur when GC transform to tumour cells in cysts or solid nests compared with equine antral follicles from control mares.

5.1.2 Objectives:

1. Determine the localization and expression pattern of the functional hormone, enzyme and receptor markers inhibin, aromatase, CYP17 and AMHR2, in equine antral follicles from control mares and in GCT using IHC.
2. Determine any associations between predictive follicle and mare factors and the control FW expression pattern of these functional markers.
3. Determine any associations between GCT category and the expression pattern of these functional GC or THC markers, and compare control FW with diseased GCT cysts or solid nests in their expression pattern.
4. Measure and compare GC nuclear circumference in very healthy (VH), healthy (H) and early atretic (EA) antral follicles, GCT cysts, and solid GC islets within GCT.

5.2 Materials and Methods:

5.2.1 Animal and tissue samples

Forty follicle walls (FW, average size of the follicles was 21.4mm), were dissected from normal ovaries of sixteen mares (age range from 1.5 to 20 years old), and classified into four categories based on histological health status with ten follicles in each category: very healthy (VH) healthy (H), early atretic (EA) and late atretic follicles (LA) as described in chapter 4. The FW were processed for H&E sections, and the same blocks were then used for immunohistochemistry.

Ten GCT tissue samples from five mares (two samples were collected from the GCT of each mare, from one cystic and one solid area of the GCT) were processed for H&E sections, and cystic and solid areas within each section were histologically classified into four categories: GCT 1 (a very large cyst like structure with the cyst wall stretched like a FW and resembling the very healthy and healthy FW categories), GCT 2 (the cystic structure is round like a small antral follicle, with a GC layer surrounding the cyst antrum and containing antral, intermediate and basal GC), GCT 3 (the cystic structure is round, but only has a single cell layer surrounding a fluid antrum, with cells resembling antral GC) and GCT4 (solid nests of GC residing within and clearly discernable from the surrounding interstitial/stromal tissue).

For the study of nuclear size= circumference, 15 FW were dissected from the normal ovaries of 10 mares, representing 5x VH, 5x H and 5x EA follicles, and ten GCT tissue samples were recovered from five mares as described above. All samples were routinely processed for H&E sections.

5.2.2 Immunohistochemistry (IHC) technique on follicle wall and GCT sections

The IHC was performed as described in detail in Chapter 2. The tissues were embedded in wax blocks at the required orientation to give a cross section of the FW or GCT cyst (Thermo Histostar embedding centre), sectioned at a thickness of 2.5 μm (Thermo Finesse NE+ Microtome) and rehydrated. Sections then underwent Heat-Induced Epitope Retrieval (HIER) followed by incubation in the first antibody solution at room temperature using the Dako Autostainer (Agilent, Dako, USA). The first and second antibodies are as detailed and using the listed dilutions as presented in Table 5-1. Please note that while the ‘inhibin’ antibody was in fact raised against the N-terminus of the human inhibin alpha subunit (with inhibin being a dimer of inhibin alpha and inhibin beta subunits), high alpha subunit expression is normally a prerequisite for high inhibin protein expression; thus the result description will refer to ‘inhibin’ protein expression and not just expression of the alpha subunit.

Table 5-1: IHC antibodies

No.	Antibodies	Antigen Retrieval	Antibodies dilution	Secondary Antibodies
11	INHIBIN alpha clone R1 Dako Cat. NO. M3609	HIER Sod Citrate pH6	1:20	Dako Envision+System HRP Labelled polymer Ant-mouse Cat. No. K4001 ready to use
22	AROMATASE ABBIOTEC Cat. No. 250549	Proteinase K 15 minutes	1:100	Dako Envision+System HRP Labelled polymer Ant-Rabbit Cat. No. K4003 ready to use
33	CYP17A1 Santa Cruz Cat. No. sc-374244	HIER Sod Citrate pH6	1:1500	Dako Envision+System HRP Labelled polymer Ant-mouse Cat. No. K4001 ready to use
44	AMHR2 N-Term Antibodies-online Cat. No. ABIN2616027	HIER sodium citrate pH6	1:200	Dako Envision+System HRP Labelled polymer Ant-Rabbit Cat. No. K4003 ready to use

5.2.3 IHC and nuclear measurements

Images for immunohistochemical evaluation of the protein expression pattern were captured using a Leica DM4000B microscope (Leica Microsystems, Switzerland) and Leica Application Suite software (version 4.3.0; Leica Microsystems, Switzerland), whereas images for nuclear circumference measurements under oil immersion were captured using an Olympus BX51 microscope and Stream Basic (version 1.9.2; Olympus soft Imaging Solutions GmbH). All images were analysed by the same operator, and each one was given a score relating to stain intensity and distribution pattern, and a percentage to show coverage of the specific cell layer analysed (%area). For the stain intensity, score 0 means no stain, 1 is low, 2 is medium and 3 is high stain intensity; in relation to the spread or distribution score 1 reflects continuous distribution, while score 2 reflects individual cells being stained, and 3 clusters of cells being stained. The percentage of the area covered was considered a better measurement than absolute cell numbers, as, for example, in GCT3 the number of GC was actually reduced, but protein expression may still have been seen in a high % of the GC.

Nuclear circumferences of 15 basal, 15 intermediate and 15 antral GC in 3 views (5 GC in each location) across each section were measured for five VH, H and EA follicles using Image J software. The GCT nuclear circumferences were similarly measured in 15 basal, 15 intermediate and 15 antral GC in three GCT1 views per section, and in 25 basal, 25 intermediate and 25 antral GC in five GCT2 cysts across each section, for a total of 10 GCT sections. For GCT3 25 antral GC were also measured in five cysts (5x GC per cyst) per section, and for GCT4 45 GC were measured in 3 different solid GC nests (15x GC per GC nest) per section. More views were analysed across the GCT sections for GCT2 and GCT3 due to their smaller cystic structure and varied distribution in the section.

The magnification of the microscope binocular was 10X, therefore, each IHC section was viewed at 200X magnification, and nuclear circumference was measured at 1000x magnification under oil immersion. Stain intensity, distribution and %area were estimated over the whole section. The measurements were based on a previous study in ovarian human samples (Hes et al., 2011) where they classified the intensity staining as negative, weak, moderate or strong. Their distribution score was focal (<50% of positive neoplastic cells) or diffuse (>50% of positive neoplastic cells) while our distribution categories included a continuous vs. individual vs. cluster like distribution.

5.2.4 Statistical analysis

The Null Hypotheses tested using statistical analyses were:

1) For IHC results: no differences exist in Inhibin, Aromatase, CYP17A1 and AMHR2 stain intensity classified as 0 (=no stain) and 1 (=weak) to 3 (=strong); stain distribution classified as 1 (=continuous), 2 (=individual) and 3 (clusters); and %area stained estimated (%area) subjectively by the same operator, between:

- a) Follicle health categories of control FW,
- b) GCT categories of GCT samples, and
- c) FW combined (VH, H, EA, LA for theca cell layer) and GCT combined (GCT1, GCT2, GCT3, GCT4).

II) For IHC results in control FW: no correlation exists between follicle diameter or follicular fluid (FF) oestradiol (E2) and %area estimated by the same operator.

III) For nuclear circumferences: no differences exist in GC nuclear circumferences between the different locations within the GC layer, between FW and GCT categories, and between the healthy control and diseased GCT tissues.

Data were analysed using the descriptive statistic function and the normality tests in Minitab 18. Because data were not all normally distributed, statistical comparisons were carried out using Kruskal-Wallis and Mann-Whitney tests, to detect the associations between a) follicle health category in control follicle walls (VH, H, EA, and LA for Theca), and b) GCT area category (category 1,2,3,4) and individual protein expression measurements. The associations of stain intensity and distribution categories for all proteins with the follicular diameter and follicular fluid oestradiol in control FW were also tested using the Kruskal-Wallis and Mann-Whitney tests. The correlation between estimated %area and follicular diameter as well as follicular fluid oestradiol concentrations in control follicles was determined using the Spearman Rho function (Minitab 18). Nuclear circumferences of granulosa cells of the follicular wall and GCT were analysed using descriptive statistics and Kruskal-Wallis followed by Mann-Whitney tests for individual comparisons.

5.3 Results:

5.3.1 Immunohistological findings

For each follicle wall health category there were ten follicles analysed from between five to eight mares, VH follicles came from eight individual mares, H and EA follicles came from seven individual mares and LA follicles came from five individual mares. For each GCT category there were 10 sections analysed obtained from one apparently solid and one apparently cystic tissue sample per GCT recovered from five mares.

The expression of inhibin protein in GC only was detected in the follicle walls of three different health status categories; very healthy (VH), healthy (H) and early atretic (EA) but not in late atretic (LA) follicles lacking the GC compartment as shown in Figure 5-1 and Figure 5-2. The expression of inhibin protein in GC in GCT categorised as GCT1 (which looks like a healthy follicular wall), GCT2 and GCT3 (circular cystic like structures; GCT2 has antral, intermediate and basal GC, whereas GCT3 has only a few antral GC remaining), and GCT4 (solid nests of GC) in Figure 5-3 and Figure 5-4.

Examples of different inhibin stain intensity, distribution and percentage area detected in the FW and GCT sections can be seen in Figure 5-5 and Figure 5-6.

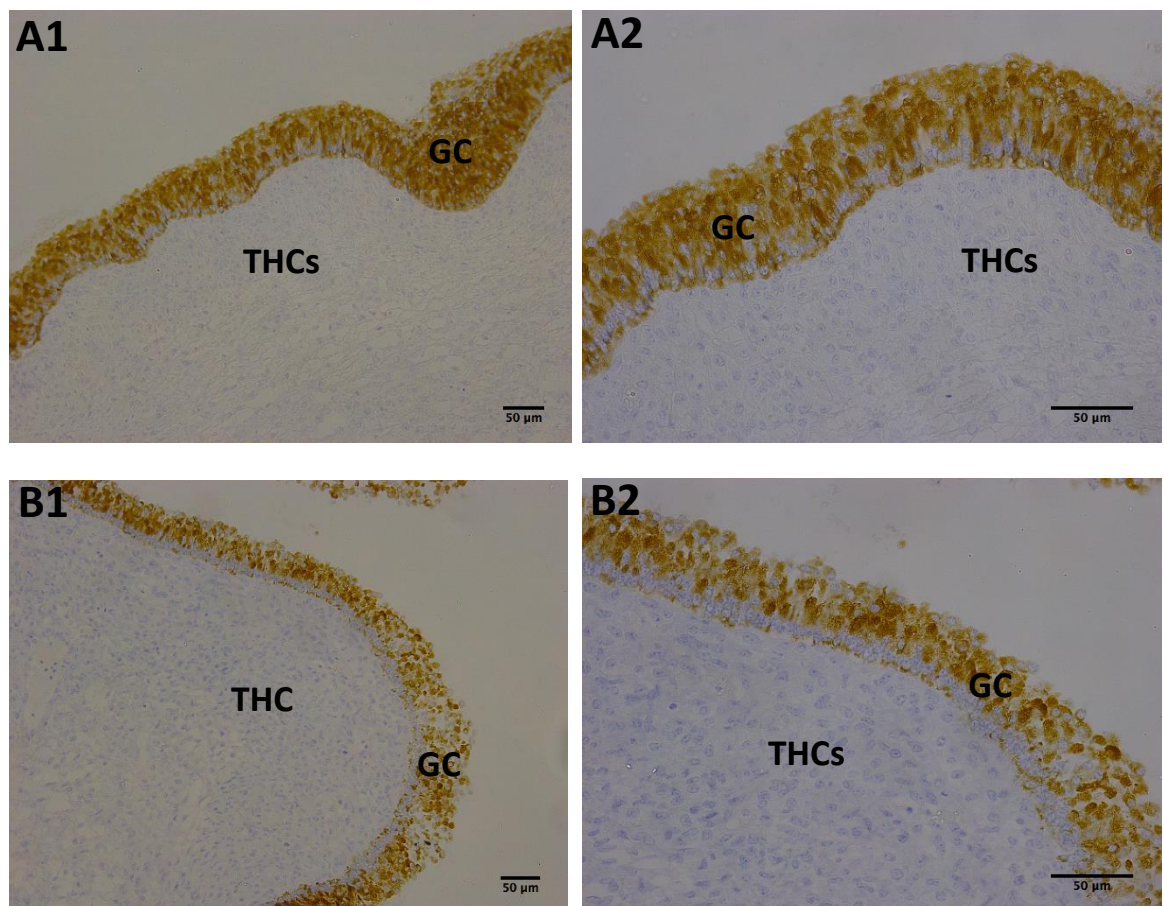


Figure 5-1: Inhibin expression exclusively in GC in VH (A1 and A2) and H (B1 and B2) follicles. A1 and B1 are at 200x magnification, and A2 and B2 are at 400x magnification.

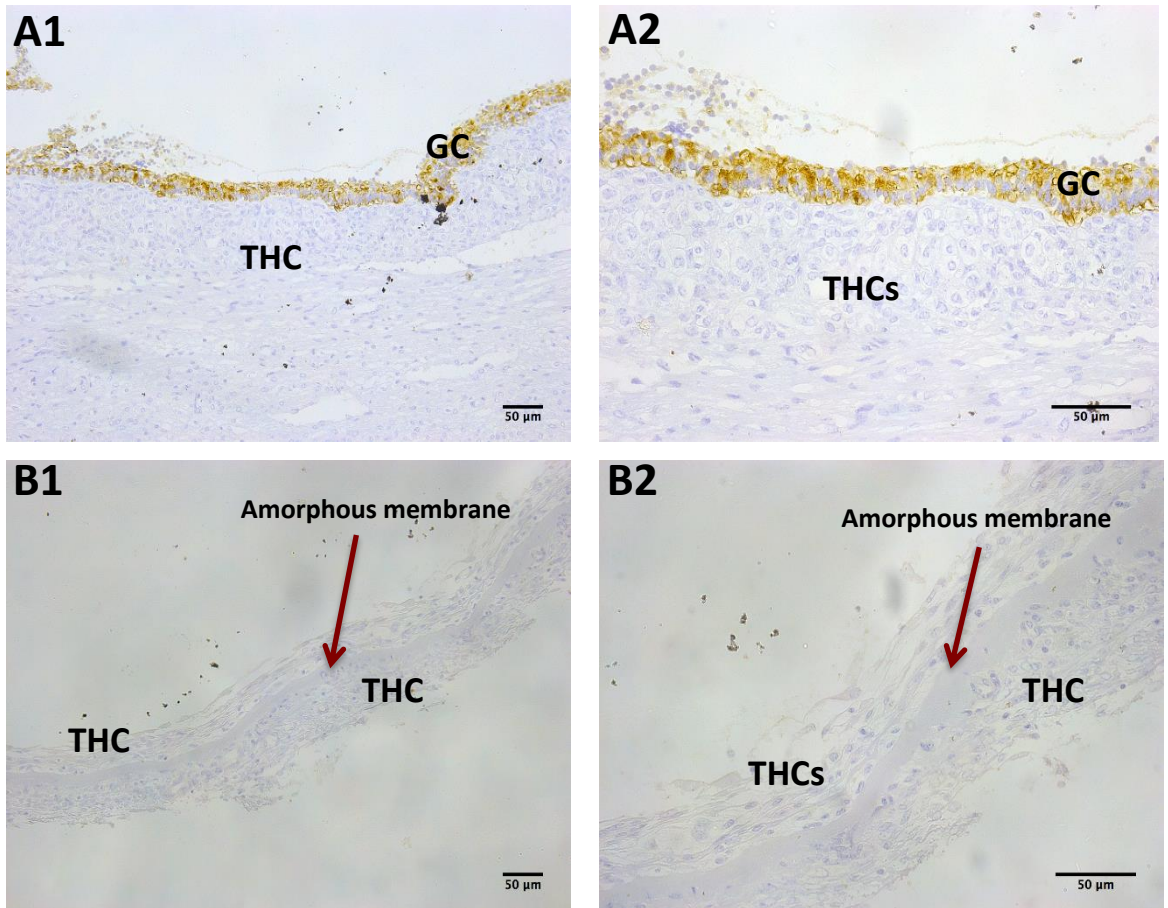


Figure 5-2: Inhibin expression exclusively in GC of EA follicles (A1 and A2). As the GC layer has disappeared in LA follicles, no positive immunoreactivity is seen (B1 and B2). A1 and B1 are at 200x magnification, and A2 and B2 are at 400x magnification.

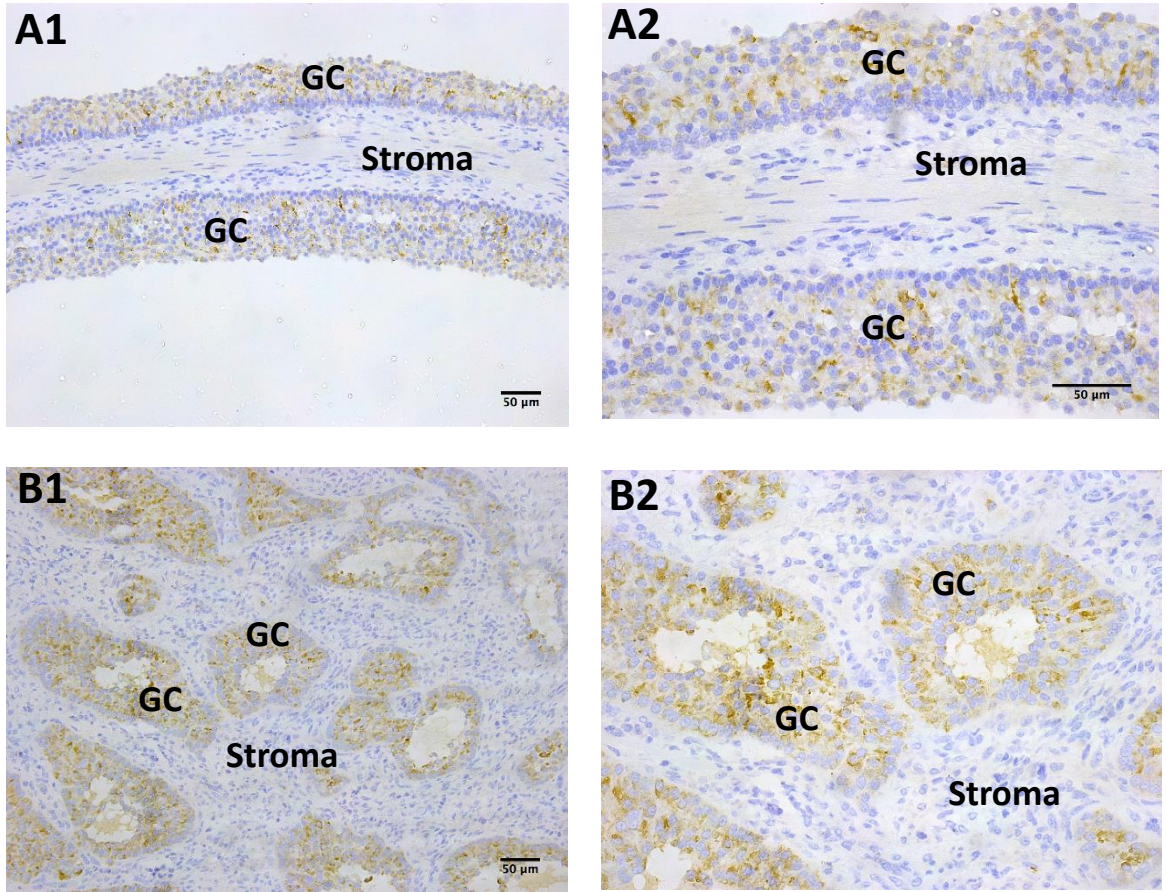


Figure 5-3: Inhibin expression exclusively in GC of GCT categorised as GCT1 (A1 and A2) and GCT2 (B1 and B2). A1 and B1 are at 200x magnification, and A2 and B2 are at 400x magnification.

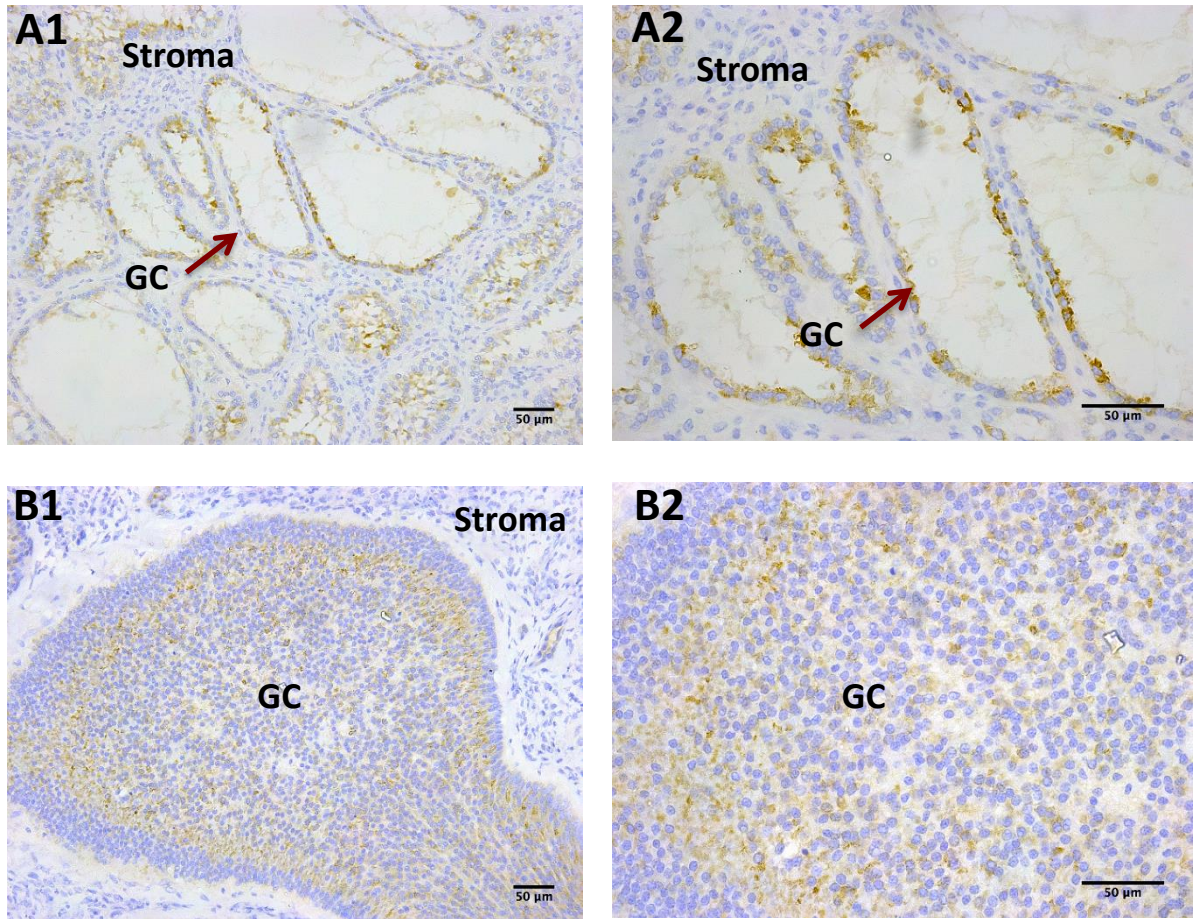


Figure 5-4: Inhibin expression exclusively in GC of GCT categorised as GCT3 (A1 and A2) and GCT4 (B1 and B2). A1 and B1 are at 200x magnification, and A2 and B2 are at 400x magnification.

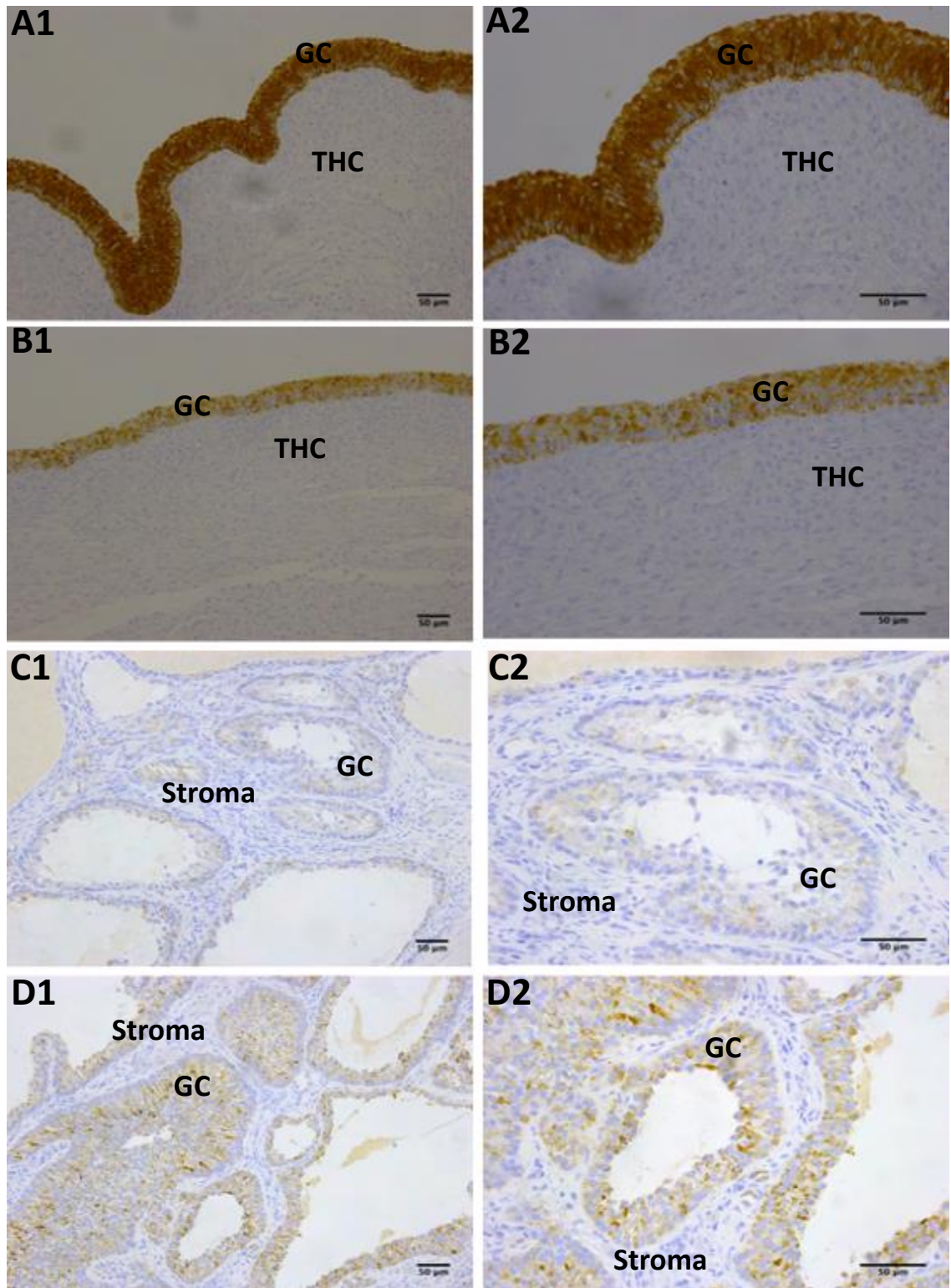


Figure 5-5: Inhibin expression exclusively in GC showing different stain intensity at 200x magnification (ABCD1) and 400x magnification (ABCD2); A1 & A2 show H follicle walls with high expression and B1 & B2 H follicle walls with medium expression, C1 & C2 show GCT2 with low expression and D1 & D2 show GCT2 with relatively high expression.

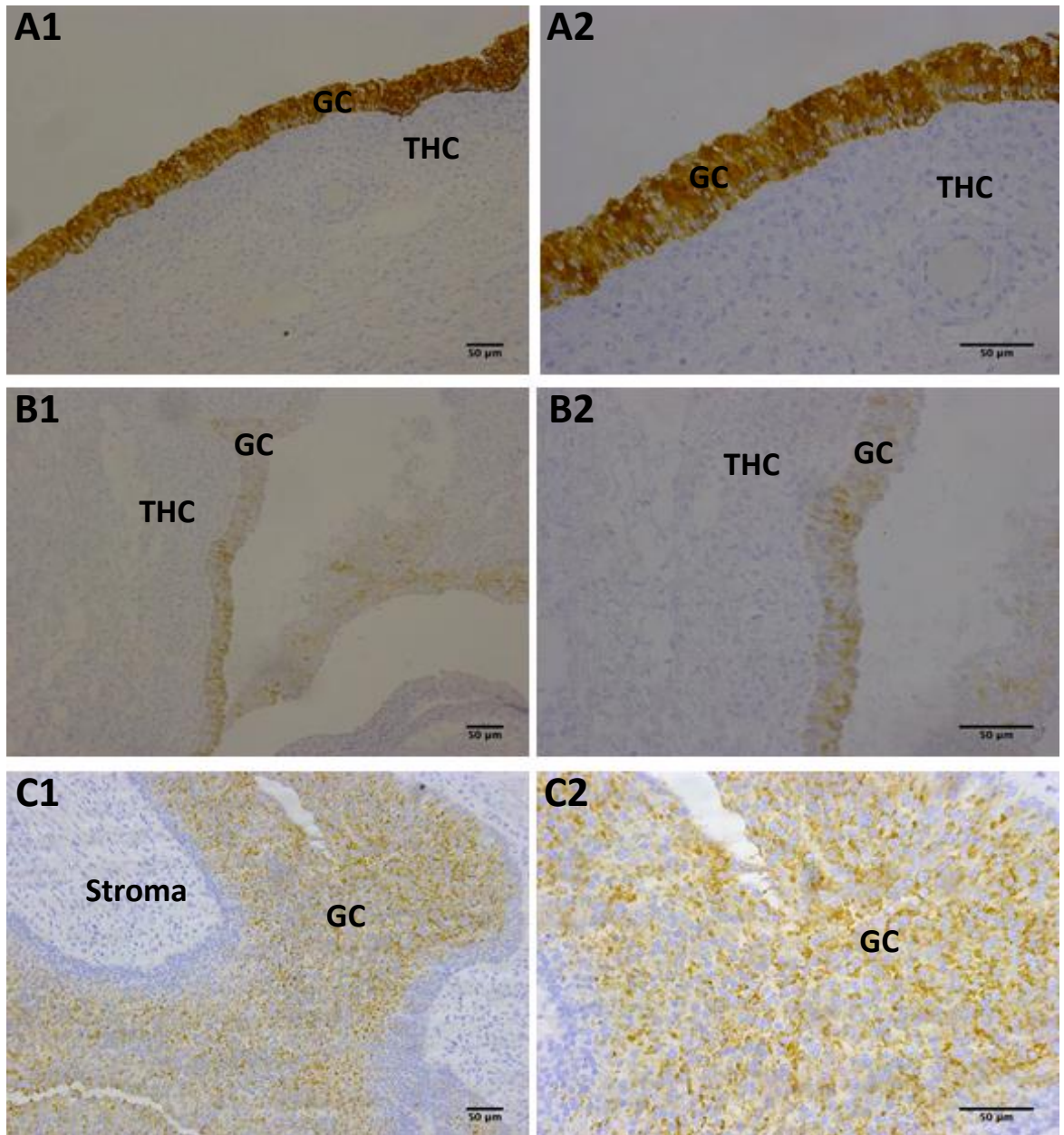


Figure 5-6: Inhibin expression exclusively in GC showing examples of different stain distribution and %area at 200x magnification (ABC1) and 400x magnification (ABC2); A1&A2 show FW with continuous distribution and almost 100% GC area covered from a H follicle, B1&B2 show FW with individual distribution and almost 70% area covered from a H follicle; C1&C2 show a GCT4 with continuous distribution and almost 90% area covered. There are no images for clustered distribution as inhibin always stained continuously or on occasion individually. No THC or stromal stain was seen.

The expression of aromatase protein was only seen in GC of the FW categorised as VH, H and EA, but not in LA lacking the GC compartment as shown below in Figure 5-7 and Figure 5-8. The expression of aromatase was not detected in any of the four GCT categories as presented in Figure 5-9 and Figure 5-10.

Examples of different aromatase stain intensity, stain distribution and %area detected in FW and GCT sections can be seen in Figure 5-11 and Figure 5-12.

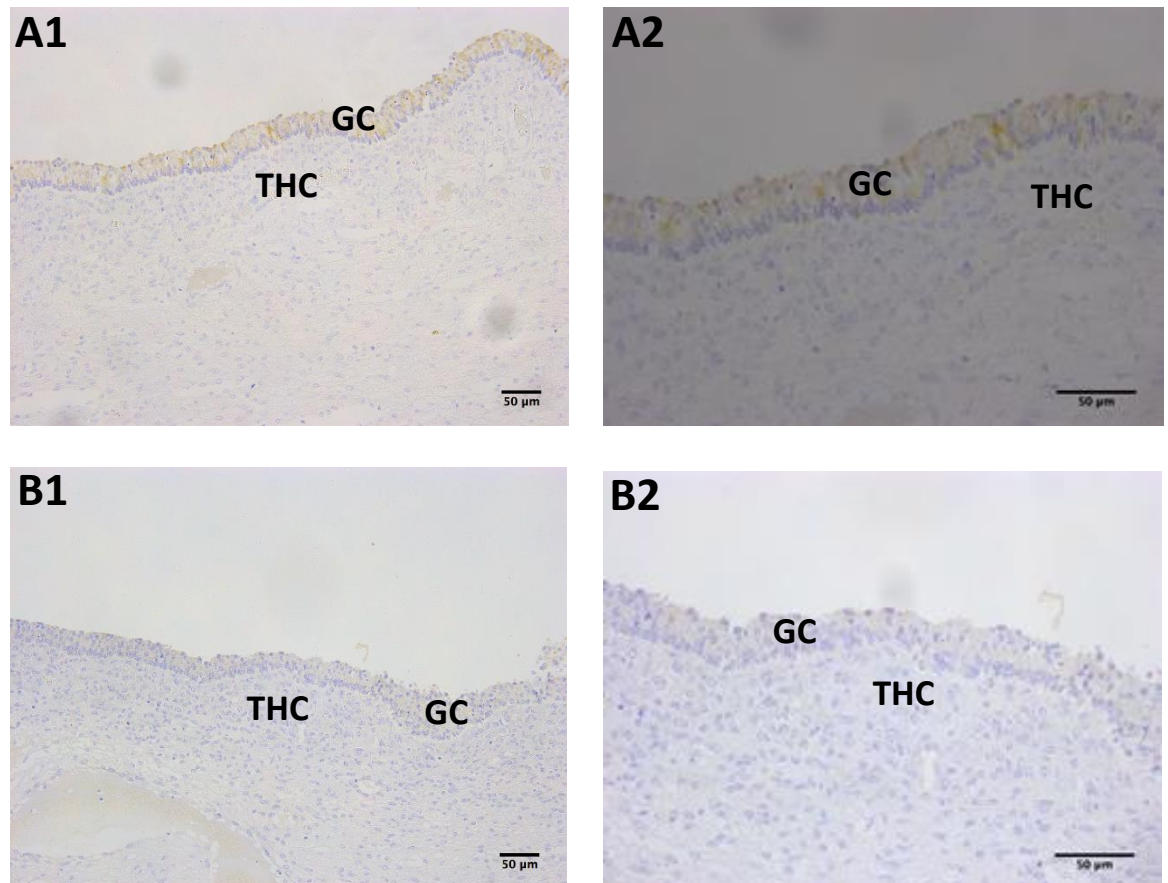


Figure 5-7: Aromatase expression exclusively in GC in VH (A1 and A2) and some cells of H (B1 and B2) FW categories. A1 and B1 are at 200x magnification, and A2 and B2 are at 400x magnification.

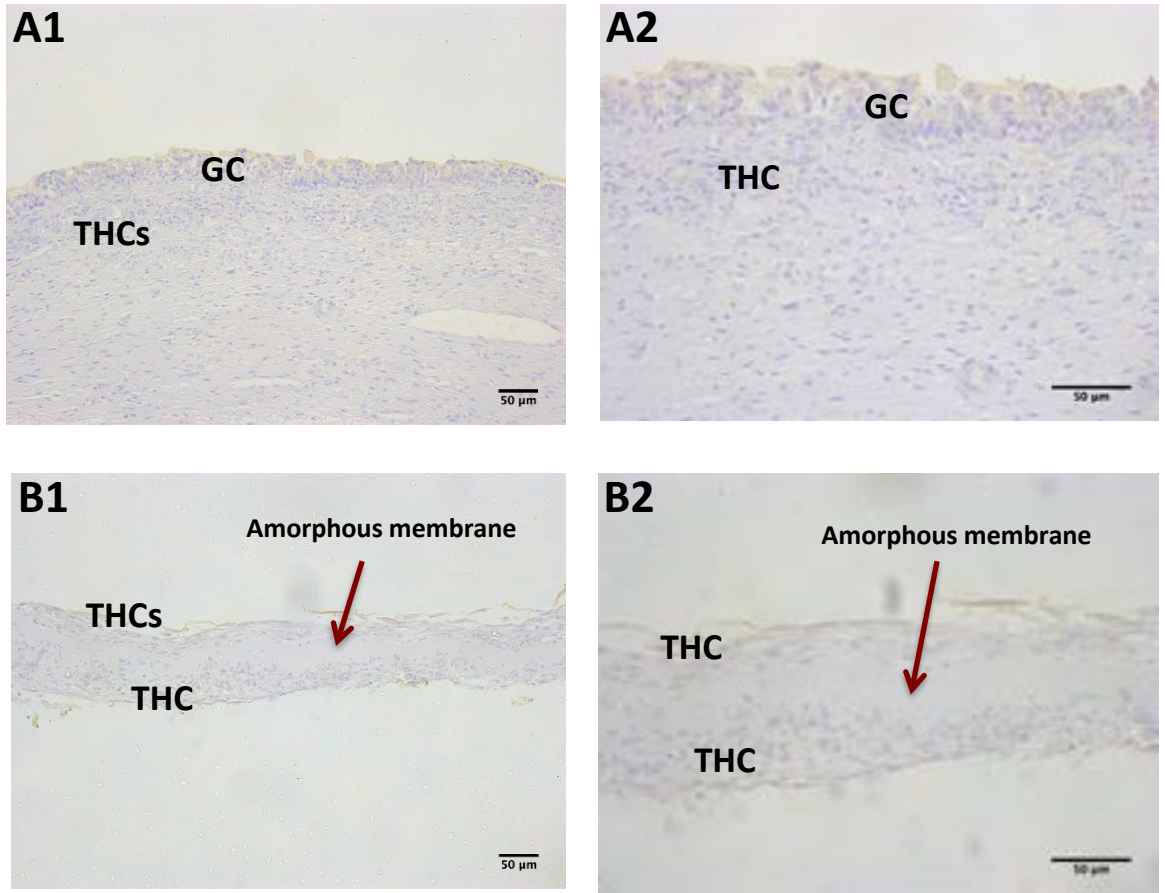


Figure 5-8: Aromatase expression exclusively in GC in cells of the EA FW category (A1 and A2) but not in LA follicles where the GC compartment is lacking (B1 and B2). A1 and B1 are at 200x magnification, and A2 and B2 are at 400x magnification.

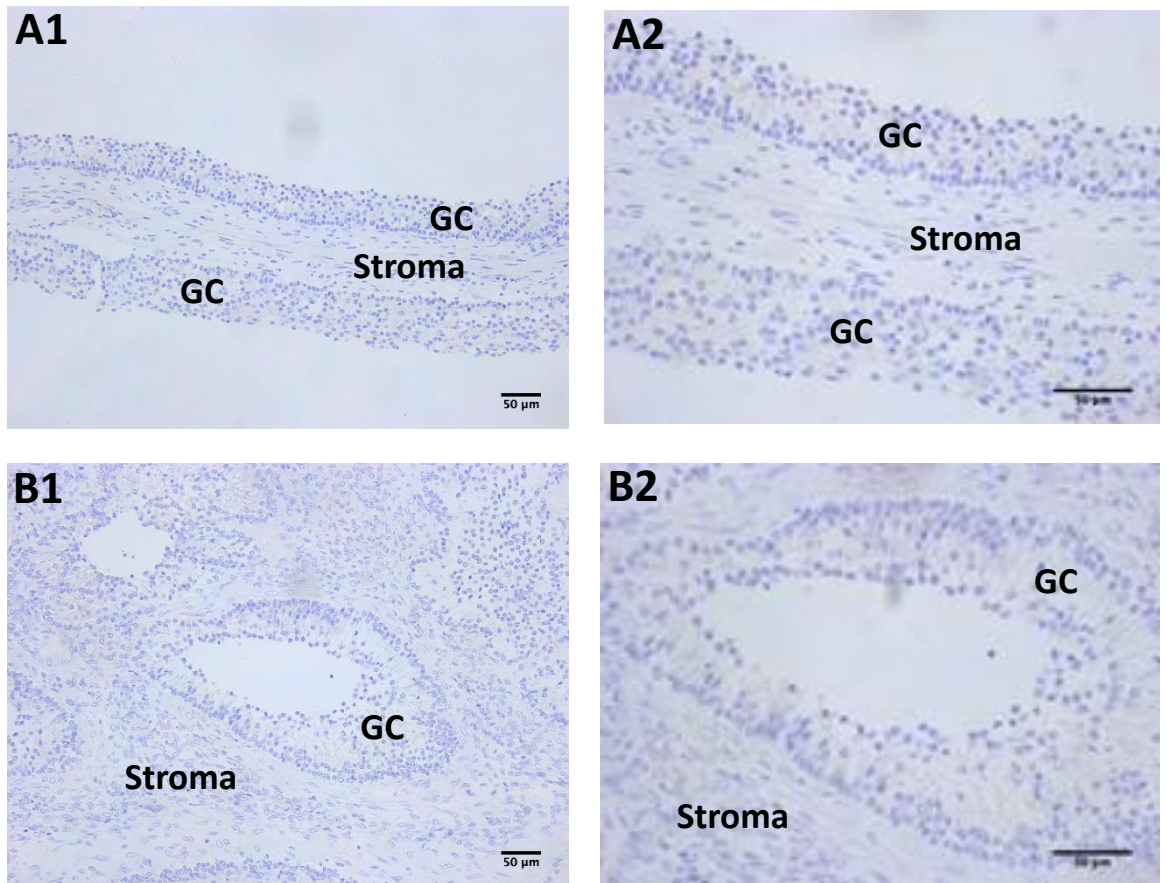


Figure 5-9: No positive aromatase immunoreactivity was seen in GCT categorised as GCT1 (A1 and A2) and GCT2 (B1 and B2). A1 and B1 are at 200x magnification, and A2 and B2 are at 400x magnification.

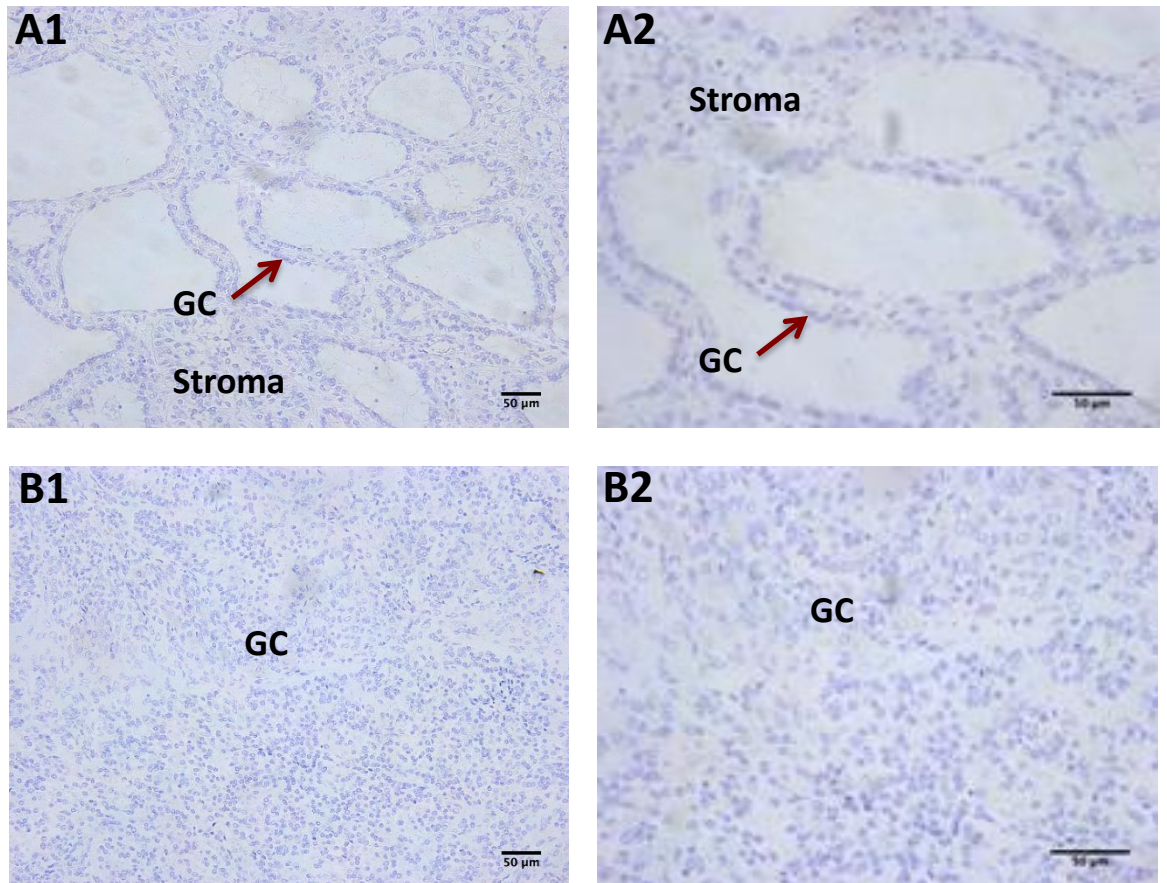


Figure 5-10: No positive aromatase immunoreactivity was seen in GCT categorised as GCT3 (A1 and A2) and GCT4 (B1 and B2). A1 and B1 are at 200x magnification, and A2 and B2 are at 400x magnification.

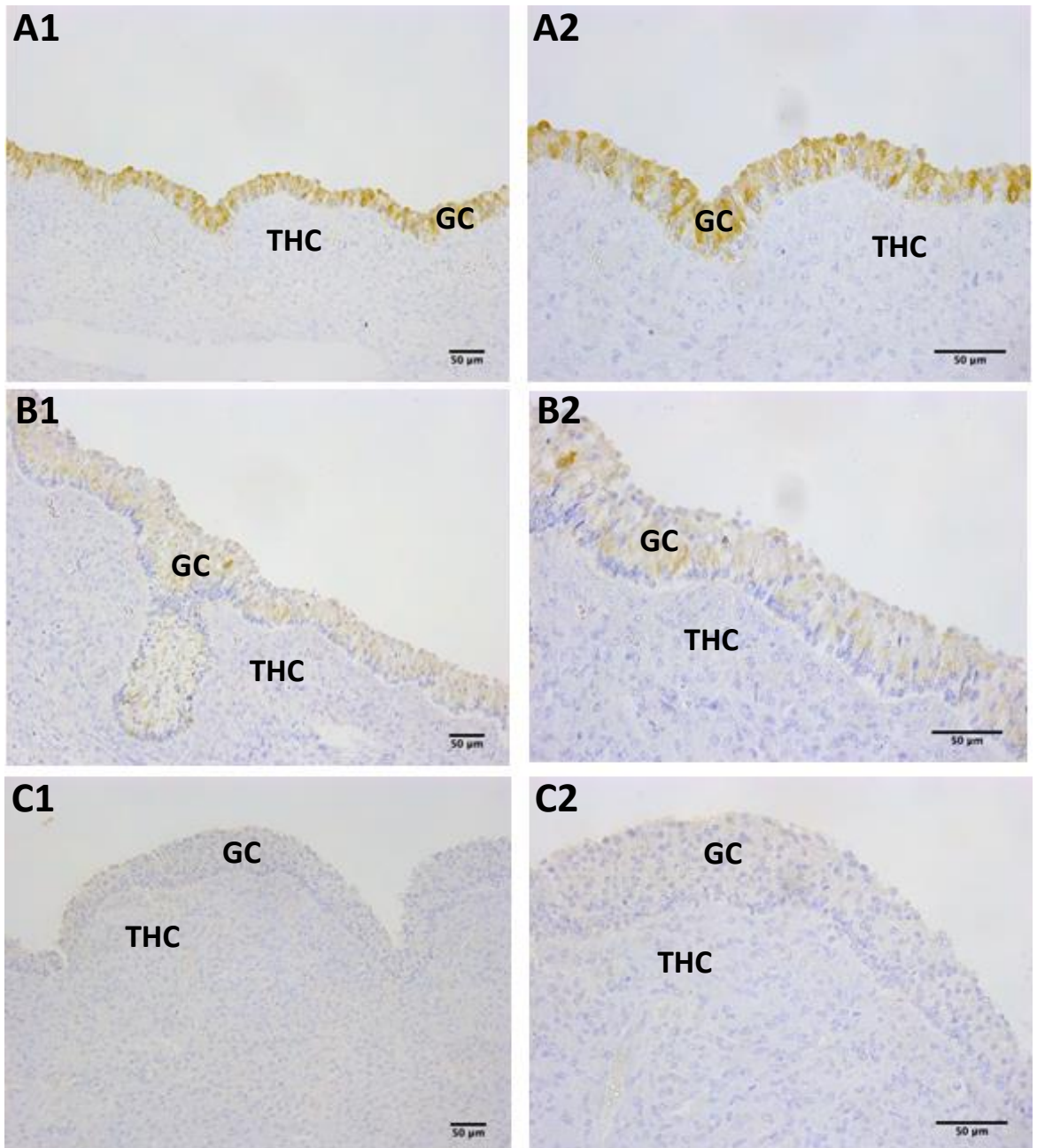


Figure 5-11: Aromatase expression exclusively in GC of FW showing different stain intensities at 200x (ABC1) magnification and 400x (ABC2) magnification; A1 & A2 show VH FW with high expression, B1 & B2 H FW with medium expression and C1 & C2 H FW with low expression.

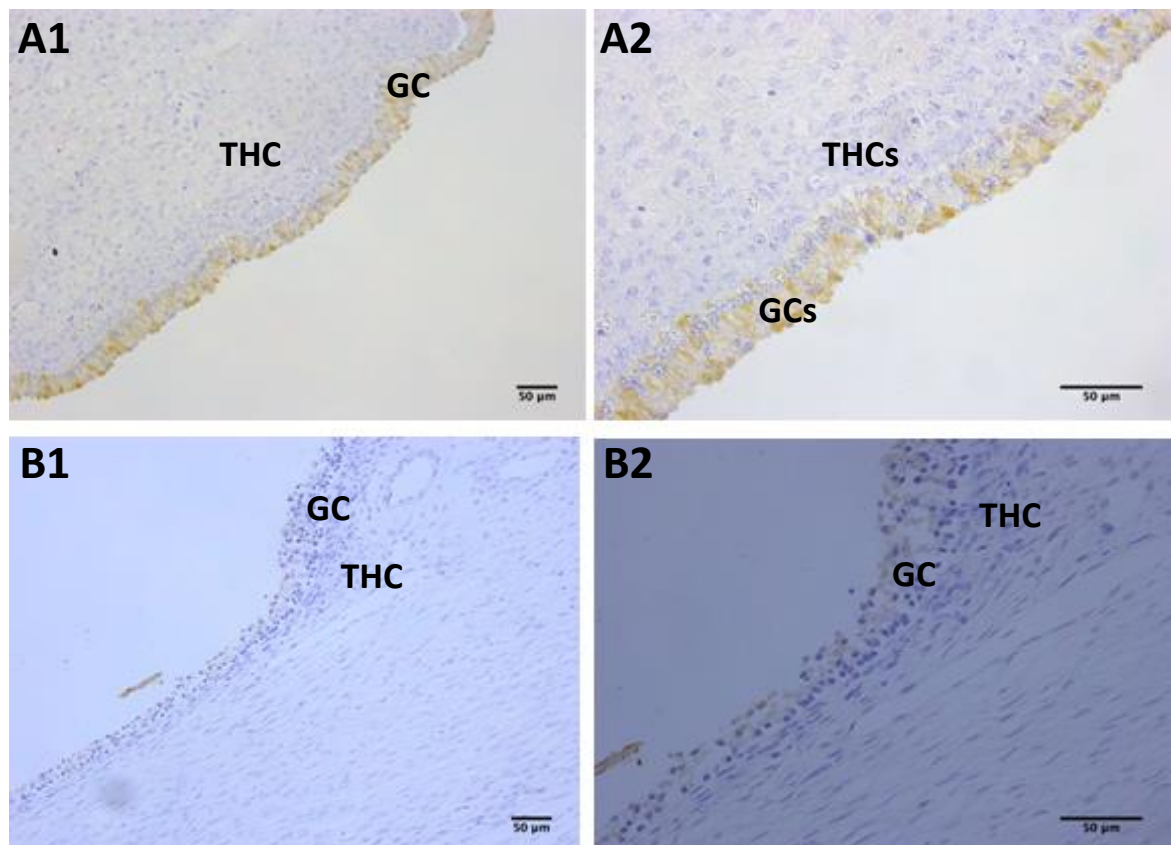


Figure 5-12: Aromatase exclusively in GC of FW showing different stain distribution and %area at 200x (ABC1) magnification and 400x (ABC2) magnification; A1&A2 show FW with continuous distribution and almost 85% GC area covered from a H follicle, B1&B2 show FW with individual distribution and almost 40% area covered from a EA follicle.

The expression of CYP17 was detected very strongly in the THC of VH and H FW categories, and strongly in EA FW with slightly less expression in THC bordering the amorphous membrane in LA FW as shown in the Figure 5-13 and Figure 5-14. The expression of CYP17 protein in THC in GCT categorised as GCT1, GCT2, GCT3 and GCT4 is shown in Figure 5-15 and Figure 5-16 and clearly showed individual clusters of cells with strong expression of CYP17 in the stromal/interstitial areas in GCT1 and 2, and individually staining interstitial cells in GCT3 and GCT4. Examples of different CYP17 stain intensity, stain distribution and percentage area detected in FW and GCT sections can be seen in Figure 5-17 and Figure 5-18. As shown in Figure 5-19 the expression of CYP17 in the LA FW category is very reduced and sometimes barely seen, and this is might be due to the reduction and degradation of large theca cells in LA follicles.

The expression of CYP17 was detected in mostly clusters but also some individual interstitial tissue or stroma cells of all GCT categories as presented in Figure 5-20. The positively immunostained cells appeared to be similar to large theca cells of FW, which supports the idea that it is these large theca-like cells

that produce androgens in GCT mares showing increased circulating androgens. It can be noticed (Figure 5-13 B2) that there was some background staining both in the cytoplasm of the granulosa cell layer above the theca and also below in the theca externa, which was unexplained but may be due to the antibody being manufactured for immunoblots and not for immunohistochemistry.

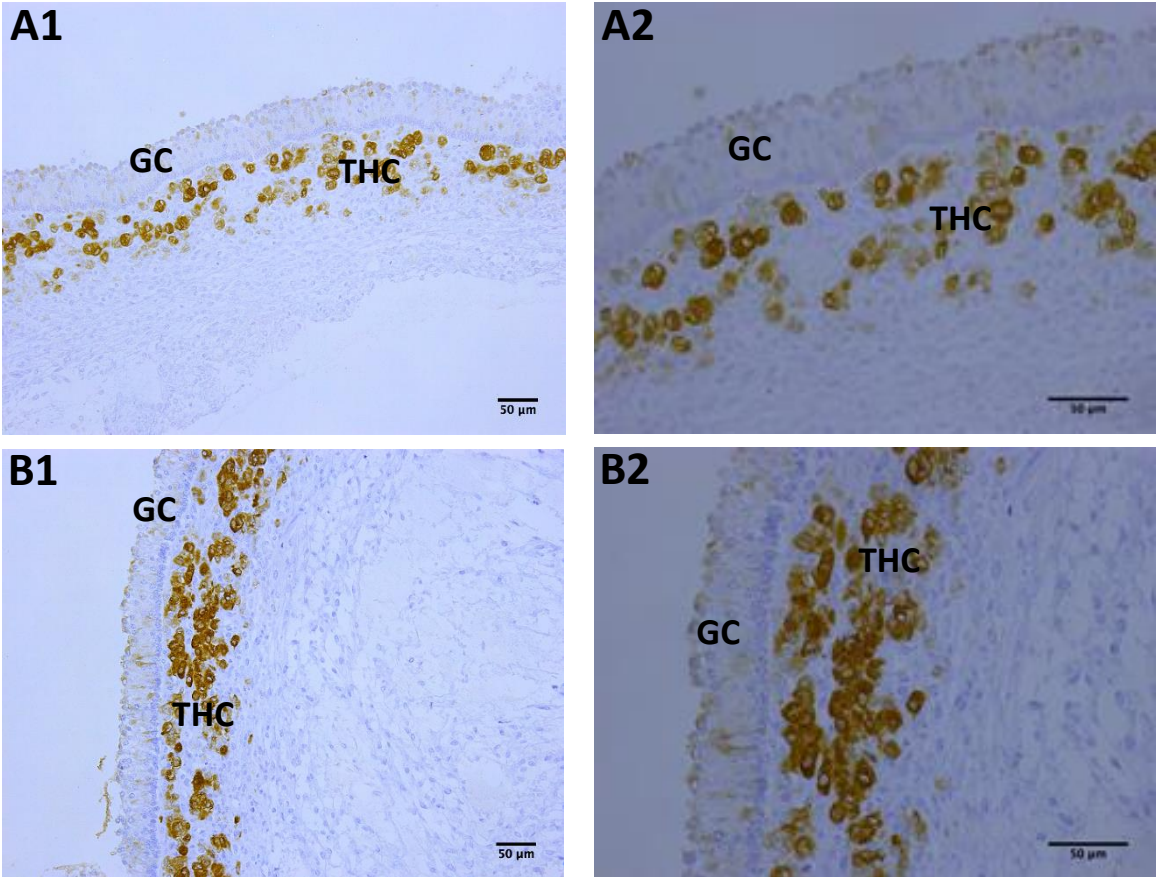


Figure 5-13: CYP17 expression in THC of VH (A1 and A2) and H (B1 and B2) FW categories. A1 and B1 are at 200x magnification, and A2 and B2 are at 400x magnification.

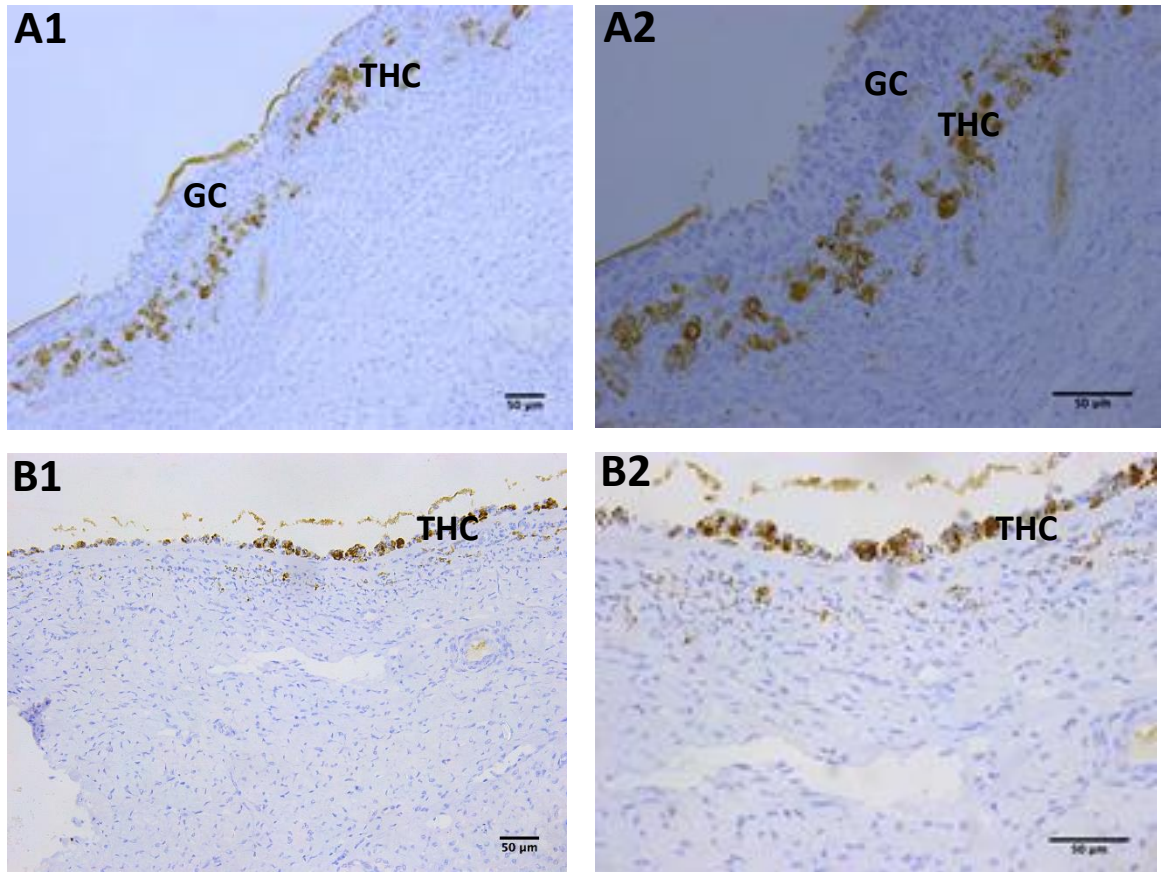


Figure 5-14: CYP17 expression in THC of EA (A1 and A2) and LA (B1 and B2) FW categories. A1 and B1 are at 200x magnification, and A2 and B2 are at 400x magnification.

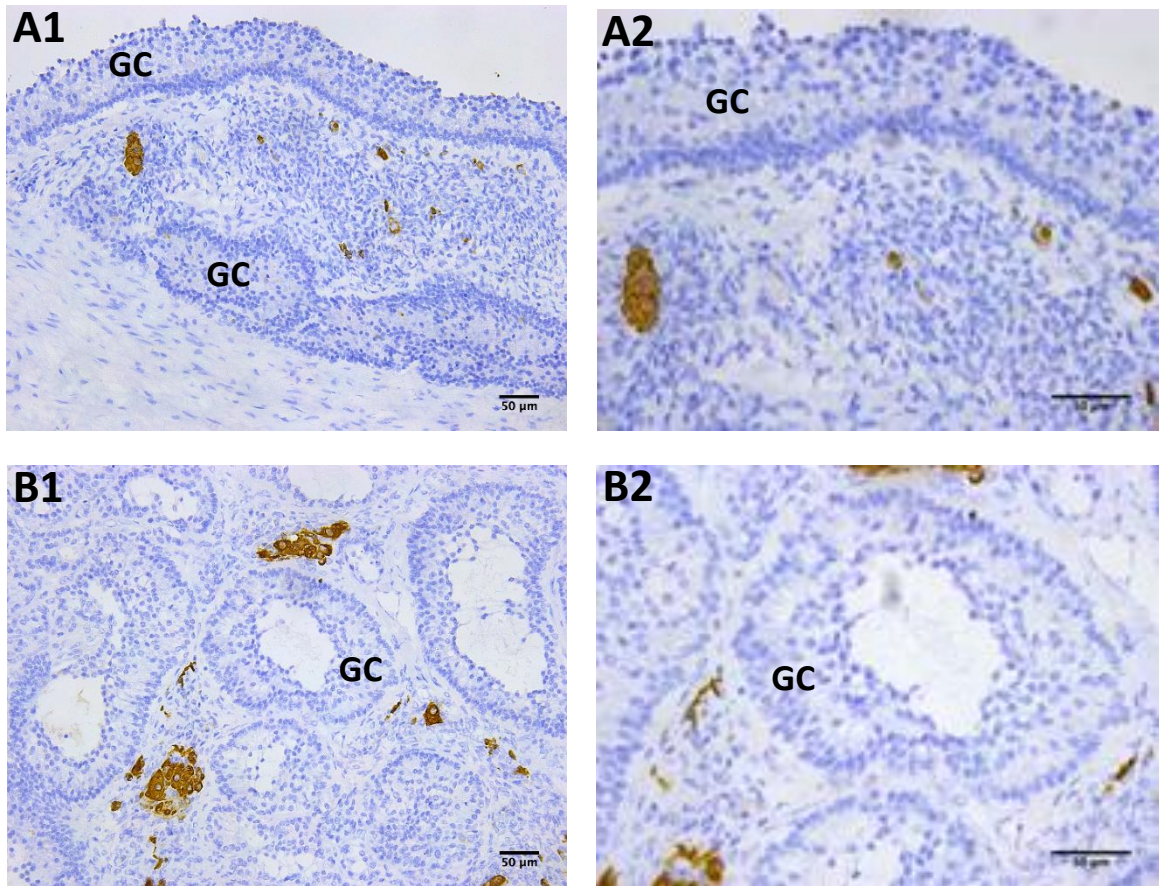


Figure 5-15: CYP17 expression in interstitial stromal tissue of GCT1 (A1 and A2) and GCT2 (B1 and B2) categories. A1 and B1 are at 200x magnification, and A2 and B2 are at 400x magnification.

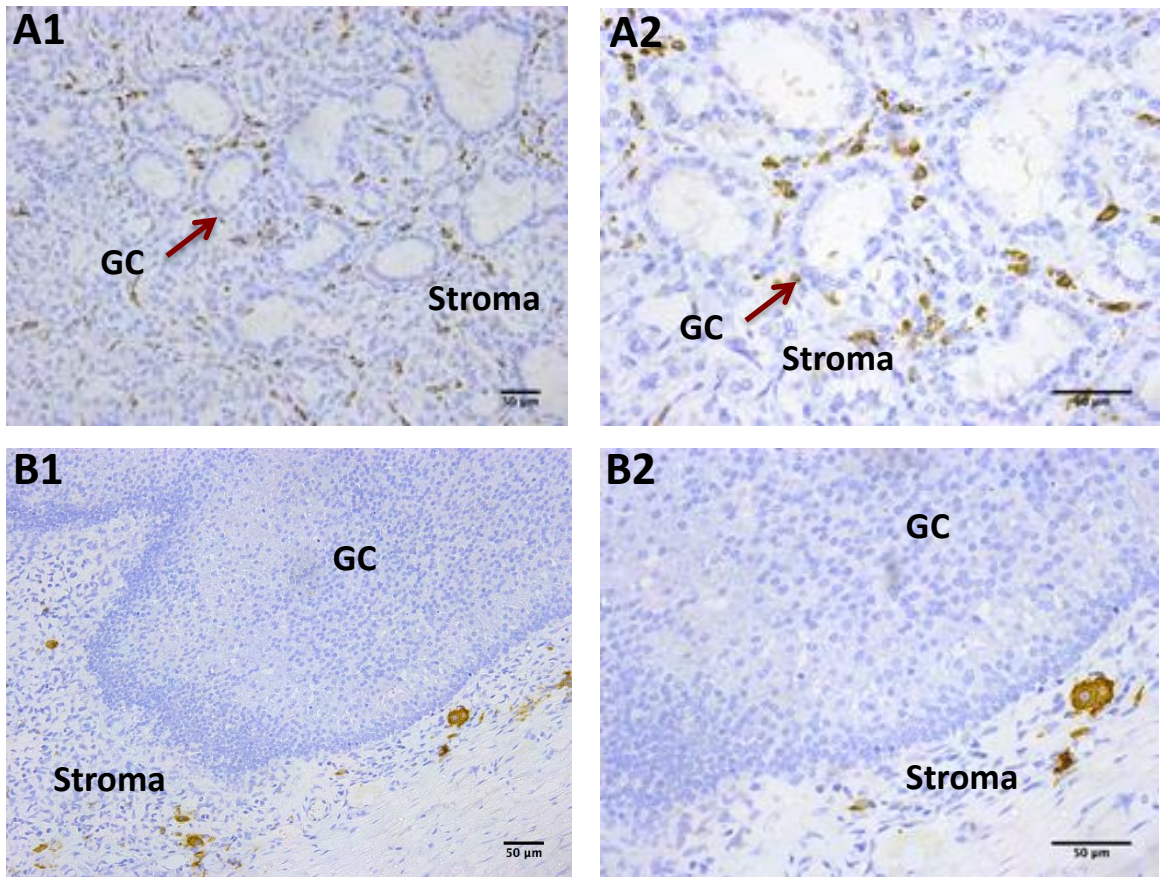


Figure 5-16: CYP17 expression in interstitial stromal tissue of GCT3 (A1 and A2) and GCT4 (B1 and B2) categories. A1 and B1 are at 200x magnification, and A2 and B2 are at 400x magnification.

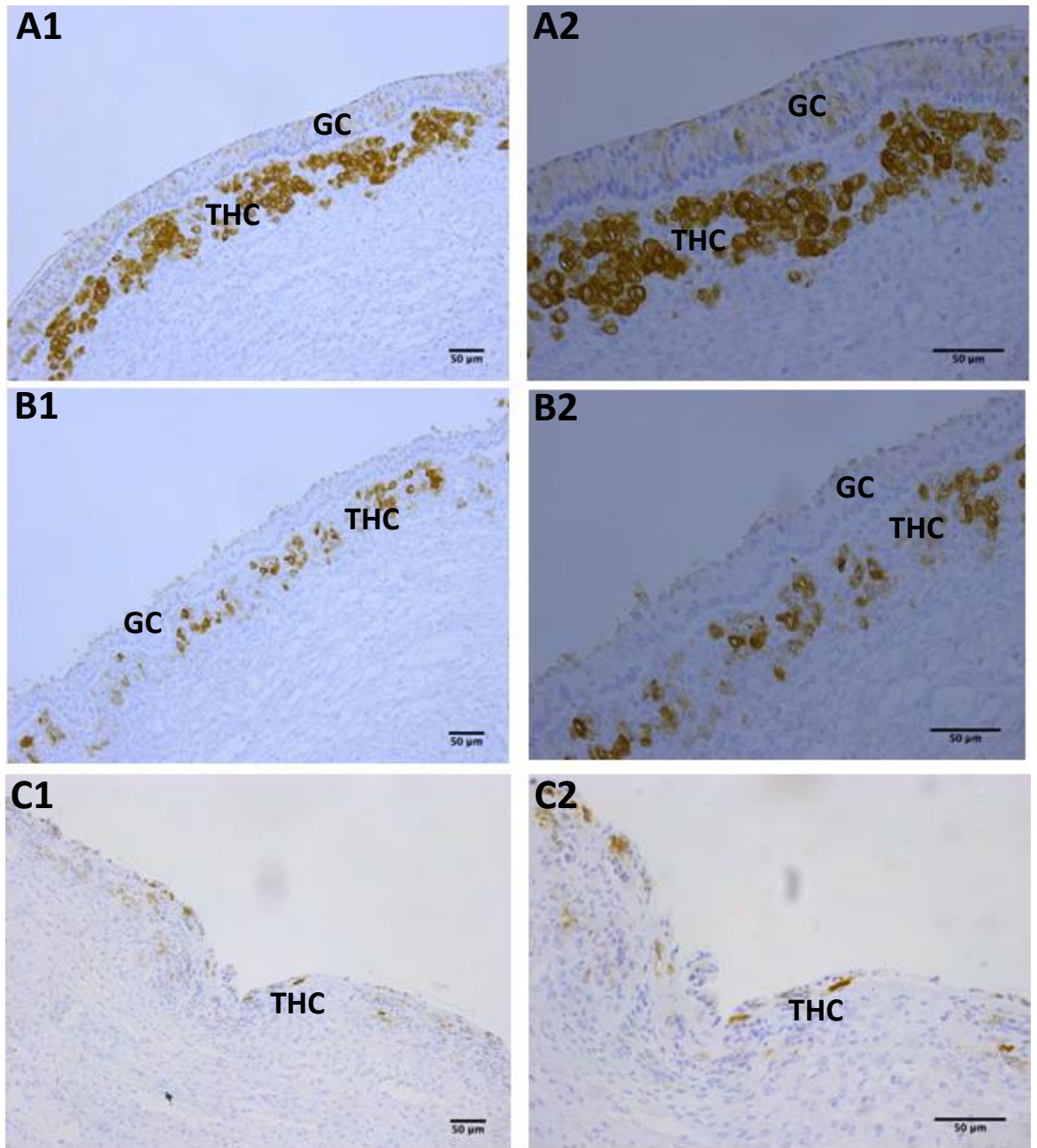


Figure 5-17: CYP17 expression in THC showing different stain intensity at 200x magnification (ABC1) and 400x magnification (ABC2); A1 & A2 show a VH follicle with high expression, B1 & B2 a H follicle with medium expression and C1 & C2 a LA follicle with low expression.

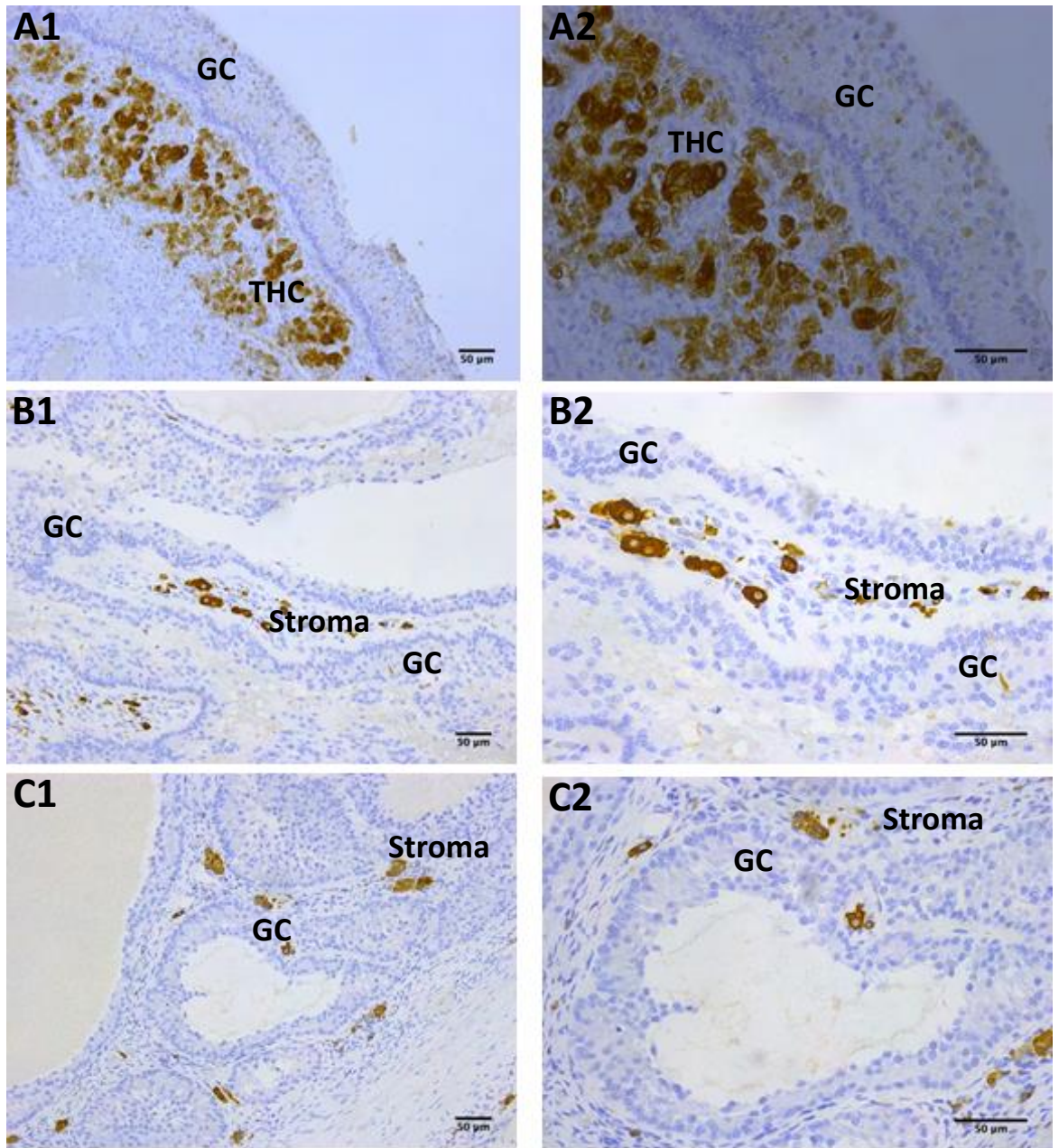


Figure 5-18: CYP17 expression in THC and interstitial stromal tissue showing different stain distribution and %area examples with 200x magnification (ABC1) and 400x magnification (ABC2); A1&A2 show frequent clustering and almost 70% GC area covered from a VH FW, B1&B2 show less frequent clustering and almost 25% area covered from GCT1, and C1&C2 shows individual cells and very small clusters and only 10% area covered from a GCT3.

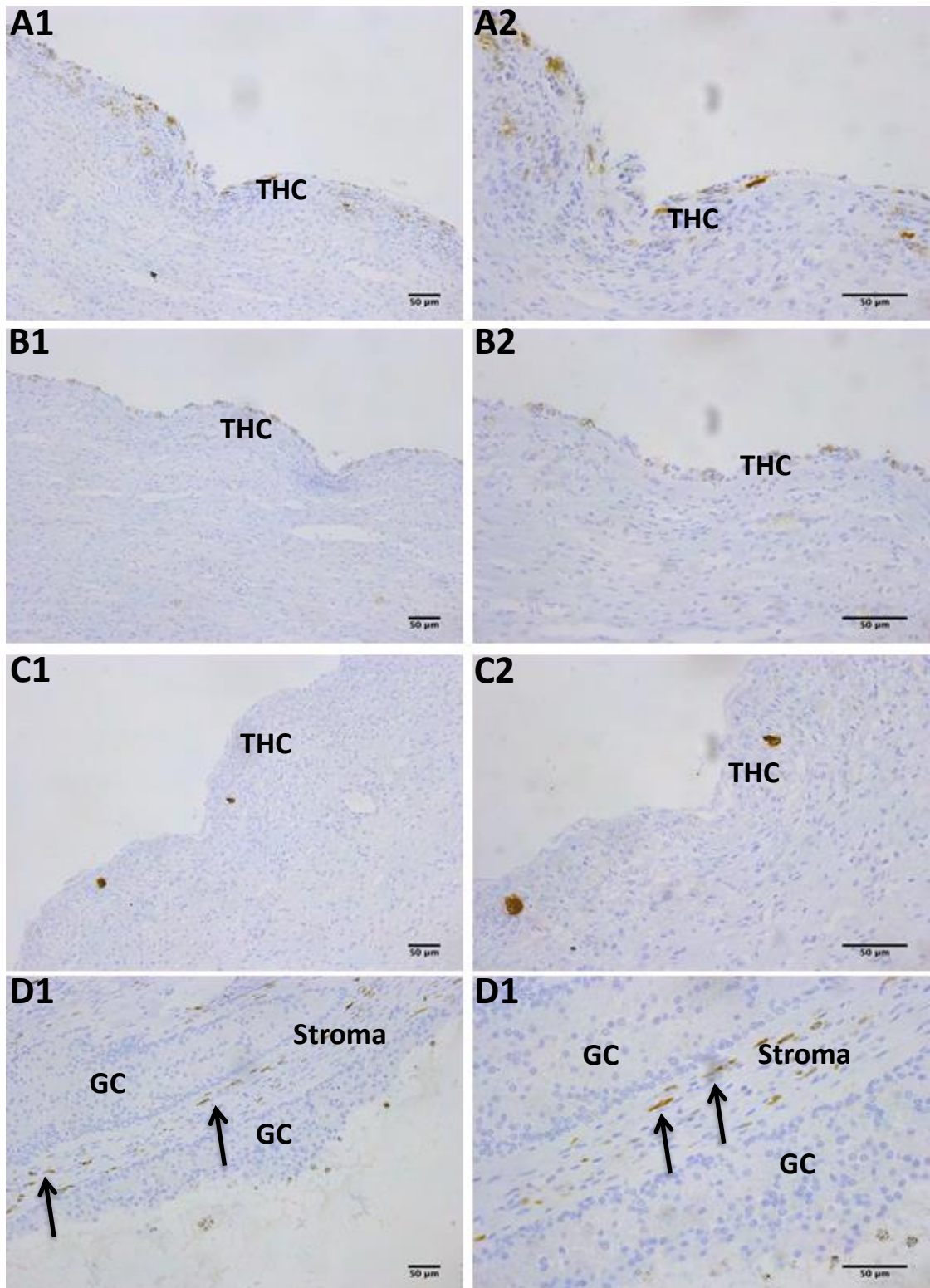


Figure 5-19: CYP17 expression in THC and interstitial stromal tissue showing a severe reduction in staining of LA FW and GCT categories with 200x magnification (ABCD1) and 400x magnification (ABCD2); A1&A2 show a low stain from a LA FW, B1&B2 shows even less staining from another LA FW, C1&C2 shows only two localised small clusters or individual cells from a LA FW, and D1&D2 shows a low number of flat interstitial cells stained from GCT1 (Black arrows).

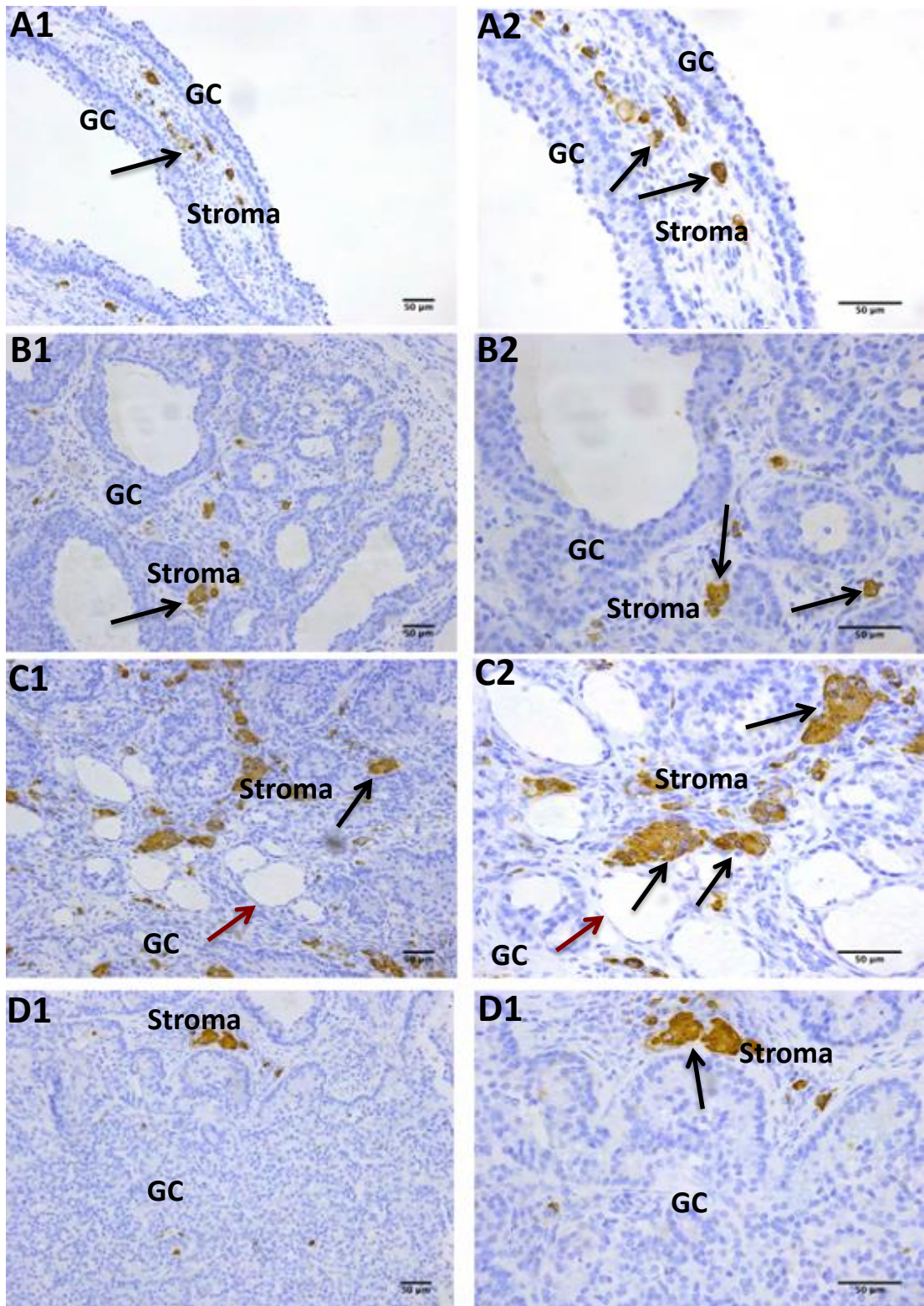


Figure 5-20: CYP17 expression in interstitial stromal tissue cells in GCT some of which appear like individual or clustered Large THC (Black arrows) at 200x magnification (ABCD1) and 400x magnification (ABCD2); A1&A2 show GCT1, B1&B2 GCT2, C1&C2 GCT3 and D1&D2 an example of GCT4.

The expression of AMHR2 protein was frequently detected in GC and THC (clusters of large THC) in the three FW categories VH, H and EA, but in LA follicles AMHR2 expression was detected only in individual THCs as shown in Figure 5-21 and Figure 5-22. The expression of AMHR2 was detected in all GCT categories both in the GC and the interstitial/stromal tissue as presented in Figure 5-23 and Figure 5-24.

Examples of different stain intensity, stain distribution and percentage area stained detected in FW and GCT sections can be seen in Figure 5-25 and Figure 5-26.

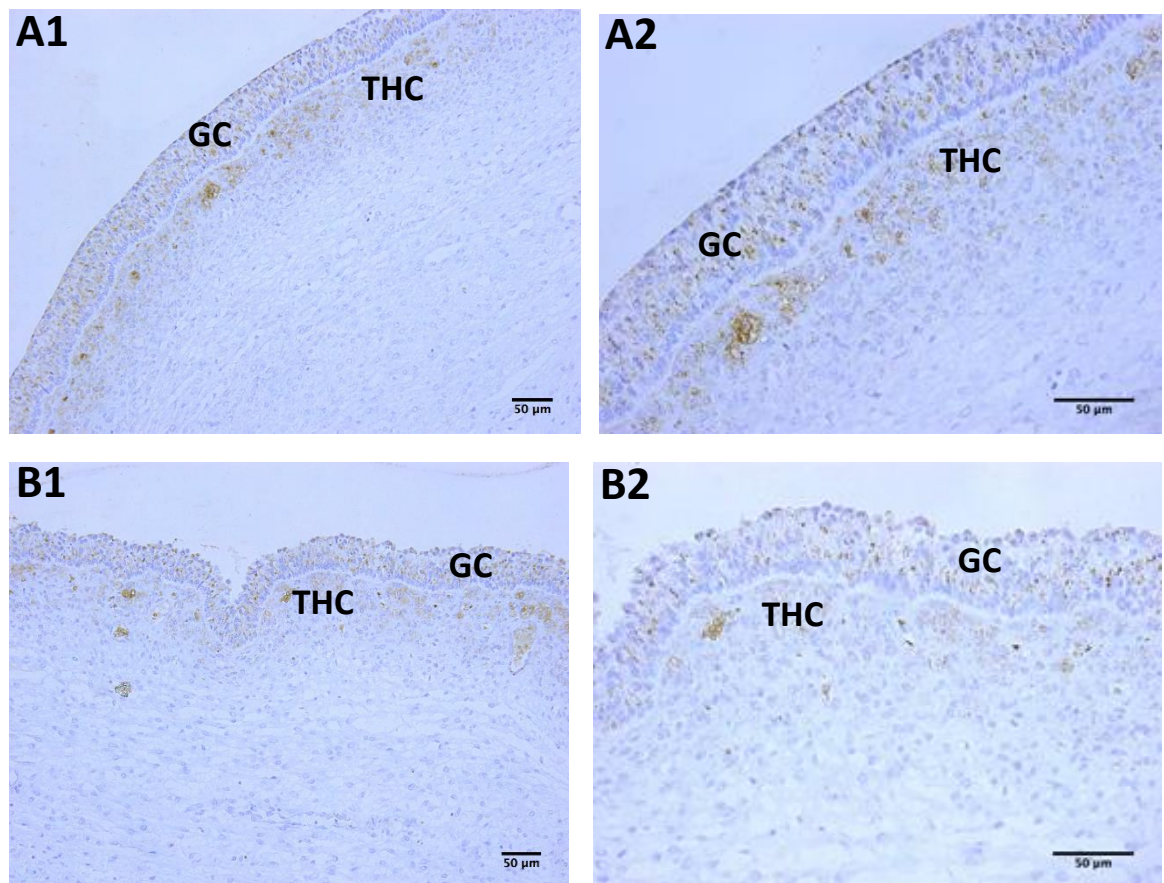


Figure 5-21: AMHR2 protein expression in GC and THC of VH (A1 and A2) and H FW (B1 and B2). A1 and B1 are at 200x magnification, and A2 and B2 are at 400x magnification.

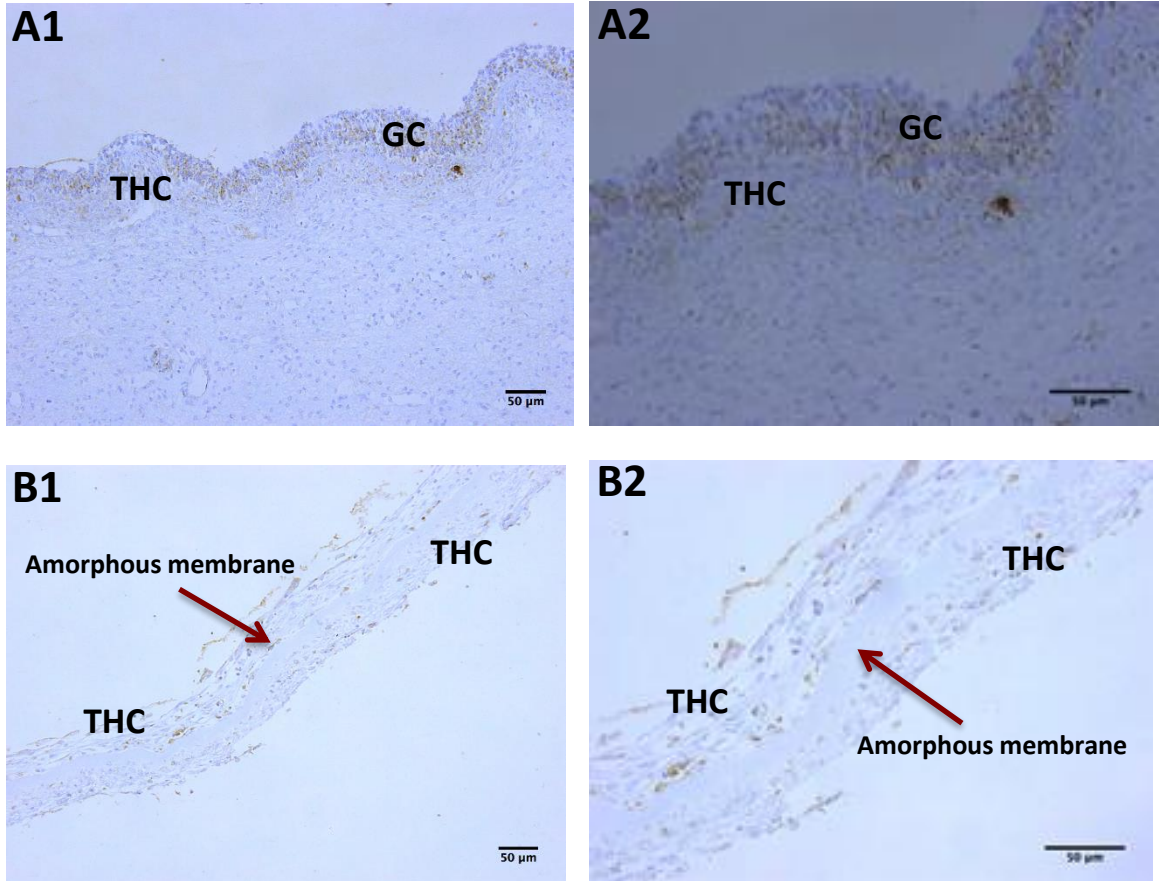


Figure 5-22: AMHR2 protein expression in GC and THC of an EA follicle (A1 and A2), and AMRH2 expression in individual THC of LA FW (B1 and B2). A1 and B1 are at 200x magnification, and A2 and B2 are at 400x magnification.

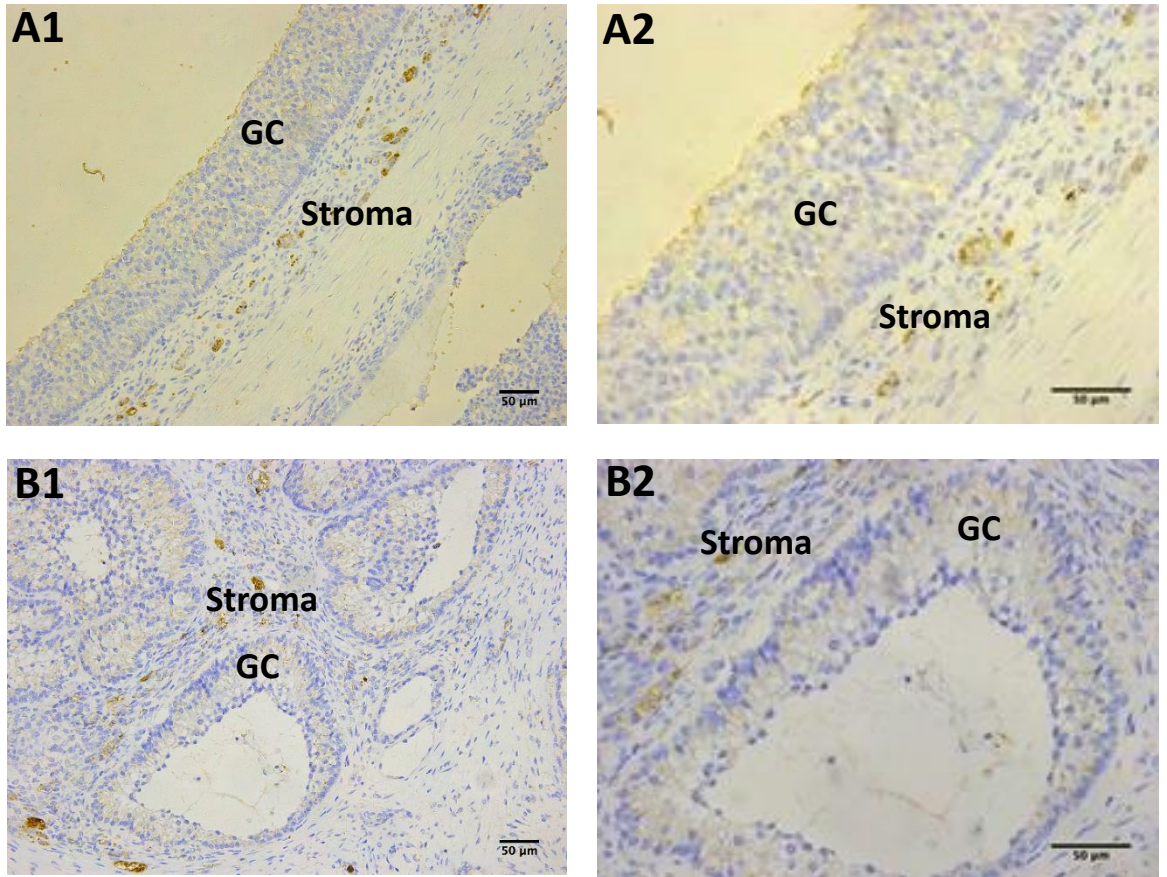


Figure 5-23: AMHR2 protein expression in GC and interstitial/stromal theca like cells in GCT1 (A1 and A2) and GCT2 categories (B1 and B2). A1 and B1 are at 200x magnification, and A2 and B2 are at 400x magnification.

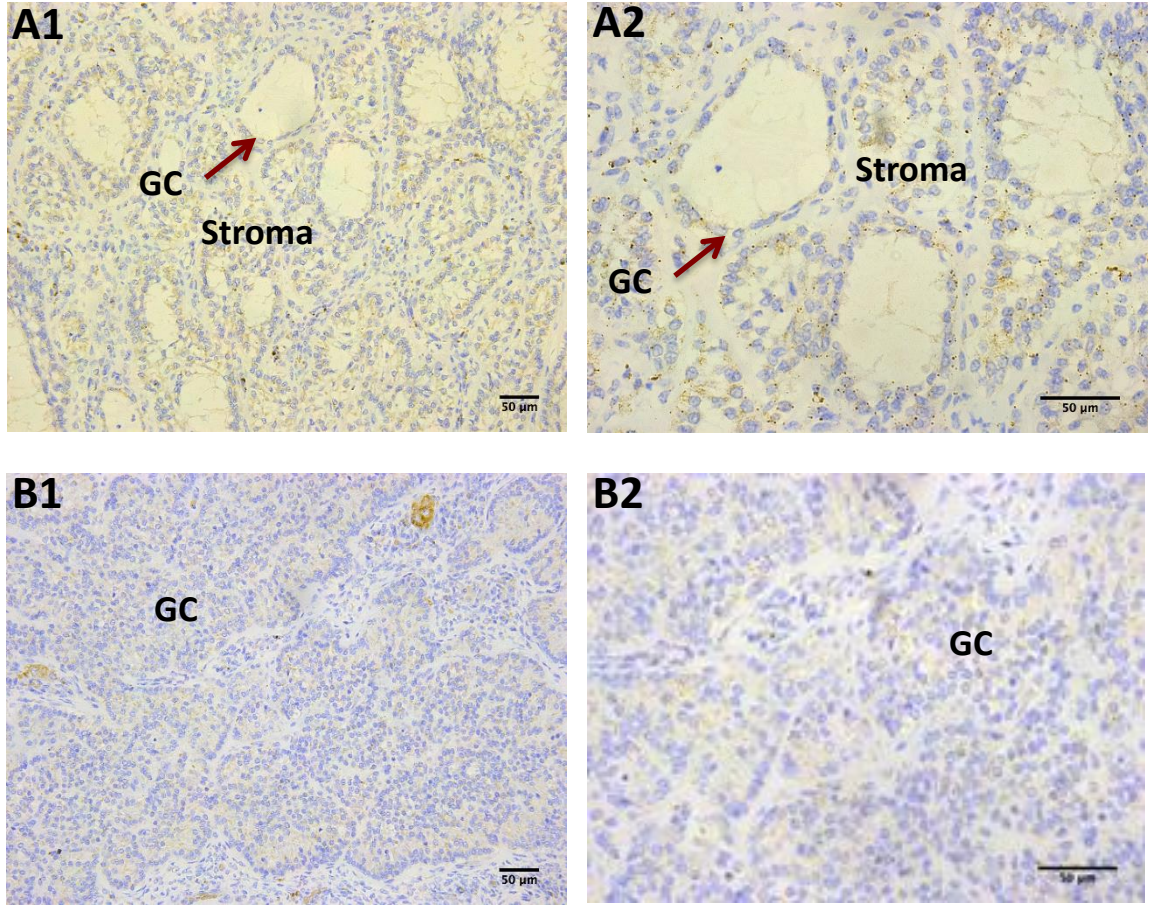


Figure 5-24: AMHR2 protein expression in GC and interstitial/stromal theca like cells in GCT3 (A1 and A2) and GCT4 categories (B1 and B2). A1 and B1 are at 200x magnification, and A2 and B2 are at 400x magnification.

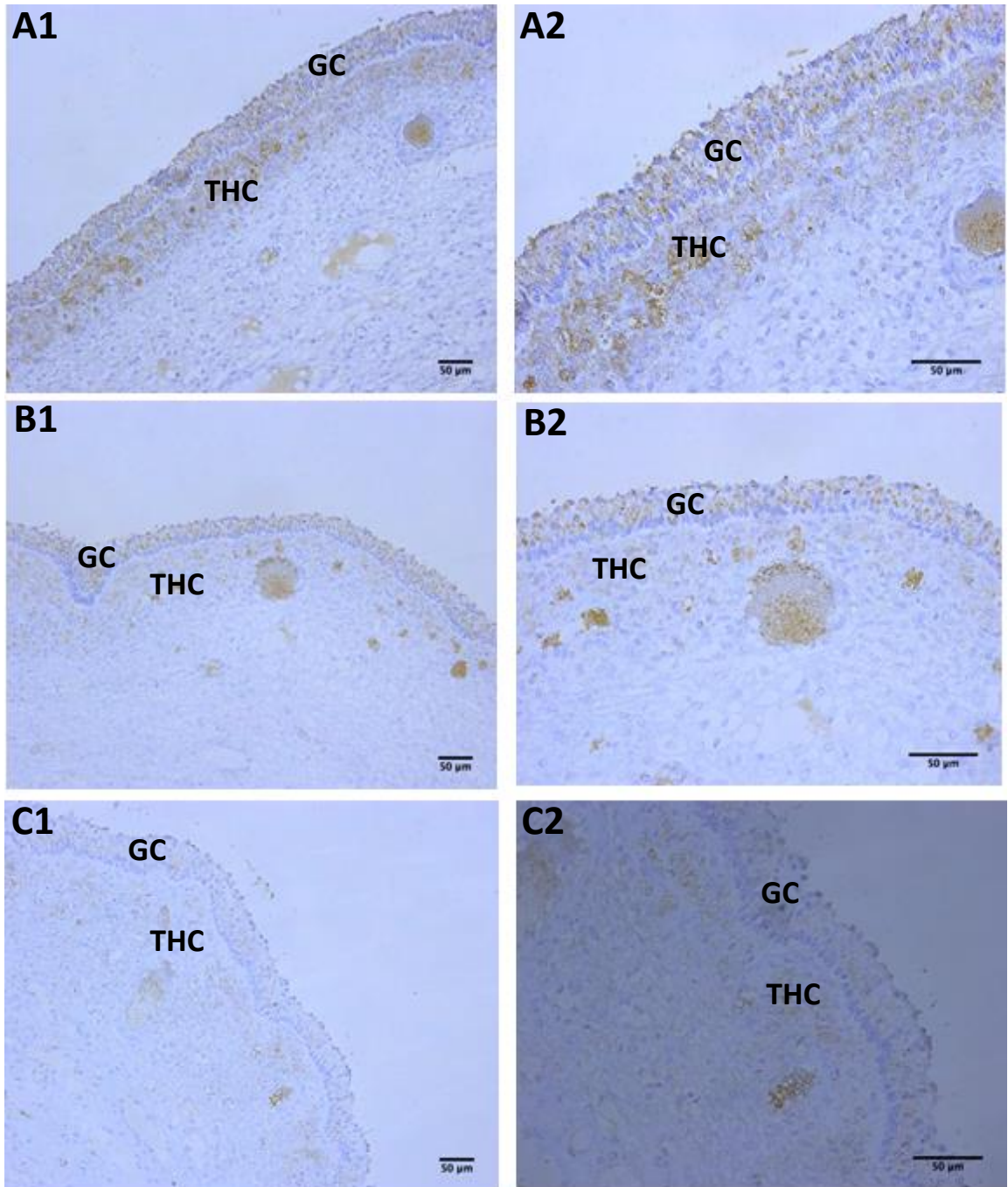


Figure 5-25: AMHR2 expression in GC and THC of FW showing different stain intensity at 200x magnification (ABC1) and 400x magnification (ABC2); A1 & A2 show H FW with high expression, B1 & B2 VH FW with medium expression and C1 & C2 VH FW with low expression.

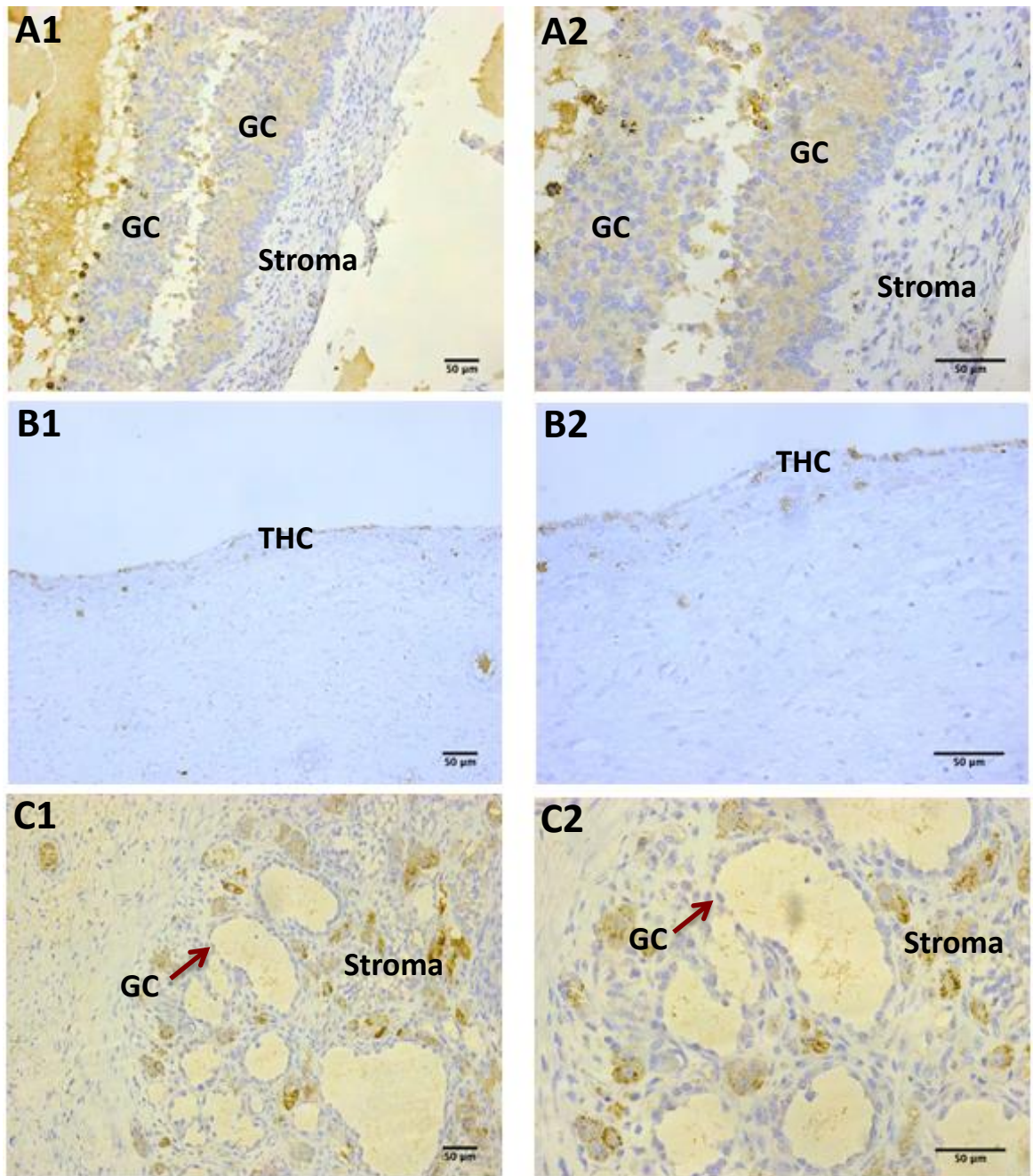


Figure 5-26: AMHR2 expression in GC and THC layer or interstitial stromal tissue of GCT showing different stain distribution and %area at 200x magnification (ABC1) and 400x magnification (ABC2); A1&A2 show continuous distribution and 100% GC area covered from GCT1, B1&B2 show individual distribution and approximately 25% area covered from a LA FW, and C1&C2 show clusters and approximately 30% of the interstitial area covered from a GCT3.

5.3.2 Analysis of the association between follicle health or GCT category and FW and GCT functional parameters

5.3.2.1 The association between FW health status categories and follicular wall diameter (FWD) and follicular fluid oestradiol (FFE2) concentration

There was no association between FW health status categories and FWD ($p=0.536$) but there was an association between FW health status categories and FFE2 concentration ($P < 0.001$) as presented in Table 5-2. Specifically EA and LA categories had significantly lower FFE2 concentrations than VH and H categories.

Table 5-2: Association between FW health status and FWD and FFE2 concentration

Outcome variable	FW categories Mean \pm SE Mean (Median) No. = each group has 10 distributed Follicles				P-value
	VH	H	EA	LA	
FWD mm	18.9 \pm 1.8 (20.1) N=8 mares	23.4 \pm 2.1(22.6) N=7 mares	21.8 \pm 2.22 (20.8) N=7 mares	20.3 \pm 2.9 (17.7) N=5 mares	0.536
FF E2 Concentration ng/ml	210.5\pm87.8 N=8 E2=10 (follicle no.)	174.8\pm45.4 N=7 E2=10 (follicle no.)	26.9\pm14.6 N=5 E2=5 (follicle no.)	6.8\pm3.1 N=4 E2=9 (follicle no.)	<0.001

5.3.2.2 The association between FW and GCT categories and inhibin GC stain intensity, distribution and percentage area covered

There was no association between FW and GCT categories and inhibin stain intensity and distribution. But EA follicles tended to have a smaller %area covered in GC, confirmed using Mann Whitney, compared with VH and H follicles, and a significant difference was also detected between GCT categories with respect to inhibin GC percentage area covered ($P= 0.012$) as presented Table 5-3. A Mann Whitney test among GCT categories detected a significant reduction in inhibin GC percentage area covered in GCT3 compared with both GCT1 and GCT2 ($P < 0.005$) (Figure 5-27).

Table 5-3: Association between FW and GCT categories and inhibin GC stain intensity, distribution and percentage area covered.

Outcome variable	FW categories Mean \pm SE Mean (or median) No. = each group has 10 distributed Follicles				P-value	GCT categories Mean \pm SE Mean (or median) No. = each group has 10 tissue samples from 5 mares (1mare=2 samples)				P-value
	VH	H	EA	LA		GCT1	GCT2	GCT3	GCT4	
Inhibin GC stain intensity	2.8 \pm 0.1(3)	2.7 \pm 0.2 (3)	2.1 \pm 0.3 (2.5)	-	0.293	1.2 \pm 0.1(1)	1.6 \pm 0.2 (2)	1.6 \pm 0.2 (2)	1.7 \pm 0.2 (2)	0.298
Inhibin GC stain distribution	1.0 \pm 0.0 (1)	1.1 \pm 0.1(1)	1.4 \pm 0.2 (1)	-	0.284	1.0 \pm 0.0 (1)	1.0 \pm 0.0 (1)	1.0 \pm 0.0 (1)	1.0 \pm 0.0 (1)	1.000
Inhibin GC percentage area covered	95.5 \pm 2.6 ^a	95.0 \pm 3.0 ^a	58.5 \pm 14.7 ^b	-	0.105	78.5\pm1.8^a	78.5\pm1.98^a	69.5\pm0.9^b	73.0\pm3.5^{ab}	0.012

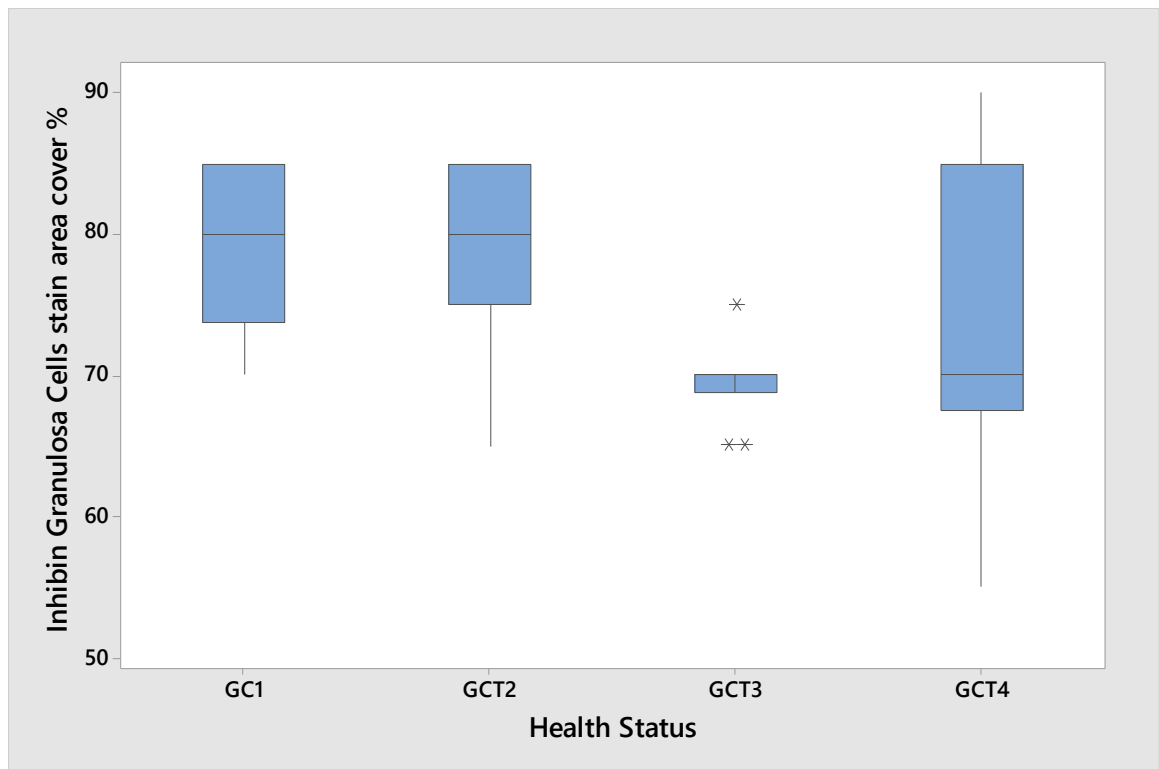


Figure 5-27: Inhibin GC percentage area covered among GCT categories

5.3.2.3 The association between FW and GCT categories and aromatase GC stain intensity, distribution and percentage area covered.

Aromatase was not expressed in any GC of the GCT categories but it was expressed in VH, H and EA FW categories. However, there were no significant differences amongst the categories in any of the aromatase parameters (Table 5-4 and Figure 5-28)

Table 5-4: Association between FW categories and aromatase GC stain intensity, distribution and percentage area covered.

Outcome variable	Follicle wall categories Mean \pm SE Mean No. = each group has 10 distributed Follicles				P-value
	VH	H	EA	LA	
Aromatase GC stain intensity	0.9 \pm 0.3 (1)	1.0 \pm 0.2 (1)	0.9 \pm 0.2 (1)	-	0.871
Aromatase GC stain distribution	1.1 \pm 0.3 (1)	1.4 \pm 0.3 (2)	1.3 \pm 0.3 (2)	-	0.744
Aromatase GC %area	47.0 \pm 11.5	37.0 \pm 9.6	26.0 \pm 7.7	-	0.358

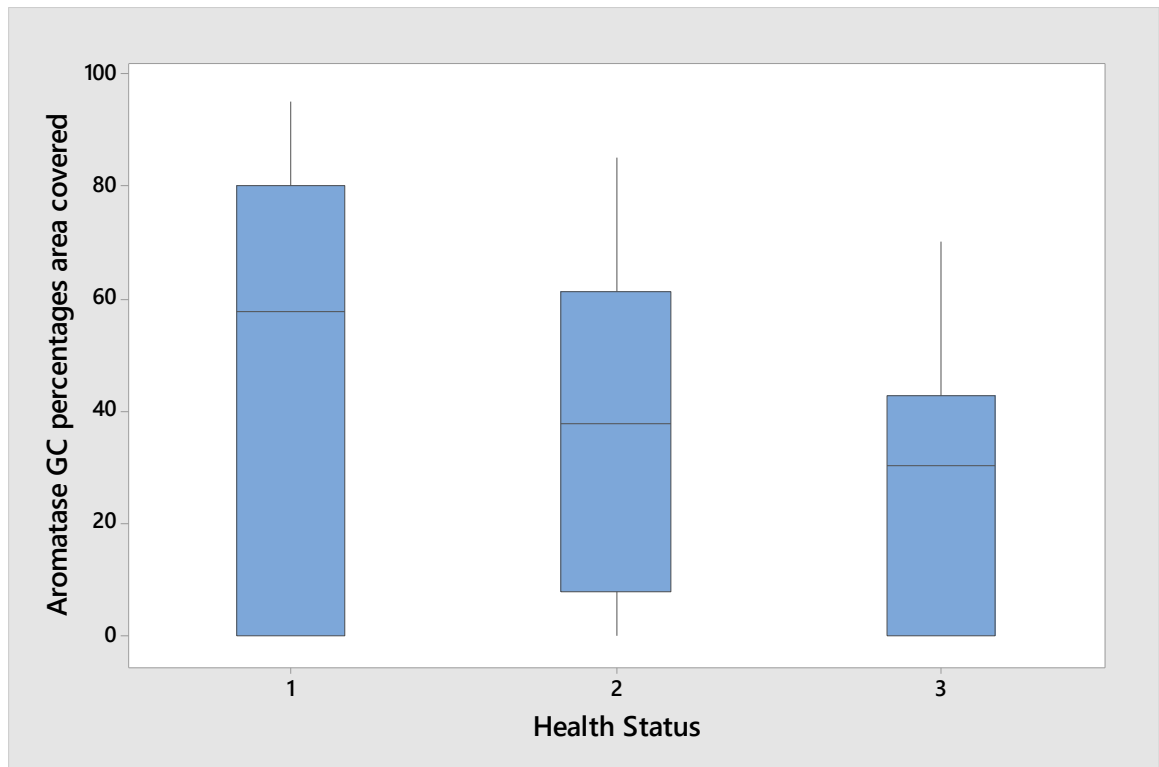


Figure 5-28: Aromatase GC percentage area covered among FW categories. 1 (VH), 2 (H), and 3 (EA)

5.3.2.4 The association between FW and GCT categories and CYP17 stain THCs intensity, distribution and percentage area covered.

There was no expression of CYP17 on GC as expected, because it is expressed only in theca cells of FW, and a low number of interstitial cells of GCT. As shown in Table 5-5 below a significant difference was detected in the THC stain intensity and percentage area covered with respect to FW health status categories ($P=0.003$ and $P<0.001$). Both stain intensity and percentage area covered were significantly lower in the LA FW compared with other FW.

Table 5-5: Association between FW and GCT categories and CYP17 THC stain intensity, distribution and percentage area covered.

Outcome variable	Follicle wall categories Mean ± SE Mean (median) No. = each group has 10 distributed Follicles				P-value	GCT categories Mean ± SE Mean (median) No. = each group has 10 tissue samples from 5 mares (1mare=2 samples)				P-value
	VH	H	EA	LA		GCT1	GCT2	GCT3	GCT4	
CYP17 THC stain intensity	3.0±0.0 (3)	2.9±0.1 (3)	3.0±0.0 (3)	1.0±0.4 (1)	0.003	2.9±0.1 (3)	3.0±0.0 (3)	2.5±0.3 (3)	3.0±0.0 (3)	0.611
CYP17 THC stain distribution	3.0±0.0 (3)	3.0±0.0 (3)	3.0±0.0 (3)	1.8±0.5 (3)	0.319	3.0±0.0 (3)	3.0±0.0 (3)	3.0±0.0 (3)	3.0±0.0 (3)	1.000
CYP17 THC percentage area covered	79.5±1.7	76.0±3.1	66.5±3.2	11.2±4.8	<0.001	6.6±1.6	9.4±2.0	10.2±2.4	8.5±1.7	0.615

5.3.2.5 The association between FW and GCT categories and AMHR2 stain intensity, distribution and percentage area covered.

There was a decrease of AMHR2 GC stain intensity and percentage area covered in atretic FW categories (EA and LA) compared to healthy FW categories (VH and H) ($P < 0.05$). The same reduction was also seen in THC stain intensity and percentage area ($P = 0.001$ and < 0.001 , respectively) with a change in distribution in atretic follicles as presented in Table 5-6. GCT3 showed a significantly lower AMHR2 GC stain intensity and percentage area compared with the other GCT categories, with an altered distribution. This alteration in the distribution was also seen in THC (interstitial cell) AMHR2 expression in GCT3 and GCT4 compared with the other two GCT categories.

Table 5-6: Association between FW and GCT categories and AMHR2 GC and THC stain intensity, distribution and %area

Outcome variable	Follicle wall categories Descriptive Stat Mean \pm SE Mean (median) No. = each group has 10 Follicles				P-value	GCT categories Descriptive Stat Mean \pm SE Mean (median) No. = each group has 10 tissue samples from 5 mares (1mare=2 samples)				P-value
	VH	H	EA	LA		GCT1	GCT2	GCT3	GCT4	
AMHR2 GC stain intensity	1.6\pm0.2 (2)	1.8\pm0.1 (2)	1.0\pm0.0 (1)	-	0.007	1.2\pm0.1 (1)	1.8\pm0.1 (2)	0.8\pm0.1 (1)	1.9\pm0.3 (2)	0.004
AMHR2 GC stain distribution	1.0 \pm 0.0 (1)	1.0 \pm 0.0 (1)	1.0 \pm 0.0 (1)	-	1.000	1.6\pm0.2 (2)	1.4\pm0.2 (1)	2.4\pm0.4 (3)	1.2\pm0.2 (1)	0.034
AMHR2 GC %area	76.0\pm4.9	77.0\pm7.1	55.5\pm3.7	-	0.006	44.0\pm10.3	48.0\pm8.9	5.3\pm2.8	65.5\pm6.7	<0.001
AMHR2 THC stain intensity	1.7\pm0.2 (2)	1.8\pm0.1 (2)	1.0\pm0.0 (1)	1.0\pm0.0 (1)	0.001	1.0 \pm 0.0 (1)	1.0 \pm 0.0 (1)	1.2 \pm 0.1 (1)	1.5 \pm 0.2 (1.5)	0.179
AMHR2 THC stain distribution	1.0\pm0.0 (1)	1.0\pm0.0 (1)	2.0\pm0.0 (2)	2.0\pm0.0 (2)	<0.001	2.0\pm0.0 (2)	2.0\pm0.0 (2)	3.0\pm0.0 (3)	3.0\pm0.0 (3)	<0.001
AMHR2 THC %area	69.0\pm5.0	69.5\pm5.4	19.2\pm4.4	14.7\pm3.0	<0.001	6.9 \pm 1.9	5.0 \pm 0.0	8.1 \pm 2.5	8.5 \pm 1.1	0.252

5.3.2.6 Comparison of control FW and diseased GCT tissues

In the comparison of control healthy with diseased tissues (FW vs. GCT categories combined) significant differences were detected in inhibin GC stain intensity and percentage area covered ($P < 0.001$) with median GC stain intensity and mean percentage area covered being higher on the FW than GCT categories. In addition, significant differences were found in AMHR2 stain distribution and percentage area covered ($P < 0.005, 0.001$) with median GC stain distribution having altered in the GCT categories and mean GC percentage area being lower in GCT compared with FW as presented in Table 5-7. Also, significant differences were found with respect to CYP17 THC stain percentage area covered and the AMHR2 THC stain distribution and percentage area covered ($P < 0.001$), with mean THC percentage area of CYP17 and AMHR2 in FW categories higher than in interstitial cells of GCT, which also showed an altered distribution of AMHR2 expression as presented in Table 5-8. Exclusion of GCT3 from the GCT categories (being similar to LA FW) did not affect these results. Note that GCT did not express aromatase enzyme in GC in contrast to FW particularly from VH follicles, but also from H and EA follicles.

Table 5-7: Comparing the combined FW (VH, H and EA) with the combined GCT categories in the hormone (inhibin) and receptor (AMHR2) expression measurements in GC.

Outcome variable	Follicle wall categories Mean \pm SE Mean No. = each group 10 Follicles	GCT categories Mean \pm SE Mean No. = each group has 10 tissue samples from 5 mares (1mare=2 samples)	Overall P-value
	FW (No.=30 without LA)	GCT (No.=40 all GCT categories)	
Inhibin GC stain intensity	2.5\pm0.1	1.5\pm0.1	<0.001
Inhibin GC stain distribution	1.2 \pm 0.1	1.0 \pm 0.0	0.253
Inhibin GC percentage area	83.3\pm5.9	74.9\pm1.3	<0.001
AMHR2 GC stain intensity	1.5 \pm 0.1	1.4 \pm 0.1	0.678
AMHR2 GC stain distribution	1.0\pm0.0	1.7\pm0.1	0.002
AMHR2 GC percentage area	69.5\pm3.5	40.7\pm5.1	<0.001

Table 5-8: Comparing the combined FW (VH, H and EA) with the combined GCT categories in the enzyme (CYP17) and receptor (AMHR2) expression measurements in THC/interstitial cells.

Outcome variable	Follicle wall categories Mean \pm SE Mean No. = each group 10 Follicles	GCT categories Mean \pm SE Mean No. = each group has 10 tissues samples from 5 mares (1mare=2 samples)	Overall P-value
	FW (No.=40 all FW categories)	GCT (No.=all GCT categories)	
CYP17 THC stain intensity	2.5 \pm 0.2	2.9 \pm 0.1	0.285
CYP17 THC stain distribution	2.7 \pm 0.1	3.0 \pm 0.0	0.441
CYP17 THC percentage area	58.3\pm4.7	8.7\pm1.0	<0.001
AMHR2 THC stain intensity	1.4 \pm 0.1	1.2 \pm 0.1	0.124
AMHR2 THC stain distribution	1.5\pm0.1	2.5\pm0.1	<0.001
AMHR2 THC percentage area	43.1\pm4.7	7.1\pm0.8	<0.001

5.3.2.7 The association between inhibin stain categories and control FW diameter (FWD)

There was a significant difference in FWD of the different inhibin GCs stain intensity and distribution categories (both $P < 0.05$) as presented in Table 5-9. Clearly, follicles with high GCs stain intensity had a larger FWD (resembling the size of dominant follicles just after selection) than the follicles with lower stain intensity, and the >20mm follicle has not only most stain intensity but also a continuous distribution of stain in granulosa cells.

Table 5-9: Association between inhibin GC stain intensity and distribution and FWD.

Inhibin expression	P-value	No=30	FWD (mm) Mean ±SE Mean	FWD (mm) Median
Stain intensity GC	0.017			
0 (No stain)				
1 (Low)		5	16.3±1.9	17.5
2 (Medium)		4	16.0±2.9	15.4
3 (High)		21	23.6±1.3	22.8
Stain distribution GCs	0.039			
1 (Continuous)		25	22.4±1.3	21.9
2 (Individual)		5	16.3±1.9	17.5
3 (Clusters)		-	-	-

5.3.2.8 The association between aromatase stain categories and control FWD

A significant difference in FWD of the different aromatase GCs stain intensity and distribution categories (both $P < 0.05$) as presented in Table 5-10. The follicles with most aromatase stain and continuous distribution have larger diameters (> 25 mm) thus may be dominant follicles. In addition, it is apparent that follicles with a diameter of approximately 20mm have reduced stain intensity and those in the smaller group (18 mm) generally do not stain positively.

Table 5-10: Association between aromatase GC stain intensity and distribution and FWD.

Aromatase expression	P-value	No = 30	FWD (mm) Mean \pm SE Mean	FWD (mm) Median
Stain intensity GC	0.02			
0 (No stain)		8	18.1\pm1.1	17.8
1 (Low)		17	20.7\pm1.5	20.8
2 (Medium)		4	30.3\pm3.1	31.1
3 (High)		1	23.2	23.2
Stain distribution GC	0.045			
1 (Continuous)		6	25.9\pm3.8	25.4
2 (Individual)		16	21.3\pm1.4	20.9
3 (Clusters)			-	-

5.3.2.9 The association between CYP17 stain categories and control FWD

Neither CYP17 THC stain intensity or distribution category were associated with FWD as presented in Table 5-11. This lack of statistical significance may be due to the fact that almost all FW showed strong positive immunoreactivity, and were only categorised as having a cluster distribution.

Table 5-11: Association between CYP17 THC stain intensity and distribution and control FWD.

CYP17 expression	P-value	No =40	FWD (mm) Mean ±SE Mean	FWD (mm) Median
Stain intensity THC	0.656			
0 (No stain)		4	21.1±6.0	22.2
1 (Low)		4	21.2±4.8	18.2
2 (Medium)		1	14.3	14.3
3 (High)		31	21.3±1.1	20.8
Stain distribution THC	0.964			
1 (Continuous)				
2 (Individual)				
3 (Clusters)		36	21.1±1.1	20.6

5.3.2.10 The association between AMHR2 stain categories and control FWD

No differences were detected in the FWD of different AMHR2 stain intensity or distribution categories, in either GC or THC, as presented in Table 5-12. It should be noted that the AMHR2 stain distribution was continuous in all GC analysed, in contrast to aromatase and inhibin GC findings.

Table 5-12: Association between AMHR2 GC and THC stain intensity and distribution and FWD.

AMHR2 expression (GC)	P-value	No=30	FWD (mm) Mean \pmSE Mean	FWD (mm) Median
Stain intensity GC	0.917			
0 (No stain)				
1 (Low)		16	21.6 \pm 1.9	20.8
2 (Medium)		14	21.1 \pm 1.4	21.4
3 (High)				
Stain distribution GC				
1 (Continuous)		30	21.4 \pm 1.2	20.90
2 (Individual)				
3 (Clusters)				
AMHR2 expression (THC)	P-value	No=40	FWD (mm) Mean \pmSE Mean	FWD (mm) Median
Stain intensity THC	0.955			
0 (No stain)				
1 (Low)		25	21.5 \pm 1.6	20.0
2 (Medium)		15	20.4 \pm 1.5	20.8
3 (High)				
Stain distribution THC	0.715			
1 (Continuous)		20	21.2 \pm 1.4	21.4
2 (Individual)		20	21.0 \pm 1.8	19.8
3 (Clusters)				

5.3.2.11 The association between inhibin stain categories and control FFE2 concentration

In the follicles analysed FFE2 concentration was highest as the GC inhibin stain intensity increased and when the distribution was continuous (both p-values <0.05) as presented in Table 5-13.

Table 5-13: Association between inhibin GC stain intensity and distribution and FFE2 concentration

Inhibin expression	P-value	No =25	FFE2 (ng/ml) Mean \pm SE Mean	FFE2 (ng/ml) Median
Stain intensity GC	0.027			
0 (No stain)				
1 (Low)		5	29.6\pm16.9	8.1
2 (Medium)		4	76.9\pm11.8	74.7
3 (High)		16	220.7\pm58.5	139.6
Stain distribution GC	0.012			
1 (Continuous)		20	192.0\pm48.4	119.5
2 (Individual)		5	29.6\pm16.9	8.1
3 (Clusters)		-	-	-

5.3.2.12 The association between aromatase stain categories and control FFE2 concentration

In the follicles analysed FFE2 concentration increased as aromatase stain intensity increased (P=0.039) and was higher in those that stained in a continuous pattern (p=0.02) as presented in Table 5-14.

Table 5-14: Association between aromatase stain GC intensity and distribution and control FFE2 concentration

Aromatase expression	P-value	No=25	FFE2 (ng/ml) Mean \pm SE Mean	FFE2 (ng/ml) Median
Stain intensity GC	0.039			
0 (No stain)		8	52.0\pm17.0	47.5
1 (Low)		14	154.0\pm49.0	92.2
2 (Medium)		2	308.4\pm34.5	308.4
3 (High)		1	798.2	798.2
Stain distribution GC	0.02			
1 (Continuous)		5	423\pm134	343
2 (Individual)		12	121.6\pm35.9	92.2
3 (Clusters)			-	-

5.3.2.13 The association between CYP17 stain categories and control FFE2 concentration

There was a tendency for THC with the highest stain intensity also having highest FFE2 concentrations as presented in Table 5-15. All of the stain distributions were in clusters.

Table 5-15: Association between CYP17 THC stain intensity and distribution and FFE2 concentration

CYP17 expression	P-value	No=34	FFE2 (ng/ml) Mean \pm SE Mean	FFE2 (ng/ml) Median
Stain intensity THC	0.060			
0 (No stain)		4	10.6 \pm 6.7	5.8
1 (Low)		3	5.5 \pm 2.0	6.2
2 (Medium)		1	87.1	87.1
3 (High)		26	150.1 \pm 40.1	74.7
Stain distribution THC				
1 (Continuous)				
2 (Individual)				
3 (Clusters)		30	133.6\pm35.6	70.3

5.3.2.14 The association between AMHR2 stain categories and control FFE2 concentration

In THC AMHR2 expression, FFE2 concentration was higher as stain intensity went from low to medium (P=0.013) and when the stain distribution was continuous (P< 0.001), as presented in Table 5-16.

Table 5-16: Association between AMHR2 GC and THC stain intensity and distribution and FFE2 concentration

AMHR2 expression (GC)	P-value	No=25	FFE2 (ng/ml) Mean \pm SE Mean	FFE2 (ng/ml) Median
Stain intensity GC	0.443			
0 (No stain)				
1 (Low)		11	190.3 \pm 83.4	50.6
2 (Medium)		14	135.3 \pm 34.5	97.4
3 (High)				
Stain distribution GC				
1 (Continuous)		25	159.5 \pm 40.8	76.6
2 (Individual)				
3 (Clusters)				
AMHR2 expression (THC)	P-value	No=34	FFE2 (ng/ml) Mean \pm SE Mean	FFE2 (ng/ml) Median
Stain intensity THC	0.013			
0 (No stain)				
1 (Low)		19	110.7 \pm 52.1	8.6
2 (Medium)		15	129.7 \pm 32.6	87.1
3 (High)				
Stain distribution THC	<0.001			
1 (Continuous)		20	192.7 \pm 48.3	119.5
2 (Individual)		14	14.0 \pm 5.9	4.36
3 (Clusters)				

5.3.2.15 Correlation of the percentage area covered with FWD and FFE2 concentrations.

A normality test was applied to all data relating to the protein expression percentage area covered, which demonstrated evidence of a lack of normality therefore Spearman Rho tests were applied to study any correlations as presented in Table 5-17.

Table 5-17: Correlation of the percentage area covered in GC or THC with FWD and FFE2 concentration in control follicles. FWD (NO. =30 follicles), FFE2 concentration (NO. =25 follicles).

Outcome variables	Inhibin percentage area GC		Aromatase percentage area GC		Cyp17 percentage area THC		AMHR2 percentage area GC		AMHR2 percentage area THC	
	Spearman Rho correlation coefficient	P-value	Spearman Rho correlation coefficient	P-value	Spearman Rho correlation coefficient	P-value	Spearman Rho correlation coefficient	P-value	Spearman Rho correlation coefficient	P-value
FWD	0.471	0.009	0.453	0.012	0.118	0.468	0.163	0.389	0.104	0.523
FFE2	0.504	0.010	0.548	0.005	0.617	<0.001	0.276	0.182	0.748	<0.001

Both FWD and FFE2 concentrations were positively correlated with percentage inhibin and aromatase percentage area covered in GC ($P < 0.05$). In addition FFE2 concentration was positively correlated with the CYP17 and AMHR2 percentage area covered in THC (both p values < 0.001).

In the main the follicles appearing on the right hand side of the scatter plots (representing coverage of 85-100%) for inhibin and aromatase GC percentage area covered in Figure 5-29 and Figure 5-30 were those that were classified as healthy and very healthy or as large follicles.

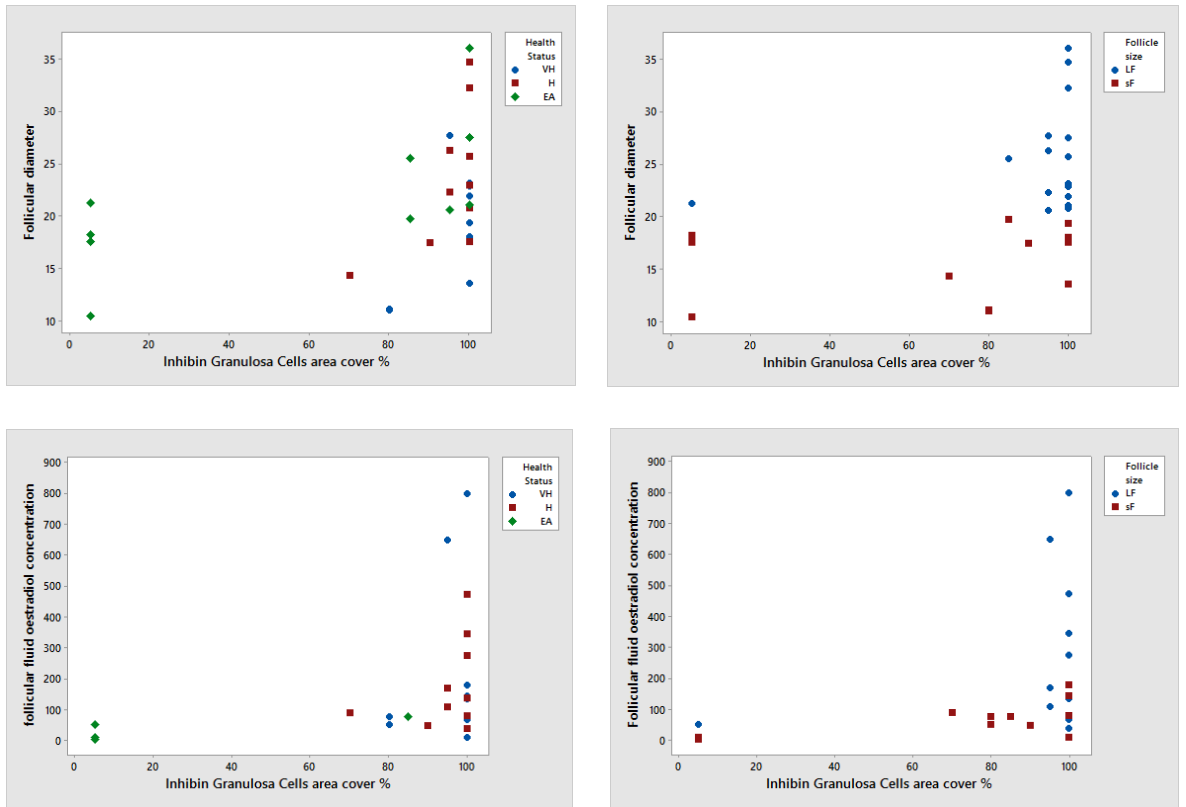


Figure 5-29: Scatter plots for inhibin GC percentage area covered versus FWD and FFE2 concentration in control FW. Health status: VH = very healthy), H = healthy, EA = early atretic. Follicle sizes are represented as LF (Large follicles from 20mm) SF (Small follicles < 20mm). FWD (No.= 30 follicles), FF E2 concentration (No.=25).

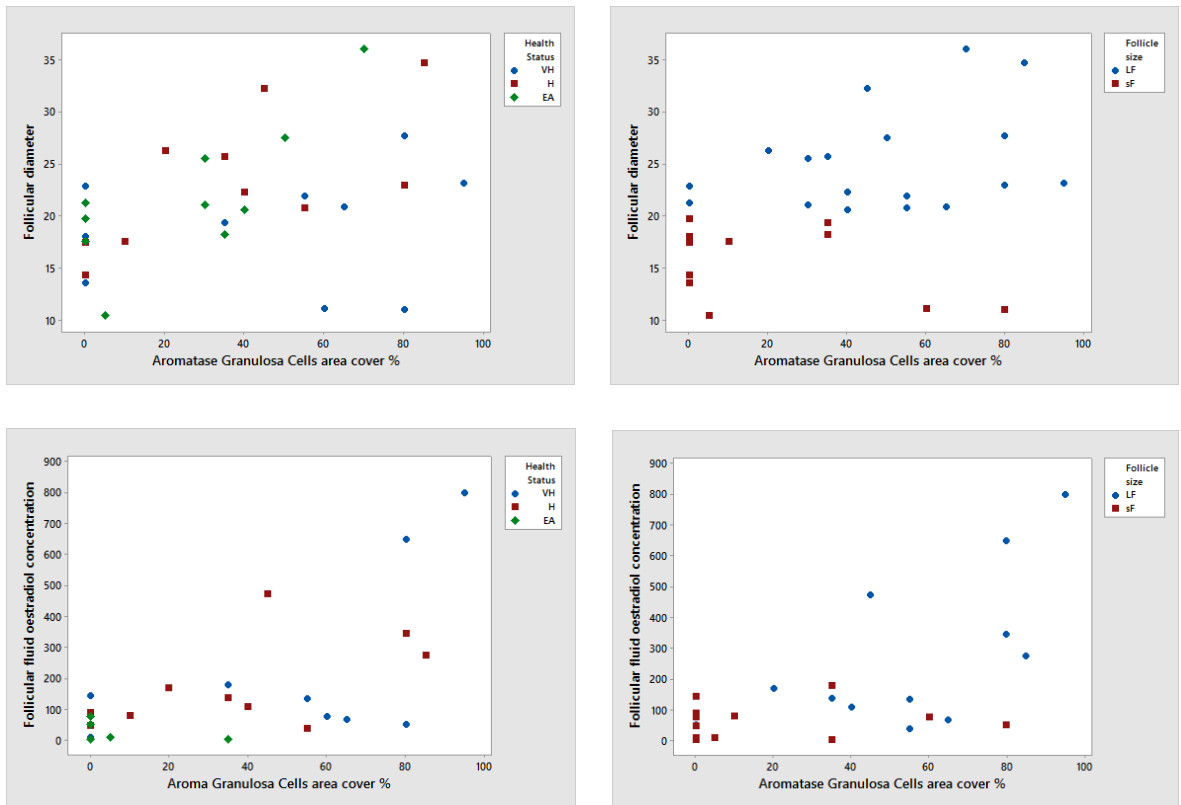


Figure 5-30: Scatter plots for aromatase GC percentage area covered versus FWD and FFE2 concentration in control FW. Health status: VH = very healthy), H = healthy, EA = early atretic. Follicle sizes are represented as LF (Large follicles from 20mm) SF (Small follicles < 20mm). FWD (No.= 30 follicles), FF E2 concentration (No.=25).

As CYP17 was only expressed in theca cells a correlation was performed for THC percentage area with FWD and FFE2 concentration, as presented in Figure 5-31 and revealed significant correlation only with FFE2 concentration (P= 0.01, Table 5-17). The majority of follicles that expressed CYP17 had between 65-85% area covered. Those that were below 50% area covered were all late atretic follicles with very low E2 production.

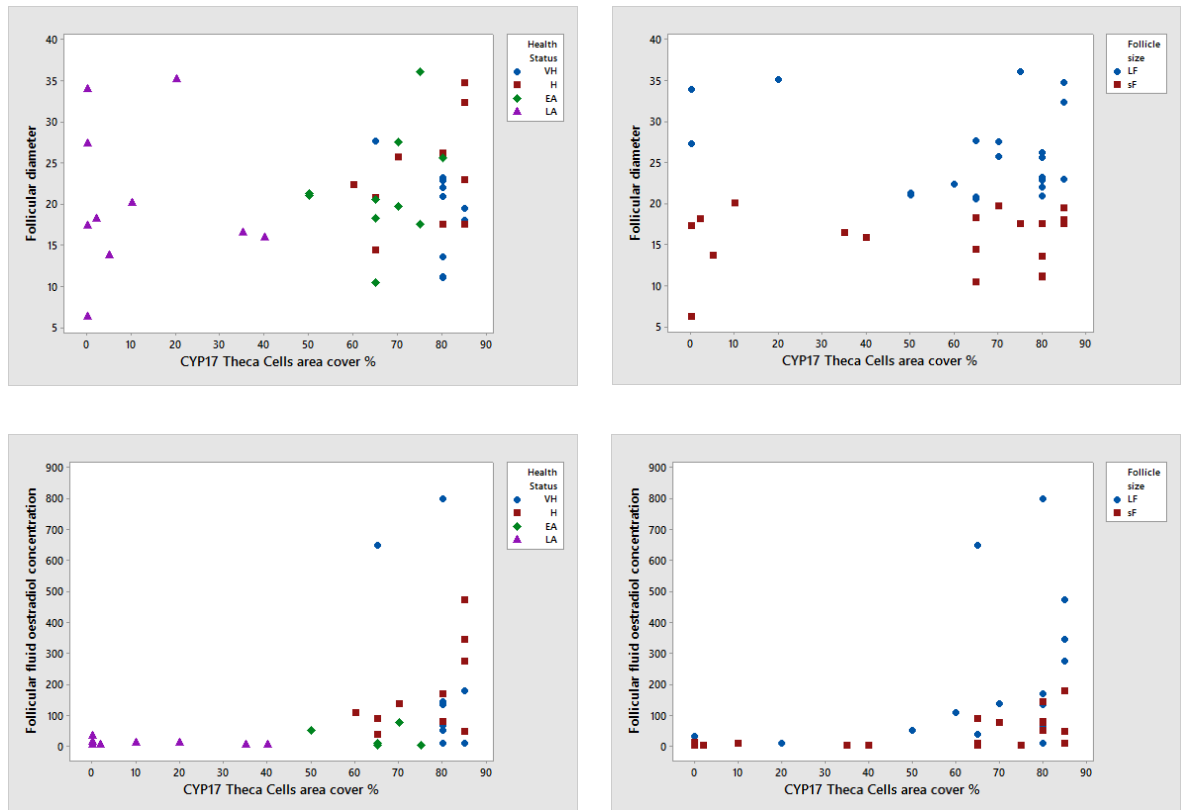


Figure 5-31: Scatter plots for CYP17 THC percentage area covered versus FWD and FFE2 concentration in control FW. Health status: VH = very healthy), H = healthy, EA = early atretic. Follicle sizes are represented as LF (Large follicles from 20mm) SF (Small follicles < 20mm). FWD (N0.=40 follicles), and FFE2 concentration (No.=30 follicles).

There were no significant correlations between AMHR2 GC percentage area covered and FWD and FFE2 concentration as presented in Table 5-17 and Figure 5-32. The THC AMHR2 percentage area covered was not correlated with FWD but there is a significant correlation with FFE2 concentration (P-value 0.01) as presented in Table 5-17 and Figure 5-33. There does appear to be a clear differentiation between follicles that have greater than 60% THC area covered and those with less than 30% area covered with all atretic follicles in the latter group and almost all healthy follicles in the former group (Figure 5-33).

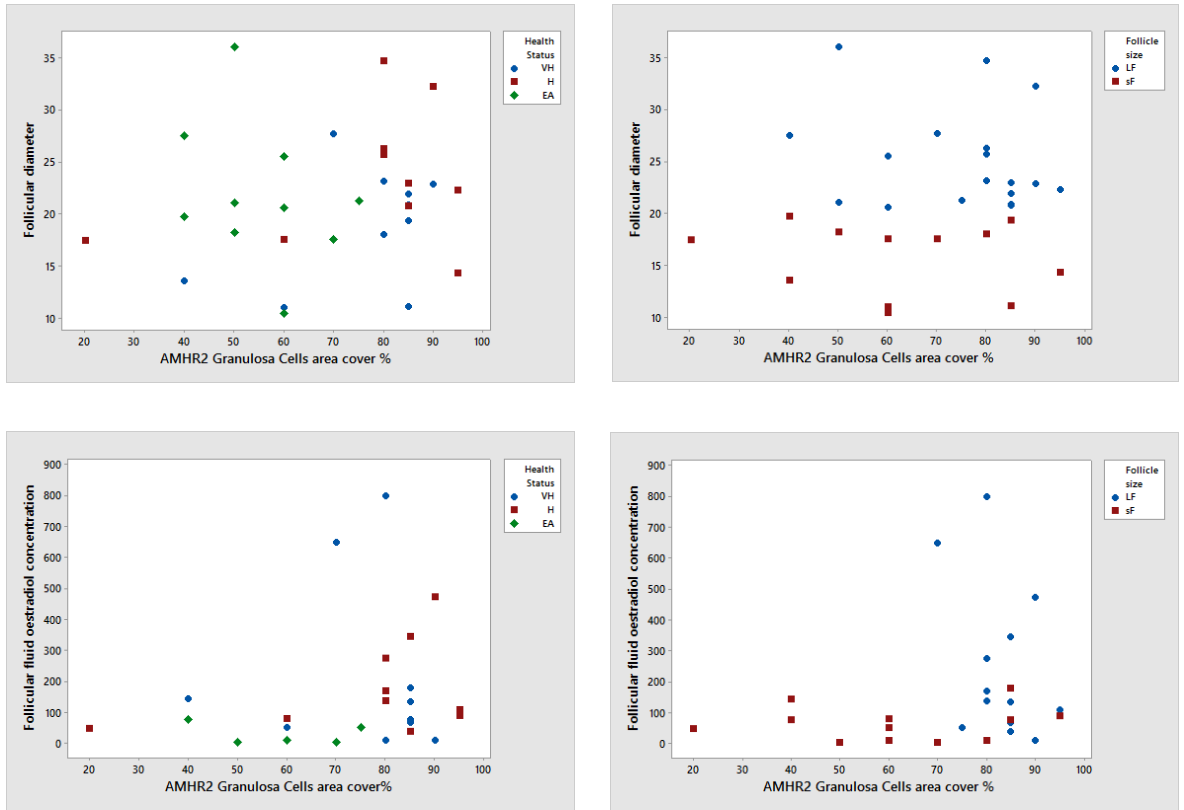


Figure 5-32: Scatter plots for AMHR2 GC percentage area covered versus FWD and FFE2 concentration in control FW. Health status: VH = very healthy), H = healthy, EA = early atretic. Follicle sizes are represented as LF (Large follicles from 20mm) SF (Small follicles < 20mm). FWD (No.= 30 follicles), FF E2 concentration (No.=25).

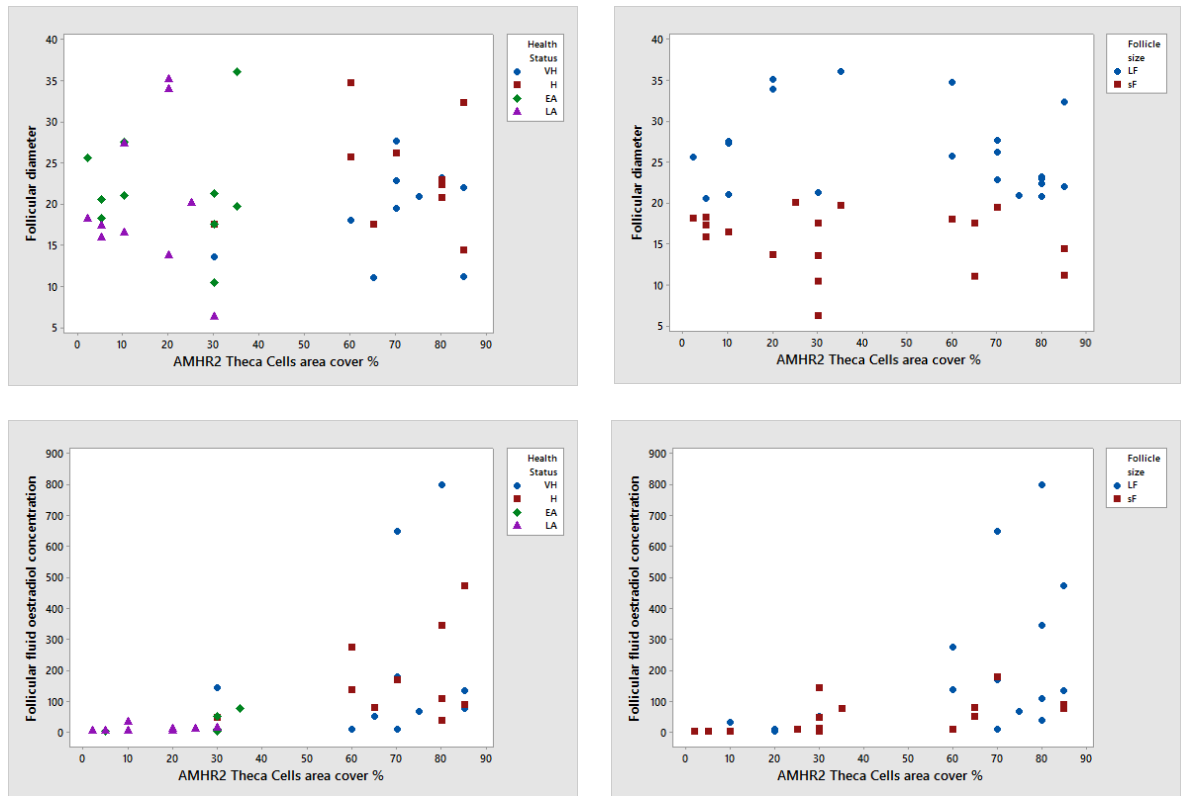


Figure 5-33: Scatter plots for AMHR2 THC percentage area covered versus FWD and FFE2 concentration in control FW. Health status: VH = very healthy), H = healthy, EA = early atretic. Follicle sizes are represented as LF (Large follicles from 20mm) SF (Small follicles < 20mm). FWD (N0.=40 follicles), and FFE2 concentration (No.=30 follicles).

5.3.3 Nuclear Circumference between FW and GCTs

The nuclear circumferences of GC (antral, intermediate and basal) were measured in follicles of different FW health categories (VH, H, EA; representative images shown in Figure 5-34 and Figure 5-35). The nuclear circumferences of GC were also measured in the different GCT categories (GCT1, GCT2, GCT4) as presented in Figure 5-36 and Figure 5-37. Late atretic FW were excluded from the analysis because LA FW have no GC. The GCT3 cysts only have a single layer of very few antral cells (Figure 5-38) so could not be included in the FW and GCT comparisons.

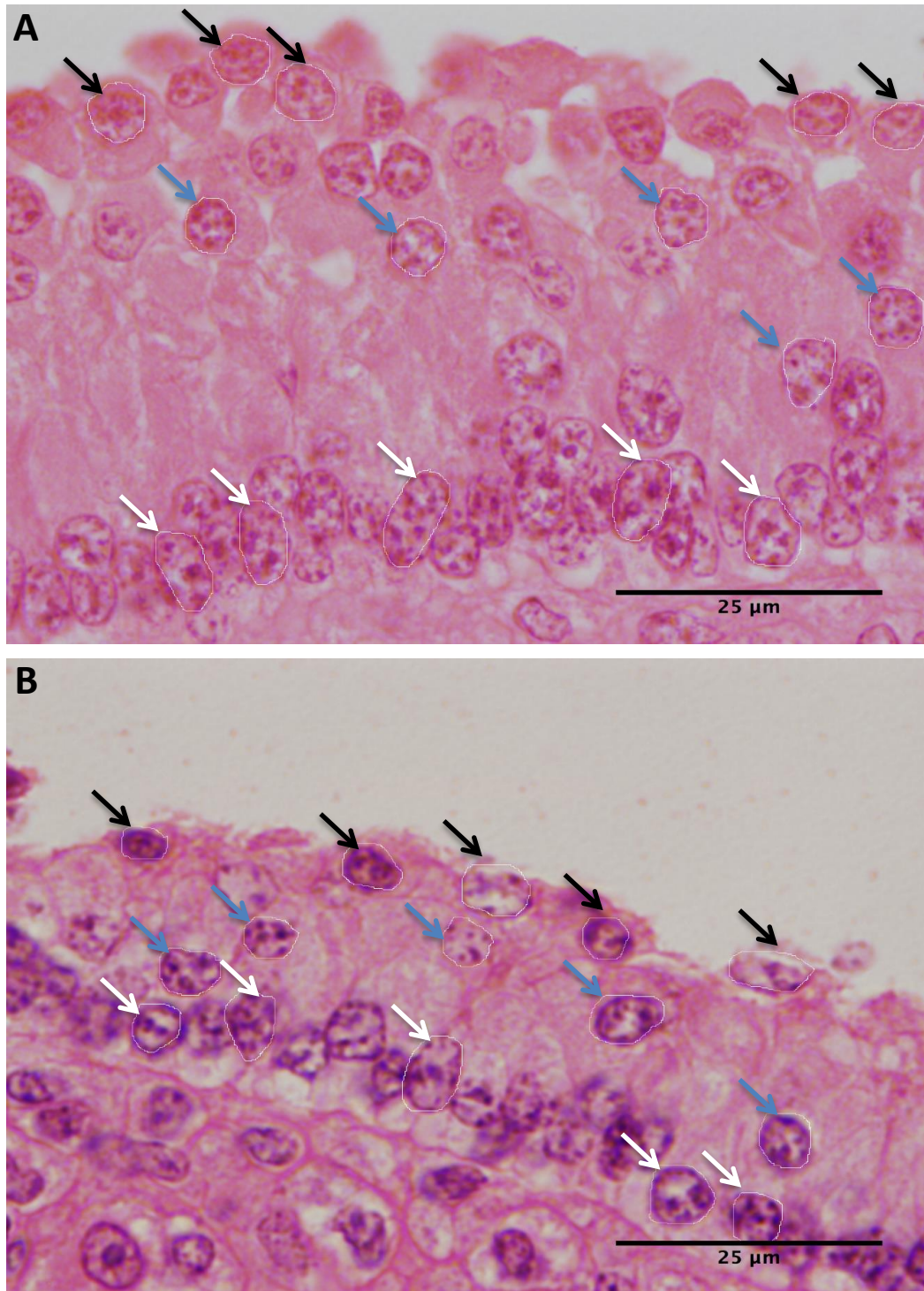


Figure 5-34: Nuclear circumferences of GC in VH (A) and H (B) FW health categories at 1000x magnification. Black arrows indicate antral GC, Blue arrows intermediate GC and White arrows basal GC.

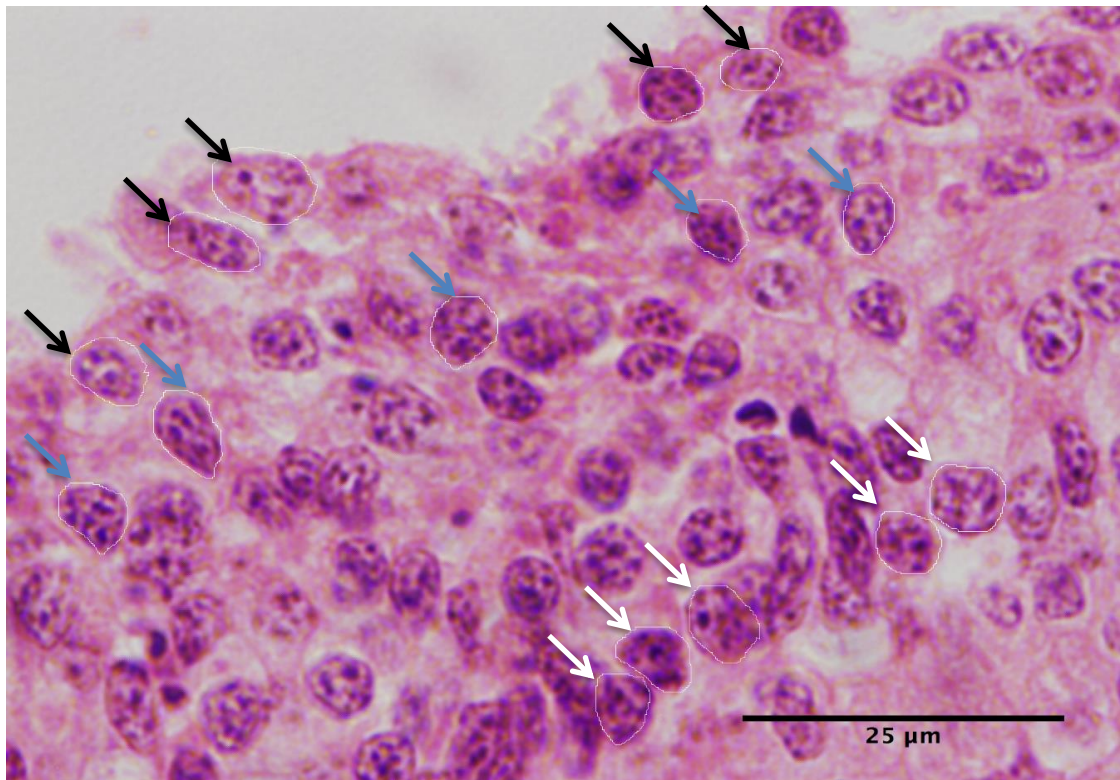


Figure 5-35: Nuclear circumferences of GC in the EA FW health category at 1000x magnification. Black arrows indicate antral GC, Blue arrows intermediate GC and White arrows basal GC.

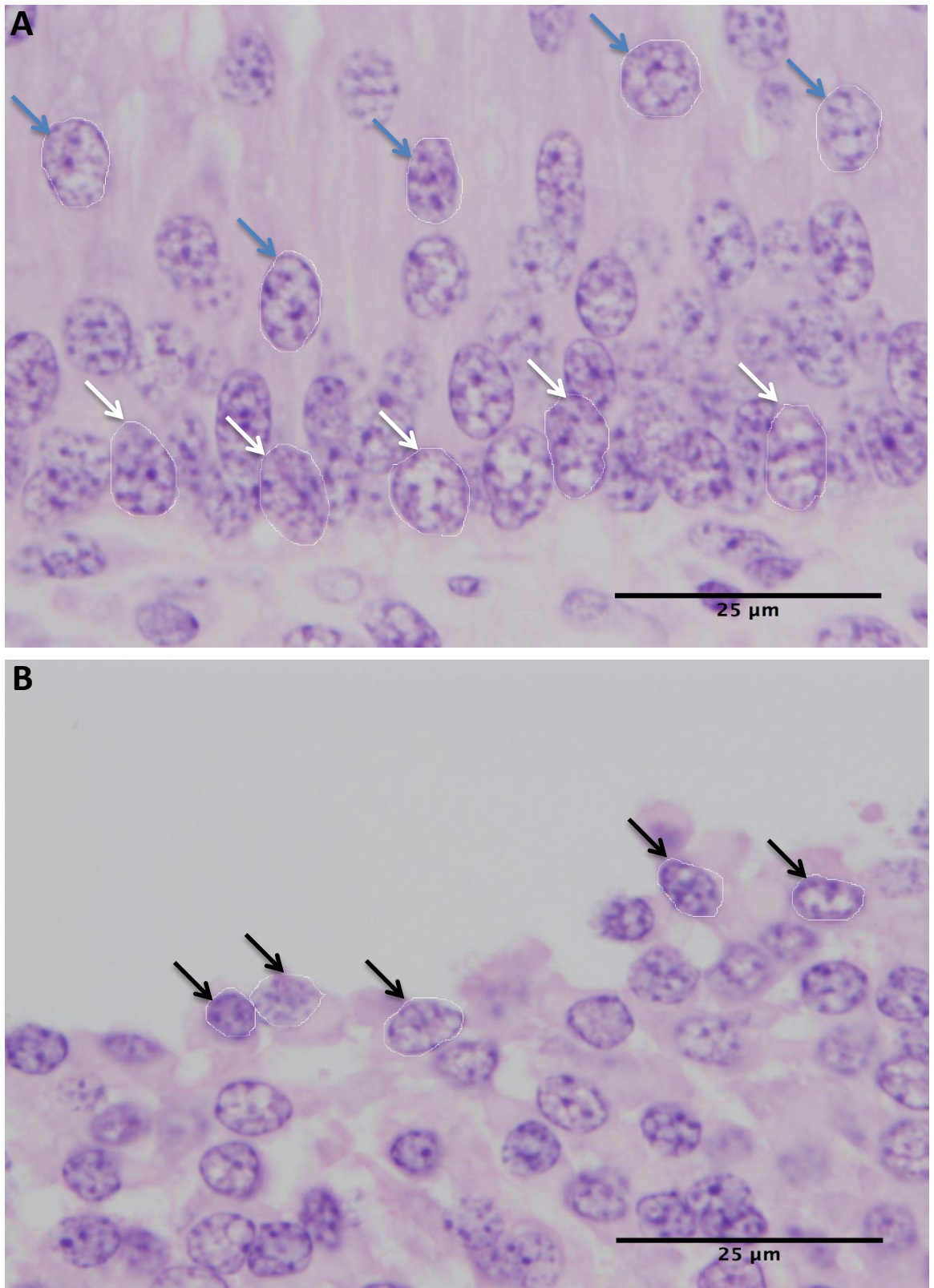


Figure 5-36: Nuclear circumferences of GC in the GCT1 category showing basal and intermediate GC (A), and antral GC (B) at 1000x magnification. Black arrows indicate antral GC, Blue arrows intermediate GC and White arrows basal GC.

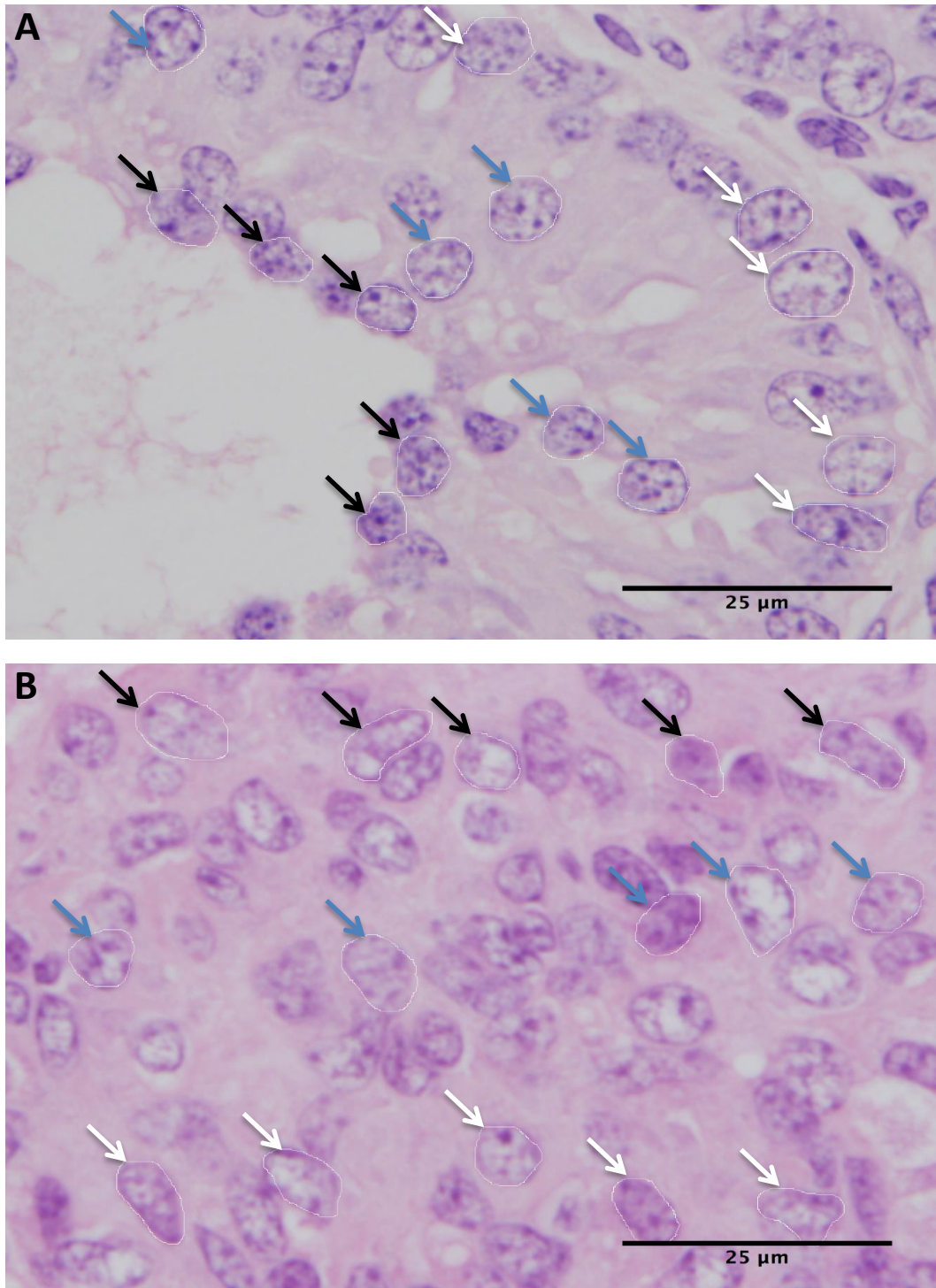


Figure 5-37: Nuclear circumference of GC in GCT categories GCT2 (A) and GCT4 (B) at 1000x magnification. In GCT2 Black arrows indicate antral (to the cyst antrum) GC, Blue arrows intermediate GC and White arrows basal GC. In the solid GC nests of GCT4 15 nuclear circumferences were measured across the view with colour of arrows only indicating the top, middle or bottom of the view.

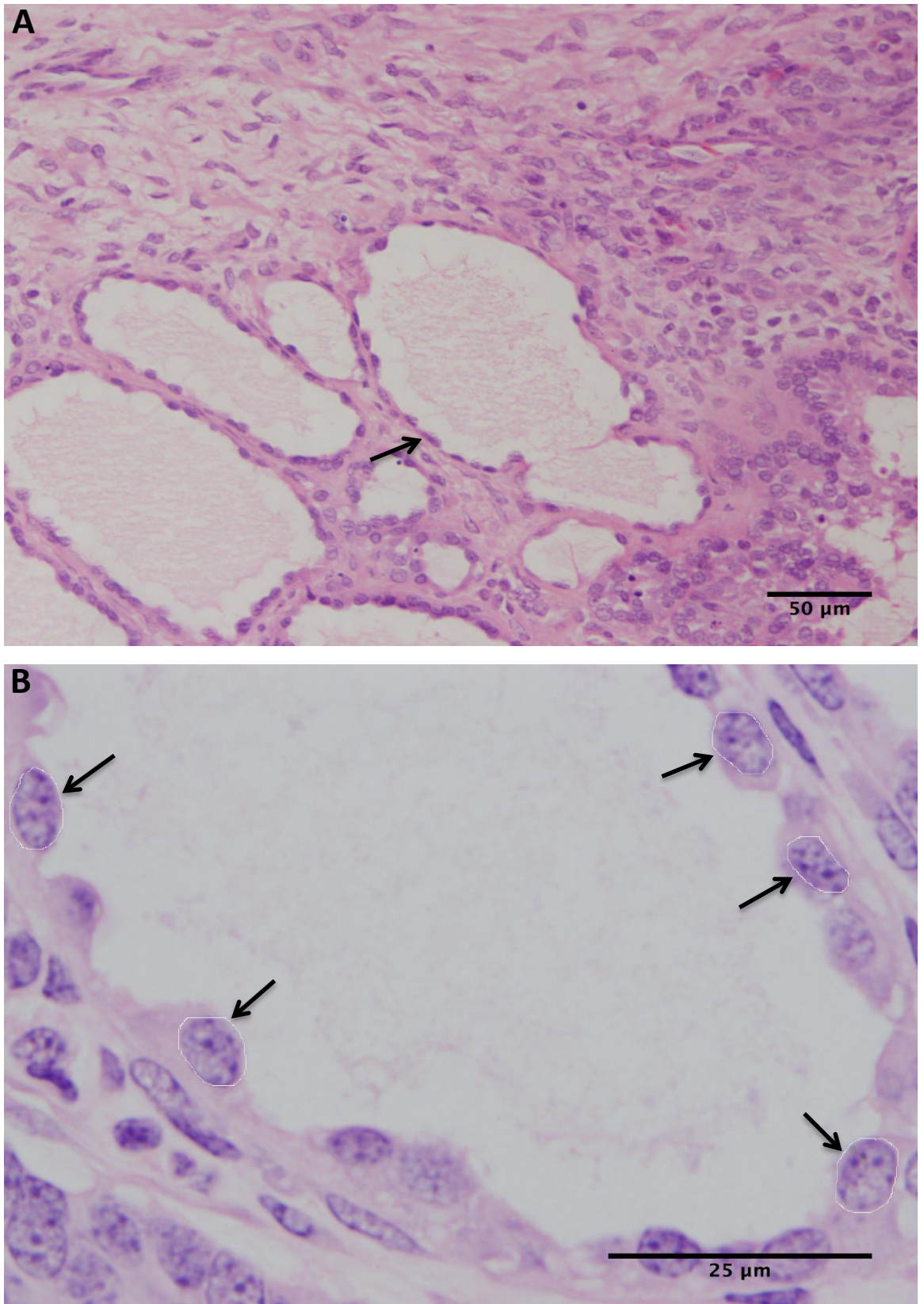


Figure 5-38: Antral (lining the cyst antrum) GC in the GCT3 category at 200x magnification (A) and 1000x magnification (B), Black arrows indicate antral GC.

5.3.3.1 Follicular wall GC nuclear circumference

Table 5-18 shows that there were no overall significant differences at $p < 0.05$ in GC nuclear circumferences of antral, intermediate or basal GC between follicles of different health status. However, Mann Whitney analysis showed that basal GC in early atretic FW had a smaller nuclear circumference than healthy basal GC ($P = 0.04$), but there was no significant difference between very healthy and early atretic follicles ($p = 0.2$). A comparison of GC in the different locations showed that antral GC have the smallest nuclear circumference (44.7 ± 1.9) followed by intermediate GC (54.5 ± 1.6), and basal GC have the largest nuclear circumference (62.9 ± 3.1), (basal vs. antral GC $P < 0.001$ and intermediate vs. antral $P = 0.001$) with a tendency between intermediate and basal GC ($P = 0.1$).

Table 5-18: Comparison of FW GC nuclear circumferences by health status. No represent 5 different follicles

FW circumferences outcomes	Health status	P-value	No	Mean \pm SE Mean	Median
Antral GC	VH	0.932	5	44.0 \pm 4.4	45.5
	H		5	45.8 \pm 2.8	47.0
	EA		5	44.4 \pm 3.2	46.1
Intermediate GC	VH	0.228	5	53.2 \pm 2.0	53.3
	H		5	58.4 \pm 2.5	61.0
	EA		5	51.9 \pm 3.2	49.6
Basal GC	VH	0.101	5	66.0 \pm 6.2	68.4
	H		5	69.7 \pm 3.2	72.2
	EA		5	53.0 \pm 4.0	52.6

There was no significant difference between large and small follicles in terms of GC nuclear circumferences as presented in Table 5-19. However, it does appear that as one goes from antral, through intermediate to basal GCs the nuclear circumference increases similar to what was shown above.

Table 5-19: Comparison of follicle size categories in their FW GC nuclear circumferences.

FW circumferences outcomes	F. Size Cat.	P-value	No	Mean \pm SE Mean	Median
Antral GC	LF	0.289	9	43.0 \pm 2.6	44.1
	SF		6	47.3 \pm 2.5	47.9
Intermediate GC	LF	0.637	9	55.3 \pm 2.0	56.9
	SF		6	53.3 \pm 2.7	53.5
Basal GC	LF	0.906	9	63.5 \pm 4.5	63.1
	SF		6	61.9 \pm 4.4	64.8

There were no significant associations between mare factors such as breeding season, breed category, age or disease status and the GCs nuclear circumferences (data not presented).

5.3.3.2 GCT nuclear circumferences

The mean of the antral GC in the GCT3, which was excluded from the overall analysis, was (62.6 ± 3.1 , Median 58.29). There were no significant differences in nuclear granulosa cell layers circumferences between GCT1 and GCT2 as presented in Table 5-20. A Mann Whitney test was used to detect any associations of location (antral, intermediate and basal) with GC nuclear circumference in GCT 1 and GCT2. It revealed that basal nuclear GC were significantly larger than intermediate ($P= 0.03$) and antral nuclear GC ($P= 0.001$).

Table 5-20: Effect of categories on GCT GC nuclear circumferences. No. represent 5 different GCT tumours which were used for each GCT category.

GCT circumferences outcomes	Health status	P-value	No	Mean±SE Mean	Median
Antral GCs	GCT1	0.251	5	49.6±3.4	48.0
	GCT2		5	57.8±4.6	59.3
Intermediate GCs	GCT1	0.602	5	64.7±9.0	55.3
	GCT2		5	63.2±4.2	60.0
Basal GCs	GCT1	0.602	5	75.0±7.7	67.7
	GCT2		5	71.6±2.3	72.8

When the antral, intermediate and basal nuclear GC in the GCT categories were combined as presented in Table 5-21 it was found that the nuclear circumference of GC in solid nests of GCT4 were significantly larger than antral GC in GCT1 and GCT2 (P= 0.01), and the combined GC nuclear circumference tended to be smaller in GCT1 and GCT2 versus GCT4.

Table 5-21: Comparison of health status and combined nuclear GC layers within GCT categories.

GCT circumferences outcomes combined	Health status	P-value	No	Mean±SE Mean	Median
Antral, Intermediate & Basal GCs	GCT1	0.057	15	63.1±4.7	61.0
Antral, Intermediate & Basal GCs	GCT2		15	64.2±2.6	65.1
Combined GCs (Solid, no Antral, Intermediate & basal)	GCT4		15	74.0±4.1	68.2

5.3.3.3 FW and GCT comparison

The comparison between FW and GCT GCs nuclear circumferences showed that there were overall differences in antral and intermediate cell layers as presented in Table 5-22. Mann Whitney tests revealed significant differences between the nuclear circumferences of antral GC (51.5±2.2) and intermediate GC (61.3±2.5) (P= 0.001), between antral GCs and basal GCs (68.9±2.6) (P < 0.001) and between intermediate GCs and basal GCs (P= 0.011).

Table 5-22: Comparison of all categories of FW and GCT in their GC nuclear circumferences. Note that GCT4 did not have different GC layers, but top, middle and bottom nuclei were measured within one view.

FW & GCT circumferences outcomes	Health status	P-value	No	Mean±SE Mean	Median
Antral GC	VH	0.014	5	44.0±4.4	45.5
	H		5	45.8±2.8	47.0
	EA		5	44.4±3.2	46.1
	GCT1		5	49.6±3.4	48.0
	GCT2		5	57.9±4.6	59.3
	GCT4		5	67.6±5.7	64.6
Intermediate GC	VH	0.026	5	53.2±2.0	53.3
	H		5	58.4±2.5	61.0
	EA		5	51.9±3.2	49.6
	GCT1		5	64.7±9.0	55.3
	GCT2		5	63.2±4.2	60.0
	GCT4		5	76.2±7.8	72.5
Basal GC	VH	0.126	5	66.0±6.2	68.4
	H		5	69.7±3.2	72.2
	EA		5	53.0±4.0	52.6
	GCT1		5	75.0±7.7	67.7
	GCT2		5	71.7±2.3	72.8
	GCT4		5	78.1±8.3	73.3

Even when GCT4 (being solid) was excluded from the analysis performed above, no changes to the overall results were observed.

Table 5-23 shows that in GCTs the nuclear circumference (67.1 ± 2.3) is increased by approximately 20% compared with those from the control follicle walls (54.0 ± 1.7), which differs significantly (P-value < 0.001). In addition, Mann Whitney tests revealed a significant difference between all antral GC of FW (44.7 ± 1.9) and all antral GC of GCT (52.8 ± 2.8) (P= 0.03). Moreover, there is a strong location effect with differences between antral GC (48.0 ± 1.8) and intermediate GC (58.3 ± 2.3) (P < 0.001), antral GC and basal GC (67.0 ± 2.6) (P < 0.001) and between intermediate GC and basal GC (P= 0.01).

Table 5-23: Comparison of the GC nuclear circumference between all VH, H and EA FW combined and all GCT1, GCT2 and GCT4 combined.

FW (VH, H& EA) & GCT (GCT1, GCT2& GCT4 (solid)) Combined circumferences outcomes	Health status	P-value	No	Mean± SE Mean	Median	Confidence
Antral, Intermediate & Basal GC	1 (FW)	<0.001	45	54.0±1.7	52.6	95.01%
	2 (GCT)		45	67.1±2.3	65.1	

5.4 Discussion

In support of previous studies we show that follicular differentiation markers such as inhibin expression in GC and CYP17 expression in THC are maintained in GCT tumour cells, while aromatase expression is not seen in GCT, although essential for follicular oestradiol synthesis and thus differentiation. The expression of the receptor AMHR2 was detected in both GC and THC compartments in antral follicles, but also in GCT indicating there is not only known GC AMH expression, but tumour GC and the theca like interstitial cells can respond to AMH. We show contrasting results to a previous study Ellenberger et al. (2007) which found that late stage III of atresia based on (Kenney et al., 1979) classification has the highest expression of inhibin. Our study shows that LA follicles have no inhibin expression as the GC layer is lost. However, we do show that EA follicles still have a high level of inhibin expression. In an experiment conducted by (Nagamine et al., 1998) a difference in inhibin subunit expression was found between large healthy and small healthy follicles, with large follicles expressing α and β A subunits, but small follicles only expressing the α subunit. In our experiment only inhibin α expression was examined in large and small follicles, and there was no significant difference between these size categories.

It has been reported that 2 mares managed to preserve their pregnancy while having GCT (Watson, 1994). Chopin et al. (2002) have another interesting

outcome in that the mare was cycling and conceived while high levels of inhibin were secreted in plasma. A majority of GCT is associated with the presence of high systemic concentrations of inhibin which suppress FSH release. When the tumour was recorded in pregnant mares it is unclear whether the GCT transformation occurred before or after the pregnancy developed (Ball et al., 2014). In our study, one case had GCT ovariectomy 12 days after foaling, so might have developed GCT during her pregnancy or shortly before without influencing cyclicity.

The expression of inhibin and AMH has previously been detected in the cytoplasm of GC in GCT (Evkuran Dal et al., 2013) and this together with our findings makes inhibin and AMH or AMHR2 useful GCT markers. Davis et al. (2005) showed that inhibin α subunit antibody moderately immunostained the cytoplasm of granulosa cells in GCT which is similar to our findings. The significant difference of inhibin expression among GCT categories in our study was due to low number of GC in GCT 3 that reduced the amount of stain intensity and percent area covered.

Expression of aromatase is confined to GC (Belin et al., 2000). Our findings support this as aromatase expression was seen in all GC of VH, H and EA follicles, but not in LA follicles as they lack the GC layer. Moreover, aromatase expression was not detected in any of our equine GCT categories. The immunostaining of aromatase in granulosa cells is generally high; we did not see any THC staining using the aromatase antibody in contrast to another study (Almadhidi et al., 1995).

We only found CYP17 expression in THC of antral follicles, and in clusters of theca like cells in the interstitial tissue or stroma in GCT. This partly supports other reports of thecal CYP17 expression (Albrecht and Daels, 1997). The THC CYP17 stain intensity and distribution pattern differed between FW health with clusters of CYP17 expressing large theca cells extending previous reports describing thecal androgen production (Watson et al., 2004). There were no differences seen between GCT categories, but this makes sense as there is no clear theca compartment, only interstitial tissue and stroma.

The AMH expression in normal equine ovaries is mainly confined to preantral and small antral follicles but not seen in primordial follicles with one layer of flattened granulosa cells (Ball et al., 2008b). In addition, when the small antral follicle size reached approximately 2-3 mm the expression of AMH increased, however, when follicles reached > 30 mm in diameter the AMH expression decreased. In our study of equine follicle walls, a reduction of AMHR2 expression was detected in early atretic follicles and AMHR2 completely disappeared in late atretic follicles where the granulosa cells are missing and the THC layer is much reduced. Similar to other reports of AMH expression in equine follicles and GCT (Almeida et al., 2011a, Ball et al., 2008b), our results showed the same localization of AMHR2 for both control follicles (apart from LA follicles) and GCT. The expression of AMHR2 reduced in intensity due to the reduction of GC numbers in EA and their sloughing in LA follicles, and this effect was mimicked in the different GCT categories, where GC numbers severely declined in GCT3. In GCT immunolabelling for AMH expression decreases in large polyhedral, Leydig like cells were seen (Ball et al., 2013), however, we show maintained expression of AMHR2 in the interstitial/stromal compartment of all GCT categories.

When comparing between FW and GCT, the thecal CYP17 and AMHR2 expression differed due to the presence of large numbers of THC in FW from VH, H and EA follicles, while only nests or clusters of theca like cells were seen in the four GCT categories.

The follicle with the largest diameter also expressed more inhibin and aromatase due to the presence of a large number of GC. As a result intrafollicular concentrations of oestradiol increased, as both inhibin and aromatase will upregulate steroid hormone production in GC and THC; we know that inhibin supports thecal androgen production which can then be used as the precursor for oestradiol synthesis in GC, and in our study the intrafollicular oestradiol concentrations and CYP17 expression were correlated, with FFE2 increasing simultaneously with CYP17 expression in THC. The intrafollicular oestradiol concentration was also associated with thecal AMHR2 stain distribution pattern, for instance, follicles with low follicular fluid oestradiol concentration showed an individual staining which might reflect the follicles becoming atretic, while

high oestradiol concentration was associated with continuous distribution of AMHR2 expression.

It was noticed that inhibin expression in GC was very low in follicles shown on the left in the scatter plots, being small and mostly classified as atretic.

The basal GC were found to have larger nuclear circumferences in both FW and GCT cysts of GCT1 and 2 compared with antral and intermediate GC, with a consecutive decline from basal to intermediate to antral GC. This makes sense in normal ovaries and follicle walls as the basal layer is the proliferating layer within the GC compartment during follicle growth. Accordingly, the basal GC nuclei in healthy follicles were also larger than those in EA category follicles. The size of basal GC nuclei did not differ between large or small follicles and was not affected by any predictive mare factors (breeding season, breed, age and disease). When the nuclear circumferences of GC were compared between FW and GCT, the size of the antral GC nuclei (in GCT 1-3) was found to be larger in GCT, and this might be due to the degree of proliferation in GC during tumour development. In the solid nests of GCT4 all GC nuclei are like basal GC nuclei in shape and size, and it appears that they are just multiplying but keeping the phenotype of the basal layer. The nuclear circumference of GC within solid islets appeared to vary more between tumours than the nuclear circumference of GC within cysts, and nuclei of GC in solid nests tended to be larger than antral GC nuclei.

5.5 Conclusion

Location within the normal antral follicle GC compartment and tumour cyst walls, atresia, tumour transformation, and GCT category affect GC nuclear size with largest nuclei likely reflecting highest DNA content and increased nuclear activity.

Chapter 6 Mutation of the forkhead box L2 (*FOXL2*) gene and *FOXL2* expression in control ovaries and GCT of mares

6.1 Introduction

The *FOXL2* transcription factor has been shown to regulate ovarian function in vitro and in vivo in the mouse as a model species. Firstly, *FOXL2* is crucially involved in sex differentiation of the gonads, where it downregulates *SOX9* expression and thus leads to ovary differentiation in the embryo, and also maintains the ovarian/follicular phenotype in the adult female, as downregulation of *FOXL2* expression causes transformation of follicles to seminiferous tubules and the appearance of Sertoli like cells (Caburet et al., 2012).

Secondly, *FOXL2* maintains the ovarian reserve and represses granulosa cell (GC) proliferation by affecting cell cycle progression, gonadotrophin response and steroidogenesis. It is considered to regulate cell (oxidative) stress response (Benayoun et al., 2011) and its over expression induces apoptosis of a GC cell line (KGN cells) in vitro (Kim et al., 2011). In contrast to this apoptotic function, *FOXL2* enhances the (anti-apoptotic) oestrogen conversion by inducing the aromatase gene *CYP19A1* (Benayoun et al., 2009). Thus, *FOXL2* can play a positive or negative part in GC apoptosis regulation.

The *FOXL2* transcription factor gene is one of the genetic determinants of premature ovarian failure in women: Several mutation variants (including deletions and heterozygous single nucleotide mutations) have been described which lead to the BPES / premature ovarian failure syndrome, as well as premature ovarian failure without BPES (Gersak et al., 2004). This illustrates that resultant alterations in the *FOXL2* protein and its cellular localization can lead to premature activation and thus premature depletion of the follicle reserve in women. Similar to the human BPES syndrome, *FOXL2* mRNA expression has been localised in murine developing eyelids as well as in murine adult ovarian follicles thus constituting an animal model for this syndrome (Pisarska et al., 2011).

Thus the wildtype protein is considered to have repressive and apoptotic functions, while altered proteins may be involved in the dysregulation of GC proliferation and follicular development: A single nucleotide polymorphism (SNP) in the *FOXL2* gene sequence within the winged helix (DNA binding) domain has been identified in human adult type GCT, resulting in an altered protein which may be causally involved in tumour progression (Cheng et al., 2013). The point mutation is a C-G (Cytosine-Guanine) mutation at nucleotide position 402 in the human coding sequence (C402G; NCBI NM_023067.4), which causes a substitution of the highly conserved cysteine with tryptophan at amino acid position 134 (C134W; NCBI NP_075555.1) (Bugno et al., 2008). This SNP was identified in almost all adult-type GCT biopsies and in varying percentages of other ovarian tumours if they contained GC, but not in circulating leucocyte DNA, thecal or epithelial ovarian tumours (Pisarska et al., 2011).

Elucidating the pathogenesis of GCT in women is very important; GCT constitute 2-5% of all ovarian cancers and have a high risk of recurrence after surgery (Shah et al., 2009, Schumer and Cannistra, 2003), and there is a clear need for early diagnosis and better prognostic markers, with high mortality at 20-30% due to poor diagnosis of recurrent and advanced stages (Schumer and Cannistra, 2003); unfortunately, surgery is still the only treatment option. In fact, there are four important functions by which wildtype *FOXL2* may normally be a tumour suppressor according to Caburet et al. (2012): first, encouraging apoptosis of extremely damaged cells, and transcriptomic analyses have indeed revealed that apoptotic pathways are downregulated by the known mutation (Benayoun et al., 2013); second, encouraging stability of genome and DNA repair; third, reducing entry into the cell cycle, and transcriptomic analyses have also revealed that cell cycle genes were activated by the known mutation (Benayoun et al., 2013), and finally, obstructing growth factor signalling.

It may be that localized somatic (granulosa) cell mutations of the *FOXL2* gene occur or accumulate in adult women, which then enhances GCT progression and invasiveness despite surgery (Shah et al., 2009). As in women, GCT are also the most frequent gonadal tumour in mares, with similar morphological and functional (inhibin and AMH producing) features to the human adult type GCT, which mainly consist of granulosa cells but might also be composed of theca

cells, lutein cells and/or fibroblasts. In human GCT granulosa cells are aligned in trabecular, insular, macro and micro-follicular or diffuse cellular patterns (Wang and Lai, 2014), which is very similar to equine GCT. In mare's surgical removal of the diseased ovary while invasive is in almost all reported cases completely curative and restores fertility, but similar to women may not prevent the occurrence of GCT on the other ovary. Both in the human condition and in the mare the pathogenesis of GCT is unclear, and while *FOXL2* mRNA and protein expression, and the (GC) somatic mutation have now been studied in human ovaries, the involvement of the *FOXL2* gene in equine ovarian function and GCT development is completely unknown (Shah et al., 2009, Koebel et al., 2009).

At the time of study a partial equine coding sequence (cds) for *FOXL2* existed on the public database (NCBI EF202823.1), which contained the winged helix domain with a 100% match to the human sequence, and thus spanned the human C402G mutation locus (shown in Figure 6-1). This allowed the amplification and sequencing of *FOXL2* DNA in our follicular and GCT samples. Subsequently, the equine genome database with full nucleotide (predicted) coding sequence and translated protein sequence of the *FOXL2* gene became available, allowing direct matching to the human adult-type GCT SNP (C405G in the equine cds NCBI XM_023621016.1) and the predicted amino-acid change (C135W in the equine amino acid sequence NCBI XP_023476784.1). Therefore, this study firstly aimed to isolate the relevant partial *FOXL2* gene from mare ovarian tissues to then identify whether the human *FOXL2* SNP (C402G) occurred in DNA extracted from mare GCT tissues, but not in normal antral follicles. Secondly, in order to begin clarify *FOXL2* roles in ovarian, and specifically follicular function in the mare, an excellent ovarian model species for women, this study also aimed to describe any alterations in *FOXL2* expression in antral follicles of different health and developmental stages compared with the expression in different cystic or solid GCT samples.

```

humanFOXL2  MMASYPEPEDAAGALLAPETGRTVKEPEGPPSPGKGGGGGGTAPEKPDPAQKPPYSYVALIAMAIRESA
equineFOXL2  -----

humanFOXL2  EKRLTLSGIYQYIIAKFFPYEKNNKGWQNSIRHNLSLNECFIKVPREGGGERKGNWTLDPACEDMFEKGN
equineFOXL2  --RLTLSGIYQYIIAKFFPYEKNNKGWQNSIRHNLSLNECFIKVPREGGGERKGNWTLDPACEDMFEKGN

humanFOXL2  YRRRRRMKRPFPPPAHFQPGKGLFGAGGAAGCGVAGAGADGYGYLAPPKYLQSGFLNNSWPLPQPPSPM
equineFOXL2  YRRRRRMKRPFPPPAHFQPGKGLFGAGGAAGCGVAGAGADGYGYLAPPKYLQSGFLNNS-----

humanFOXL2  PYASCQMAAAAAAAAAAAAAAGPGSPGAAAVVKGLAGPAASYGPYTRVQSMPHPHHAHHLHAAAAPPAP
equineFOXL2  -----

humanFOXL2  PHHGAAPPQGQLSPASPATAAPPAPAPTSAPGLQFACARQPELAMMHCSYWDHDSKTGALHSRLDL
equineFOXL2  -----

```

Figure 6-1: Equine and Human *FOXL2* gene sequences

Human GCT generally consisted of granulosa cells and might be composed of theca cells, lutein cells and/or fibroblasts. Those granulosa cells aligned in trabecular, grand like, insular, macro and micro-follicular or diffuse cellular patterns (Wang and Lai, 2014).

6.1.1 Aim:

The overall aim was to identify any ovary-specific mutation in the *FOXL2* gene in mare control ovaries and GCT, and then begin describe the expression and putative function of the *FOXL2* gene in follicle and GCT development in mares.

6.1.2 Objectives:

1. Using molecular techniques, we aimed to isolate and sequence the partial *FOXL2* gene from ovarian biopsies including antral follicle walls, and from GCT biopsies, which include solid areas and cysts.
2. Identify whether a comparative point mutation exists in equine GCTs: an area not previously researched to our knowledge.
3. Determine the localization of the *FOXL2* protein in GCT cysts and solid areas, and in antral follicle walls from VH, H, EA and LA categories.

6.2 Materials and Methods

6.2.1 Next Generation Sequencing (NGS)

This experiment was taking place because of the impossibility of generating single and uncontaminated by primer dimer PCR products from extracted DNA of all fixed ovaries, which led to overlapping sequences using the BigDye protocol (Biosystems, 2016) and the in-house Genetic Analyzer. Therefore, the decision was taken to perform one last (primer 3) PCR on freshly extracted DNA samples and send PCR products for next generation sequencing (NGS) to Glasgow Polyomics, University of Glasgow. Prior to NGS the quality of PCR products and a small number of DNA samples extracted from fixed and frozen follicle walls and GCT was checked using the Agilent Bioanalyzer; again there was evidence of primer dimers in the PCR products. However, this did not interfere with NGS, and the short primer sequences were easily removed during the subsequent bioinformatic processing (described in chapter 2)

6.2.1.1 Tissue samples

DNA was extracted from ten control samples (seven solid ovarian stroma and three antral FW areas dissected from healthy ovaries of five mares) and 10 GCT samples (one cystic and/or one solid area dissected from GCT of seven mares) as presented in Table 6-1.

6.2.1.2 Molecular techniques

DNA was extracted using the Qiagen DNeasy® Blood & tissue kit, Cat. Number 69504 (Qiagen., 2006) according to manufacturer's instructions, using either the AE buffer (Qiagen DNeasy kit, 10 mM Tris-HCL, 0.5 mM EDTA, pH 9.0) used for eluting the DNA, or a lower pH buffer (10 mM Tris-HCL, 1 mM EDTA buffer at pH8) used for gel DNA extraction and also in final elution from the filter (see Table 6-1).

A PCR amplification of a 119bp sequence spanning the human SNP (C→G point mutation, nucleotide position 183 in the published equine sequence EF202823.1) was carried out on the 20 samples using the primer set 3 designed by Primer-BLAST (NCBI) as presented in Figure 6-2 (5' to 3' Forward primer:

CAACCTCAGCCTCAACGAGT $T_M=59.4$ °C, 5' to 3' Reverse primer
GGTAGTTGCCCTTCTCGAACA $T_M=59.8$ °C, see also Table 2-3 in Chapter 2.
Primers were initially prepared to 100pmol/μl with (molecular grade) water. For the PCR, a Primer Mix of both Forward and Reverse primers was prepared to 20pmol/μl of each primer, to give an 800nM concentration. The PCR reactions were prepared using Applied Biosystems AmpliTaq Gold® reagents (Biosystems., 2010). Each 30μl reaction contained 3.0μl 10x Buffer II, 2.4μl MgCl₂, and sufficient molecular grade water to bring the final reaction volume to 30μl. This volume was centrifuged and treated with 9999 units of UV to eradicate any potential DNA contaminants. Subsequently, 0.6μl Invitrogen (10mM) dNTP mix was added, along with 0.3μl AmpliTaq Gold® DNA Polymerase and 1.2μl of the primer mix (0.6μl Forward, 0.6μl: 20pmol mix). The final mix was then transferred into 500μl PCR tubes, and 40x PCR cycles were run as outlined in Chapter 2, cycling between 95°C (30 seconds), 55°C (30 seconds) and 72°C (2 minutes). Subsequently, PCR product (DNA) concentration was checked using the NanoDrop 1000 spectrophotometer before submission to Glasgow Polyomics.

A 2% agarose gel electrophoresis was also run with 5μl of PCR product at 125 Volts, until the dye reach approximately three quarter across the gel to confirm the correct product size following PCR. Then the remaining 25μl of PCR product underwent purification with 20μl of elution buffer PE to elute the samples using Qiagen QIAquick® PCR Purification Kit as described in Chapter 2.

For NGS, libraries were prepared using the NEBNext Ultra II DNA Library Prep kit for Illumina (New England BioLabs), single index with no size selection, and then libraries were sequenced on the Illumina HiSeq 4000 sequencer with a maximum read length of 2x75bp, and coverage of approximately 50,000 reads per sample (Glasgow Polyomics, University of Glasgow). Sequencing data were visualised using Integrative Genomics Viewer (IGV, version 2.4.14) and a summary table was prepared by the bioinformatician Dr. Hamilton from Glasgow Polyomics using the FreeBayes (<https://github.com/ekg/freebayes/blob/master/README.md>; (Garrison and Marth, 2012) program to call the variants. Prior to alignment, the reads were trimmed to remove any sequencing adapters and any low quality bases, where the average quality PHRED score

(https://www.illumina.com/documents/products/technotes/technote_Q-Scores.pdf) over four bases was lower than 20. In addition, reads that were trimmed to less than 54 bases were discarded. Nucleotide variants occurring at a frequency from 10% in the reads from one sample were considered relevant, with the REFerence and ALTerNative nucleotide listed in the summary table.

```

1 aggctcacgc tgtccggcat ctaccagtac atcatcgcca agttcccgtt ctacgagaag
61 aacaagaagg gctggcagaa tagcatccgc cacaacctca gcctcaacga gtgcttcac
121 aaggtgccgc gggagggcgg cggcgagcgc aagggcaact actggacgct ggacccggcc
181 tgcgaggaca tgttcgagaa gggcaactac cggcgccgcc gccgcatgaa gcggccctc
241 cggccgccgc cagcgcaact ccagcccggc aaggggctct tcggggcggg aggcgccgcg
301 ggcggctgcg gtgtggcggg cgcgggggcc gacggctacg gctacctggc gcccccaag
361 tacctgcagt cgggcttct caacaactcg t

```

Figure 6-2: The nucleotide sequence of Equine FOXL2 (EF202823.1), with the position of forward and reverse primers shown and the expected site of the mutation highlighted in yellow and primer in blue.

Table 6-1: PCR products for GCTs and for controls

PCR Product	Mare ID	Sample Name	Tissues	Buffer	Concentration (ng/ μ L)
GCT	1	GCT1	Fixed solid	AE buffer	53.50
	2	GCT 2A	Fixed solid	AE buffer	34.62
		GCT 2B	Frozen cystic	AE buffer	32.77
		GCT 2C	Frozen solid	AE buffer	35.02
	3	GCT 3	Fixed solid	AE buffer	45.45
	4	GCT4	Fixed solid	AE buffer	14.82
	5	GCT5	Fixed solid	AE buffer	108.82
	6	GCT6	Fixed solid	AE buffer	35.69
	7	GCT 10A	Fresh solid	AE buffer	87.74
		GCT 10B	Fresh cystic	AE buffer	84.40
NON GCT	1	NON GCT 1	Fixed stroma	Tris-HCl PH 8	15.36
	2	NON GCT5	Fixed stroma	Tris-HCl PH 8	6.25
	3	NON GCT 7B	Fresh L. Follicle wall	AE buffer	49.08
	4	NON GCT 8A	Fixed stroma L. Ovary	Tris-HCl PH 8	15.76
		NON GCT 8B	Fixed L. Follicle wall	Tris-HCl PH 8	13.91
		NON GCT 8C	Fixed stroma R. Ovary	Tris-HCl PH 8	12.39
		NON GCT 8D	Fixed R. Follicle wall	Tris-HCl PH 8	10.99
	5	NON GCT 9A	Fixed stroma	AE buffer	134.06
		NON GCT 9B	Fixed follicle wall	AE buffer	42.92
		NON GCT 9C	Fixed stroma	Tris-HCl PH 8	17.64

6.2.2 Immunohistochemistry (IHC) procedures

6.2.2.1 Tissue samples

Existing wax blocks were used from 40 antral follicle walls (40x Control FW samples) (average size of follicles was 21.4mm) dissected from the ovaries of 16 mares (age range from 1.5 to 20 years old), which had previously been categorised using H&E sections as Very Healthy (VH, n=10), Healthy (H, n=10), Early Atretic (EA, n=10) and Late Atretic (LA, n=10) (Chapter 4). Existing wax blocks were also used from the cystic and solid tissue sample dissected from the GCT of five mares (10x GCT samples) where cystic and solid areas were also previously categorised using H&E sections as GCT1-4 as described in Chapter 5.

6.2.2.2 IHC technique

The IHC was performed as described in detail in Chapter 2. Following embedding of the tissue samples in a wax block (Thermo Histostar embedding centre), sectioning at a thickness of 2.5 μm (Thermo Finesse NE+ Microtome) and rehydrating, sections underwent Heat-Induced Epitope Retrieval (HIER) followed by incubation at room temperature using the Dako Autostainer (Agilent, Dako, USA) with the anti-FOXL2 goat polyclonal antibody (Abcam, Cat. No. ab5096) diluted at 1:600. Subsequently, the ImmPRESS HRP anti-goat IgG (peroxidase) secondary antibody raised in horses was used according to the suppliers' instructions (Vector Laboratories, Cat. No. MP-7405).

6.2.2.3 IHC Measurements

Images for immunohistochemistry were captured using a Leica DM4000B microscope (Leica Microsystems, Switzerland) and Leica Application Suite software (version 4.3.0; Leica Microsystems, Switzerland) as described previously in Chapter 5. The magnification of the microscope binocular was 10X and the 20x objective was used, therefore, each section was evaluated at 200X magnification. Stain intensity, distribution and percentage area were estimated over the whole view. The measurements were based on a previous study in ovarian human samples (Hes et al., 2011). They classified the nuclear immunoreactivity intensity as negative (coded as 0 for analysis), weak (coded as 1), moderate (coded as 2) or strong (coded as 3) intensity. Their evaluation of the distribution was scored as focal (<50% of positive neoplastic cells) or diffuse (>50% of positive neoplastic cells), while our distribution categories included continuous (coded as 1) vs. individual (coded as 2) vs. cluster like (coded as 3) distribution as presented in Figure 6-13 and also in chapter 5 (Figure 5-6, 5-12, 5-18 and 5-26).

6.2.3 Statistical analysis

The Null Hypotheses tested using statistical analyses were:

- I) For **NGS** results: no difference exists between FW and GCT samples in the percentage of alternate = T reads (mutated from the reference = C read) at position 117 of the reference sequence NCBI EF202823.1.

II) For IHC results: no differences exist in FOXL2 stain intensity classified as 0 (=no stain) or 1 (=weak) to 3 (=strong); stain distribution classified as 1 (=continuous), 2 (=individual) or 3 (clusters); and percentage area stained (percentage area) estimated subjectively by the same operator, between:

- d) Follicle health categories of control FW,
- e) GCT categories of GCT samples, and
- f) FW combined (VH, H, EA, LA for theca only) and GCT combined (GCT1, GCT2, GCT3, GCT4).

III) For IHC results: in control FW no correlation exists between follicle diameter or follicular fluid (FF) oestradiol (E2) and %area FOXL2 immunoreactivity estimated by the same operator.

Data were analysed using the descriptive statistic function and the normality tests in Minitab 18. Because data were not all normally distributed, statistical comparisons were carried out using Kruskal-Wallis and Mann-Whitney tests, to detect the effect of GCT on alternate read percentage (mare being the statistical unit so multiple samples from the same mare were averaged), and associations between a) follicle health category in control follicle walls (VH, H, EA, and LA for Theca), and b) GCT area category (category 1, 2, 3, 4) and FOXL2 histological measurements. Associations between stain intensity and distribution of FOXL2 expression and the follicular diameter and follicular fluid oestradiol of control FW were also tested using the Kruskal-Wallis and Mann-Whitney tests. The correlation between estimated percentage area of FOXL2 immunoreactivity and follicular diameter as well as follicular fluid oestradiol concentrations of control FW was determined using the Spearman Rho function (Minitab 18).

6.3 Results

6.3.1 Next generation sequencing of PCR products

The reads sequenced from the PCR samples were aligned to the equine *FOXL2* cDNA sequence available on NCBI (EF202823.1, (Bugno et al., 2008)) and visualized in Integrative Genomics Viewer (IGV, <http://software.broadinstitute.org/software/igv/home>) as in Figure 6-3.

a) Human mutation SNP C→G

The SNP (C402G) was not identified in GCT or control samples at a frequency of more than 5% reads

b) Different mutation C→T identified in variable proportion of reads.



Figure 6-3: This screenshot shows multiple reads sequenced from one control sample with the mutation from C → T shown in position 117 bp of the reference sequence EF202823.1. Please note that the alternate base is in red when it differs from the reference base.

Although the target number of reads for the sequences was 1000, the coverage initially ranged from 52,000-90,000. Following processing of sequencing data the number of reads analysed ranged from 24,855-64,897 total reads. An interesting point mutation C→T was identified in 18 out of 20 samples, at bp117 of the reference sequence (Figure 6-4). In sample number 10 the mutation was called in 9.4% of reads, but the bioinformatician considered this low frequency <10% as not conclusive (Table 6-3). On average %Ref reads in GCT and control samples were 67.31% and 76.53%; respectively, and %Alt reads in GCT and control samples were 32.68% and 23.46%, respectively. Bearing in mind, the average calculation was done on 17 samples excluding the 0/0 GT and also sample number 10 (Table 6-3) because the %Alt was less than 10% (which the bioinformatician considered as the GT 0/0). The wild type and mutated read

sequences were aligned to the *FOXL2* gene sequences to show the mutation as presented in Figure 6-5 using

(<https://blast.ncbi.nlm.nih.gov/Blast.cgi>).

Also shown (Figure 6-4) are examples of random sequencing errors indicated by the individual red lines distal to the frequent mutation identified, which occur when a large number of reads are sequenced. However, because they occur only in a small number of reads it is not identified as a variant genotype. This likely happened in the two GCT samples number 3 and 4 (Table 6-2).

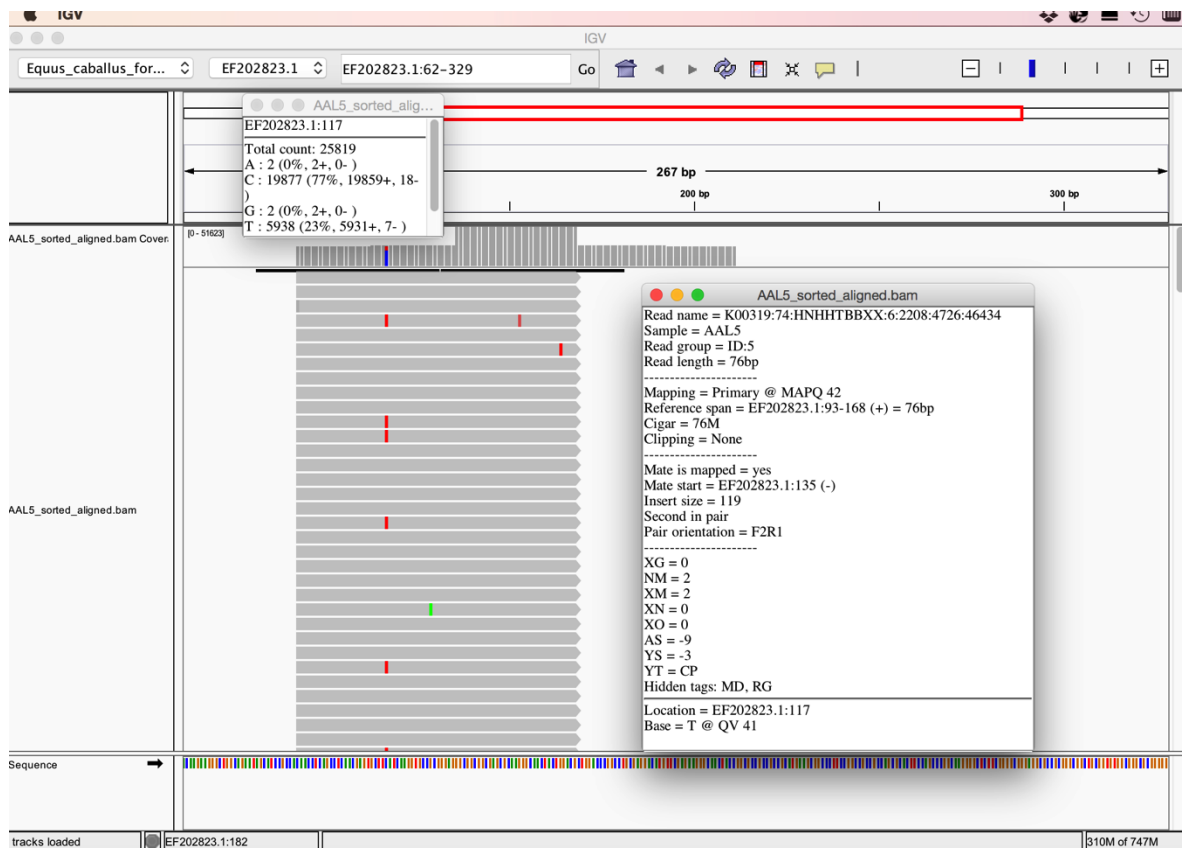


Figure 6-4: The number and percentages of mutation localisation

Original Sequence

Equus_caballus_forkhead_box_L2_gene.fa (FOXL2) EF202823.1

```

1  aggctcagc tgtccggcat ctaccagtac atcatcgcca agttcccgtt ctacgagaag
61  aacaagaagg gctggcagaa tagcatccgc cacaacctca gcctcaacga gtgcttatc
121 aaggtgccgc gggagggcgg cggcgagcgc aagggcaact actggacgct ggaccggcc
181 tgcgaggaca tgttcgagaa gggcaactac cggcgccgcc gccgcatgaa gggcccttc
241 cggccgccgc cagcgcaact ccagcccggc aaggggtctt tcggggcggg aggcgccgcg
301 ggcggctgcg gtgtggcggg cgcgggggcc gacggctacg gctacctggc gcccccaag
361 tacctgcagt cgggcttctt caacaactcg t

```

'Mutated' Sequence

```

1  aggctcagc tgtccggcat ctaccagtac atcatcgcca agttcccgtt ctacgagaag
61  aacaagaagg gctggcagaa tagcatccgc cacaacctca gcctcaacga gtgctttatc
121 aaggtgccgc gggagggcgg cggcgagcgc aagggcaact actggacgct ggaccggcc
181 tgcgaggaca tgttcgagaa gggcaactac cggcgccgcc gccgcatgaa gggcccttc
241 cggccgccgc cagcgcaact ccagcccggc aaggggtctt tcggggcggg aggcgccgcg
301 ggcggctgcg gtgtggcggg cgcgggggcc gacggctacg gctacctggc gcccccaag
361 tacctgcagt cgggcttctt caacaactcg t

```

Original	AGGCTCACGCTGTCCGGCATCTACCAGTACATCATCGCCAAGTTC	60
Mutation	AGGCTCACGCTGTCCGGCATCTACCAGTACATCATCGCCAAGTTC	60
Original	AACAAGAAGGGCTGGCAGAATAGCATCCGCCACAACCTCAGCCTCAACGAGTGCTT ^C ATC	120
Mutation	AACAAGAAGGGCTGGCAGAATAGCATCCGCCACAACCTCAGCCTCAACGAGTGCTTT ^T ATC	120
Original	AAGGTGCCGCGGGAGGGCGGGCGGAGCGCAAGGGCAACTACTGGACGCTGGACCCGGCC	180
Mutation	AAGGTGCCGCGGGAGGGCGGGCGGAGCGCAAGGGCAACTACTGGACGCTGGACCCGGCC	180
Original	TG ^C GAGGACATGTTTCGAGAAGGGCAACTACCGCGCCGCCCGCCGCATGAAGCGGCCCTTC	240
Mutation	TG ^C GAGGACATGTTTCGAGAAGGGCAACTACCGCGCCGCCCGCCGCATGAAGCGGCCCTTC	240
Original	CGGCCCGCCAGCGCACTTCCAGCCCAGGGGGCTCTTCGGGGCGGGAGGCGCCGCG	300
Mutation	CGGCCCGCCAGCGCACTTCCAGCCCAGGGGGCTCTTCGGGGCGGGAGGCGCCGCG	300
Original	GGCGGCTGCGGTGTGGCGGGCGGGGGCCGACGGCTACGGCTACCTGGCGCCCCCAAG	360
Mutation	GGCGGCTGCGGTGTGGCGGGCGGGGGCCGACGGCTACGGCTACCTGGCGCCCCCAAG	360
Original	TACCTGCAGTCGGGCTTCCTCAACAACCTCGT	391
Mutation	TACCTGCAGTCGGGCTTCCTCAACAACCTCGT	391

Figure 6-5: Mutated sequences aligned with original *FOXL2* gene sequence. The yellow highlighted is the new identified SNP and the green highlighted would be the original human SNP

This C117T mutation (based on the reference sequence) was found in almost all samples except two, and it was the only single nucleotide polymorphism (SNP) identified (based on showing in 10% or more of the sequenced reads) for all of the PCR products. All samples showing the mutation were heterozygous. The detailed percentage results for the REference base and the ALternate base are

presented for the GCT samples in Table 6-2 and for the control samples in Table 6-3.

Table 6-2: GCT samples: GT is Genotype, DP is Depth, RO is Reference allele count, QR is Reference allele quality, AO is Alternate count, QA is Alternate quality and GL is Genotype likelihood (0/0 is Ref and 1/1 is Alt and both are Homozygous, 0/1 is Heterozygous). * Please note that Freebayes identified 'no mutation' in samples 3 and 4 because %Alt is less than 10%, thus we consider the genotype of the sample as 0/0.

NO.	GCT samples	EF202823.1							
	POSITION	117							
	Reference allele count (Ref)	C							
	Alternate allele count (Alt)	T							
	FORMAT	GT:DP:RO:QR:AO:QA:GL	GT	Depth	Ref count	Alt count	% Ref	% Alt	
1	GCT 6	0/1:32648:22416:911927:10229:414743:-36312.3,0,-81058.8	0/1	32,648	22,416	10,229	68.66%	31.33%	
2	GCT 3	0/1:28052:21004:855242:7047:284122:-23991.7,0,-75392.5	0/1	28,052	21,004	7,047	74.88%	25.12%	
3*	GCT 2B	0/0:45954:44292:1801022:1659:67183:0,-4687.52,-156046	0/0	45,954	44,292	1,659	96.38%	3.61%	
4*	GCT 2C	0/0:37286:34937:1421096:2346:95129:-1140.41,0,-120477	0/0	37,286	34,937	2,346	93.70%	6.29%	
5	GCT 2A	0/1:25817:19536:793847:6277:254514:-21352.2,0,-69892.1	0/1	25,817	19,536	6,277	75.67%	24.31%	
6	GCT 10A	0/1:29372:15217:618145:14154:574050:-51653.8,0,-55622.4	0/1	29,372	15,217	14,154	51.81%	48.19%	
7	GCT 10B	0/1:32974:16876:686541:16097:652908:-58755.4,0,-61782.3	0/1	32,974	16,876	16,097	51.18%	48.82%	
8	GCT 1	0/1:31678:22730:924471:8945:362293:-31256.8,0,-81852.9	0/1	31,678	22,730	8,945	71.75%	28.24%	
9	GCT 4	0/1:35591:23824:968738:11767:477050:-42027.8,0,-86279.7	0/1	35,591	23,824	11,767	66.94%	33.06%	
10	GCT 5	0/1:24924:19342:785530:5581:226339:-18622.6,0,-68949.8	0/1	24,924	19,342	5,581	77.60%	22.39%	
	Average of %Ref and %Alt without samples 3 and 4						72.86%	27.14%	

Table 6-3: Control samples. * Please note that Freebayes identified the mutation in sample 10 but as %Alt is less than 10% we consider the genotype of the sample as 0/0.

NO.	CONTROL samples	EF202823.1							
	POSITION	117							
	Reference allele count (Ref)	C							
	Alternate allele count (Alt)	T							
	FORMAT	GT:DP:RO:QR:AO:QA:GL	GT	Depth	Ref count	Alt count	% Ref	% Alt	
1	NON GCT 1	0/1:24855:19117:777978:5736:231604:-19191.7,0,-68365.4	0/1	24,855	19,117	5,736	76.91%	23.08%	
2	NON GCT 9A	0/1:34451:27270:1108023:7180:291167:-23490.3,0,-97007.4	0/1	34,451	27,270	7,180	79.16%	20.84%	
3	NON GCT 9B	0/1:24233:18072:735967:6161:248844:-21066,0,-64907	0/1	24,233	18,072	6,161	74.58%	25.42%	
4	NON GCT 9C	0/1:29034:21846:889043:7185:290043:-24417.4,0,-78327.4	0/1	29,034	21,846	7,185	75.24%	24.75%	
5	NON GCT 5	0/1:31712:24248:987350:7460:301173:-25071.1,0,-86827	0/1	31,712	24,248	7,460	76.46%	23.52%	
6	NON GCT 7B	0/1:36636:23069:938356:13566:550071:-48962.6,0,-83908.2	0/1	36,636	23,069	13,566	62.97%	37.03%	
7	NON GCT 8A	0/1:26566:21309:868048:5253:211952:-16814.1,0,-75862.7	0/1	26,566	21,309	5,253	80.21%	19.77%	
8	NON GCT 8B	0/1:35036:25288:1029935:9723:393263:-33834.9,0,-91135.3	0/1	35,036	25,288	9,723	72.18%	27.75%	
9	NON GCT 8C	0/1:28162:21682:883582:6480:262164:-21712.4,0,-77640	0/1	28,162	21,682	6,480	76.99%	23.01%	
10*	NON GCT 8D	0/1:64897:58783:2386158:6109:247386:-11521.4,0,-204011	0/0	64,897	58,783	6,109	90.58%	9.41%	
	Average of %Ref and %Alt without sample 10						76.53%	23.46%	

6.3.1.1 PCR sequence analysis

There was no significant difference between GCT (n=7 mares) and control samples (n=5 mares; P= 0.4) in the average \pm SE Mean reference nucleotide percentage (Ref%), (specifically, 72.8 \pm 4.3% for GCT (eight samples in total from seven mares, after excluding the two samples no.3&4), and 74.5 \pm 3.0% for controls (nine samples in total from five mares, after excluding sample no.10)). Conversely, the average \pm SE Mean Alternative nucleotide percentage (Alt%) was 27.2 \pm 4.3% for GCT and 25.5 \pm 3.0% for controls (P= 0.4).

The mutation was identified in almost all GCT and control samples, with GCT samples ranging from 5 to 48.5 Alt%, and control samples ranging from 20 to 37 Alt%. While the range appeared to be greater in GCT compared with control samples, a two-variance test showed no difference (P> 0.3). In addition, this mutation does not lead to a change in amino acid (phenylalanine is encoded by both TTC and TTT) within the protein as presented in Figure 6-6 using (<https://www.ebi.ac.uk/Tools/msa/>). Moreover, there is no difference between the equine FOXL2 protein compared with the human reference protein spanning and including the site of the mutation (Figure 6-7).

Original Sequence

```

aggctcacgctgtccggcatctaccagtacatcatcgccaagttcccgttctacgagaag
R L T L S G I Y Q Y I I A K F P F Y E K
aacaagaagggctggcagaa tagcatccgccacaacctcagcctcaacgagtgcttcatc
N K K G W Q N S I R H N L S L N E C F I
aaggtgccgcgggagggcgccggcgagcgcaagggcaactactggacgctggaccggcc
K V P R E G G G E R K G N Y W T L D P A
tgcgaggacatgttcgagaagggcaactaccggcgccgcccgcgcatgaagcggcccttc
C E D M F E K G N Y R R R R R M K R P F
cggccgcccagcgcacttccagcccggcaaggggctcttcggggcgggaggcgccgcg
R P P P A H F Q P G K G L F G A G G A A
ggcggctgcggtgtggcgggcgcgggggccgacggctacggctacctggcggcccccaag
G G C G V A G A G A D G Y G Y L A P P K
tacctgcagtcgggcttctcaacaactcgt
Y L Q S G F L N N S

```

'Mutated' Sequence

```

aggctcacgctgtccggcatctaccagtacatcatcgccaagttcccgttctacgagaag
R L T L S G I Y Q Y I I A K F P F Y E K
aacaagaagggctggcagaa tagcatccgccacaacctcagcctcaacgagtgcttcatc
N K K G W Q N S I R H N L S L N E C F I
aaggtgccgcgggagggcgccggcgagcgcaagggcaactactggacgctggaccggcc
K V P R E G G G E R K G N Y W T L D P A
tgcgaggacatgttcgagaagggcaactaccggcgccgcccgcgcatgaagcggcccttc
C E D M F E K G N Y R R R R R M K R P F
cggccgcccagcgcacttccagcccggcaaggggctcttcggggcgggaggcgccgcg
R P P P A H F Q P G K G L F G A G G A A
ggcggctgcggtgtggcgggcgcgggggccgacggctacggctacctggcggcccccaag
G G C G V A G A G A D G Y G Y L A P P K
tacctgcagtcgggcttctcaacaactcgt
Y L Q S G F L N N S

```

Blast of Original/Reference with mutated version seen

```

Original  RLTLSGIYQYIIAKFFPFYEKNKKGWQNSIRHNLSLNECFIKVPREGGGERKGNWTLDDPA  60
Mutation  RLTLSGIYQYIIAKFFPFYEKNKKGWQNSIRHNLSLNECFIKVPREGGGERKGNWTLDDPA  60

Original  CEDMFEKGNYYYYRRRRMCRPFRPPPAHFQPGKGLFGAGGAAGGCGVAGAGADGYGLAPPK  120
Mutation  CEDMFEKGNYYYYRRRRMCRPFRPPPAHFQPGKGLFGAGGAAGGCGVAGAGADGYGLAPPK  120

Original  YLQSGFLNNS  130
Mutation  YLQSGFLNNS  130

```

Figure 6-6: Original *FOX L2* gene sequences and mutated sequences aligned with amino acids code showing no alternative changes within protein.

```

humanFOXL2  MMASYPEPEDAAGALLAPETGRTVKEPEGPPSPGKGGGGGGTAPEKPDPAQKPPYSYVALIAMAIRESA
equineFOXL2  -----

humanFOXL2  EKRLTLSGIYQYIIAKFFPYEKNKKGWQNSIRHNLSLNECFIKVPREGGGERKGNWTLDPACEDMFEKGN
equineFOXL2  --RLTLSGIYQYIIAKFFPYEKNKKGWQNSIRHNLSLNECFIKVPREGGGERKGNWTLDPACEDMFEKGN

humanFOXL2  YRRRRRMKRPFPPPAHFQPGKGLFGAGGAAGGCGVAGAGADGYGYLAPPKYLQSGFLNNSWPLPQPPSPM
equineFOXL2  YRRRRRMKRPFPPPAHFQPGKGLFGAGGAAGGCGVAGAGADGYGYLAPPKYLQSGFLNNS-----

humanFOXL2  PYASCQMAAAAAAAAAAAAAAGPGSPGAAAVVKGLAGPAASYGPYTRVQSMPHPHAHHLHAAAAPPAP
equineFOXL2  -----

humanFOXL2  PHHGAAAPPPGQLSPASPATAAPPAPAPTSAPGLQFACARQPELAMMHCSYWDHDSKGTALHSRLDL
equineFOXL2  -----

```

Figure 6-7: Human vs. Equine *FOXL2* gene with known sites of mutation highlighted.

6.3.2 Immunohistochemical findings

For each follicle wall (FW) health category there were ten follicles analysed from between five and eight mares (eight VH mares, seven H and EA mares, and five LA mares). For each GCT category there were 10 sections analysed obtained from five mares (one apparently solid and one apparently cystic tissue sample per mare).

The expression of *FOXL2* protein in GC and THC in FW categorised as very healthy (VH), healthy (H), early atretic (EA) and late atretic (EA) is shown below in Figure 6-8 and Figure 6-9. The expression of *FOXL2* protein in GCT cysts categorised as GCT1 (which resemble long stretches of healthy follicular walls), GCT2 (circular cystic like structures where antral, intermediate and basal GC are clearly discernible enclosing the fluid-filled cyst), GCT3 (circular cysts but with only very few antral GC lining the cyst), and GCT4 (solid variably sized nests of GC embedded in the stroma) is shown in Figure 6-10 and Figure 6-11.

Examples of different stain intensity, distribution and %area detected in FW and GCT sections can be seen in Figure 6-12 and Figure 6-13.

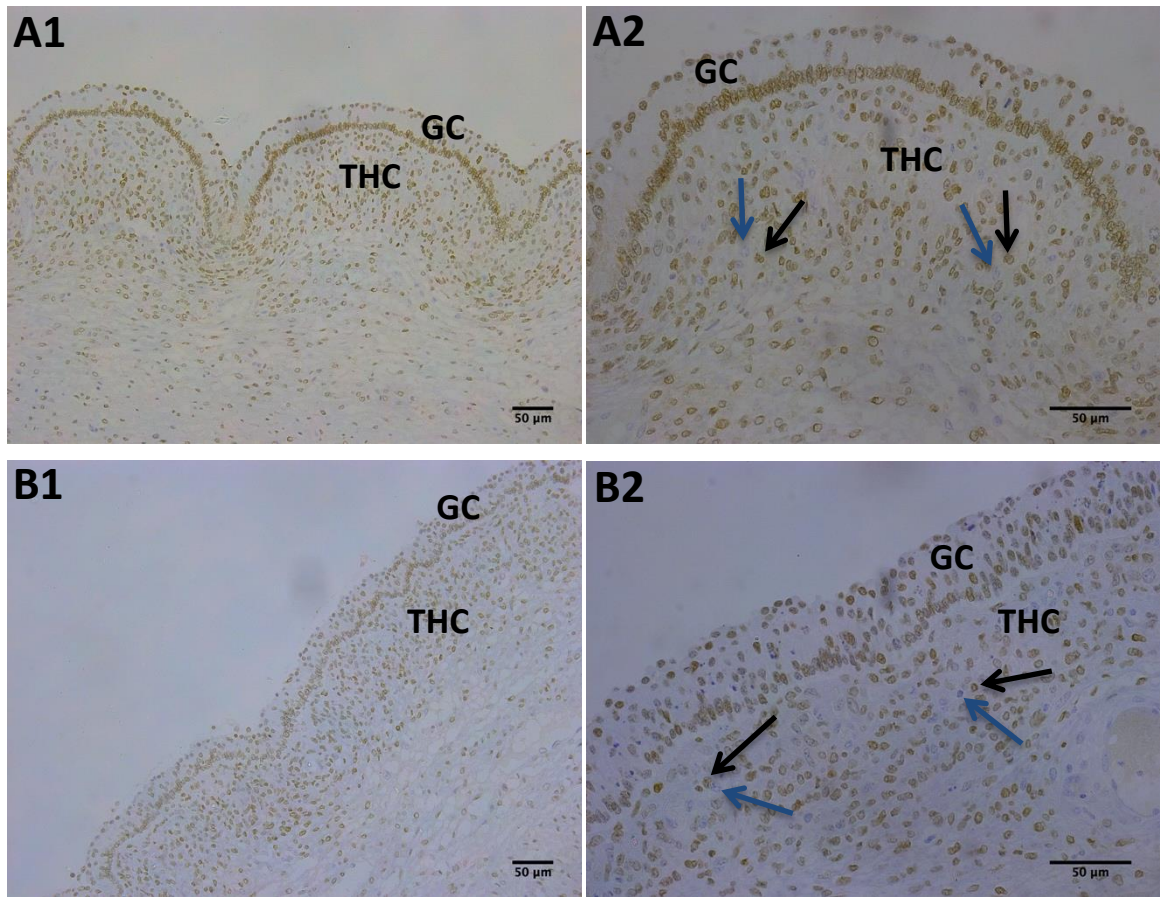


Figure 6-8:FOXL2 expression in GC and THC in VH and H FW categories; A1 shows VH with 200x and A2 with 400x magnification; B1 shows H with 200x and B2 with 400x magnification. Black arrow shows positive nuclear stain, Blue arrow shows negative nuclear stain.

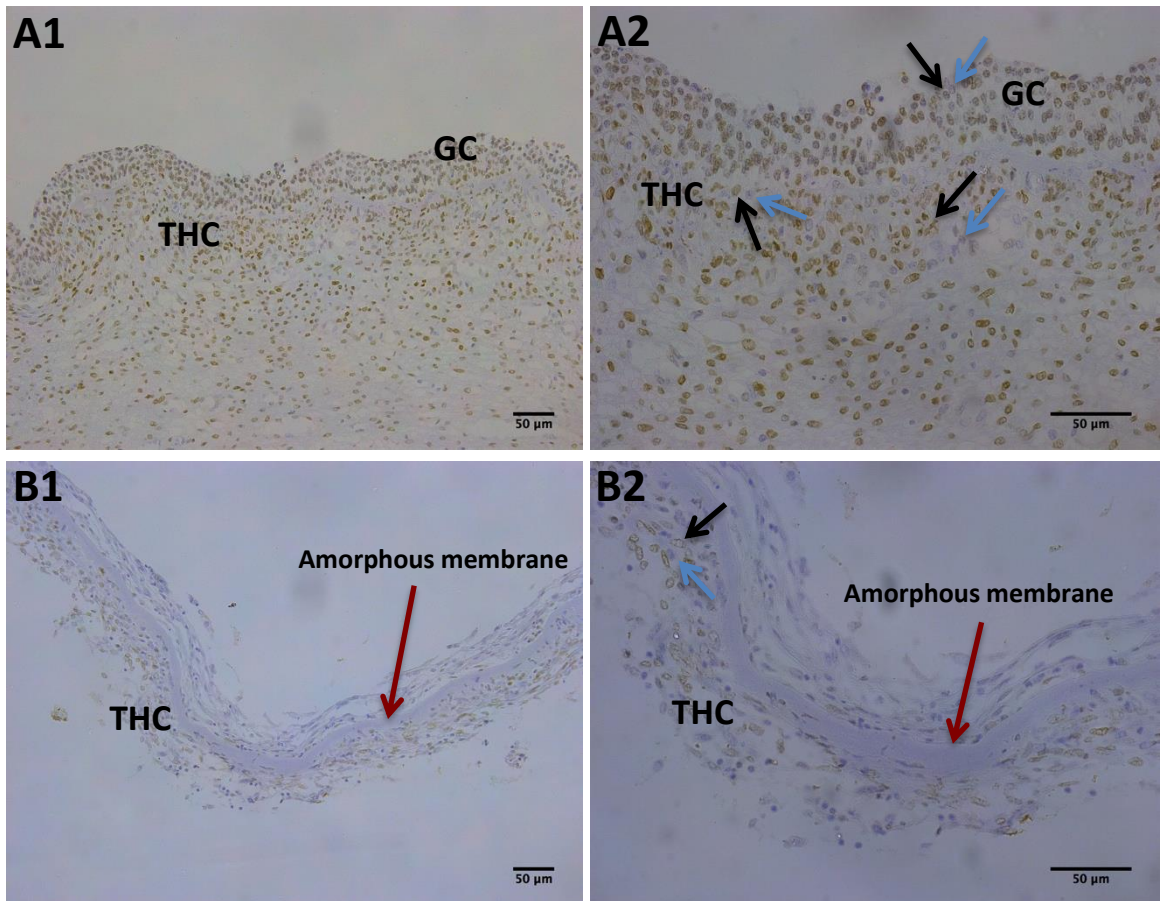


Figure 6-9: FOXL2 expression in GC and THC in EA and LA FW; A1 shows EA with 200X and A2 with 400x magnification. B1 shows LA with 200x and B2 with 400x magnification. Black arrow shows positive nuclear stain, Blue arrow shows negative nuclear stain.

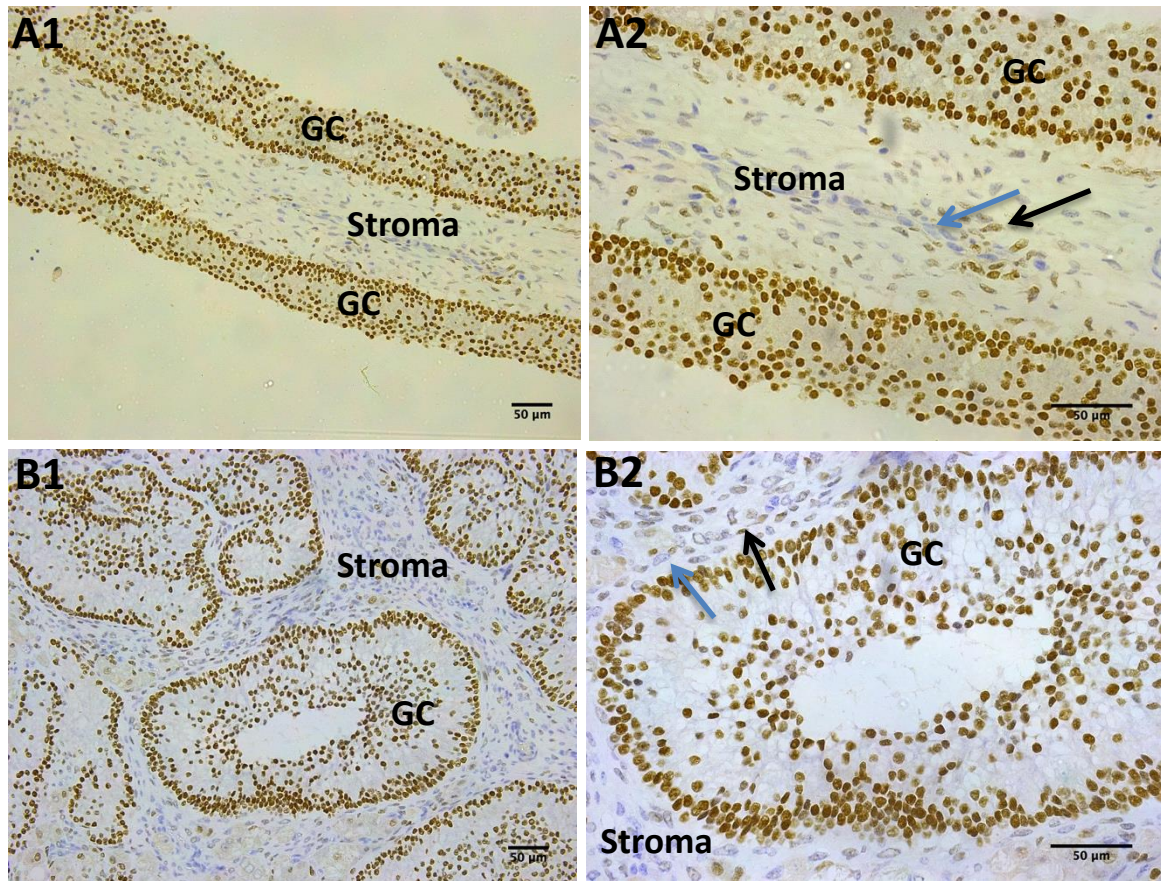


Figure 6-10: FOXL2 expression in GC and few interstitial cells (Stromal cells) of GCT1 and GCT2 categories; A1 shows GCT1 with 200x and A2 with 400x magnification, B1 shows GCT2 with 200x and B2 with 400x magnification. Black arrow shows positive mesenchymal nuclear stain, Blue arrow shows negative mesenchymal irregular nuclear stain.

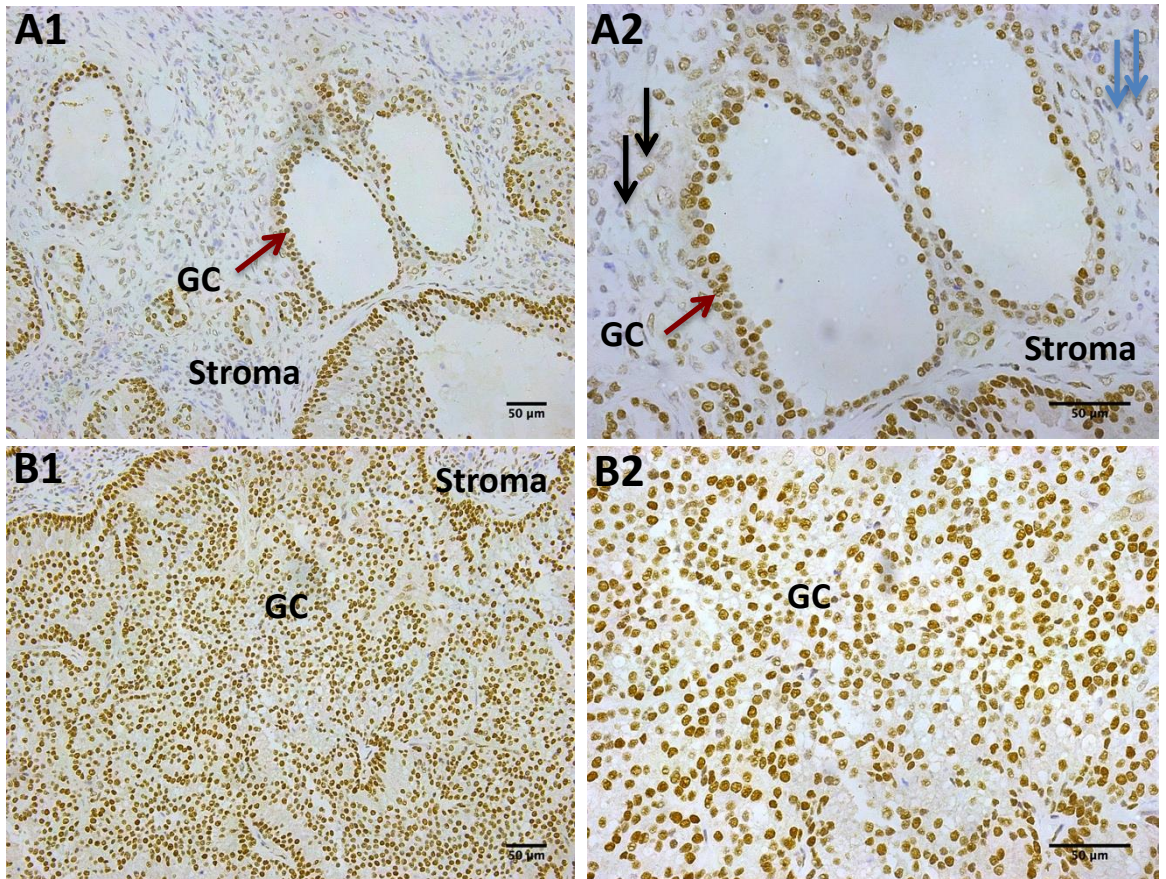


Figure 6-11: FOXL2 expression in GC and few interstitial cells (Stromal cells) of GCT3 and GCT4 categories; A1 shows GCT3 with 200x and A2 with 400x magnification, B1 shows GCT4 with 200x and B2 with 400x magnification. Black arrow shows positive mesenchymal nuclear stain, Blue arrow shows negative mesenchymal irregular nuclear stain.

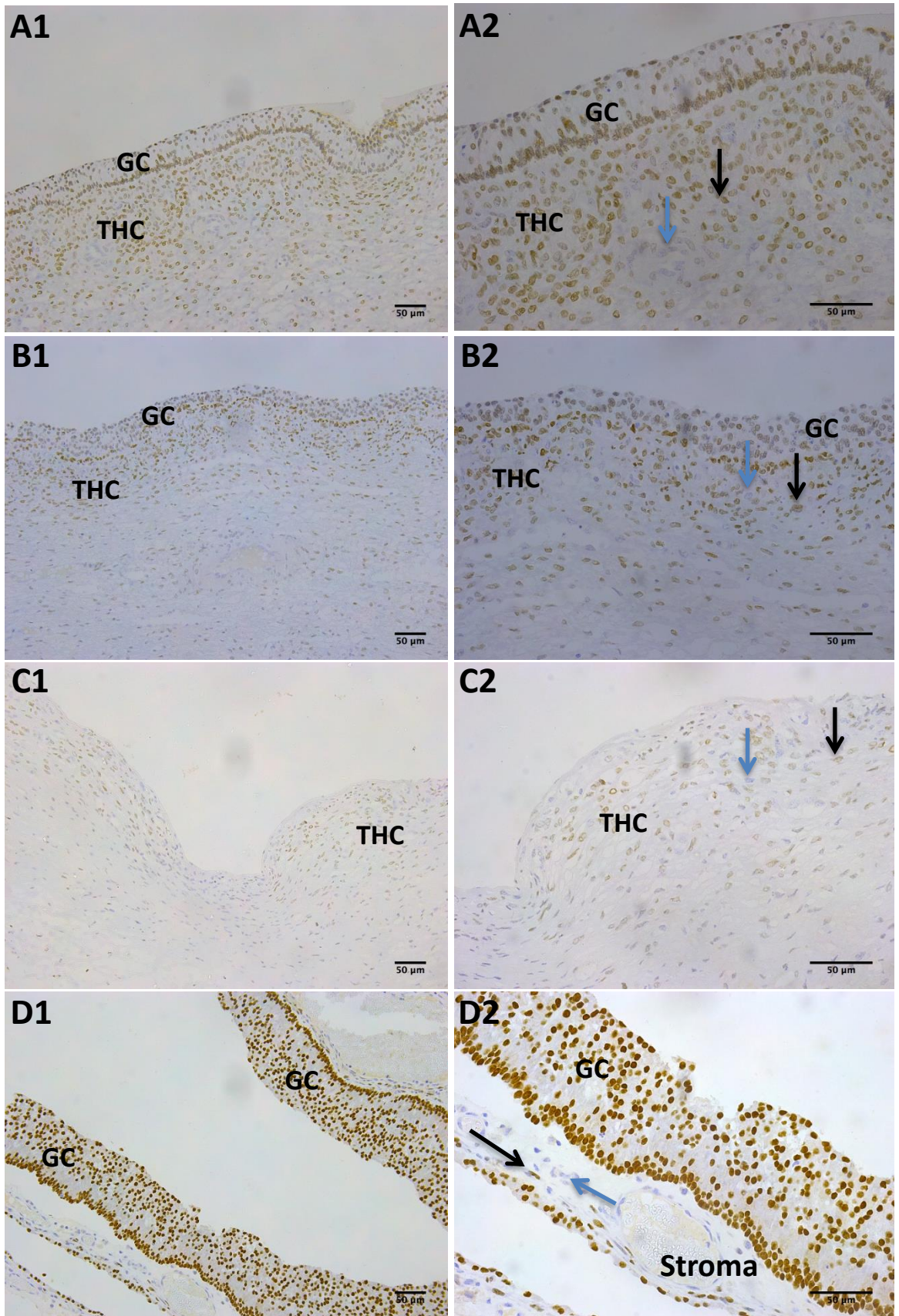


Figure 6-12: FOXL2 expression in GC and THC showing different stain intensity with 200x (ABCD1) and 400x magnification (ABCD2); A1 & A2 from VH FW with high expression, B1&B2 with medium expression from EA FW, C1 & C2 with Low expression from LA FW, D1&D2 from GCT1 with high expression. Black arrow shows positive mesenchymal irregular nuclear stain, Blue arrow shows negative mesenchymal irregular nuclear stain.

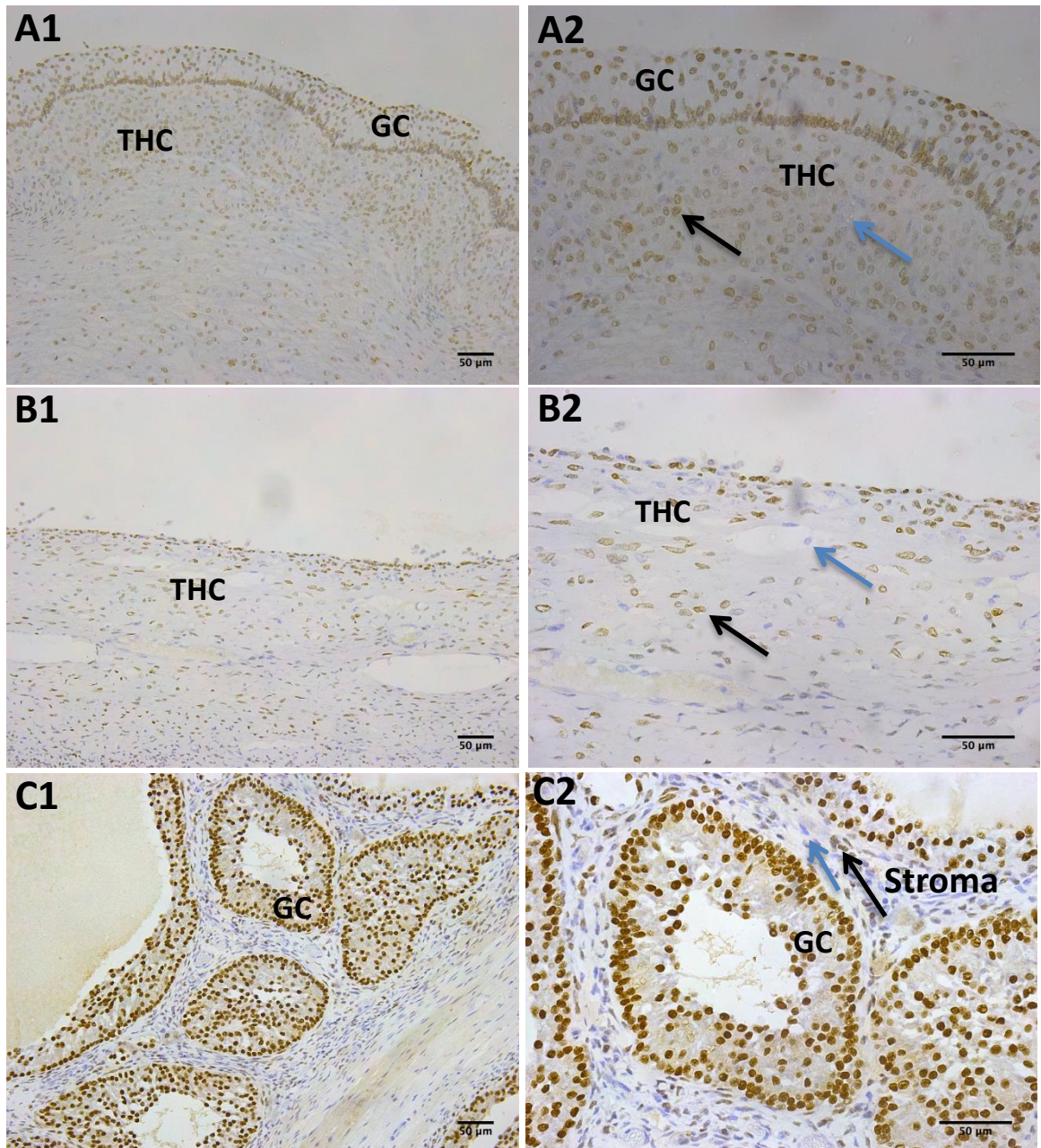


Figure 6-13: FOXL2 expression in GC and THC showing different stain distribution and %area with 200x (ABC1) and 400x magnification (ABC2); A1&A2 show continuous distribution and almost 90% GC and THC area covered from VH FW, B1&B2 show individual distribution and almost 50% area covered from LA FW; C1&C2 show continuous distribution and almost 100% area covered from a GCT2. There are no images for clustered distribution as FOXL2 always stained continuously or in a few occasions individually. Black arrow shows positive mesenchymal irregular nuclear stain, Blue arrow shows negative mesenchymal irregular nuclear stain.

6.3.2.1 The association between FW and GCT categories and FOXL2 GC and THC stain intensity, distribution and percentage area covered

As shown in Table 6-4 there was no effect of FW category on FOXL2 GC stain intensity and distribution estimates. However, a significant difference was detected between FW categories with respect to FOXL2 GC percentage area ($P < 0.05$), with EA follicles showing a reduction in percentage area. In FW THC layer

the stain intensity and percentage area decreased ($P < 0.01$) in EA and further in LA follicles, and the stain distribution changed from continuous to individual cells ($P < 0.05$). In GCTs there were no differences in stain intensity, distribution or percentage area between the different categories ($P > 0.7$).

Table 6-4: Association between FW and GCT categories and FOXL2 GC and THC stain intensity, distribution and percentage area covered

Outcome variable	FW categories Mean \pm SE Mean (median) No. = each group has 10 distributed follicles				P-value	GCT categories Mean \pm SE Mean (median) No. = each group has 10 tissue samples from 5 mares (1 mare=2 samples)				P-value
	VH	H	EA	LA		GCT1	GCT2	GCT3	GCT4	
FOXL2 GC stain intensity	2.8 \pm 0.1 (3)	2.8 \pm 0.1 (3)	2.2 \pm 0.3 (2.5)	-	0.285	3.0 \pm 0.0 (3)	3.0 \pm 0.0 (3)	3.0 \pm 0.0 (3)	3.0 \pm 0.0 (3)	1.000
FOXL2 GC stain distribution	1.0 \pm 0.0 (1)	1.0 \pm 0.0 (1)	1.3 \pm 0.2 (1)	-	0.419	1.0 \pm 0.0 (1)	1.0 \pm 0.0 (1)	1.0 \pm 0.0 (1)	1.0 \pm 0.0 (1)	1.000
FOXL2 GC %area	92.5 \pm 1.3 ^a	97.5 \pm 1.1 ^a	78.5 \pm 6.1 ^b	-	0.005	99.0 \pm 0.7	100.0 \pm 0.0	100.0 \pm 0.0	98.0 \pm 1.5	0.760
FOXL2 TH stain intensity	2.8 \pm 0.1 (3) ^a	2.8 \pm 0.1 (3) ^a	1.9 \pm 0.2 (2) ^b	1.5 \pm 0.2 (1.5) ^b	<0.001	1.0 \pm 0.0 (1)	1.0 \pm 0.0 (1)	1.0 \pm 0.0 (1)	1.0 \pm 0.0 (1)	1.000
FOXL2 TH stain distribution	1.0 \pm 0.0 (1) ^a	1.0 \pm 0.0 (1) ^a	1.0 \pm 0.0 (1) ^a	1.6 \pm 0.2 (2) ^b	0.048	2.0 \pm 0.0 (2)	2.0 \pm 0.0 (2)	2.0 \pm 0.0 (2)	2.0 \pm 0.0 (2)	1.000
FOXL2 TH %area	90.0 \pm 1.5 ^a	93.5 \pm 1.3 ^a	76.0 \pm 1.3 ^b	44.5 \pm 4.4 ^c	<0.001	12.5 \pm 3.7	10.5 \pm 1.4	11.5 \pm 0.8	11.0 \pm 1.8	0.754

6.3.2.2 FW and GCT categories comparison

In the comparison of health status (FW vs. GCT categories combined) and FOXL2 GC measurements, significant differences were found in FOXL2 granulosa stain intensity and percentage area covered ($P < 0.01$) with means lower in FW categories compared to GCT categories (2.6 ± 0.1 , 89.5 ± 2.5 ; respectively) and (3.0 ± 0.0 , 99.3 ± 0.4 ; respectively) as presented in Table 6-5. In addition, significant differences were seen in theca stain intensity, stain distribution and percentage area covered ($P < 0.01$) with means higher in theca stain intensity and percentage area in FW categories compared to GCT categories (2.3 ± 0.1 , 76.0 ± 3.3 ; respectively) and (1.0 ± 0.0 , 11.4 ± 1.1 ; respectively) but the THC stain was more individual in the GCT categories (1.2 ± 0.1 , 2.0 ± 0.0 ; respectively; $P < 0.01$). Exactly the same results were obtained when GCT3 was excluded from GCT categories in the GC comparisons (GCT3 cysts resemble atretic follicle walls, with severe loss of GC, thus almost resemble LA FW with no GC).

Table 6-5: Comparing the difference in combined health status of GC and THC in FW and GCT categories on FOXL2 stain measurements

Outcome variable	FW categories Mean \pm SE Mean No.=30 without LA	GCT categories Mean \pm SE Mean No.=40 all GCT	Overall P-value
	FW categories	GCT categories	
FOXL2 GC stain intensity	2.6\pm0.1	3.0\pm0.0	0.033
FOXL2 GC stain distribution	1.1 \pm 0.1	1.0 \pm 0.0	0.476
FOXL2 GC %area	89.5\pm2.5	99.3\pm0.4	0.000
	No.=40 all FW	No.=40 all GCT	
FOXL2 TH stain intensity	2.3\pm0.1	1.0\pm0.0	0.000
FOXL2 TH stain distribution	1.2\pm0.1	2.0\pm0.0	0.000
FOXL2 TH % area	76.0\pm3.3	11.4\pm1.1	0.000

6.3.2.3 The association between FOXL2 stain categories and control FW diameter (FWD)

To determine whether the different FOXL2 protein expression measurements were only found in specific follicle size classes, the effects of stain intensity or distribution categories on the control FWD were tested. Interestingly, a

tendency ($P \leq 0.1$) was found with three smaller (< 20 mm) follicles showing lower GC stain intensity category and more individual distribution (Table 6-6). When follicles in the low and medium category (19.5 ± 2.4 mm FWD) were combined and compared with follicles in the high GC stain intensity category (22.2 ± 1.3 mm FWD), no significant differences were revealed ($P = 0.1$).

Table 6-6: Effect of FOXL2 GC and THC stain intensity and distribution on FWD

FOXL2 expression	P-value	No=30	FWD (mm) Mean \pm SE Mean	FWD (mm) Median
Stain intensity GC	0.143			
0 (No stain)				
1 (Low)		3	15.4 \pm 2.5	17.5
2 (Medium)		6	21.5 \pm 3.1	20.5
3 (High)		21	22.2 \pm 1.3	21.9
Stain distribution GC	0.053			
1 (Continuous)		27	22.0 \pm 1.2	21.3
2 (Individual)		3	15.4 \pm 2.5	17.5
3 (Clusters)				
FOXL2 expression	P-value	No=40	FWD (mm) Mean \pm SE Mean	FWD (mm) Median
Stain intensity THC	0.770			
0 (No stain)				
1 (Low)		7	20.1 \pm 3.3	18.2
2 (Medium)		16	22.5 \pm 1.9	21.1
3 (High)		17	20.2 \pm 1.4	20.7
Stain distribution THC	0.705			
0 (No stain)				
1 (Continuous)		34	21.3 \pm 1.1	20.8
2 (Individual)		6	20.2 \pm 3.9	19.0
3 (Clusters)				

6.3.2.4 The association between FOXL2 stain categories and control Follicular fluid oestradiol (FFE2) concentration

The association between different FOXL2 protein expression (stain) measurements and control FFE2 concentration was tested and there were significant differences in FFE2 concentrations between the different FOXL2 GC stain intensity and distribution categories ($P < 0.05$) and the FOXL2 THC stain intensity and distribution categories (P -value 0.01, < 0.05 ; respectively) as presented in Table 6-7. Follicles showing increasing GC and THC FOXL2 stain intensity and continuous distribution had higher median FFE2 concentrations. A Mann Whitney test was followed between GCs stain intensity after combining low

and medium (19.5 ± 2.4) and compared them to high (22.2 ± 1.3) and revealed no significant difference but there was a significant difference when stain intensity low (3.9 ± 2.1) and high were compared ($P < 0.05$).

Table 6-7: Effect of FOXL2 GC and THC stain intensity and distribution on FFE2 concentration

FOXL2 expression	P-value	No=25	FFE2 (ng/ml) Mean \pm SE Mean	FFE2 (ng/ml) Median
Stain intensity GC	0.021			
0 (No stain)				
1 (Low)		3	4.0 \pm 2.1	2.5
2 (Medium)		6	223 \pm 109	62
3 (High)		16	164.8 \pm 47.7	119.5
Stain distribution GC	0.006			
1 (Continuous)		22	180.7 \pm 44.6	97.4
2 (Individual)		3	4.0 \pm 2.1	2.5
3 (Clusters)				
FOXL2 expression	P-value	No=34	FFE2 Mean \pm SE Mean	FFE2 Median
Stain intensity TH	0.003			
0 (No stain)				
1 (Low)		7	7.5 \pm 3.9	2.5
2 (Medium)		11	191.6 \pm 89.7	46.0
3 (High)		16	118.0 \pm 22.7	97.4
Stain distribution TH	0.006			
1 (Continuous)		28	142.8 \pm 37.5	74.7
2 (Individual)		6	8.3 \pm 4.5	3.7
3 (Clusters)				

6.3.2.5 Correlation of FOXL2 protein stain percentage area covered with control FWD and FFE2.

Following a normality test, indicating evidence of a lack of normality Spearman Rho tests were applied for the correlation analyses as presented in Table 6-8.

Table 6-8: Correlation of GC and THC percentage area covered and FWD and FFE2 concentration. FWD (NO.=30 follicles) and FFE2 concentration (NO.=25 follicles)

Outcome variables	FOXL2 percentage area covered GC		FOXL2 percentage area covered THC	
	Spearman Rho correlation coefficient	P-value	Spearman Rho correlation coefficient	P-value
FWD	0.371	0.043	0.028	0.862
FFE2	0.530	0.006	0.632	0.000

There were significant correlations between FFE2 concentrations and FOXL2 GC and THC percentages area stained ($P < 0.01$). The follicles appearing on the left hand side of the scattered plots for GC percentage area stained in Figure 6-14 are EA or small with low E2 in follicular fluid. All follicles showing 100% of GC expressing FOXL2 are healthy.

The follicles appearing on the left hand side of the scattered plots for THC percentage area stained in Figure 6-15 are LA with low E2 in follicular fluid. All follicles showing 85% or more of THC expressing FOXL2 are VH or H.

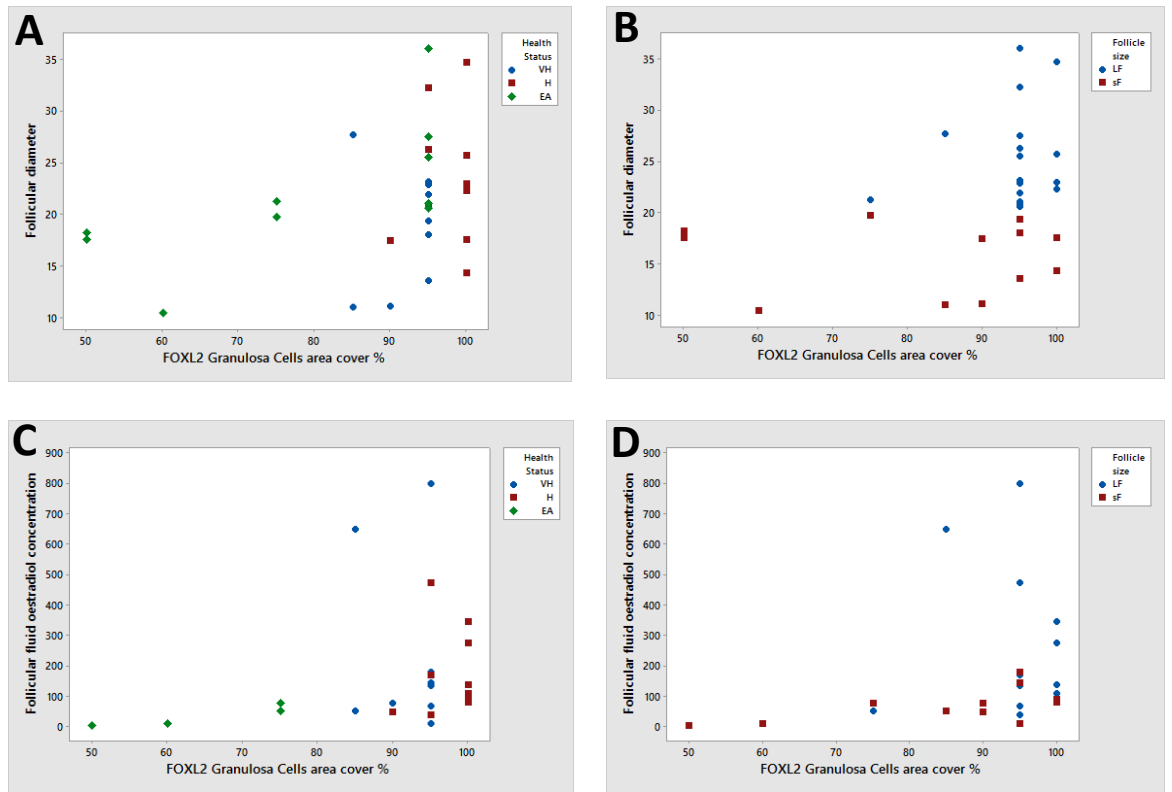


Figure 6-14: Correlation of FOXL2 GC percentage area covered with FWD (A&B) and FFE2 (C&D) concentration. A & C follicles are characterised by health status categories (VH blue, H red and EA green), B & D follicles are characterised by follicle size categories (Large follicle (LF) blue, small follicle (sF) red).

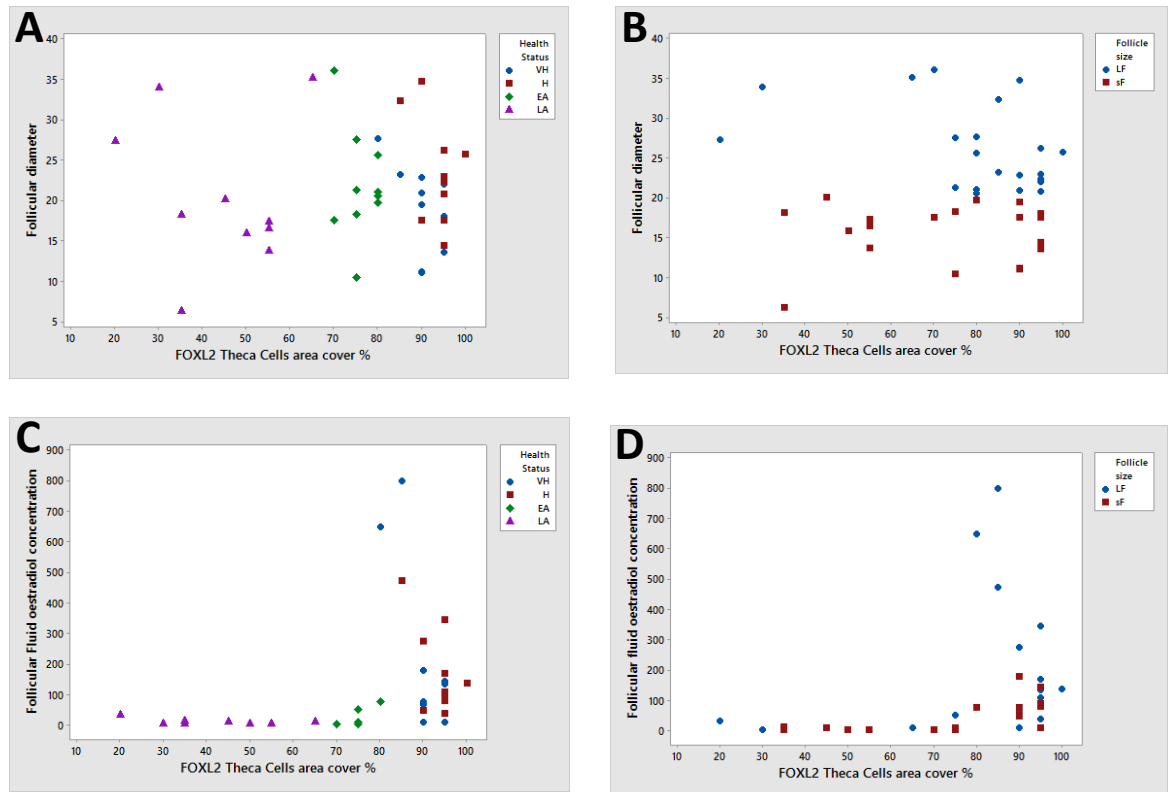


Figure 6-15: Correlation of FOXL2 THC percentage area covered in FWD (A&B) and FFE2 concentration (C&D). A & C follicle are characterised by health status categories (VH blue, H red and EA green, LA purple), B & D follicle are characterised by follicle size categories (Large follicle (LF) blue, small follicle (sF) red).

6.4 Discussion

To our knowledge there is only one equine *FOXL2* sequence currently available on NCBI and this came from whole blood DNA of an intersex horse with a male body conformation and stallion-like behaviour (Bugno et al., 2008). Our study firstly identified for the first time partial *FOXL2* gene sequence in DNA extracted from equine ovarian stroma and follicle walls, and (based on almost all of the protein being expressed in GC) most likely from the somatic tumour granulosa cells of GCT; secondly characterised *FOXL2* protein expression in equine antral follicles of different health status, and in different GCT cysts and solid tumour tissue; and thirdly identified a frequently occurring point mutation in the coding sequence of the *FOXL2* gene. However, in our study of seven different GCT cases, which were different in age profile of mares, the human SNP sequence (C402G) was not identified sufficiently frequently to call it a mutation. Therefore, it is unlikely in equine GCT, in contrast to human GCT, that the existence of this specific human *FOXL2* mutation, which alters the protein amino-acid sequence, plays a role in mare GCT development. However, it would

be worthwhile confirming this finding with a much larger number of GCT cases and fresh or directly frozen rather than formalin-fixed materials.

Another SNP (C->T) was found at a different location upstream (closer to the 5' end of the cds) and was detected frequently enough (23-27%) to be called a mutation. However, there was no difference between GCT and control FW allele percentage, and it would not have changed the amino acid sequence unlike the human 402 C-G mutation. Based on the fact that our study identified a new FOXL2 SNP in a very small amplified gene region and the potential importance of FOXL2 in GCT development, we conclude that the whole equine *FOXL2* gene needs to be sequenced and compared between GCT and control FW samples.

The FOXL2 protein was abundantly expressed in VH and H antral follicle GC and THC compartments, with a decline in protein expression (%area, intensity and also distribution) when atresia is initiated (EA follicles) or has progressed (LA follicles). In fact murine studies have shown FOXL2 expression in earlier stages of follicle development, where FOXL2 expression was detected in primordial, primary and larger secondary follicles, but also in cumulus cells of preovulatory follicles, therefore, it proposed to play a critical role in separate stages of follicle development (Pisarska et al., 2011). Our study has extended such information and shown a general relationship with health and atresia in equine follicles. Our study also characterised FOXL2 expression in growing antral cohort and dominant follicles, and, for the first time, also identified a positive relationship between FOXL2 protein expression in GC and THC and intrafollicular oestradiol, which is a known marker for differentiated follicle function. The wildtype FOXL2 protein has been shown to stimulate the aromatase promotor in vitro, while repressing CYP17 expression in steroidogenic cells, so here we present new functional data to support this same relationship for equine antral follicles, and their GC and THC compartments. Thus FOXL2 may be an important physiological regulator of differentiated and controlled follicle growth. Interestingly, follicle diameter per se was not related to FOXL2 expression.

The antibody used will bind to both wildtype and mutant protein, but in our study we only saw nuclear localization of FOXL2 in both follicle wall cells and GCT tumour cells, no cytoplasmic aggregates. This is similar to previously published human studies, where independent of whether the 402C-G SNP was

found in adult GCT of women, the mutation did not change the nuclear localisation of the FOXL2 protein (Shah et al., 2009) (Jamieson et al., 2010).

Very high expression of FOXL2 in tumour GC was seen (it must be assumed that it is the wildtype protein) independent of (cyst or solid) GCT category, which went beyond that of healthy antral follicles. In contrast the interstitial or stromal tissue in GCT only contained very few stained theca cells, compared to the theca layer of healthy FW. Interestingly, a severe reduction in GC numbers in GCT3 which resembles what happens in LA follicles, did not lead to a reduction in FOXL2 staining of GC, indicating dysregulated FOXL2 expression in tumours compared with control follicles.

Another fundamental difference to the differentiated FW from control mares is the complete absence of aromatase expression in GCT, confirmed by a lack of increased circulating oestradiol in affected mares. Yet the proliferating GC appear very healthy and show very high FOXL2 expression. Thus, FOXL2 appears to be a marker of health or proliferation in tumour GC independent of GCT category and size of the GC compartment, as the expression did not appear to be affected by the reduction of GC numbers in GCT3, for example. But FOXL2 expression in GCT is clearly disconnected from steroid (oestradiol) production in contrast to FW. At this stage it is not clear where the fundamental switch or transformation occurs, but the following questions need to be addressed: Does oestradiol in differentiating follicles of dominant follicle size regulate FOXL2 expression, and does FOXL2 then act to limit GC proliferation? Is FOXL2 (wildtype or mutant) expression directly regulating GC survival or proliferation as shown in GCT1-4 and itself disconnected from hormone control when GC transformation to tumour cells occurs?

Interestingly, while GC in GCT show very high FOXL2 expression compared to FW GC, the interstitial or stromal area in GCT was characterised by very low FOXL2 expression independent of GCT category. This may be due to the fact that there were very few theca like cells in GCT leading to such a reduced expression pattern in the surrounding interstitial or stromal tissue compared with a relatively higher THCA expression in control FW.

Finally, it may now be possible to use FOXL2 as an immunomarker for specific GCT diagnosis when equine ovarian tumour samples are submitted to pathology. In women, all cases of GCT patients positively expressed nuclear FOXL2 protein (Hes et al., 2011, Takahashi et al., 2013, Yanagida et al., 2017, Jamieson et al., 2010) and FOXL2 has been found a successful immunomarker for sex cord stromal tumours but not other ovarian tumours, due to its high sensitivity and specificity (80% and 90%, respectively) independent of the presence of the specific point mutation (Al-Agha et al., 2011, Geiersbach et al., 2011, McCluggage et al., 2013, Kommoss et al., 2013).

6.5 Conclusion

The specific human SNP (C402G) did not occur in equine GCT in our samples but we did identify another frequent mutation in the small region amplified in both FW and GCT. Further comparative studies of SNPs within the full equine *FOXL2* gene may thus reveal mutations with functional significance in GCT formation. The nuclear transcription factor FOXL2 is expressed in both granulosa and theca FW compartments even at the onset of histological atresia, but expression is highly upregulated in healthy follicles producing most estradiol. In GCT *FOXL2* is abundantly expressed in the granulosa compartment only independent of GCT category.

Chapter 7 General Discussion

The main objectives of the work presented in this thesis were to:

- Determine the prevalence of mare ovarian pathology and GCT in electronic veterinary records collected in the UK from seven practices and investigate whether any predictive factors might lead to those diseases
- Determine the histomorphological changes in ovarian follicle wall health categories by measuring the GC and THC counts, thickness and the intrafollicular FFE2 concentration.
- Determine the effect of FW health and GCT categories on the expression of different marker proteins using IHC, and comparing the GC nuclear circumference between FW and GCT categories.
- Determine whether *FOXL2* gene mutation exist in mares as it does in humans using molecular techniques, and investigate its protein localization in FW and GCT categories.

Ovarian tumours in the Western World are considered as the most fatal malignant disease in human gynaecology (Cheng et al., 2013). Approximately 5% of those cancers are GCT, which occur normally at the age of 50-60 years old. The percentage of GCT incidence in equine is considered to be the same, however, it is not a fatal disease and most mares recover after unilateral or bilateral ovariectomy. If it is unilateral they recover fertility and can still produce offspring (Watson, 1994, Troedsson et al., 2003).

The first study in chapter 3 looked at the data collected from seven practices around the UK to investigate through a text mining approach using WordStat/Simstat software the estimation of the prevalence of ovarian tumours particularly GCT, and ovarian pathology in general. Three dictionaries were created with different words and phrases to assist the searching in data mining (see Appendices). Those dictionaries allow recovering large text data on ovarian pathology and GCT, however, very few cases were relevant and considered as a true positive result. The reason of that was the software pulled out all words

entered by the clinicians, which may not relate to the main specific targeted word. Examples of that are: writing a suggested GCT diagnosis or it might be ovarian cyst or samples sent to lab for GCT examination and so on. Another reasons include the spelling mistakes or the software retrieved a disease from different parts of the body such as eosinophilic granuloma.

The sensitivity and specificity of measurement of the ovarian pathology and GCT that were retrieved from electronic veterinary medical records were high (100%, 99.7% and 100%, 99.6%, respectively). We could not identify a previous estimate of the true prevalence of either ovarian pathology or GCT derived from a large population of horses. Anecdotal reports, and clinical experience, would suggest that these conditions are indeed rare, and it is possible that the estimates derived here of 0.25% for ovarian pathology and up to 0.1% for GCT are realistic. They would represent 1 in 400 mares suffering some form of ovarian pathology and 1 in 1000 mares sustaining a GCT. However, it is also possible that due to the nature of the data recorded these estimates are underestimates of the true population prevalence.

The scoring analysis and univariable and multivariable logistic regression created in this chapter for ovarian pathology and GCT allows for predictive factors to be identified for development of both diseases. Those factors included some that were a common veterinary routine investigation such as previous respiratory and orthopaedic examinations, which could easily be detected in a randomly selected control population but appeared to be less likely in mares that are prone to ovarian pathology. An eye treatment category had an unexplained positive relationship with ovarian pathology but this may be an accidental finding due to the high possibility for most control and ovarian pathology mares to previously have had an eye treatment. In comparison, logistic regression analysis identified previous reproduction and sedation categories particularly reproductive investigation that was related to a subsequent GCT diagnosis. However, none of those factors listed were found highly associated with GCT and considered as good predictive factors.

It is likely that the variation in the age of mares when they are diagnosed with GCT were similar in our study and the previous literature, which confirmed that

most ages were susceptible to GCT (Watson, 1994, Charman and McKinnon, 2007).

Although data were retrieved successfully, we did not identify predictive factors that could indicate that GCT development was to be expected.

The second study, detailed in chapter 4, examined the histology of the normal follicular wall in terms of health status and aimed to confirm this by measuring the GC and THC cell counts and GC and THC thickness layer, plus examine the association between those measurements and different follicle and mare parameters. There was a significant association between FWD and disease categories with non-diseased follicles having a larger diameter than diseased ones. Additionally, larger follicles from the VH and H categories had higher E2 production compared to smaller sized follicles from the EA and LA categories. This is in agreement with a previous study by Sessions et al. (2009) which categorised the health status of follicles based on the intrafollicular concentration of E2, with the healthier follicles having high FF E2 concentrations.

While investigating the effect of breeding season on GC layer, it was found that the thickness of the basal GC increased gradually from the transitional period to the winter season, which may indicate changes in differentiation and follicle type as follicles fail to complete development. We also know that the E2 concentrations increase dramatically from small follicles to reach a peak in preovulatory follicles (Mlodawska et al., 2018), and indeed our study found highest intrafollicular concentration in a large follicle. We also detected an effect of age on the GC layer, specifically the percentage of basal GC and intermediate GC counts which were significantly higher in prepubertal than in young adult mares. This, however, may be more related to the fact that there were differences in the proportions of healthy and atretic follicles recovered from the different age groups of mares.

Significant differences were found between health categories in terms of THC thickness and counts. The number of small THC in LA was increased compared to VH, H and EA whereas the large THC counts decreased in number in LA compared to VH, H and EA. This finding appears to support a previous study by

Watson and Al-zi'abi (2002) where they stated that there was difference in THC interna layer thickness between preovulatory follicle which had a thick layer of polyhedral thecal cells and transitional anovulatory follicles which had a thin and undeveloped THC.

The number of large THC counts was increased during winter compared to summer and transition, whereas the small THC counts decreased in winter compared to summer and transition. The THC thickness was significantly different between winter and summer as follicles showed increased THC thickness when recovered in winter than in summer.

The percentages of small and large THC counts were also significantly associated with age, as prepubertal follicles had reduced small THC counts compared to adults but with increased large THC counts. The THC thickness also differed between prepubertal age and adults over 10 years in which the THC layer was thickest.

When examining the effect of disease on THC thickness a significant difference was seen between diseased and non-diseased groups, with a thicker layer in follicles from diseased mares. However, all these mare factors need to be examined in multivariate analyses for independent effects, as it appears that more healthy and estrogenic follicles were, for example, recovered from prepubertal animals late in the year.

The third study described in chapter 5 focused on immunohistochemistry of very relevant hormone, enzyme and receptor protein expression in control FW and GCT categories. The expression of inhibin immunostaining as a percentage of GC area in the VH and H groups and GCT1 and GCT2 was higher than in EA and GCT3, which is due to the low number of GC in EA and GCT3; and this also reduced the immunostaining area covered. This has also been reported in previous studies (Davis et al., 2005, Evkuran Dal et al., 2013). This GC stain reduction was also detected in aromatase expression in FW categories when they become atretic, and similar to previous studies where no aromatase expression was seen in advanced atresia, the GC layer and therefore inhibin and aromatase expression disappeared completely in our study when follicles become LA, (Watson and Thomson (1996). This is also an agreement with another former

study addressing the presence of aromatase expression in GC recovered from dominant follicles (Belin et al., 2000), and as in our images, it was confirmed that the only place of aromatase expression in the mare's ovary is the GC layer (Mlodawska et al., 2018). In our study aromatase was not expressed in THC similar to (Mlodawska and Slomczynska, 2010) but in contrast to a previous report (Almadhidi et al. (1995) where it was observed that aromatase was expressed in the theca interna. Aromatase was also not expressed in any GC of GCT categories in our study. In contrast, research showed that aromatase was expressed slightly in three mares with GCT disease (Watson and Thomson, 1996) but this could be due to the presence of high amount of testosterone possibly inducing the enzyme. None of the mares from which GCT samples were collected reported a sign of stallion like behaviour, itself an indication of high circulating concentrations of testosterone, and in this case the thecal cell androgen production would be involved (Rodger et al., 1998). In our study the expression of CYP17 was detected in clusters of THC within GCT, and only in the THC compartment of FW, and this finding is similar to what was stated by Albrecht and Daels (1997). We also found that aromatase stain intensity and percentage area covered reduced with atresia.

In comparison between combined FW and GCT categories, the FW categories of inhibin and AMHR2 have higher GC stain intensity and percentage area covered. The FW CYP17 and AMHR2 IHC images show higher THC percentage area covered than within the GCT categories, while the THC distribution of both CYP17 and AMHR2 is more in clusters in GCT than in FW categories.

Measuring the association between inhibin and aromatase expression, and FW diameter and E2 concentration in control FW revealed that follicles with large diameter and high amount of E2 production had higher GC stain intensity as well as a continuous distribution. In contrast, no associations were found between CYP17 and AMHR2 expression and FW diameter but there was an association with E2 concentration, which revealed that the THC stain intensity expression and continuous distribution increased with a high level of E2 production.

The follicles with large diameter and a high level of intrafollicular E2 concentration expressed more GC stain percentage area covered by inhibin and aromatase protein, and the follicles with large diameter are highly correlated

with THC CYP17 percentage area covered. This is in agreement with a previous study by Bashir et al. (2016) which found the intrafollicular steroid hormone concentrations were elevated with an expansion of follicular diameter. However, this correlation does not exist for AMHR2 GC and THC expression.

When investigating GC nuclear circumferences, a potential marker for DNA content and proliferation, in FW health categories, it was found that basal GC in EA are smaller than those in healthy follicles. None of the following different follicle and mare parameters; follicle size, breeding season, breed and disease status had an effect on GC nuclear circumferences. In addition, location played a role as the basal GC were found to be larger than intermediate and antral GC, and this applied to both FW and GCT categories. In comparison of combined GCT and FW samples, it was found that GC nuclei were larger in GCT, particularly in GCT4 and the basal location.

The final study in this thesis illustrated in chapter 6, investigated a partial sequence of the Equine *FOXL2* gene, which had only once before been extracted from whole blood DNA of an intersex horse with a male body confirmation and stallion like behavior (Bugno et al., 2008). To the best of our knowledge, this equine *FOXL2* gene sequence and the mutation found is the only one documented from ovarian samples, and there are no previous published reports of *FOXL2* protein expression in equine ovarian follicles and GCT tissues.

The *FOXL2* gene sequence was amplified from fixed, frozen and fresh ovarian stroma, control FW and GCT cysts and solid areas. However, the human SNP sequence (C402G) was not detected adequately repeatedly to call it a mutation. However, another SNP upstream (closer to the 5'end) of the human SNP was found (C>T, with T found in 23%-27%of reads) and frequently enough to be called a mutation. There was no difference between FW and GCT allele proportions, and with no predicted amino acid sequence change, this point mutation was considered to have the same significance as the human 402 C-G mutation.

The *FOXL2* expression was localized to the nuclei of GC and THC of FW and GCT. The findings of our study are in agreement with a previous human study that detected the nuclear localization of *FOXL2* staining (Jamieson et al., 2010). It was found that there was a variation of GC %area and THC stain intensity as well

as % area between follicle health categories, with a decrease seen with atresia. This was probably due to the low concentration of E2 produced in atretic follicles. On the other hand, and in contrast to the regulated expression of FOXL2 in antral follicles, there was no association between the different GCT categories and FOXL2 tumour expression. When combined GCT and FW data were compared, the GCT categories appeared to have an extra level of GC stain intensity and % area covered. Knowing that in our study GCT had no distinct large THC compartment, the FOXL2 stain intensity and %area covered in the interstitial/ stromal tissue definitely declined.

A strong correlation was found with follicular E2 production and FW health categories in which the healthier follicles with high intrafollicular E2 concentrations showed more FOXL2 stain intensity and %area. In contrast, GCT had also a very strong GC stain intensity and %area covered but without concomitant E2 production. This suggests that proliferation in GC in GCT is independent of E2 production. It is possible that this important difference in the regulation of FOXL2 expression leads to tumour transformation in GC.

Diagnosis of GCT regularly occurs in adult humans before the menopausal stage, however, it might occur earlier (Verdin and De Baere, 2012). Normal expression of *FOXL2* in the adult ovary is really significant to avoid somatic trans-differentiation of GC and Theca cells from their usual characteristic features to testis specific Sertoli and Leydig like cells, respectively. Despite patients hetero- or homozygous for the *FOXL2* mutation having a significant GCT incidence, a previous study by Rosario et al. (2013) reported that there was no significant correlation between tumour size and stage and the *FOXL2* mutation (Leung et al., 2016).

Detection of *FOXL2* mutation in mares might help us in early diagnosis and perhaps even future therapy of GCT. The *FOXL2* mutation C134W has been found in Japanese patients but not very commonly, thus the authors suggested that further experiments should be conducted on a large number of patients to illustrate the exact prevalence (Oseto et al., 2014). Therefore, further study with many fresh equine GCT cases is recommended as well as examining the complete *FOXL2* gene to identify any further significant mutations.

Overall Conclusion

Text mining could facilitate predicting future GCT by providing further predictive factors in a larger data set. The result of the text mining also revealed the possibility of performing prevalence estimation of different disease conditions despite the limitations that were found. Studying different functional proteins immunohistochemically in control follicle walls and GCT tissue can effectively detect variations that could potentially identify biomarkers for GCT. The result of the GC nuclear circumference comparison between FW and GCT revealed location differences, but also that GC nuclei in GCT were larger than the one in FW. This might be due to the GC having transformed to tumours showing enhanced proliferation. The FOXL2 SNP (C402G) mutation was not detected in our GCT samples but another upstream mutation was detected in both FW and GCT, therefore, this study is a basis for future analyses of the *FOXL2* gene in control ovaries and equine GCT.

Limitations

Few limitations were associated with this study: we only had seven ovaries diagnosed with GCT available for this study, with two obtained before the study started and five collected during three years. It would be helpful if they were collected all at one time, as well as having larger numbers of GCT samples. In addition, a single operator performed the cell counts and thickness measurements, as well as IHC analyses described in this thesis, and it may be advisable to validate a second operator for future analyses.

In text mining, the data were not recorded for research purposes for instance, therefore, some horse records confusingly had the same ID number and there was missing information, as the clinician did not always record the subsequent laboratory results.

During hormonal assay of oestradiol in follicular fluid the only Gamma counter available for reading the samples became dysfunctional, and the RIA assay used for more than 20 years became unavailable. This resulted in choosing an

alternative assay approach, i.e. the human ELISA kit. When designing the immunohistochemical analyses and choosing relevant marker proteins, some antibodies for protein expression were not available such as HSD3B1, which would have been very useful to investigate follicle function, and might have assisted us in finding the function of the large theca cells. Furthermore, the CYP17 antibody that was used in this study was in fact manufactured for immunoblot assay and had never been used in IHC.

In the final study, there was no previous research found reporting the function and regulation of the equine *FOXL2* gene in granulosa and theca cells of follicles, and in GCT, which could assist the investigation of the human C402G or any other SNP mutation.

Future Work

The results of this study suggest further work including:

Presence of amorphous eosinophilic band of deposit in LA follicles is indicative of atresia, and in some studies this layer is described as hyaline (Pedersen et al., 2003). However, as tests for collagen (eg. Masson's Trichrome stain) were not carried out in our experiment, it was not possible to determine definitively that this band is made of collagen. These assays could be done in future experiments so as to confirm the development and composition of this membrane.

As GCTs were discovered within the testis of human males showing the characteristic *FOXL2* gene mutation in at least one case (Lima et al., 2012) this would also be of interest for future study in the equine industry, as testicular primary neoplasms are rare with no reports of granulosa/sex cord tumours so far; in such a study abdominal cryptorchid testicular tumours would very much need to be considered. Further equine studies can also be done in the future to investigate the regulation of gene expression that *FOXL2* targets as a transcription factor, such as StAR and CYP19A (Rosario et al., 2012), as well as some further candidates among FSH-responsive genes (Benayoun et al., 2013), and also other intraovarian regulators of apoptosis (Cheng et al., 2013).

The expression of follistatin requires *FOXL2* gene activity controlling activin A, and this may have significance for granulosa cells. Therefore, overexpression of the wild-type *FOXL2* might operate as a cancer inhibitor by reducing activin A-stimulated cell proliferation (Cheng et al., 2014). This kind of experiment could be a future study in horses. It has been documented that plasma from human cases of GCT might support GCT diagnosis by examining the *FOXL2* mutation (McConechy et al., 2014). Thus, in future, DNA can be extracted from plasma of mares with and without GCT to detect any significant *FOXL2* mutations and assist in the diagnosis of GCT.

Appendices

Appendix 1 Method of using the software SimStat/WordStat

The data file should be downloaded and saved in the computer then Simstat should be clicked. If the data can not be opened in Simstat then it needs to be imported by clicking file, data and then import, however if the data already exist in Simstat just click open. After that, search for where the data has been stored and before opening the data make sure that in the box where the file type should be written is in provalis project ppj. Thus the file imported in the “supported file box” should be ppj, and then can be opened easily. Always in Simstat and Wordstat enough time should be given either for importing data or loading because it seems that it not loading or this also during searching. Click the statistic on the tool bar and choose X-Y as presented in Figure 7-1, then put ID in independent and Text in dependent after that click ok as presented in Figure 7-2. Again go to statistic and click on content analysis at the bottom of choices. This will shift the screen from Simstat to Wordstat where the dictionaries that have been prepared by the researcher appear, so the software can search for particular words as presented in Figure 7-3.

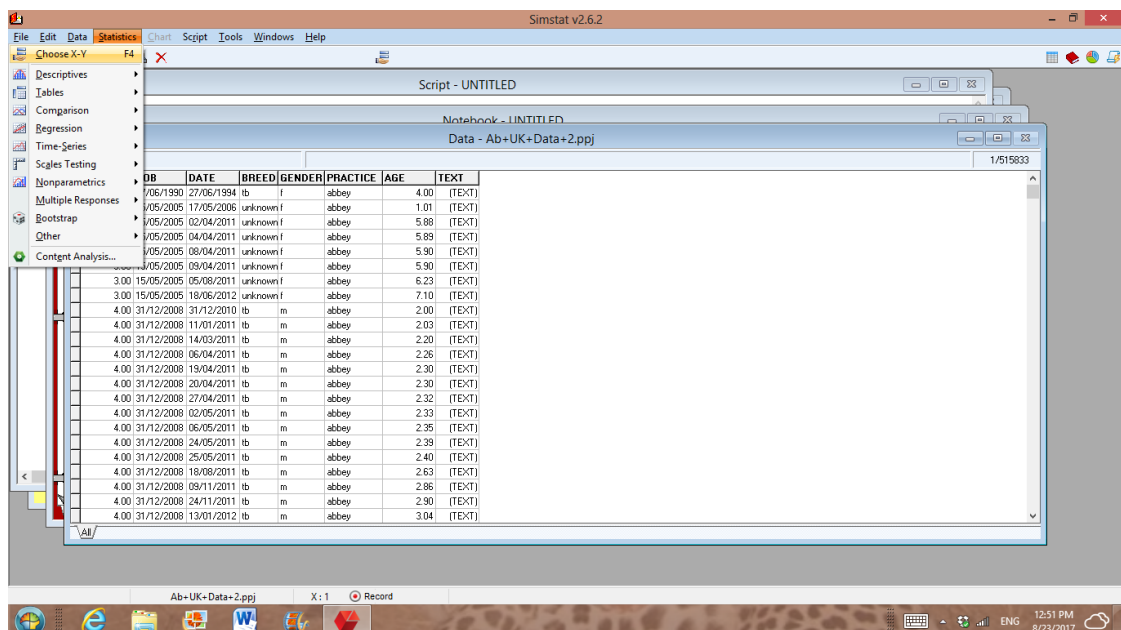


Figure 7-1: Choosing X_Y

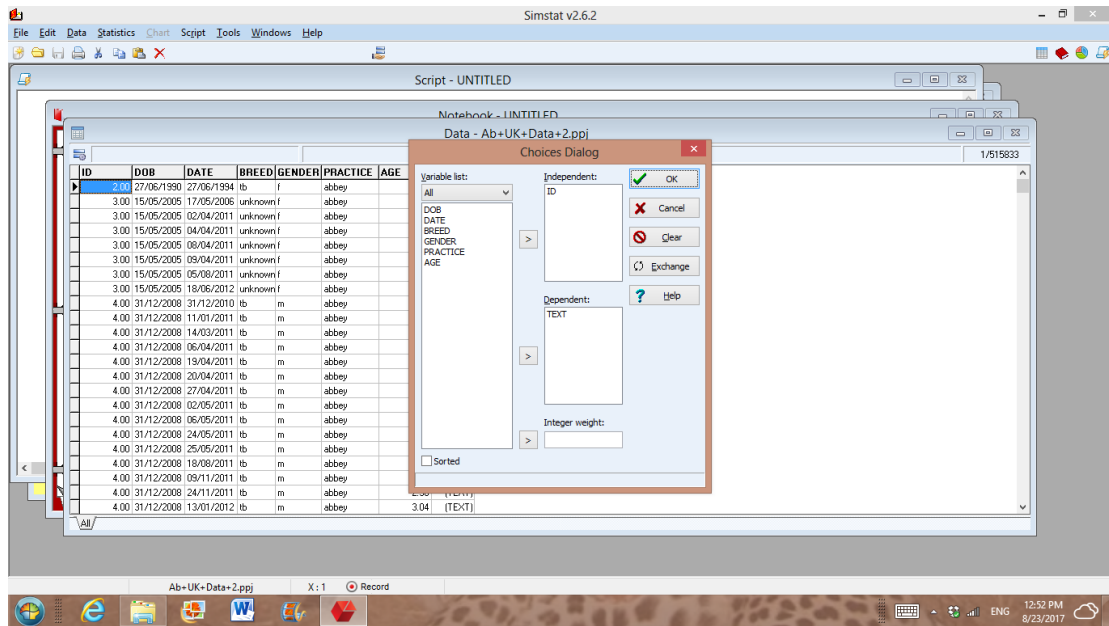


Figure 7-2: Adding ID to independent column and Text to dependent column

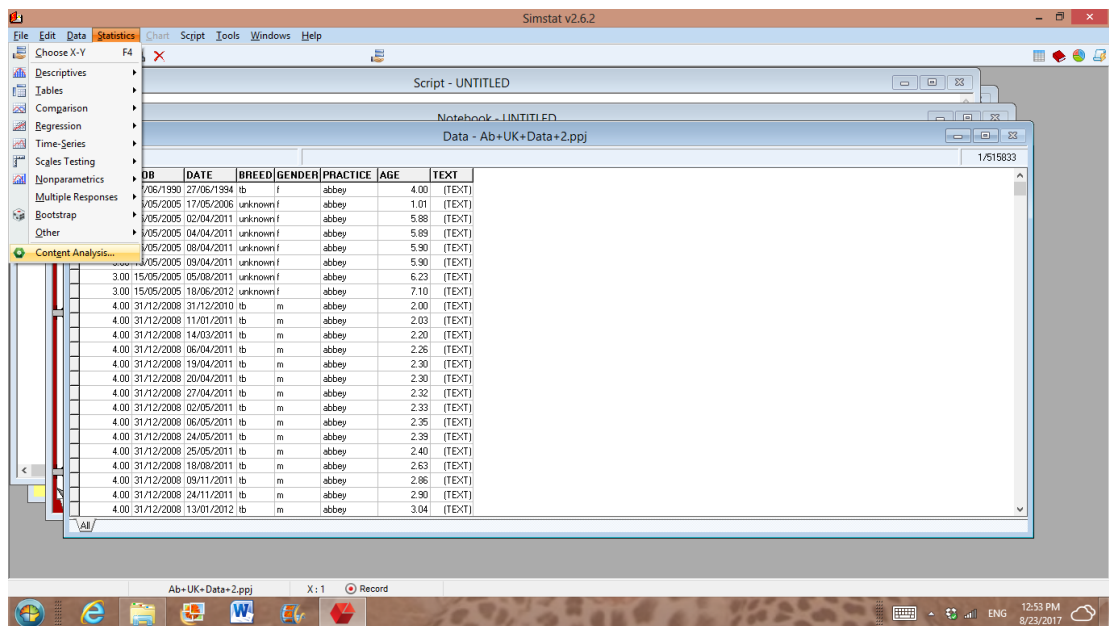


Figure 7-3: Shifting from Simstat to Wordstat by clicking on content analysis

When Wordstat appears on screen click the file open to choose the particular dictionary that has been made as presented in Figure 7-4 then tick box that near categorisation to check the level as presented in Figure 7-5.

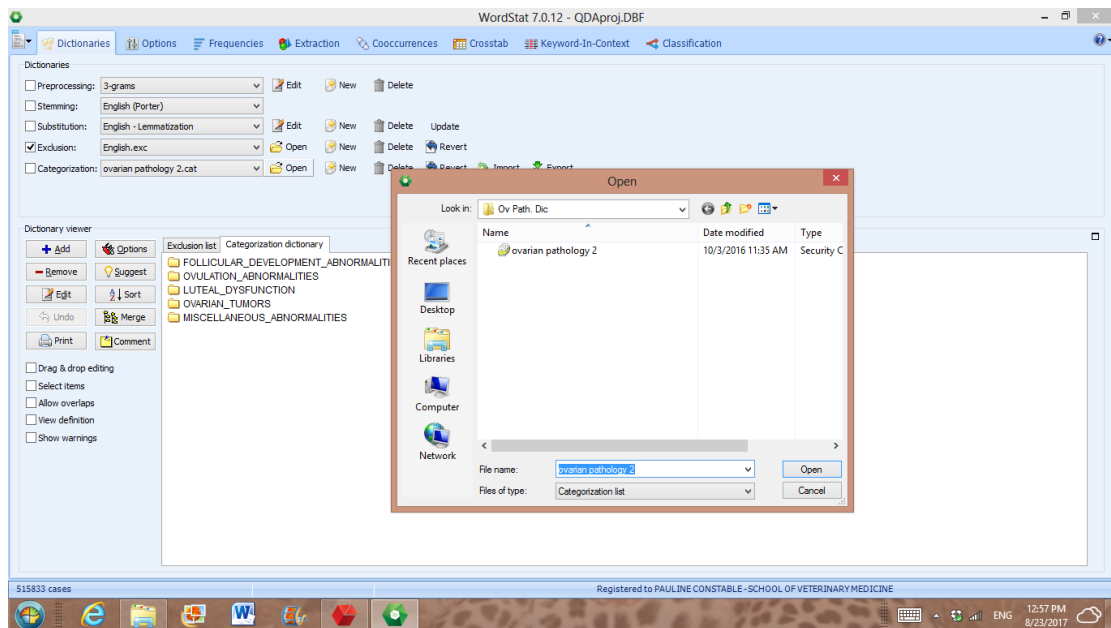


Figure 7-4: Choosing dictionary

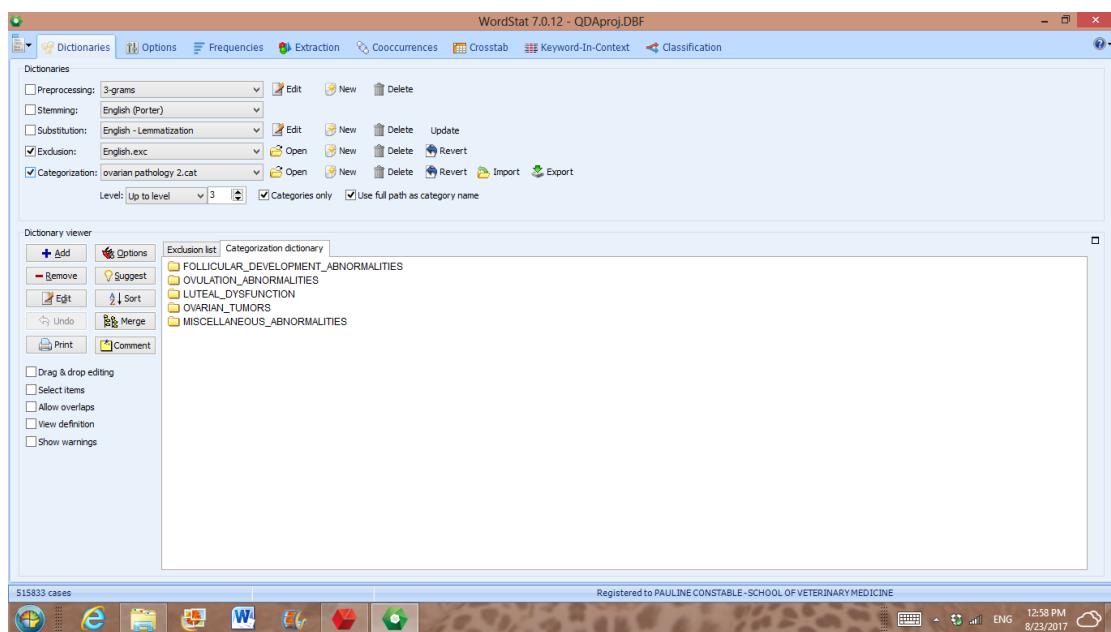


Figure 7-5: Put tick in the box near categories

After running dictionary on Wordstat by clicking on Keyword-In-Context and leave it for a while to search bearing in mind this might take a couple of minutes depending on the data size the Keyword box should be filtered and chose one category, after that the text will appear on screen. See examples of these steps as presented below on Figure 7-6, Figure 7-7 and Figure 7-8.

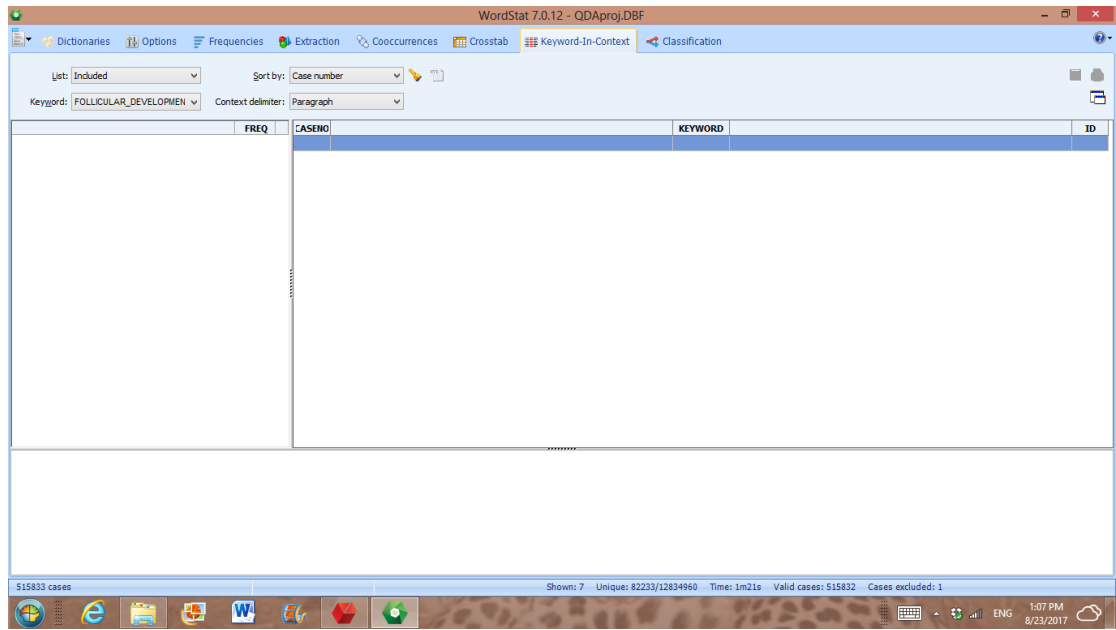


Figure 7-6: Clicking on Keyword-In-Content

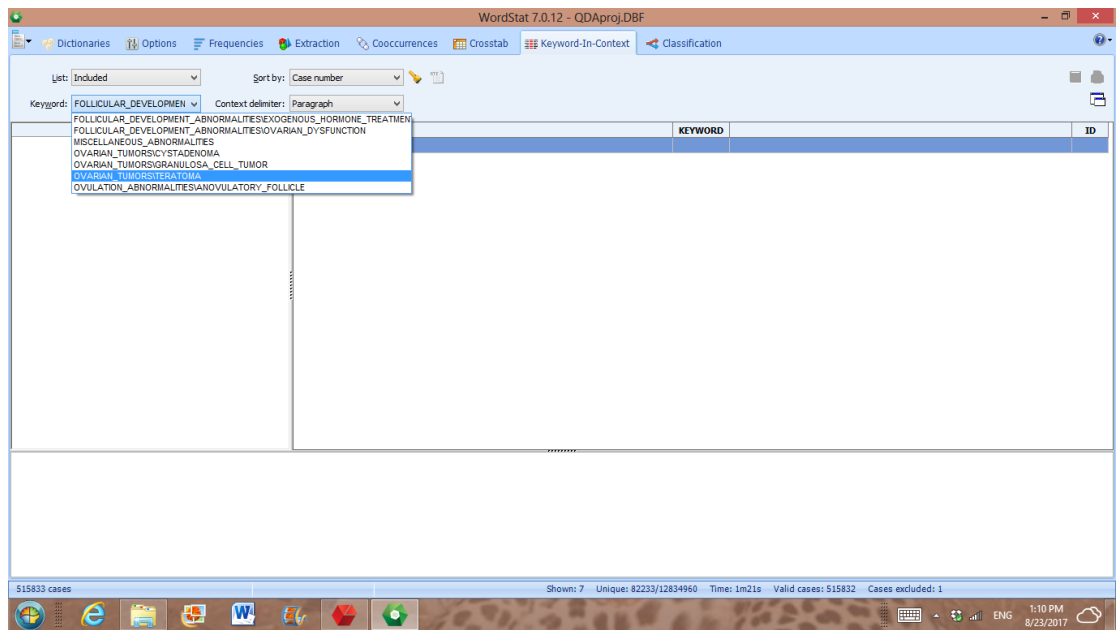


Figure 7-7: Choosing a category or subcategory from the box near keyword

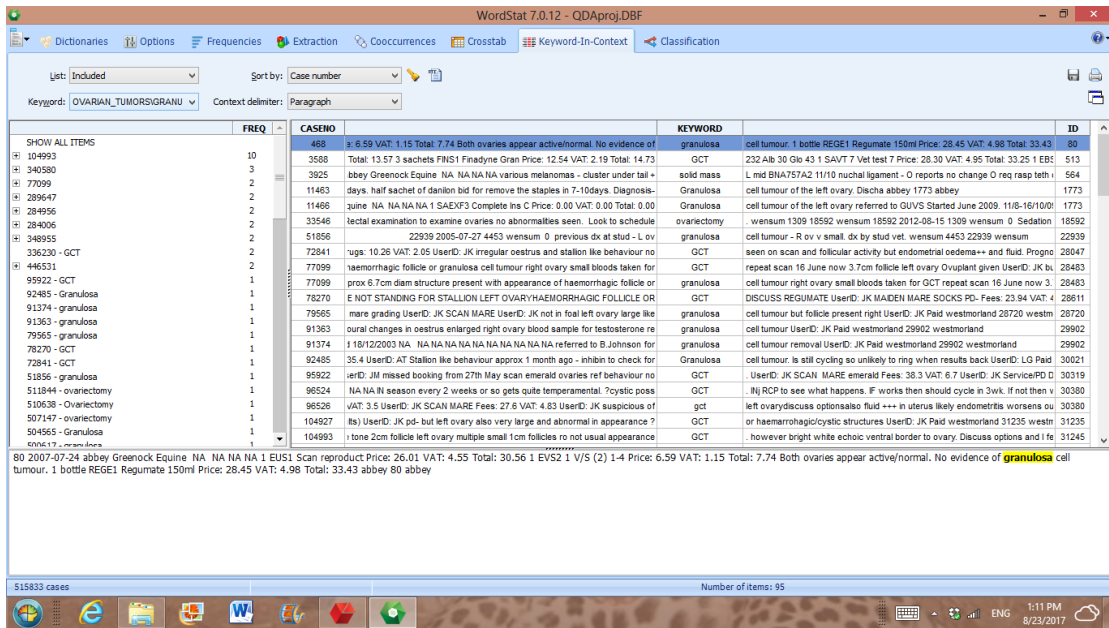


Figure 7-8: Case no., Keyword and Text appeared on the screen with highlighted keyword

Click on Frequency to check if any words have been leftover which can be useful to the dictionary, bearing in mind that always give plenty of time to the program to think. In order to check those words in alphabetical order click on the top of these words underneath the box of leftover words beside Frequency then words can be checked. If any useful word has been detected click on it and keep pressing then drag it to the dictionary at the left of the screen where the exclusion list is and chose the preferable file. See examples of these steps below as presented on Figure 7-9, Figure 7-10, Figure 7-11 and Figure 7-12.

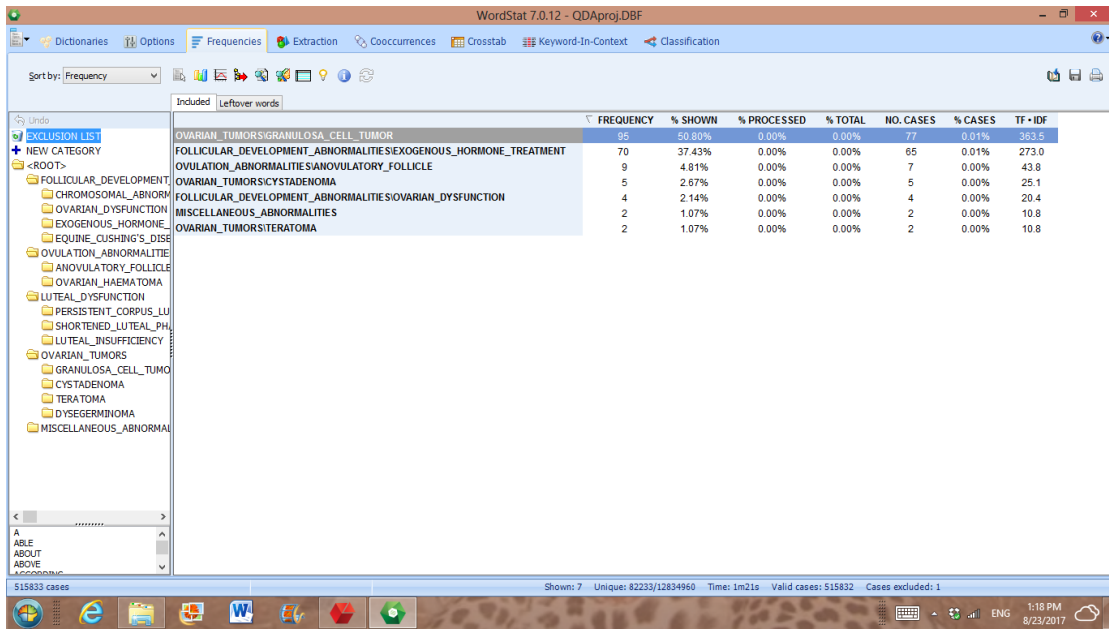


Figure 7-9: Clicking on Frequency showed the frequency and percentages of cases on categories

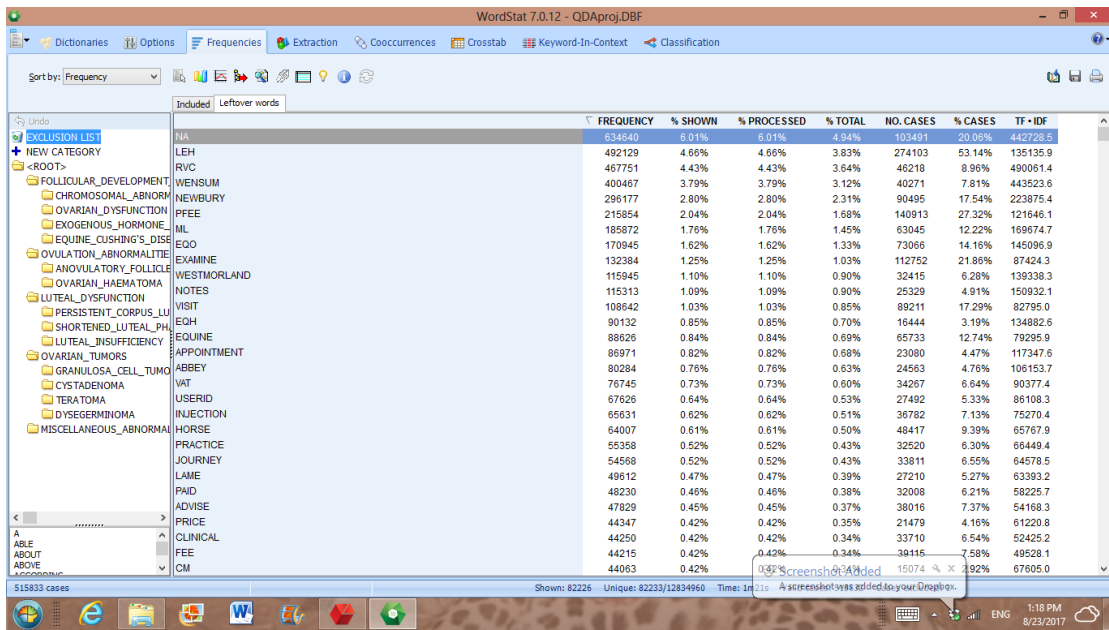


Figure 7-10: Clicking on Leftover words showed words with no alphabetical order

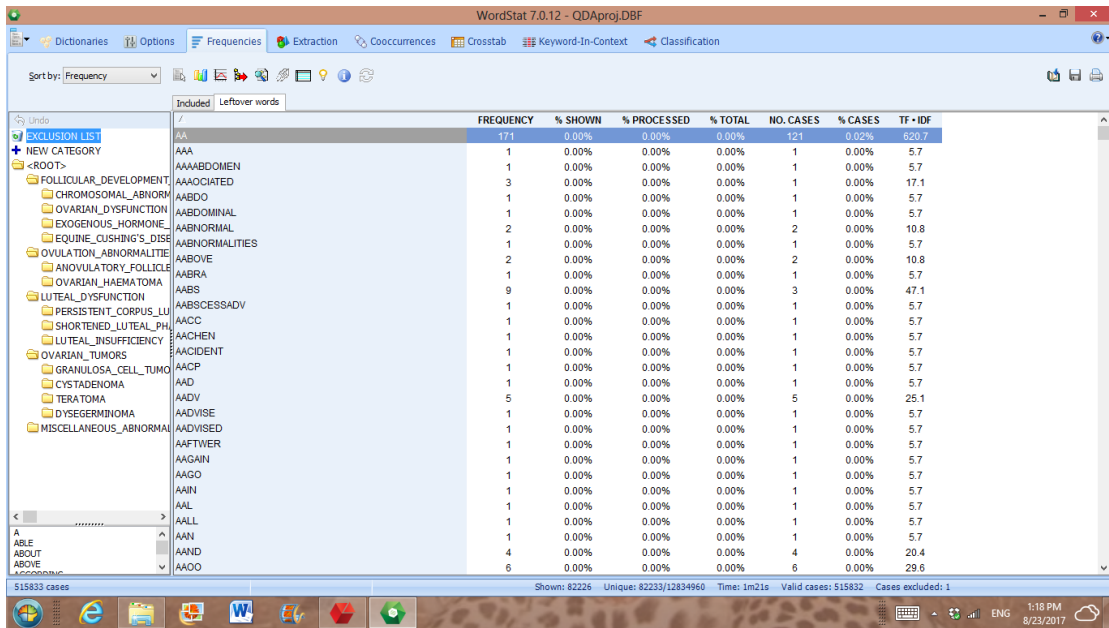


Figure 7-11: Tabbing on top of the first word from the list of leftover words arranged them alphabetically

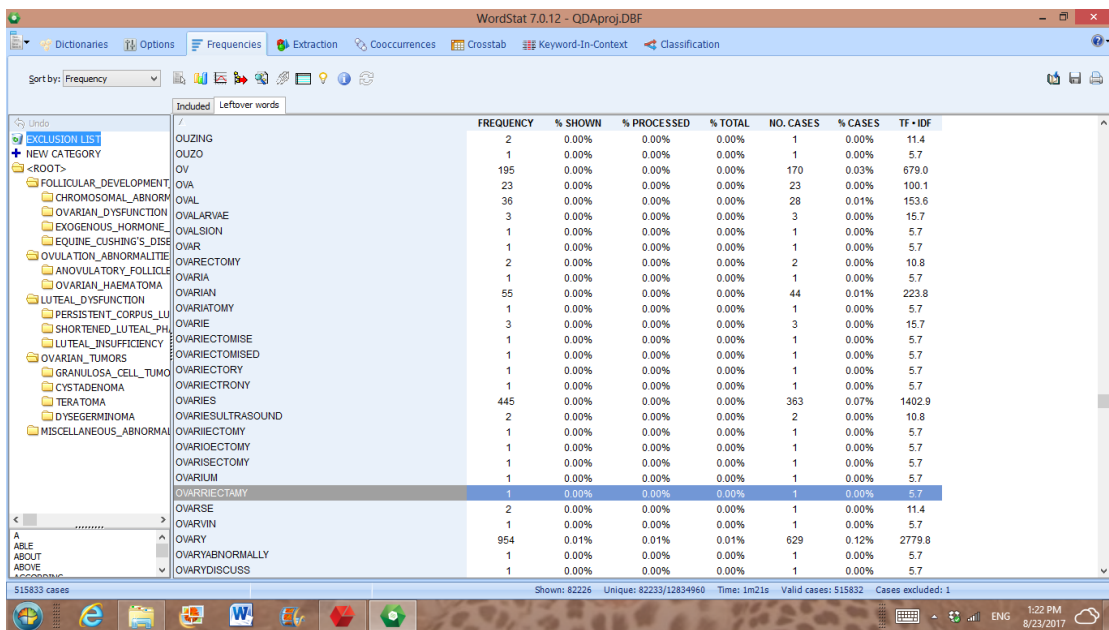


Figure 7-12: Choosing the required or useful word and drag it to the dictionary

Exporting data can be achieved by clicking the red arrow as presented Figure 7-13 then export data matrix as shown in Figure 7-14.

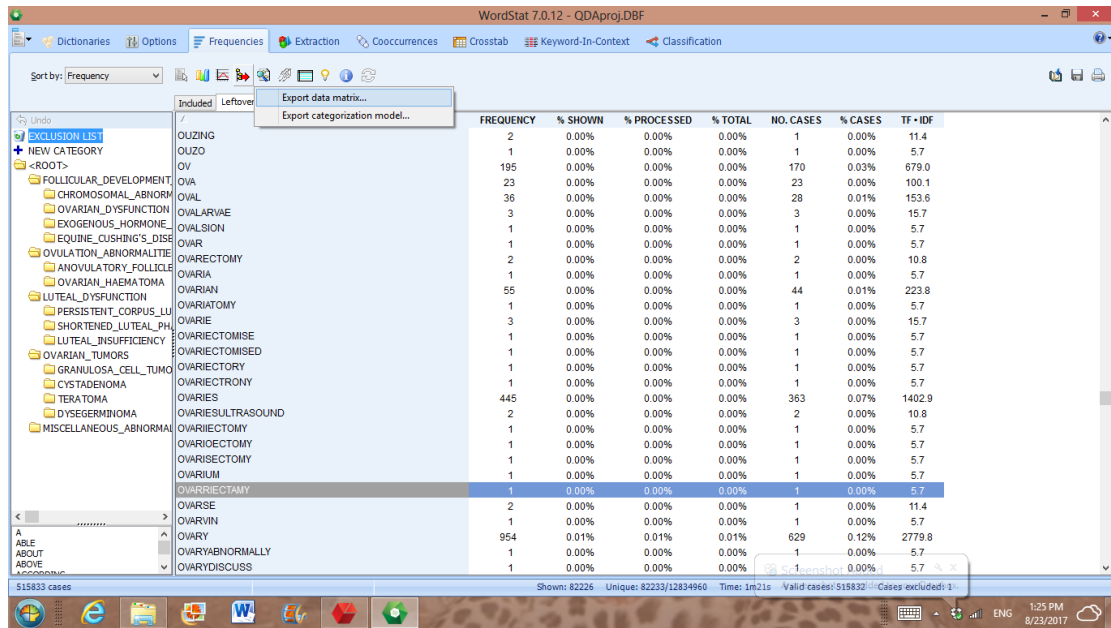


Figure 7-13: Clicking the Red arrow to export data matrix

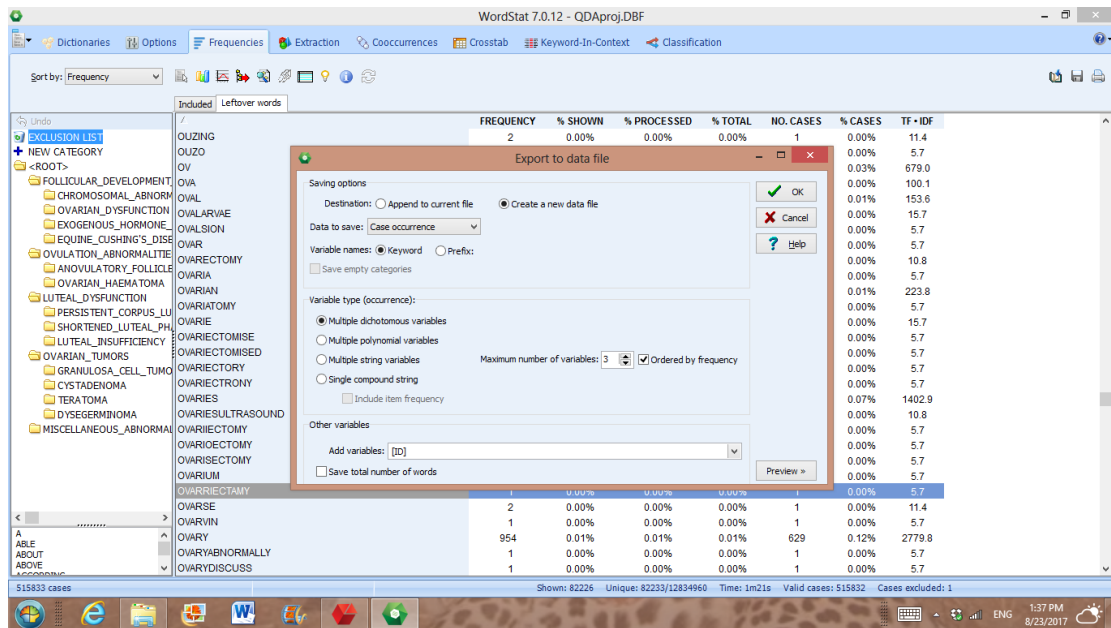


Figure 7-14: A box for exporting data to file appeared

After the button ok has been pressed it will transfer to Save Word Frequency list as presented in Figure 7-15, so the searcher should choose a name and save it in a particular place but be aware of changing the file type. It is recommended to be save as comma separated files (CSV) as presented in Figure 7-16 then the file can be examine by searching for word, ID, or any things.

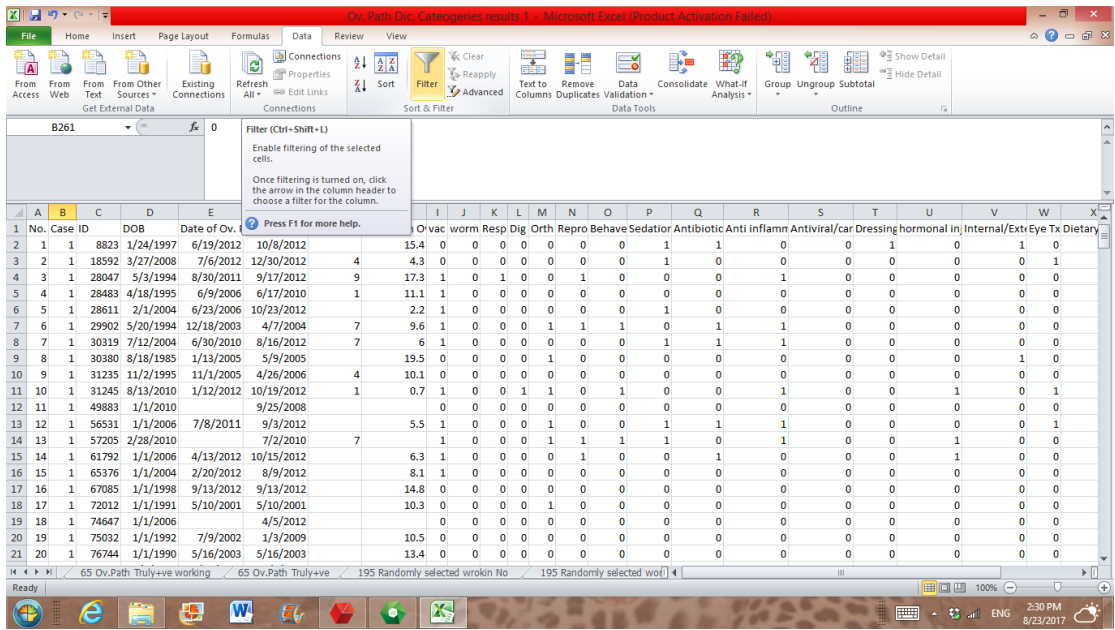
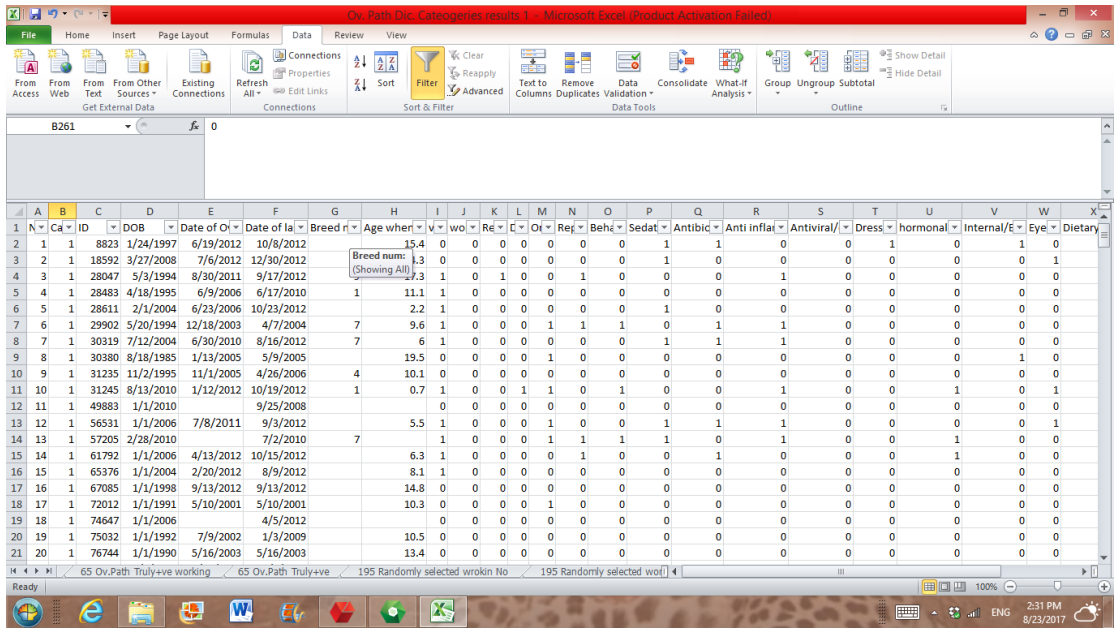


Figure 7-17: Tabbing filter



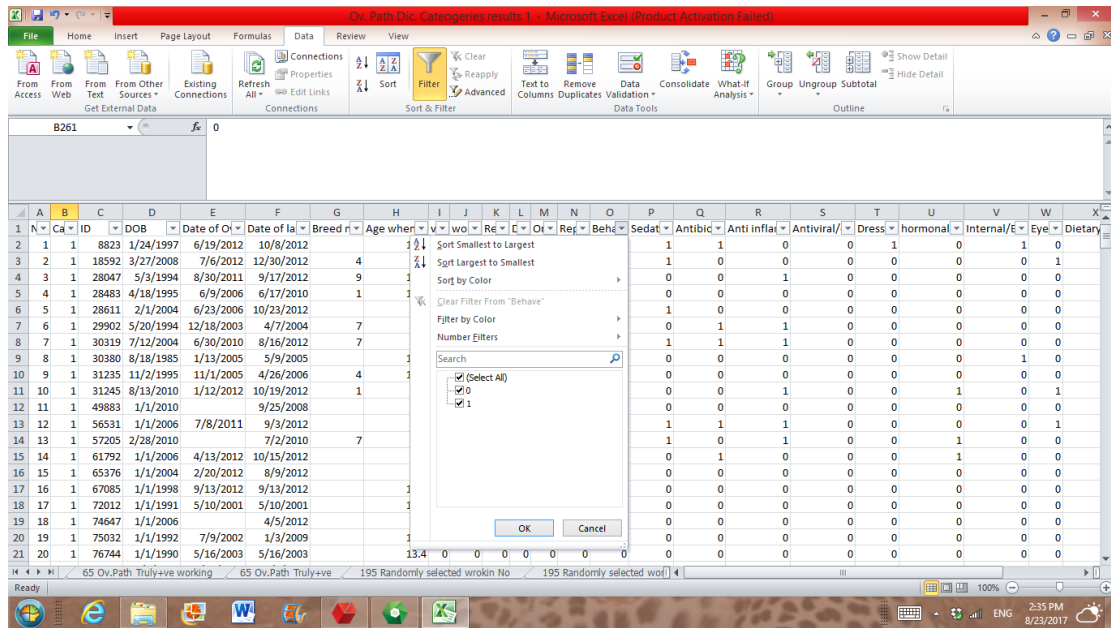


Figure 7-19: Sorting from largest to smallest or vice versa

The numbers of ID should be written down or extracted in new sheet to help searching in the original data that been saved in computer and search for individual cases. Bearing in mind that some repetition of ID numbers might be found.

Sometimes filtering is not always helpful because when the information seeker wants to choose the specific gender such as female having ovarian granulosa cell tumour the filtering will come out with all female not the one that have GCT which is according to ID numbers. Therefore, the best way is using pivot table. Clicking on it to highlight all cells can use pivot table and the box will appear on the screen. Examples of creating pivot table are as shown below and presented in Figure 7-20, Figure 7-21, Figure 7-22, and Figure 7-23.

Create pivot table by clicking on

- Select a table or range
- New work sheet
- Then press ok button
- Drag the ID number to Row labels then drag the breed to Report filter
- Then from the sheet click (All) this will delete all ticks which besides All, F, M, Mnx, Unknown then click on select Multiple items

- Click on F then click ok

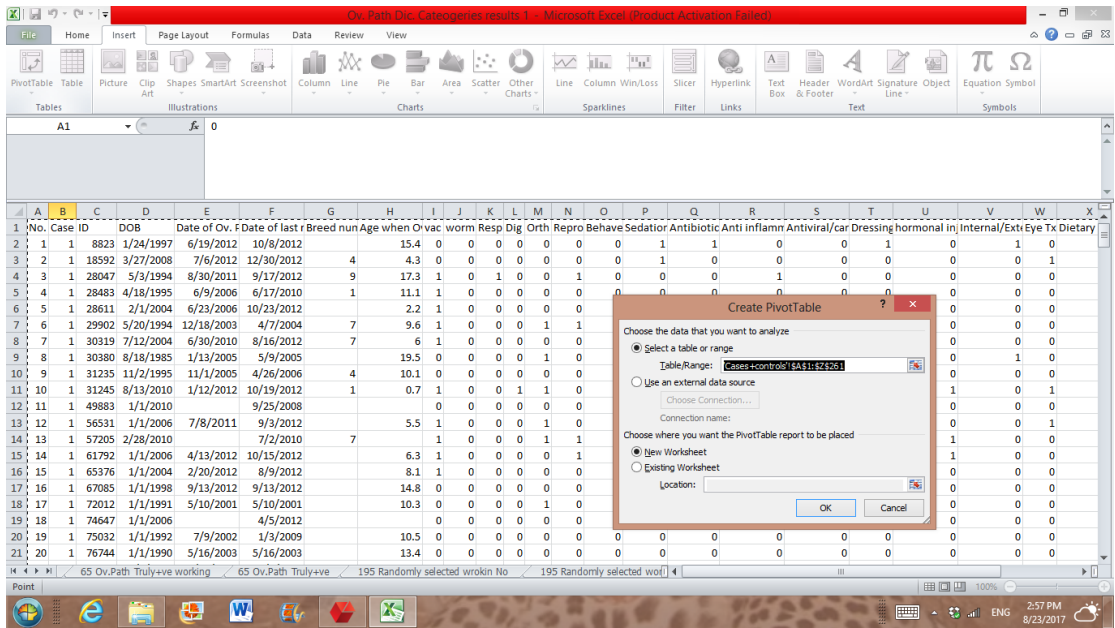


Figure 7-20: creating pivot table by selecting table/range and choose new worksheet

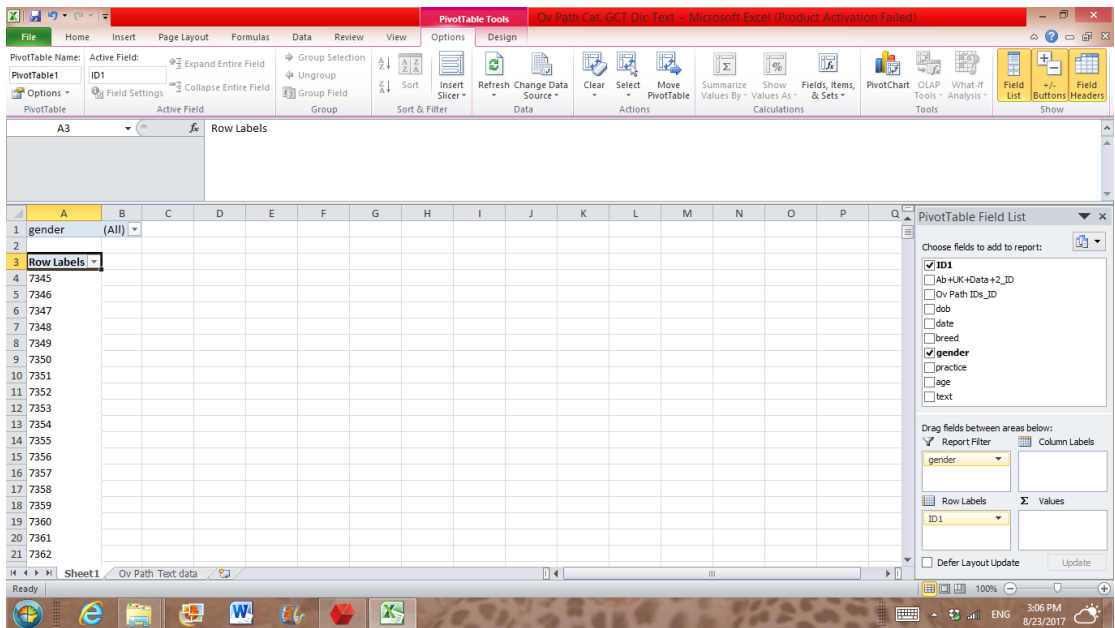


Figure 7-21: Dragging ID number to raw labels

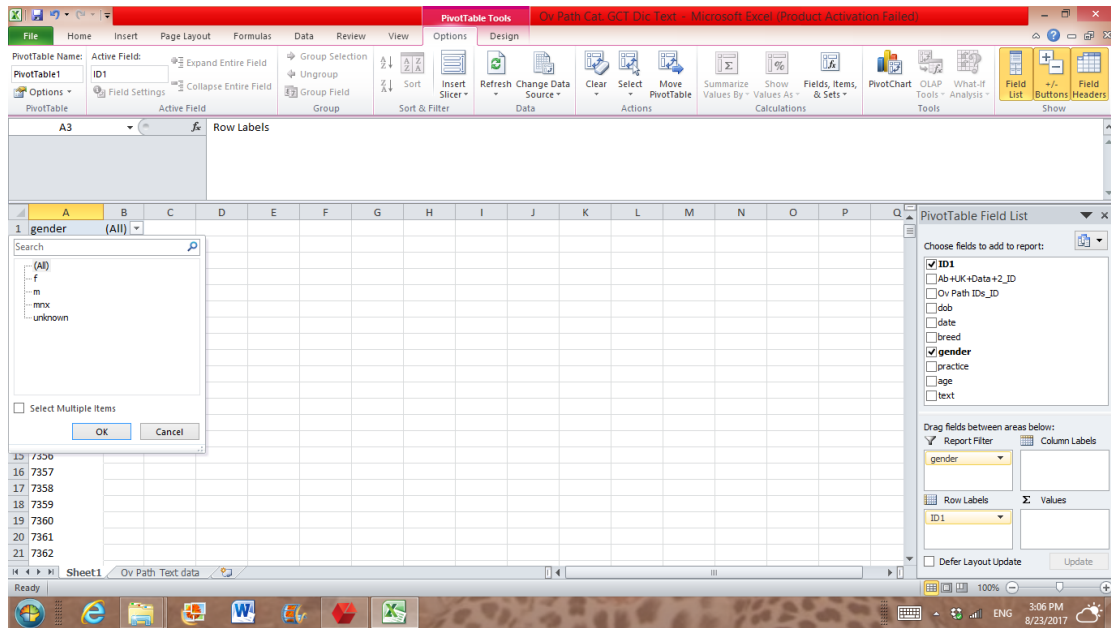


Figure 7-22: Choosing the gender for example by clicking all to delete the ticks from all boxes

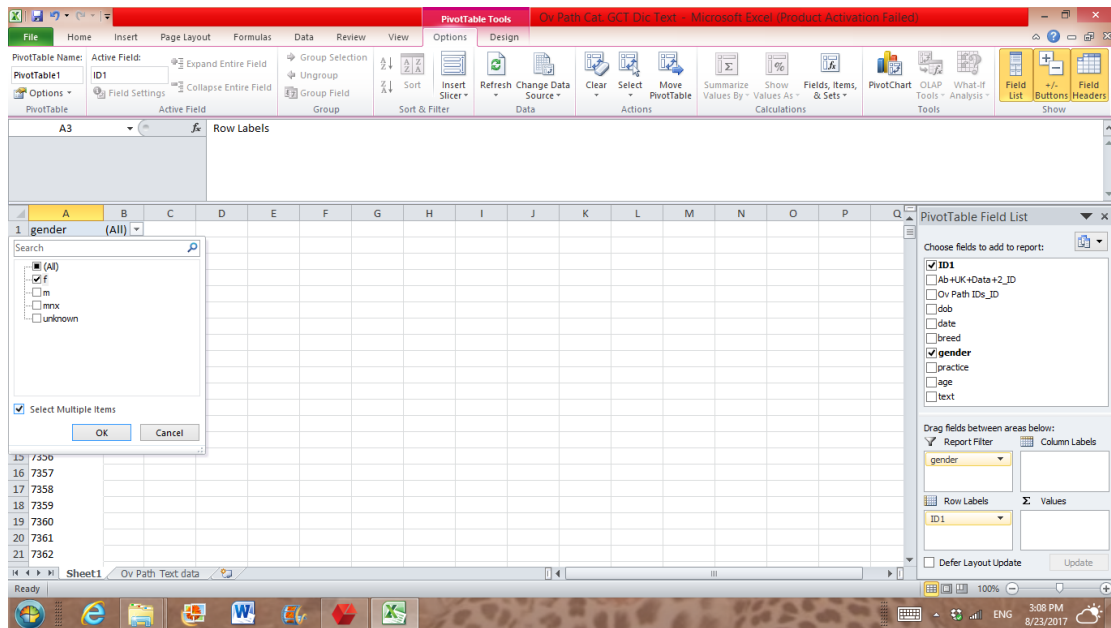


Figure 7-23: Choose the required gender e.g female then tab select multiple items then ok

Moreover, ID numbers can be arranged from smallest to largest or vice versa by filtering and clicking on Row Labels where the ID numbers based then choose through the options appears as presented in Figure 7-24 and when it is done it can be by clicking on the icon undo. In order to know how many females, the female column should be highlighted by drag the column from top to bottom, however it is time consuming. Therefore, the easiest way is by clicking on the top cell and go to the bottom one then press shift and click on it. The count will be found at the bottom on the right hand side of the screen.

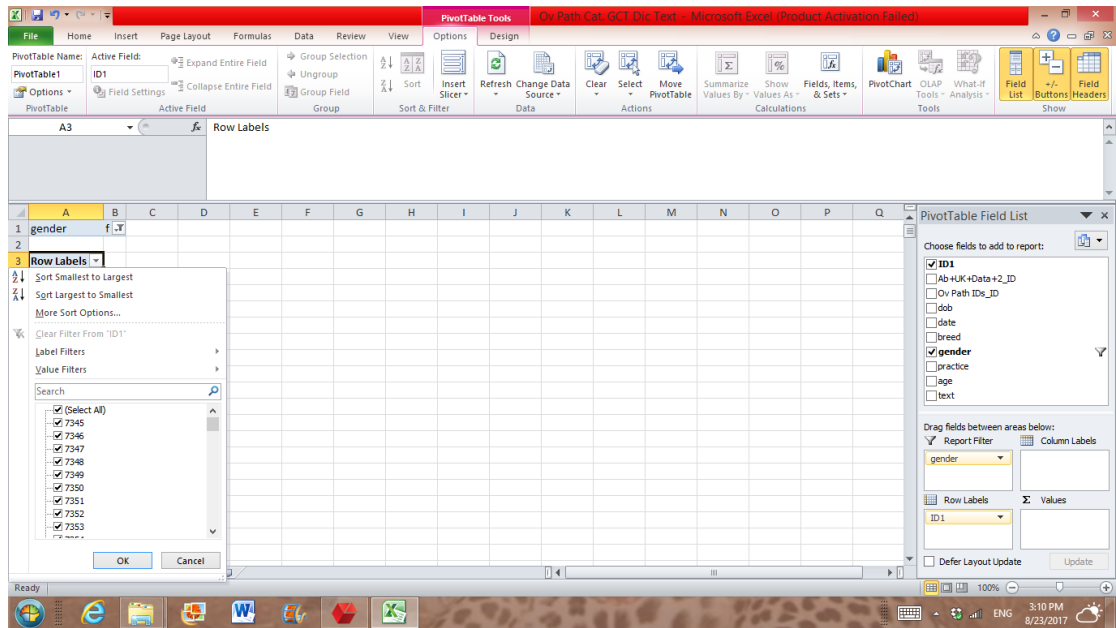


Figure 7-24: Filtering ID number from smallest to largest or vice versa by clicking the Row labels

Searching for particular ID to find how many entries for this animal go to main data then open home and click on find and select after that click on find then option as presented in Figure 7-25.

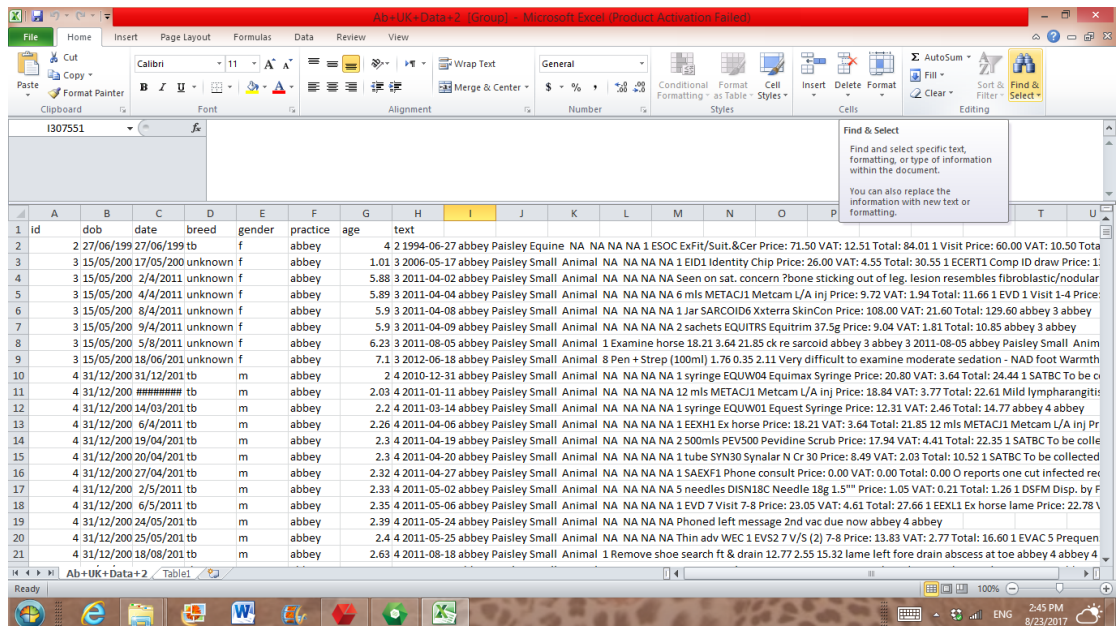


Figure 7-25: Clicking on find and select to search for particular D number

Put the of the ID number in (Find what) and click the box (options >>) then make sure you click the tick in the box near Match entire cell contents. Then click (Find next) as presented in Figure 7-26, Figure 7-27 and Figure 7-28. This will

identified the rows of ID numbers, so those entries can be read through or copy and paste somewhere save.

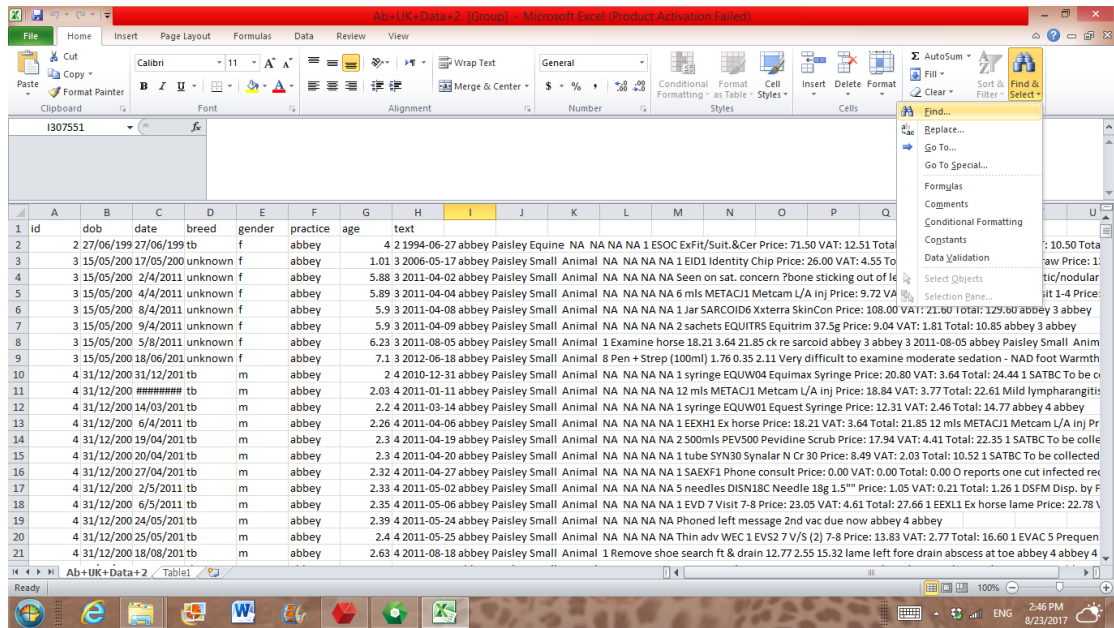


Figure 7-26: clicking on Find

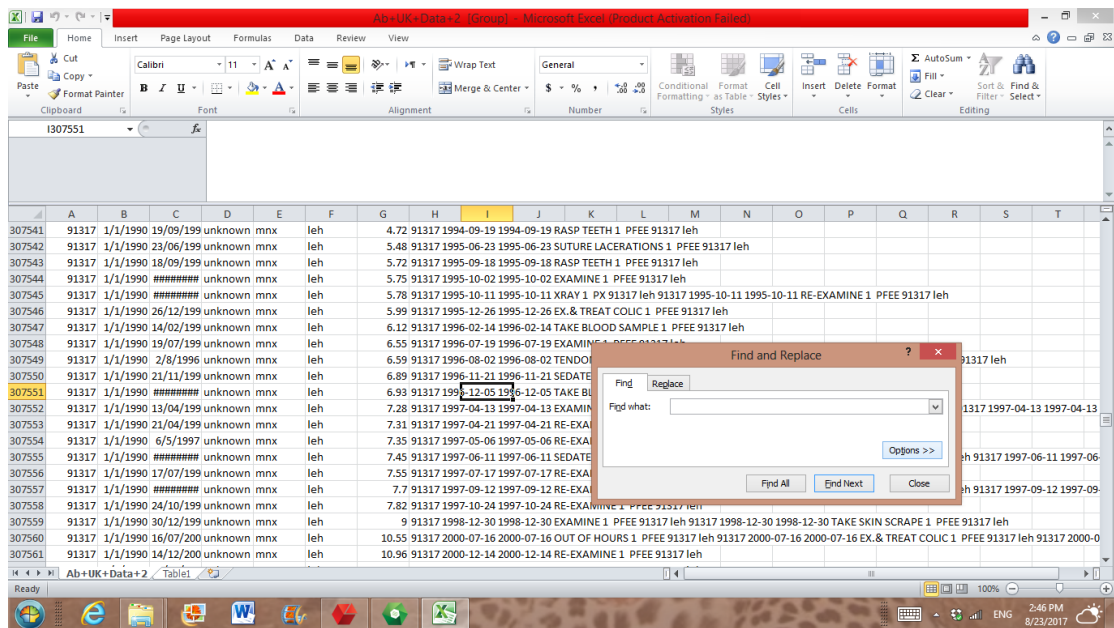


Figure 7-27: The box of Find and replace appeared

The screenshot shows a Microsoft Excel spreadsheet with a 'Find and Replace' dialog box open. The dialog box has 'Find what:' set to '2345' and the 'Match entire cell contents' checkbox checked. The spreadsheet data is as follows:

ID	Date	Name	Sex	Breed	Other Info
15309	2340 14/04/198	##### welsh	m	abbey	15.57 2340 1996-11-05 abbey Paisley Equine NA NA NA NA 1 V09 Visit Price: 17.26 VAT: 3.02 Total: 20.28 1 EIV Inj. horse i/v Price: 1.91 VAT: 0.33 T...
15310	2341 19/11/199 21/11/200	##### pony	m	abbey	13.02 2341 2008-11-21 abbey Paisley Equine NA NA NA NA 1 EVS219 V/S (2) 19-20 Price: 25.04 VAT: 4.38 Total: 29.42 1 EEXP2 PPE 2 Stage Price: 64.4...
15311	2341 19/11/199 24/11/200	##### pony	m	abbey	13.02 2341 2008-11-24 abbey Paisley Equine NA NA NA NA Rainrash along back 21/11/08. This horse passed a 2 stage vetting at Darwhilling Farm c...
15312	2342 1/1/2006 8/1/2011	##### unknown	unknown	abbey	5.02 2342 2011-01-08 abbey Paisley Equine NA NA NA NA 1 needle DISN19A Needle 19g 1" Price: 0.07 VAT: 0.01 Total: 0.08 1 syringe DISS20 Dis.5...
15313	2342 1/1/2006 21/02/201	##### unknown	unknown	abbey	5.14 2342 2011-02-21 abbey Paisley Equine NA NA NA NA 1 EVAC 4 Frequenza TE 1s Price: 27.07 VAT: 5.41 Total: 32.48 abbey 2342 abbey
15314	2342 1/1/2006 22/03/201	##### unknown	unknown	abbey	5.22 2342 2011-03-22 abbey Paisley Equine NA NA NA NA 12 mls METACJ1 Metcam L/A Inj Price: 19.44 VAT: 3.89 Total: 23.33 1 EIB I/V Injection Pri...
15315	2342 1/1/2006 6/4/2011	##### unknown	unknown	abbey	5.26 2342 2011-04-06 abbey Paisley Equine NA NA NA NA 1 EVAC 5 Frequenza TE 2n Price: 27.07 VAT: 5.41 Total: 32.48 abbey 2342 abbey
15316	2342 1/1/2006 7/6/2011	##### unknown	unknown	abbey	5.43 2342 2011-06-07 abbey Paisley Equine NA NA NA NA 1 EVAC 5 Frequenza TE 2n Price: 27.07 VAT: 5.41 Total: 32.48 abbey 2342 abbey
15317	2343 1/1/2006 #####	##### unknown	unknown	abbey	5.61 2343 2011-08-10 abbey Paisley Equine NA NA NA NA 1 EVAC 5 Frequenza TE 2n Price: 27.07 VAT: 5.41 Total: 32.48 abbey 2342 abbey
15318	2344 ##### 25/09/200	##### pony	m	abbey	6.98 2344 2006-09-25 abbey Paisley Equine NA NA NA NA 1 EVAC 5 Frequenza TE 2n Price: 27.07 VAT: 5.41 Total: 32.48 abbey 2342 abbey
15319	2345 #####	##### wb	m	abbey	4 2345 2005-08-11 abbey Paisley Equine NA NA NA NA 1 EVAC 5 Frequenza TE 2n Price: 27.07 VAT: 5.41 Total: 32.48 abbey 2342 abbey
15320	2346 15/07/198 15/07/200	##### tb	m	abbey	20.01 2346 2007-07-15 abbey Greenock Sma NA NA NA NA 1 EVAC 5 Frequenza TE 2n Price: 27.07 VAT: 5.41 Total: 32.48 abbey 2342 abbey
15321	2346 15/07/198 18/08/200	##### tb	m	abbey	20.11 2346 2007-08-18 abbey Greenock Sma NA NA NA NA 1 EVAC 5 Frequenza TE 2n Price: 27.07 VAT: 5.41 Total: 32.48 abbey 2342 abbey
15322	2346 15/07/198 #####	##### tb	m	abbey	20.41 2346 2007-12-08 abbey Greenock Sma NA NA NA NA 1 EVAC 5 Frequenza TE 2n Price: 27.07 VAT: 5.41 Total: 32.48 abbey 2342 abbey
15323	2346 15/07/198 #####	##### tb	m	abbey	20.42 2346 2007-12-10 abbey Greenock Sma NA NA NA NA 1 EVAC 5 Frequenza TE 2n Price: 27.07 VAT: 5.41 Total: 32.48 abbey 2342 abbey
15324	2346 15/07/198 #####	##### tb	m	abbey	20.42 2346 2007-12-12 abbey Greenock Sma NA NA NA NA 1 EVAC 5 Frequenza TE 2n Price: 27.07 VAT: 5.41 Total: 32.48 abbey 2342 abbey
15325	2346 15/07/198 15/12/200	##### tb	m	abbey	20.43 2346 2007-12-15 abbey Greenock Sma NA NA NA NA 1 EVAC 5 Frequenza TE 2n Price: 27.07 VAT: 5.41 Total: 32.48 abbey 2342 abbey
15326	2346 15/07/198 3/3/2008	##### tb	m	abbey	20.65 2346 2008-03-03 abbey Greenock Sma NA NA NA NA 1 EVAC 5 Frequenza TE 2n Price: 27.07 VAT: 5.41 Total: 32.48 abbey 2342 abbey
15327	2346 15/07/198 23/06/201	##### tb	m	abbey	22.96 2346 2010-06-23 abbey Greenock Sma NA NA NA NA 1 EVAC 5 Frequenza TE 2n Price: 27.07 VAT: 5.41 Total: 32.48 abbey 2342 abbey
15328	2346 15/07/198 8/9/2010	##### tb	m	abbey	23.17 2346 2010-09-08 abbey Greenock Sma NA NA NA NA 1 EVAC 5 Frequenza TE 2n Price: 27.07 VAT: 5.41 Total: 32.48 abbey 2342 abbey
15329	2346 15/07/198 #####	##### tb	m	abbey	23.26 2346 2010-10-11 abbey Greenock Small Animal NA NA NA NA 1 SAEXF1 Phone consult Price: 0.00 VAT: 0.00 Total: 0.00 can take pictures com...

Figure 7-28: Write the ID number required on the box of find what then tick the box close to Match entire cell contents

Appendix 2 Dictionary used in Text mining

2.1 Ovarian Tumour dictionary

TERATOMA

TERATOM* (1)

TERATOC* (1)

CYSTADENOMA

BENIN_CYST (1)

CYCTIC (1)

CYSTAD* (1)

CYST_LIKE_STRUCTURE (1)

CYSTIC (1)

DYSGERMINOMA

DYSCARCINOMA (1)

DYSGERM* (1)

MALIGNANT_OVAR* (1)

GRANULOSA CELL TUMOUR

GRANULOS (1)

GRANULOSAL (1)

GRANULOSE (1)

GRANULOSIS (1)

GRANULOUSA (1)

OVARY (1)

HONEYCOMB_STRUCTURE (1)

HONEYCB (1)

OVARIECTOMY (1)

OVARIATOMY (1)

OVARIES (1)

OVARIAN (1)

LARGE_OVAR* (1)

OVARIE (1)

ENLARGED_OVAR* (1)

BIG_OVAR* (1)

THECA_CELL_TUMOR* (1)

STALLION_LIKE_BEHAVIOUR (1)

STALLION_LIKE_BEHAVIOR (1)

INHIBIN_CONC* (1)

GTCT (1)

GCT (1)

GRANULOSA (1)

GRANNULOSA (1)

GRANLOSA (1)

ANTI_MULLARIAN_HORMON* (1)

AMH (1)

2.2 Ovarian pathology dictionary

FOLLICULAR_DEVELOPMENT_ABNORMALITIES

CHROMOSOMAL_ABNORMALITIES

ABNORMAL_GONAD* (1)

CHROMOSOM*_ABNORMALITIES (1)

ABNORMAL_CHROMOSOM* (1)

GONADAL_DYSGENESIS (1)

GONADAL_ABNORMALIT* (1)

OVARIAN_DYSFUNCTION

INFERTILE (1)

INFERTILITY (1)

SUBFERTILE_MARE (1)

INFERTILE_MARE (1)

EXOGENOUS_HORMONE_TREATMENT

ANABOLIC_STEROID (1)

P4 (1)

PROGESTIN (1)

PROGESTERONE (1)

EQUINE_CUSHING'S_DISEASE

ANDROGEN_PRODUCTION (1)

DECREASE_GONADOTROPIN (1)

HYPOTHALAMUS_COMPRESSION (1)

ANTERIOR_PITUTATRY_COMPRESSION (1)

OVULATION_ABNORMALITIES

ANOVULATORY_FOLLICLE

CYSTIC_OVAR* (1)

HAEMORRHAGIC_FOLLICLE (1)

HEMORRHAGIC_FOLLICLE (1)

OVARIAN_BIOPSY (1)

OVULATION_FAILURE (1)

PERSISTENT_ANOVULATORY_FOLLICLE (1)

PAF (1)

OVARIAN_HAEMATOMA

BIG_CH (1)

ENLARGED_CH (1)

ENLARGED_CORPORA_HAEMORRHAGICA (1)

OVARIAN_HAEMOATOMA (1)

OVARIAN_HEMATOMA (1)

LUTEAL_DYSFUNCTION

PERSISTENT_CORPUS_LUTEUM

PERSISETENT_CL (1)

DESTRUCTED_CL (1)

FAILED_REGRESSION_CL (1)

SHORTENED_LUTEAL_PHASE

PREMATURE_LUTEOLYSIS (1)

SHORT_LUTEAL_PHASE (1)

LUTEAL_INSUFFICIENCY

LUTEAL_DYSFUNCTION (1)

LUTEAL_INSUFFICIENCY (1)

OVARIAN_TUMORS

GRANULOSA_CELL_TUMOR

GRANULOSA (1)

GRANULOSA_CELL_TUMOR* (1)

GRANULOSA_TUMOR (1)

GCT (1)

GTCT (1)

MULTICYSTIC (1)

HONEYCOMB*_STRUCTURE (1)

HONEYCOMBED_STRUCTURE (1)

HONEYCOMBED_APPEARANCE (1)

SOLID_MASS (1)

POLYCYSTIC (1)

LARGE_CYST* (1)

INACTIVE_OVAR* (1)

ATROPHIED_OVAR* (1)

AFFECTED_OVAR* (1)

TRANSITIONAL_OVAR* (1)

SMALL_OVAR* (1)

OVARIAN_ENLARGEMENT (1)

LARGE_OVAR* (1)

BIG_OVAR* (1)

ENLARGED_OVAR* (1)

NYMPHOMANIA (1)

MARE_NYMPHOMANIA (1)

CONTRALATERAL_OVAR* (1)

OVARIECTOMY (1)

REMOVE_OVAR* (1)

OVARICTOMY (1)

CLOPTOMY (1)

OVARIAN_NEOPLASMA (1)

OVARIAN_TUMOR* (1)

OESTROGEN_PRODUCING_TUMOR* (1)

CYSTADENOMA

CYSTADENOMA* (1)

CYST_LIKE_STRUCTURE (1)

BENIGN_CYST (1)

TERATOMA

TERATOM* (1)

TERATOC* (1)

TERATOMAS (1)

DYSEGERMINOMA

MALIGNANT_OVAR* (1)

DYSGERMINOMA (1)

MISCELLANEOUS_ABNORMALITIES

FIMBRIAL_CYST* (1)

FOSSA_CYST* (1)

IRREGULAR ESTRUS (1)

IRREGULAR HEAT (1)

IRREGULAR OESTRUS (1)

MULLERIAN_CYST* (1)

OVARIAN_ABSCESS* (1)

PAROVARIAN_CYST* (1)

PREPUBERTY (1)

ABNORMAL ESTRUS (1)

ABNORMAL OESTRUS (1)

ABNORMAL HEAT (1)

ABNORMAL CYCLICITY (1)

POSTPARTUM HEAT (1)

POSTPARTUM_ANOESTRUS (1)

REDUCED_FERTILITY (1)

SEASONAL_ANESTRUS (1)

SEASONAL_HEAT (1)

SEASONAL_ANOESTRUS (1)

WOLFFIAN_DUCT_CYST* (1)

2.3 GCT dictionary

OVARIAN_PATHOLOGY

BIG_OVAR* (1)

MARE_SCAN (1)

@SCAN [SCAN AND MARE /A /S] (1)

*LARGE*_OVAR* (1)

FIRM_OVAR* (1)

CYST

@CYSTS [CYST* NEAR OVAR* /A /S5] (1)

@POLY [POLYCYST* NEAR OVAR* /A /S5] (1)

@MULTICYST [MULTICYST* NEAR OVAR* /A /S5] (1)

TUMOUR

@TUMOUR

[OVAR* NEAR TUMO*R NEAR MASS NEAR NEOPLAS* NEAR CANSER /A /S5/D5/D5/D5] (1)

@TUMOUR [TUMO*R AND OVAR* /A /S] (1)

SOLID_MASS (1)

GCT

GCT (1)

GRANCULOSA (1)

GRANLOSA (1)

GRANULOS (1)

GRANULOSA (1)

GRANNULOSA (1)

GRANULOSAL (1)

GRANULOSE (1)

GRANULOSIS (1)

GRANULOUSA (1)

GTCT (1)

TUMORS (1)

TUMOURS (1)

BEHAVIOUR

NEIGHING (1)

STIKING (1)

STALLION_LIKE (1)

UNRULY (1)

List of References

- AGRESTI, A. & COULL, B. 2000. Agresti, A., and Coull, B. A. (1998), "Approximate is better than 'exact' for interval estimation of binomial proportions," *The American Statistician*, 52, 119-126: Comment by Rindskopf and reply - Response. *American Statistician*, 54, 88-88.
- AL-AGHA, O. M., HUWAIT, H. F., CHOW, C., YANG, W., SENZ, J., KALLOGER, S. E., HUNTSMAN, D. G., YOUNG, R. H. & GILKS, C. B. 2011. FOXL2 Is a Sensitive and Specific Marker for Sex Cord-Stromal Tumors of the Ovary. *American Journal of Surgical Pathology*, 35, 484-494.
- ALBRECHT, B. A. & DAELS, P. F. 1997. Immunolocalization of 3 beta-hydroxysteroid dehydrogenase, cytochrome P450 17 alpha-hydroxylase/17,20-lyase and cytochrome P450 aromatase in the equine corpus luteum of dioestrus and early pregnancy. *Journal of Reproduction and Fertility*, 111, 127-133.
- ALMADHIDI, J., SERALINI, G. E., FRESNEL, J., SILBERZAHN, P. & GAILLARD, J. L. 1995. IMMUNOHISTOCHEMICAL LOCALIZATION OF CYTOCHROME-P450 AROMATASE IN EQUINE GONADS. *Journal of Histochemistry & Cytochemistry*, 43, 571-577.
- ALMEIDA, J., BALL, B. A., CONLEY, A. J., PLACE, N. J., LIU, I. K. M., SCHOLTZ, E. L., MATHEWSON, L., STANLEY, S. D. & MOELLER, B. C. 2011a. Biological and clinical significance of anti-Mullerian hormone determination in blood serum of the mare. *Theriogenology*, 76, 1393-1403.
- ALMEIDA, J., CONLEY, A. J., MATHEWSON, L. & BALL, B. A. 2011b. Expression of steroidogenic enzymes during equine testicular development. *Reproduction*, 141, 841-848.
- ANHOLT, R. M., BEREZOWSKI, J., JAMAL, I., RIBBLE, C. & STEPHEN, C. 2014a. Mining free-text medical records for companion animal enteric syndrome surveillance. *Preventive Veterinary Medicine*, 113, 417-422.
- ANHOLT, R. M., BEREZOWSKI, J., RIBBLE, C. S., RUSSELL, M. L. & STEPHEN, C. 2014b. Using Informatics and the Electronic Medical Record to Describe Antimicrobial Use in the Clinical Management of Diarrhea Cases at 12 Companion Animal Practices. *Plos One*, 9.
- ASSIS NETO, A. C., BALL, B. A., BROWNE, P. & CONLEY, A. J. 2010. Cellular localization of androgen synthesis in equine granulosa-theca cell tumors: Immunohistochemical expression of 17 alpha-hydroxylase/17,20-lyase cytochrome P450. *Theriogenology*, 74, 393-401.
- AURICH, C. 2011. Reproductive cycles of horses. *Animal Reproduction Science*, 124, 220-228.
- BAILEY, M. T., CHRISTMAN, S. A., WHEATON, J. E., TROEDSSON, M. H., O'BRIEN, T. D., ABABNEH, M. M. & SANTACHI, E. 2000. Inhibin localization in equine

granulosa-theca cell tumours and inhibin forms in tumour fluid. *Journal of reproduction and fertility. Supplement*, 247-55.

- BAILEY, M. T., TROEDSSON, M. H. T. & WHEATON, J. E. 2002. Inhibin concentrations in mares with granulosa cell tumors. *Theriogenology*, 57, 1885-1895.
- BALL, B. A., ALMEIDA, J. & CONLEY, A. J. 2013. Determination of serum anti-Mullerian hormone concentrations for the diagnosis of granulosa-cell tumours in mares. *Equine Veterinary Journal*, 45, 199-203.
- BALL, B. A., CONLEY, A. J., ALMEIDA, J., ESTELLER-VICO, A., CRABTREE, J., MUNRO, C. & LIU, I. K. M. 2014. A Retrospective Analysis of 2,253 Cases Submitted for Endocrine Diagnosis of Possible Granulosa Cell Tumors in Mares. *Journal of Equine Veterinary Science*, 34, 307-313.
- BALL, B. A., CONLEY, A. J. & LIU, I. K. M. 2008a. Expression of anti-Mullerian hormone in equine granulosa cell tumors. *Proceedings of the 54th Annual Convention of the American Association of Equine Practitioners, San Diego, California, USA, 6-10 December 2008*, 272-273.
- BALL, B. A., CONLEY, A. J., MACLAUGHLIN, D. T., GRUNDY, S. A., SABEUR, K. & LIU, I. K. M. 2008b. Expression of anti-Mullerian hormone (AMH) in equine granulosa-cell tumors and in normal equine ovaries. *Theriogenology*, 70, 968-977.
- BASHIR, S. T., ISHAK, G. M., GASTAL, M. O., ROSER, J. F. & GASTAL, E. L. 2016. Changes in intrafollicular concentrations of free IGF-1, activin A, inhibin A, VEGF, estradiol, and prolactin before ovulation in mares. *Theriogenology*, 85, 1491-1498.
- BEACHLER, T. M., BAILEY, C. S., MCKELVEY, K. A., DAVIS, J. L., EDWARDS, A., DIAW, M., VASGAARD, J. M. & WHITACRE, M. D. 2016. Haemoperitoneum in a pregnant mare with an ovarian haematoma. *Equine Veterinary Education*, 28, 359-363.
- BELIN, F., GOUDET, G., DUCHAMP, G. & GERARD, N. 2000. Intrafollicular concentrations of steroids and steroidogenic enzymes in relation to follicular development in the mare. *Biology of Reproduction*, 62, 1335-1343.
- BENAYOUN, B. A., ANTTONEN, M., L'HOTE, D., BAILLY-BECHET, M., ANDERSSON, N., HEIKINHEIMO, M. & VEITIA, R. A. 2013. Adult ovarian granulosa cell tumor transcriptomics: prevalence of FOXL2 target genes misregulation gives insights into the pathogenic mechanism of the p.Cys134Trp somatic mutation. *Oncogene*, 32, 2739-2746.
- BENAYOUN, B. A., BATISTA, F., AUER, J., DIPIETROMARIA, A., L'HOTE, D., DE BAERE, E. & VEITIA, R. A. 2009. Positive and negative feedback regulates the transcription factor FOXL2 in response to cell stress: evidence for a regulatory imbalance induced by disease-causing mutations. *Human Molecular Genetics*, 18, 632-644.

- BENAYOUN, B. A., GEORGES, A. B., L'HOTE, D., ANDERSSON, N., DIPIETROMARIA, A., TODESCHINI, A.-L., CABURET, S., BAZIN, C., ANTTONEN, M. & VEITIA, R. A. 2011. Transcription factor FOXL2 protects granulosa cells from stress and delays cell cycle: role of its regulation by the SIRT1 deacetylase. *Human Molecular Genetics*, 20, 1673-1686.
- BIOSYSTEMS, A. 2016. Applied_Biosystems. BigDye® Terminator v3.1 Cycle Sequencing Kit User Guide. Carlsbad, CA:.
- BIOSYSTEMS., A. 2010. AmpliTaq Gold® DNA Polymerase, LD. Foster City, CA: Applied Biosystems.
- BRADLEY, C. A., ROLKA, H., WALKER, D. & LOONSK, J. 2005. BioSense: implementation of a National Early Event Detection and Situational Awareness System. *MMWR supplements*, 54, 11-9.
- BROWN, L. D., CAI, T. T., DASGUPTA, A., AGRESTI, A., COULL, B. A., CASELLA, G., CORCORAN, C., MEHTA, C., GHOSH, M. & SANTNER, T. J. 2001. Interval estimation for a binomial proportion - Comment - Rejoinder. *Statistical Science*, 16, 101-133.
- BUGNO, M., ZABEK, T., GOLONKA, P., PIENKOWSKA-SCHELLING, A., SCHELLING, C. & SLOTA, E. 2008. A case of an intersex horse with 63,X/64,XX/65,XX,del(Y)(q?) karyotype. *Cytogenetic and Genome Research*, 120, 123-126.
- BUSTAMANTE, R. M. I. 1998. Granulosa theca cell tumors in 93 mares. *Revista Científica-Facultad De Ciencias Veterinarias*, 8, 222-228.
- CABURET, S., GEORGES, A., L'HOTE, D., TODESCHINI, A.-L., BENAYOUN, B. A. & VEITIA, R. A. 2012. The transcription factor FOXL2: At the crossroads of ovarian physiology and pathology. *Molecular and Cellular Endocrinology*, 356, 55-64.
- CARNEVALE, E. M., MCKINNON, A. O. & SQUIRES, E. L. 1988. ULTRASONIC CHARACTERISTICS OF THE PREOVULATORY FOLLICLE DIRECTLY PROCEEDING AND DURING OVULATION IN THE MARE. *Theriogenology*, 29, 232-232.
- CATONE, G., MARINO, G., MANCUSO, R. & ZANGHI, A. 2004. Clinicopathological features of an equine ovarian teratoma. *Reproduction in Domestic Animals*, 39, 65-69.
- CHANDRA, A. M. S., WOODARD, J. C. & MERRITT, A. M. 1998. Dysgerminoma in an Arabian filly. *Veterinary Pathology*, 35, 308-311.
- CHAPMAN, W. W., CHRISTENSEN, L. M., WAGNER, M. M., HAUG, P. J., IVANOV, O., DOWLING, J. N. & OLSZEWSKI, R. T. 2005. Classifying free-text triage chief complaints into syndromic categories with natural language processing. *Artificial Intelligence in Medicine*, 33, 31-40.

- CHAPMAN, W. W., DOWLING, J. N. & WAGNER, M. M. 2004. Fever detection from free-text clinical records for biosurveillance. *Journal of Biomedical Informatics*, 37, 120-127.
- CHARMAN, R. E. & MCKINNON, A. O. 2007. A granulosa-theca cell tumour in a 15-month-old Thoroughbred filly. *Australian Veterinary Journal*, 85, 124-125.
- CHENG, J.-C., CHANG, H.-M., QIU, X., FANG, L. & LEUNG, P. C. K. 2014. FOXL2-induced follistatin attenuates activin A-stimulated cell proliferation in human granulosa cell tumors. *Biochemical and Biophysical Research Communications*, 443, 537-542.
- CHENG, J.-C., KLAUSEN, C. & LEUNG, P. C. K. 2013. Overexpression of Wild-Type but Not C134W Mutant FOXL2 Enhances GnRH-Induced Cell Apoptosis by Increasing GnRH Receptor Expression in Human Granulosa Cell Tumors. *Plos One*, 8.
- CHOPIN, J. B., CHOPIN, L. K., KNOTT, L. M., DE KRETSEK, D. M. & DOWSETT, K. F. 2002. Unusual ovarian activity in a mare preceding the development of an ovarian granulosa cell tumour. *Australian Veterinary Journal*, 80, 32-36.
- COCQUET, J., PAILHOUX, E., JAUBERT, F., SERVEL, N., XIA, X., PANNETIER, M., DE BAERE, E., MESSIAEN, L., COTINOT, C., FELLOUS, M. & VEITIA, R. A. 2002. Evolution and expression of FOXL2. *Journal of Medical Genetics*, 39, 916-921.
- CRABTREE, J. 2011. Review of seven cases of granulosa cell tumour of the equine ovary. *Veterinary Record*, 169, 251-U41.
- CRABTREE, J. 2013. Review of seven cases of granulosa cell tumour of the equine ovary. *Veterinary Record Case Reports*, 1, ed4635-ed4635.
- CRABTREE, J. R., BRENNAN, M. J., FOOTE, A. K. & PYCOCK, J. F. 2013. Granulosa cell tumour: An interesting case in a pregnant mare. *Equine Veterinary Education*, 25, 4-10.
- CUERVO-ARANGO, J. & NEWCOMBE, J. R. 2010. Risk Factors for the Development of Haemorrhagic Anovulatory Follicles in the Mare. *Reproduction in Domestic Animals*, 45, 473-480.
- CURTIN, D. J. E. 2003. Ovarian hematoma in an 11-year-old Thoroughbred-Hanovarian mare. *Canadian Veterinary Journal-Revue Veterinaire Canadienne*, 44, 589-591.
- DA ENCARNACAO FIALA, S. M., AMARAL, M., RICHER, L. M., CRUZ, L. A. & RODRIGUES, R. F. 2011. Ovarian Teratoma in a Mare. *Journal of Equine Veterinary Science*, 31, 511-513.
- DANICA MARKOVIĆ¹, M. P., VOJISLAV PAVLOVIĆ³ 2003. SEASONALITY, FOLLICULOGENESIS AND LUTEOGENESIS IN MARE OVARIES. *Medicine and Biology*, Vol.10, pp. 120 - 126.

- DAVIS MOREL, M. C. G. 2015. *Equine Reproductive Physiology, Breeding and Stud Management, 4th Edition CABI*, London, UK, Library of Congress Cataloging-in-Publication Data.
- DAVIS, W. P., MEDAN, M. S., JIN, W. Z., WELLS, R. E., WATANABE, G. & TAYA, K. 2005. Immunohistochemical localization of inhibin alpha-subunit in two equine granulosa-theca cell tumors. *Journal of Equine Science*, 16, 45-49.
- DE BONT, M. P., WILDERJANS, H. & SIMON, O. 2010. Standing Laparoscopic Ovariectomy Technique with Intraabdominal Dissection for Removal of Large Pathologic Ovaries in Mares. *Veterinary Surgery*, 39, 737-741.
- DE BRUIJN, B. & MARTIN, J. 2002. Getting to the (c)ore of knowledge: mining biomedical literature. *International Journal of Medical Informatics*, 67, 7-18.
- DONADEU, F. X. & GINTHER, O. J. 2002. Follicular waves and circulating concentrations of gonadotrophins, inhibin and oestradiol during the anovulatory season in mares. *Reproduction*, 124, 875-885.
- DONADEU, F. X. & PEDERSEN, H. G. 2008. Follicle development in mares. *Reproduction in Domestic Animals*, 43, 224-231.
- DOU, M., ZHU, K., FAN, Z., ZHANG, Y., CHEN, X., ZHOU, X., DING, X., LI, L., GU, Z., GUO, M., YAN, M., DENG, X., SHEN, P. & WANG, S. 2017. Reproductive Hormones and Their Receptors May Affect Lung Cancer. *Cellular Physiology and Biochemistry*, 44, 1425-1434.
- DRAIN COURT, M. A., MARIANA, J. C. & PALMER, E. 1982. Effect of the stage of the oestrous cycle on the follicular population in pony mares. *Reproduction Nutrition Developpement*, 22, 803-812.
- DRIANCOURT, M. A., PARIS, A., ROUX, C., MARIANA, J. C. & PALMER, E. 1982. OVARIAN FOLLICULAR POPULATIONS IN PONY AND SADDLE-TYPE MARES. *Reproduction Nutrition Development*, 22, 1035-1047.
- DUVALL, E. & WYLLIE, A. H. 1986. DEATH AND THE CELL. *Immunology Today*, 7, 115-119.
- DUZ, M., PARKIN, T. & MARSHALL, J. 2016. *Biochemical and epidemiological investigations of non-steroidal anti-inflammatory drug usage and related side effects in equids*. Doctor in Philosophy , University of Glasgow.
- ELLENBERGER, C., BARTMANN, C. P., HOPPEN, H. O., KRATZSCH, J., AUPPERLE, H., KLUG, E., SCHOON, D. & SCHOON, H. A. 2007. Histomorphological and immunohistochemical characterization of equine granulosa cell tumours. *Journal of Comparative Pathology*, 136, 167-176.
- EVKURAN DAL, G., ALCIGIR, E., POLAT, I. M., VURAL ATALAY, S., CANATAN, H. E., VURAL, M. R. & KUPLULU, S. 2013. Granulosa Theca Cell Tumor in An Arabian Mare: Are Immunohistochemically Loss of GDF-9 and BMP-6

Proteins Associated with High GATA-4, Inhibin-alpha, AMH Expressions?
Kafkas Universitesi Veteriner Fakultesi Dergisi, 19, A237-A242.

- FERNANDES, T. R., GRANDI, F., MONTEIRO, L. N., SALGADO, B. S. & ROCHA, N. S. 2011. What is your diagnosis? Unilateral ovarian mass in a mare. *Veterinary Clinical Pathology*, 40, 399-400.
- FORST, S., NIEDERSTUCKE, H. & HOPPEN, H. O. 2003. Persistent anovulatory follicles in the mare. *Pferdeheilkunde*, 19, 625-627.
- GARRISON, E. & MARTH, G. 2012. Haplotype-based variant detection from short-read sequencing. arXiv preprint arXiv:1207.3907 [q-bio.GN]
- GARTEN, Y., COULET, A. & ALTMAN, R. B. 2010. Recent progress in automatically extracting information from the pharmacogenomic literature. *Pharmacogenomics*, 11, 1467-1489.
- GASTAL, E. L., GASTAL, M. O. & GINTHER, O. J. 2006. Relationships of changes in B-mode echotexture and colour-Doppler signals in the wall of the preovulatory follicle to changes in systemic oestradiol concentrations and the effects of human chorionic gonadotrophin in mares. *Reproduction*, 131, 699-709.
- GASTAL, E. L., GASTAL, M. O., WILTBANK, M. C. & GINTHER, O. J. 1999a. Follicle deviation and intrafollicular and systemic estradiol concentrations in mares. *Biology of Reproduction*, 61, 31-39.
- GASTAL, E. L., GASTAL, M. O., WILTBANK, M. C. & GINTHER, O. J. 1999b. Relationship of follicle deviation with intrafollicular and systemic estradiol concentrations in mares. *Theriogenology*, 51, 300-300.
- GASTAL, E. L., JACOB, J. C. F., GASTAL, M. O. & GINTHER, O. J. 2007. Accumulation of fluid in the infundibulum during the estrous cycle in mares. *Journal of Equine Veterinary Science*, 27, 251-259.
- GEHLEN, H., HAIST, V., BAUMGARTNER, W. & KLUG, E. 2006. Malignant dysgerminoma in an 18-year old warmblood mare. *Journal of Equine Veterinary Science*, 26, 23-26.
- GEIERSBACH, K. B., JARBOE, E. A., JAHROMI, M. S., BAKER, C. L., PAXTON, C. N., TRIPP, S. R. & SCHIFFMAN, J. D. 2011. FOXL2 mutation and large-scale genomic imbalances in adult granulosa cell tumors of the ovary. *Cancer Genetics*, 204, 596-602.
- GERARD, N., DUCHAMP, G., GOUDET, G., BEZARD, J., MAGISTRINI, M. & PALMER, E. 1998. A high-molecular-weight preovulatory stage-related protein in equine follicular fluid and granulosa cells. *Biology of Reproduction*, 58, 551-557.
- GERSAK, K., HARRIS, S. E., SMALE, W. J. & SHELLING, A. N. 2004. A novel 30 bp deletion in the FOXL2 gene in a phenotypically normal woman with primary amenorrhoea: Case report. *Human Reproduction*, 19, 2767-2770.

- GHARAGOZLOU, F., YOUSSEFI, R., AKBARINEJAD, V. & ASHRAFIHELAN, J. 2013. Elevated Serum Anti-Mullerian Hormone in an Arabian Mare with Granulosa Cell Tumor. *Journal of Equine Veterinary Science*, 33, 645-648.
- GHARAGOZLOU, F., YOUSSEFI, R., AKBARINEJAD, V., MASOUDIFARD, M. & ASHRAFIHELAN, J. 2014. Changes of serum anti-Mullerian hormone in a mare with granulosa cell tumour following surgery and reinitiation of follicular activity. *Equine Veterinary Education*, 26, 481-484.
- GINTHER, O. J. 1990. FOLLICULOGENESIS DURING THE TRANSITIONAL PERIOD AND EARLY OVULATORY SEASON IN MARES. *Journal of Reproduction and Fertility*, 90, 311-320.
- GINTHER, O. J., BEG, M. A., DONADEU, F. X. & BERGFELT, D. R. 2003. Mechanism of follicle deviation in monovular farm species. *Animal Reproduction Science*, 78, 239-257.
- GINTHER, O. J., GASTAL, E. L., GASTAL, M. O. & BEG, M. A. 2006. Conversion of a viable preovulatory follicle into a hemorrhagic anovulatory follicle in mares. *Animal Reproduction*, 3, A29-A40.
- GINTHER, O. J., GASTAL, E. L., GASTAL, M. O., SIDDIQUI, M. A. R. & BEG, M. A. 2007. Relationships of follicle versus oocyte maturity to ultrasound morphology, blood flow, and hormone concentrations of the preovulatory follicle in mares'. *Biology of Reproduction*, 77, 202-208.
- GINTHER, O. J., GASTAL, E. L., RODRIGUES, B. L., GASTAL, M. O. & BEG, M. A. 2008. Follicle diameters and hormone concentrations in the development of single versus double ovulations in mares. *Theriogenology*, 69, 583-590.
- GOUDET, G., BELIN, F., BEZARD, J. & GERARD, N. 1999. Intrafollicular content of luteinizing hormone receptor, alpha-inhibin, and aromatase in relation to follicular growth, estrous cycle stage, and oocyte competence for in vitro maturation in the mare. *Biology of Reproduction*, 60, 1120-1127.
- GUNDUZ, M. C., KASIKCI, G., KILICARSLAN, R., UCMAN, M., DUZGUN, O. & TEK, C. 2010. Reproductive performance following unilateral ovariectomy for treatment of ovarian tumors in 7 mares. *Turkish Journal of Veterinary & Animal Sciences*, 34, 283-287.
- HAAG, K. T., MAGALHAES-PADILHA, D. M., FONSECA, G. R., WISCHRAL, A., GASTAL, M. O., KING, S. S., JONES, K. L., FIGUEIREDO, J. R. & GASTAL, E. L. 2013. Quantification, morphology, and viability of equine preantral follicles obtained via the Biopsy Pick-Up method. *Theriogenology*, 79, 599-609.
- HARLAND, S., SMITH, C. S., MOGG, T. D., HORADAGODA, N. & DART, A. J. 2009. Surgical resection of a dysgerminoma in a mare. *Australian Veterinary Journal*, 87, 110-112.

- HEIDLER, B., AURICH, J. E., POHL, W. & AURICH, C. 2004. Body weight of mares and foals, estrous cycles and plasma glucose concentration in lactating and non-lactating Lipizzaner mares. *Theriogenology*, 61, 883-893.
- HES, O., VANECEK, T., PETERSSON, F., GROSSMANN, P., HORA, M., PEREZ MONTIEL, D. M., STEINER, P., DVORAK, M. & MICHAL, M. 2011. Mutational Analysis (c.402C > G) of the FOXL2 Gene and Immunohistochemical Expression of the FOXL2 Protein in Testicular Adult Type Granulosa Cell Tumors and Incompletely Differentiated Sex Cord Stromal Tumors. *Applied Immunohistochemistry & Molecular Morphology*, 19, 347-351.
- HINRICHS, K., FRAZER, G. S., DEGANNES, R. V. G., RICHARDSON, D. W. & KENNEY, R. M. 1989. SEROUS CYSTADENOMA IN A NORMALLY CYCLIC MARE WITH HIGH PLASMA TESTOSTERONE VALUES. *Journal of the American Veterinary Medical Association*, 194, 381-382.
- HULTGREN, B. D., ZACK, P. M., PEARSON, E. G. & KANEPS, A. J. 1987. JUVENILE GRANULOSA-CELL TUMOR IN AN EQUINE WEANLING. *Journal of Comparative Pathology*, 97, 137-142.
- JAMIESON, S., BUTZOW, R., ANDERSSON, N., ALEXIADIS, M., UNKILA-KALLIO, L., HEIKINHEIMO, M., FULLER, P. J. & ANTTONEN, M. 2010. The FOXL2 C134W mutation is characteristic of adult granulosa cell tumors of the ovary. *Modern Pathology*, 23, 1477-1485.
- JONES-DIETTE, J. S., ROBINSON, N., BRENNAN, M., COBB, M. & DEAN, R. 2014. How complete is the electronic patient record in veterinary practice? *BSAVA Congress 2014, Birmingham, UK, 3-6 April, 2014. Scientific Proceedings Veterinary Programme*, 635-635.
- KENNEY, R. M., CONDON, W., GANJAM, V. K. & CHANNING, C. 1979. Morphological and biochemical correlates of equine ovarian follicles as a function of their state of viability or atresia. *Journal of reproduction and fertility. Supplement*, 163-71.
- KIERNAN, J. 2008. *Histological and Histochemical Methods: Theory and Practice*. 4th ed. Bloxham, UK: Scion.
- KIM, J. H., YOON, S., PARK, M., PARK, H. O., KO, J. J., LEE, K. & BAE, J. 2011. Differential apoptotic activities of wild-type FOXL2 and the adult-type granulosa cell tumor-associated mutant FOXL2 (C134W). *Oncogene*, 30, 1653-1663.
- KNUDSEN, O. & VELLE, W. 1961. OVARIAN OESTROGEN LEVELS IN NON-PREGNANT MARE - RELATIONSHIP TO HISTOLOGICAL APPEARANCE OF UTERUS AND TO CLINICAL STATUS. *Journal of Reproduction and Fertility*, 2, 130-&.
- KOEBEL, M., GILKS, C. B. & HUNTSMAN, D. G. 2009. Adult-Type Granulosa Cell Tumors and FOXL2 Mutation. *Cancer Research*, 69, 9160-9162.
- KOMMOSS, S., ANGLÉSIO, M. S., MACKENZIE, R., YANG, W., SENZ, J., HO, J., BELL, L., LEE, S., LORETTE, J., HUNTSMAN, D. G. & GILKS, C. B. 2013.

FOXL2 molecular testing in ovarian neoplasms: diagnostic approach and procedural guidelines. *Modern Pathology*, 26, 860-867.

- LAM, K., PARKIN, T., RIGGS, C. & MORGAN, K. 2007. Use of free text clinical records in identifying syndromes and analysing health data. *Veterinary Record*, 161, 547-551.
- LEFEBVRE, R., THEORET, C., DORE, M., GIRARD, C., LAVERTY, S. & VAILLANCOURT, D. 2005. Ovarian teratoma and endometritis in a mare. *Canadian Veterinary Journal-Revue Veterinaire Canadienne*, 46, 1029-1033.
- LEUNG, D. T. H., FULLER, P. J. & CHU, S. 2016. Impact of FOXL2 mutations on signaling in ovarian granulosa cell tumors. *International Journal of Biochemistry & Cell Biology*, 72, 51-54.
- LIMA, J. F., JIN, L., DE ARAUJO, A. R. C., ERIKSON-JOHNSON, M. R., OLIVEIRA, A. M., SEBO, T. J., KEENEY, G. L. & MEDEIROS, F. 2012. FOXL2 Mutations in Granulosa Cell Tumors Occurring in Males. *Archives of Pathology & Laboratory Medicine*, 136, 825-828.
- MATTIN, M., O'NEILL, D., CHURCH, D., MCGREEVY, P. D., THOMSON, P. C. & BRODBELT, D. 2014. An epidemiological study of diabetes mellitus in dogs attending first opinion practice in the UK. *Veterinary Record*, 174, 349-+.
- MATTIN, M. J., BOSWOOD, A., CHURCH, D. B., LOPEZ-ALVAREZ, J., MCGREEVY, P. D., O'NEILL, D. G., THOMSON, P. C. & BRODBELT, D. C. 2015. Prevalence of and Risk Factors for Degenerative Mitral Valve Disease in Dogs Attending Primary-care Veterinary Practices in England. *Journal of Veterinary Internal Medicine*, 29, 847-854.
- MCCLUGGAGE, W. G., SINGH, N., KOMMOSS, S., HUNTSMAN, D. G. & GILKS, C. B. 2013. Ovarian Cellular Fibromas Lack FOXL2 Mutations A Useful Diagnostic Adjunct in the Distinction From Diffuse Adult Granulosa Cell Tumor. *American Journal of Surgical Pathology*, 37, 1450-1455.
- MCCONECHY, M. K., FARKKILA, A., YANG, W., ANDERSSON, N., NG, Y., UNKILA-KALLIO, L., MCALPINE, J. N., GILKS, B., ANTTONEN, M. & HUNTSMAN, D. G. 2014. Circulating tumor DNA: FOXL2 402C-G mutation can be identified in plasma from adult granulosa cell tumor patients with recurrent disease. *Cancer Research*, 74.
- MCCUE, P. M. 1993. Equine granulosa cell tumors. *Proceedings of the Annual Convention of the American Association of Equine Practitioners*, 38, 587-593.
- MCCUE, P. M. 1998. Neoplasia of the female reproductive tract. *Veterinary Clinics of North America-Equine Practice*, 14, 505-+.
- MCCUE, P. M., LEBLANC, M. M., AKITA, G. Y., PASCOE, J. R., WITHERSPOON, D. M. & STABENFELDT, G. H. 1991. GRANULOSA-CELL TUMORS IN 2 CYCLING MARES. *Journal of Equine Veterinary Science*, 11, 281-282.

- MCCUE, P. M. & MCKINNON, A. O. 2011. Ovarian abnormalities. *Equine reproduction, Volume 2*, 2123-2136.
- MCCUE, P. M., ROSER, J. F., MUNRO, C. J., LIU, I. K. M. & LASLEY, B. L. 2006. Granulosa cell tumors of the equine ovary. *Veterinary Clinics of North America-Equine Practice*, 22, 799-+.
- MCCUE, P. M. & SQUIRES, E. L. 2002. Persistent anovulatory follicles in the mare. *Theriogenology*, 58, 541-543.
- MCKINNON, A. O. 1997. Ovarian abnormalities. In: Ranaten NW, McKinnon AO, editors. *Equine diagnostic ultrasonography*. Baltimore: Williams and Wilkins, 1997. p 233-51.
- MCLENNAN, M. W. & KELLY, W. R. 1977. HYPERTROPHIC OSTEOPATHY AND DYSGERMINOMA IN A MARE. *Australian Veterinary Journal*, 53, 144-146.
- MEINECKE, B. & GIPS, H. 1987. STEROID-HORMONE SECRETORY PATTERNS IN MARES WITH GRANULOSA-CELL TUMORS. *Journal of Veterinary Medicine Series a-Zentralblatt Fur Veterinarmedizin Reihe a-Physiology Pathology Clinical Medicine*, 34, 545-560.
- MIHM, M., BAKER, P. J., IRELAND, J. L. H., SMITH, G. W., COUSSENS, P. M., EVANS, A. C. O. & IRELAND, J. J. 2006. Molecular evidence that growth of dominant follicles involves a reduction in follicle-stimulating hormone dependence and an increase in luteinizing hormone dependence in cattle. *Biology of Reproduction*, 74, 1051-1059.
- MLODAWSKA, W., GRZESIAK, M., KOCHAN, J. & NOWAK, A. 2018. Intrafollicular level of steroid hormones and the expression of androgen receptor in the equine ovary at puberty. *Theriogenology*, 121, 13-20.
- MLODAWSKA, W. & SLOMCZYNSKA, M. 2010. Immunohistochemical localization of aromatase during the development and atresia of ovarian follicles in prepubertal horses. *Theriogenology*, 74, 1707-1712.
- MOREL, M. C. G. D., NEWCOMBE, J. R. & HAYWARD, K. 2010. Factors affecting pre-ovulatory follicle diameter in the mare: the effect of mare age, season and presence of other ovulatory follicles (multiple ovulation). *Theriogenology*, 74, 1241-1247.
- MUELLER, K., ELLENBERGER, C. & SCHOON, H. A. 2009. Histomorphological and immunohistochemical study of angiogenesis and angiogenic factors in the ovary of the mare. *Research in Veterinary Science*, 87, 421-431.
- NAGAMINE, N., NAMBO, Y., NAGATA, S., NAGAOKA, K., TSUNODA, N., TANIYAMA, H., TANAKA, Y., TOHEI, A., WATANABE, G. & TAYA, K. 1998. Inhibin secretion in the mare: Localization of inhibin alpha, beta(A), and beta(B) subunits in the Ovary. *Biology of Reproduction*, 59, 1392-1398.
- O'NEILL, D. 2012. VetCompass clinical data points the way forward. *Veterinary Ireland Journal*, 2, 353-356.

- O'NEILL, D., HENDRICKS, A., SUMMERS, J. & BRODBELT, D. 2012. Primary care veterinary usage of systemic glucocorticoids in cats and dogs in three UK practices. *Journal of Small Animal Practice*, 53, 217-222.
- O'NEILL, D. G., ELLIOTT, J., CHURCH, D. B., MCGREEVY, P. D., THOMSON, P. C. & BRODBELT, D. C. 2013. Chronic Kidney Disease in Dogs in UK Veterinary Practices: Prevalence, Risk Factors, and Survival. *Journal of Veterinary Internal Medicine*, 27, 814-821.
- OLIVER, C. & JAMUR, M. C. 2010. Immunocytochemical Methods and Protocols. 3rd Edition. Edited by Lorette C. Javois. Humana Press, Totowa, New Jersey.
- OSETO, K., SUZUMORI, N., NISHIKAWA, R., NISHIKAWA, H., ARAKAWA, A., OZAKI, Y., ASAI, H., KAWAI, M., MIZUNO, K., TAKAHASHI, S., SHIRAI, T., YAMADA-NAMIKAWA, C., NAKANISHI, M., KAJIYAMA, H., KIKKAWA, F. & SUGIURA-OGASAWARA, M. 2014. Mutational analysis of FOXL2 p. C134W and expression of bone morphogenetic protein 2 in Japanese patients with granulosa cell tumor of ovary. *Journal of Obstetrics and Gynaecology Research*, 40, 1197-1204.
- OSHEA, J. D. 1968. A HISTOLOGICAL STUDY OF NON-FOLLICULAR CYSTS IN OVULATION FOSSA REGION OF EQUINE OVARY. *Journal of Morphology*, 124, 313-318.
- OSWALD, J., LOVE, S., PARKIN, T. D. H. & HUGHES, K. J. 2010. Prevalence of cervical vertebral stenotic myelopathy in a population of thoroughbred horses. *Veterinary Record*, 166, 82-83.
- PEDERSEN, H. G., WATSON, E. D. & TELFER, E. E. 2003. Analysis of atresia in equine follicles using histology, fresh granulosa cell morphology and detection of DNA fragmentation. *Reproduction*, 125, 417-423.
- PENZ, J. F. E., WILCOX, A. B. & HURDLE, J. F. 2007. Automated identification of adverse events related to central venous catheters. *Journal of Biomedical Informatics*, 40, 174-182.
- PETER, A. T. & DHANASEKARAN, N. 2003. Apoptosis of granulosa cells: A review on the role of MAPK-signalling modules. *Reproduction in Domestic Animals*, 38, 209-213.
- PIERSON, R. A. 1993. Folliculogenesis and ovulation. In: Equine Reproduction. McKinnon, A, Voss J (eds.) Williams & Wilkins, Media, PA: 161.
- PIQUETTE, C. N., KENNEY, R. M., SERTICH, P. L., YAMOTO, M. & HSUEH, A. J. W. 1990. Equine granulosa-theca cell tumors express inhibin alpha- and beta A-subunit messenger ribonucleic acids and proteins. *Biology of Reproduction*, 43, 1050-1057.
- PISARSKA, M. D., BARLOW, G. & KUO, F.-T. 2011. Minireview: Roles of the Forkhead Transcription Factor FOXL2 in Granulosa Cell Biology and Pathology. *Endocrinology*, 152, 1199-1208.

- PRINGLE, M., WARD, P. & CHILVERS, C. 1995. ASSESSMENT OF THE COMPLETENESS AND ACCURACY OF COMPUTER MEDICAL RECORDS IN 4 PRACTICES COMMITTED TO RECORDING DATA ON COMPUTER. *British Journal of General Practice*, 45, 537-541.
- PYCOCK, J. F., DIELEMAN, S., DRIFJHOUT, P., VANDERBRUG, Y., OEI, C. & VANDERWEIJDEN, G. C. 1995. Correlation of plasma concentrations of progesterone and oestradiol with ultrasound characteristics of the uterus and duration of oestrous behaviour in the cycling mare. *Reproduction in Domestic Animals*, 30, 224-227.
- QIAGEN. 2006. DNeasy® Blood & Tissue Handbook. Qiagen.
- RADFORD, A. D., NOBLE, P. J., COYNE, K. P., GASKELL, R. M., JONES, P. H., BRYAN, J. G. E., SETZKORN, C., TIERNEY, A. & DAWSON, S. 2011. Antibacterial prescribing patterns in small animal veterinary practice identified via SAVSNET: the small animal veterinary surveillance network. *Veterinary Record*, 169, 310-U91.
- RAJA, U., MITCHELL, T., DAY, T. & HARDIN, J. M. 2008. Text mining in healthcare. Applications and opportunities. *Journal of healthcare information management : JHIM*, 22, 52-6.
- RAZ, T. & AHARONSON-RAZ, K. 2012. Ovarian Follicular Dynamics During the Estrous Cycle in the Mare. *Israel Journal of Veterinary Medicine*, 67, 11-18.
- RODGER, F. E., ILLINGWORTH, P. J. & WATSON, E. D. 1998. Immunolocalization of P450C17 in the mare corpus luteum. *Theriogenology*, 50, 321-333.
- RODGERS, R. J., IRVING-RODGERS, H. F., VAN WEZEL, I. L., KRUPA, M. & LAVRANOS, T. C. 2001. Dynamics of the membrana granulosa during expansion of the ovarian follicular antrum. *Molecular and Cellular Endocrinology*, 171, 41-48.
- ROECKEN, M., MOSEL, G., SEYREK-INTAS, K., SEYREK-INTAS, D., LITZKE, F., VERVER, J. & RIJKENHUIZEN, A. B. M. 2011. Unilateral and Bilateral Laparoscopic Ovariectomy in 157 Mares: A Retrospective Multicenter Study. *Veterinary Surgery*, 40, 1009-1014.
- ROSARIO, R., ARAKI, H., PRINT, C. G. & SHELLING, A. N. 2012. GSE39890: Gene knockdown and overexpression of 402C>G FOXL2 in COV434 and KGN cells. *Gene Expression Omnibus*.
- ROSARIO, R., WILSON, M., CHENG, W.-T., PAYNE, K., COHEN, P. A., FONG, P. & SHELLING, A. N. 2013. Adult granulosa cell tumours (GCT): Clinicopathological outcomes including FOXL2 mutational status and expression. *Gynecologic Oncology*, 131, 325-329.
- SALTON, G. & LESK, M. E. 1968. COMPUTER EVALUATION OF INDEXING AND TEXT PROCESSING. *Journal of the Acm*, 15, 8-&.

- SATUÉ & GARDÓN 2013. A Review of the Estrous Cycle and the Neuroendocrine Mechanisms in the Mare. *J Steroids Horm Sci*, 4.
- SCHUMER, S. T. & CANNISTRA, S. A. 2003. Granulosa cell tumor of the ovary. *Journal of Clinical Oncology*, 21, 1180-1189.
- SESSIONS, D. R., VICK, M. M. & FITZGERALD, B. P. 2009. Characterization of matrix metalloproteinase-2 and matrix metalloproteinase-9 and their inhibitors in equine granulosa cells in vivo and in vitro. *Journal of Animal Science*, 87, 3955-3966.
- SHAH, S. P., KOEBEL, M., SENZ, J., MORIN, R. D., CLARKE, B. A., WIEGAND, K. C., LEUNG, G., ZAYED, A., MEHL, E., KALLOGER, S. E., SUN, M., GIULIANI, R., YORIDA, E., JONES, S., VARHOL, R., SWENERTON, K. D., MILLER, D., CLEMENT, P. B., CRANE, C., MADORE, J., PROVENCHER, D., LEUNG, P., DEFAZIO, A., KHATTRA, J., TURASHVILI, G., ZHAO, Y., ZENG, T., GLOVER, J. N. M., VANDERHYDEN, B., ZHAO, C., PARKINSON, C. A., JIMENEZ-LINAN, M., BOWTELL, D. D. L., MES-MASSON, A.-M., BRENTON, J. D., APARICIO, S. A., BOYD, N., HIRST, M., GILKS, C. B., MARRA, M. & HUNTSMAN, D. G. 2009. Mutation of FOXL2 in Granulosa-Cell Tumors of the Ovary. *New England Journal of Medicine*, 360, 2719-2729.
- SIROIS, J., BALL, B. A. & FORTUNE, J. E. 1989. Patterns of growth and regression of ovarian follicles during the oestrous cycle and after hemiovariectomy in mares. *Equine Veterinary Journal*, 43-48.
- SIROIS, J., KIMMICH, T. L. & FORTUNE, J. E. 1990. DEVELOPMENTAL-CHANGES IN STEROIDOGENESIS BY EQUINE PREEVULATORY FOLLICLES - EFFECTS OF EQUINE LH, FSH, AND CG. *Endocrinology*, 127, 2423-2430.
- SMOK S, C. & ROJAS R, M. 2010. Follicular-Stromal Interaction in Mare Ovary During the Reproductive Cycle. *International Journal of Morphology*, 28, 697-701.
- SON, Y. S., LEE, C. S., JEONG, W. I., HONG, I. H., PARK, S. J., KIM, T. H., CHO, E. M., PARK, T. I. & JEONG, K. S. 2005. Cystadenocarcinoma in the ovary of a Thoroughbred mare. *Australian Veterinary Journal*, 83, 283-284.
- TAKAHASHI, A., KIMURA, F., YAMANAKA, A., TAKEBAYASHI, A., KITA, N., TAKAHASHI, K. & MURAKAMI, T. 2013. The FOXL2 Mutation (c.402C > G) in Adult-Type Ovarian Granulosa Cell Tumors of Three Japanese Patients: Clinical Report and Review of the Literature. *Tohoku Journal of Experimental Medicine*, 231, 243-250.
- TROEDSSON, M. H. T., MCCUE, P. M. & MACPHERSON, M. L. 2003. Clinical aspects of ovarian pathology in the mare. *Pferdeheilkunde*, 19, 577-+.
- VAN DER KOLK, J. H., GEELLEN, S. N. J., JONKER, F. H., PYCOCK, J. F. & KOEMAN, J. P. 1998. Hypertrophic osteopathy associated with ovarian carcinoma in a mare. *Veterinary Record*, 143, 172-173.

- VANCAMP, S. D., MAHLER, J., ROBERTS, M. C., TATE, L. P. & WHITACRE, M. D. 1989. PRIMARY OVARIAN ADENOCARCINOMA ASSOCIATED WITH TERATOMATOUS ELEMENTS IN A MARE. *Journal of the American Veterinary Medical Association*, 194, 1728-1730.
- VANDERZAAG, E. J., RIJKENHUIZEN, A. B. M., KALSBECK, H. C. & PEPEKAMP, N. 1996. A mare with colic caused by an ovarian tumour. *Veterinary Quarterly*, 18, 60-62.
- VANHAESEBROUCK, E., GOVAERE, J., SMITS, K., DURIE, I., VERCAUTEREN, G., MARTENS, A., SCHAUVLIEGE, S., DUCATELLE, R., HOOGEWIJS, M., DE SCHAUWER, C. & DE KRUIF, A. 2010. Ovarian teratoma in the mare: a review and two cases. *Vlaams Diergeneeskundig Tijdschrift*, 79, 32-41.
- VERDIN, H. & DE BAERE, E. 2012. FOXL2 Impairment in Human Disease. *Hormone Research in Paediatrics*, 77, 2-11.
- WALSH, S. W., MATTHEWS, D., BROWNE, J. A., FORDE, N., CROWE, M. A., MIHM, M., DISKIN, M. & EVANS, A. C. O. 2012. Acute dietary restriction in heifers alters expression of genes regulating exposure and response to gonadotrophins and IGF in dominant follicles. *Animal Reproduction Science*, 133, 43-51.
- WANG, W.-C. & LAI, Y.-C. 2014. Molecular pathogenesis in granulosa cell tumor is not only due to somatic FOXL2 mutation. *Journal of Ovarian Research*, 7.
- WATSON, E. D. 1994. INFERTILITY IN THE MARE. *Journal of Comparative Pathology*, 111, 333-351.
- WATSON, E. D. 1999. Granulosa cell tumours in the mare: - a review of 9 cases. *Equine Veterinary Education*, 11, 136-142.
- WATSON, E. D. & AL-ZI'ABI, M. O. 2002. Characterization of morphology and angiogenesis in follicles of mares during spring transition and the breeding season. *Reproduction*, 124, 227-234.
- WATSON, E. D. & AL-ZI'ABI, M. O. 2002. Angiogenesis in follicles of mares during spring transition and the breeding season. *Theriogenology*, 58, 607-608.
- WATSON, E. D., BAE, S. E., STEELE, M., THOMASSEN, R., PEDERSEN, H. G., BRAMLEY, T., HOGG, C. O. & ARMSTRONG, D. G. 2004. Expression of messenger ribonucleic acid encoding for steroidogenic acute regulatory protein and enzymes, and luteinizing hormone receptor during the spring transitional season in equine follicles. *Domestic Animal Endocrinology*, 26, 215-230.
- WATSON, E. D., HEALD, M., LEASK, R., GROOME, N. P. & RILEY, S. C. 2002a. Detection of high circulating concentrations of inhibin pro- and -alpha C immunoreactivity in mares with granulosa-theca cell tumours. *Equine Veterinary Journal*, 34, 203-206.

- WATSON, E. D., THOMASSEN, R., STEELE, M., HEALD, M., LEASK, R., GROOME, N. P. & RILEY, S. C. 2002b. Concentrations of inhibin, progesterone and oestradiol in fluid from dominant and subordinate follicles from mares during spring transition and the breeding season. *Animal Reproduction Science*, 74, 55-67.
- WATSON, E. D. & THOMSON, S. R. M. 1996. Immunolocalization of aromatase P-450 in ovarian tissue from pregnant and nonpregnant mares and in ovarian tumours. *Journal of Reproduction and Fertility*, 108, 239-244.
- YANAGIDA, S., ANGLÉSIO, M. S., NAZERAN, T. M., LUM, A., INOUE, M., IIDA, Y., TAKANO, H., NIKAIDO, T., OKAMOTO, A. & HUNTSMAN, D. G. 2017. Clinical and genetic analysis of recurrent adult-type granulosa cell tumor of the ovary: Persistent preservation of heterozygous c.402C > G FOXL2 mutation. *Plos One*, 12.
- YOSHIDA, G., TSUNODA, N., MIYAKE, Y.-I., SHAFIQUL, H. M. D., OSAWA, T., NAGAMINE, N., TANIYAMA, H., NAMBO, Y., WATANABE, G. & TAYA, K. 2000. Endocrinological studies of mares with granulosa-theca cell tumor. *Journal of Equine Science*, 11, 35-43.
- YOUNG, J. M. & MCNEILLY, A. S. 2010. Theca: the forgotten cell of the ovarian follicle. *Reproduction*, 140, 489-504.